2017-05-24

Single-Molecule Studies of Replication Kinetics in Response to DNA Damage

Divya Ramalingam Iyer
University of Massachusetts Medical School

SINGLE-MOLECULE STUDIES OF REPLICATION KINETICS IN RESPONSE TO DNA DAMAGE

A Dissertation Presented

By

DIVYA RAMALINGAM IYER

Submitted to the Faculty of the

University of Massachusetts Graduate School of Biomedical Sciences, Worcester

in partial fulfillment of the requirements for the degree of

DOCTOR OF PHILOSOPHY

(May 24, 2017)

INTERDISCIPLINARY GRADUATE PROGRAM

Dedication

I dedicate this thesis to my aunt,

ஜெயஸ்ரீ

for her unconditional love and support.

Acknowledgements

I would like to thank foremost my mentor, Dr. Nick Rhind for giving me the opportunity to conduct my PhD on such an interesting and challenging project in his lab. During the course of my PhD I have found him to be very encouraging and supportive as a mentor. I have really valued the way he is always available to discuss science with great enthusiasm even for the most improbable of experiments. He has always believed and shown faith in me even at times when the most trivial of experiments were not working for several months. He has also supported my career and helped me develop as a scientist by giving me several opportunities to present talks at conferences and write reviews.

I would like to thank Dr. Merav Socolovsky, for always making me feel like I had not one, but two mentors during my PhD. I have been very fortunate to get to work with her from the beginning of my PhD. It was great to learn from her and have her support and advice while I was trouble-shooting DNA combing. Without her encouragement and reassurance I would have long given up on this tedious technique. I think her belief and faith in me has played a very big part in helping me make it till the end.

I want to thank Dr. Paul Kaufman for personally teaching me to work with budding yeast and do CHIP experiments when I rotated with him. As a first year student it was very valuable to be taught first-hand by a principal investigator. I want to thank Dr. Dannel McCollum for teaching me how to do tetrad dissections

and several routine basics of fission yeast during my rotation. I want to thank Dr. Jennifer Benanti with whom we have had joint lab meetings. Jenny has always given great advice on every aspect of research from doing experiments to presentations. I have learnt a lot about how to be a better scientist from her.

I would like to thank all my TRAC members – Dr. Craig Peterson, Dr. Paul Kaufman, Dr. Merav Socolovsky and Dr. Scot Wolfe for always being available and showing interest in my research over the years and giving me constructive criticisms and taking time out of their busy schedules. I'm very grateful for all your inputs and support over the years.

I would like to thank Dr. Mitch McVey for being on my dissertation committee and reading my thesis.

I want to thank Livio Dukaj from Rhind lab for being the best colleague one can ask for. He has always been helpful, eager to discuss science and very understanding. I would also like to thank some former members of Rhind lab. I want to thank Dr. Nick Willis for being very meticulous and leaving me lots of resources to help me kick start my project with great ease. I want to thank Dr. Ryan George for advising me on the challenges of navigating through graduate school, career transitions and being ever ready to discuss (and curse) combing and DNA replication at great lengths. I want to thank Ryan Holmes for being a great friend and always bringing a smile with his colorful anecdotes from his part-time job as a bartender. I want to thank Maximiliaan Huisman for being a fabulous colleague and 3D-printing coverslip platforms exactly as designed by

us. I want to thank members of Benanti lab particularly Tyler for being a great colleague and Heather for being so helpful with protocols and reagents.

I want to thank Genomic Vision, a combing company in France with whom I collaborated for my review experiments. I want to thank Julien Cottineau and Eszter Takacs for being understanding, helpful and patient with all my emails and questions.

I would also like to thank the Biochemistry and Molecular Pharmacology Department for providing their support, encouragement and a collegial atmosphere over the years. I would like to thank Dr. Melissa Moore's lab for sharing equipment.

I want to thank several friends at UMass Medical School and elsewhere who have made my journey through graduate school enjoyable – Dipti, Nidhi, Sandhya, Arvind, Mayuri, Ebru, Cha San, Meghana, Ribhu, Sugandha, Siva, Sungwook, Neha, Ken, Sreya, Pallavi, Subhalaxmi, Ami, Swapnil, Janani, Venkatesan, Viknesh, Swetha, Meetu, Ozge, Darshana, Deepa, Upasna, Fengyun, Shailaja, Ram, Irene, Ivery and Rajesh.

I want to thank my best friend Sonal, who is also a PhD candidate at UMass Medical School close to defending soon and with whom I have been fortunate to be with since my undergraduate days. It has been phenomenal to have her as a friend over the last twelve years through all the ups and downs from starting and completing undergraduate studies to moving to a foreign country for a PhD. I feel incredibly fortunate to have met a friend with whom I can share my thoughts

without even expressing a word. No matter how difficult things got in personal or professional life over the last twelve years she has always been there to support me and made it easier to smile. Thank you for always being there.

Finally I want to thank my parents and my sister for all their help and support over the years.

Abstract

In response to DNA damage during S phase, cells slow DNA replication. This slowing is orchestrated by the intra-S checkpoint and involves inhibition of origin firing and reduction of replication fork speed. Slowing of replication allows for tolerance of DNA damage and suppresses genomic instability. Although the mechanisms of origin inhibition by the intra-S checkpoint are understood, major questions remain about how the checkpoint regulates replication forks: Does the checkpoint regulate the rate of fork progression? Does the checkpoint affect all forks, or only those encountering damage? Does the checkpoint facilitate the replication of polymerase-blocking lesions? To address these questions, we have analyzed the checkpoint in the fission yeast *Schizosaccharomyces pombe* using a single-molecule DNA combing assay, which allows us to unambiguously separate the contribution of origin and fork regulation towards replication slowing, and allows us to investigate the behavior of individual forks. Moreover, we have interrogated the role of forks interacting with individual sites of damage by using three damaging agents—MMS, 4NQO and bleomycin—that cause similar levels of replication slowing with very different frequency of DNA lesions. We find that the checkpoint slows replication by inhibiting origin firing, but not by decreasing fork rates. However, the checkpoint appears to facilitate replication of damaged templates, allowing forks to more quickly pass lesions. Finally, using a novel analytic approach, we rigorously identify fork stalling events in our combing data

and show that they play a previously unappreciated role in shaping replication kinetics in response to DNA damage.

Table of Contents

List of Tables

List of Figures

List of copyrighted Materials Produced by the Author

- Chapter I is mainly compiled from the following published reviews. Extra sections have been added to make it suitable for this thesis.

  - **Iyer DR**, Rhind N. The Intra-S Checkpoint Responses to DNA Damage. Genes 2017, 8(2), 74, doi:10.3390/genes8020074
  - **Iyer DR**, Rhind N. Checkpoint regulation of replication forks: global or local? Biochem Soc Trans. 2013 Dec;41(6):1701-5. doi: 10.1042/BST20130197. (License no. 4083120501429)

- Chapter II is compiled from the following methods paper which has been accepted and the manuscript, which is under review.

  - **Iyer DR**, Rhind N. Replication Fork Slowing and Stalling are Distinct, Checkpoint-Independent Consequences of Replicating Damaged DNA. (re-submitted to PLOS Genetics)
  - **Iyer DR**, Das S, Rhind N. Analysis of DNA Replication in Fission Yeast by Combing. Fission Yeast : A Laboratory Manual. Cold Spring Harb Protoc; doi:10.1101/pdb.prot092015 (in press).

- Chapter III is mostly from the following manuscript, which is under review.
  - **Iyer DR**, Rhind N. Replication Fork Slowing and Stalling are Distinct, Checkpoint-Independent Consequences of Replicating Damaged DNA. (re-submitted to PLOS Genetics)

- Chapter IV is a part of a larger study published by Stefano Santaguida et al. from Angelika Amon's lab at MIT.
  - Santaguida S, Richardson A, **Iyer DR**, M'Saad O, Zasadil L, Knouse KA, Wong YL, Rhind N, Desai A, Amon A. Chromosome mis-segregation generates cell cycle-arrested cells with complex karyotypes that are eliminated by the immune system. 10.1016/j.devcel.2017.05.022

List of Abbreviations

AT	Ataxia telangiectasia
ATM	Ataxia telangiectasia mutated
ATR	ATM and Rad3-related
ATRIP	ATR-interacting protein
BER	Base excision repair
BrdU	5-bromo-2’-deoxyuridine
CDK	Cyclin-dependent kinase
CHIP	Chromatin immunoprecipitation
Chk1	Checkpoint kinase 1
CldU	5-chloro-2’-deoxyuridine
CPT	Camptothecin
DDK	Dbf4-dependent kinase
DSB	Double strand break
dsDNA	double stranded DNA
EdU	5-ethynyl-2’-deoxyuridine
EM	Electron microscopy
FA	Fanconi anemia
hENT1	Human equilibrative nucleoside transporter 1
HR	Homologous recombination
HU	Hydroxyurea
IdU	5-iodo-2’-deoxyuridine
iPOND	Isolation of proteins on nascent DNA
IR	Ionizing radiation
MCM	Mini-chromosome maintenance
MMS	Methyl-methane sulfonate
NER	Nucleotide excision repair
NHEJ	Non-homologous end-joining
PARP1	poly (ADP-ribose) polymerase 1

PCNA	Proliferating cell nuclear antigen
PhADE	*Ph*oto*A*ctivation, *D*iffusion, *E*xcitation
pre-RC	pre-replicative complex
RNaseH	Ribonuclease H
ROS	Reactive oxygen species
RPA	Replication protein A
SAC	Spindle assembly checkpoint
ssDNA	single stranded DNA
TIRF	Total internal reflection fluorescence
tk	Herpes simplex virus thymidine kinase
TLS	Translesion synthesis
TopBP1	Topoisomerase II binding protein 1
UV	Ultra-violet
4NQO	4-nitroquinoline 1-oxide

Preface

Chapter I is compiled from two published reviews which were written by Nick Rhind and me and are published in the journals *Biochemical Society Transactions* and *Genes*.

A part of Chapter II is compiled from the methods paper, which was written by Nick Rhind and me. Shankar Das is also a contributing author in this methods paper for his efforts in initial trouble-shooting of the technique. The methods paper has been accepted at *Cold Spring Harbor Protocols*. Chapter II also contains a part of the manuscript written by Nick Rhind and me. This manuscript is currently under review at *PLOS Genetics*.

Chapter III is mainly from the manuscript written by Nick Rhind and me and is currently under review at *PLOS Genetics*.

Chapter IV is a part of a larger study carried out by Stefano Santaguida in Angelika Amon's lab at MIT. The cells were prepared by Stefano Santaguida. Sample processing, combing and analysis were performed by me. All the figures of Chapter IV were prepared by me. This work is published as a part of a larger study (Santaguida et al., 2017) in *Developmental Cell*.

Chapter I

Introduction:

Checkpoint Regulation of Forks in Response to DNA Damage

Chapter I is compiled from two published reviews which were written by Nick Rhind and me (Iyer and Rhind, 2013; Iyer and Rhind, 2017). Extra sections have been added to make it suitable for this thesis.

Why study fork regulation in response to DNA damage?

Cells slow replication in response to DNA damage during S phase. This slowing of replication in response to DNA damage has been documented for more than half a century (Ord and Stocken, 1956; Ord and Stocken, 1958; Lajtha et al., 1958; Painter, 1967). The initial hints of checkpoint regulation of replication slowing came from Ataxia Telangiectasia (AT) patients, characterized by hypersensitivity to ionizing radiation (IR). Cells from AT patients fail to slow replication in response to IR, a characteristic termed 'radio-resistant DNA synthesis' (Painter and Young, 1980; Painter, 1981; Houldsworth and Lavin, 1980; Young and Painter, 1989). AT patients suffer from severe developmental defects and are highly predisposed to developing cancer (Gatti et al., 2001; Friedberg et al., 1995).

The symptoms of AT patients highlight the importance of checkpoint regulated slowing of replication in response to damage. Later studies in *Saccharomyces cerevisiae* and *Schizosaccharomyces pombe* showed that slowing of S phase is an evolutionarily conserved mechanism in response to DNA damage (Lindsay et al., 1998; Rhind and Russell, 1998; Paulovich and Hartwell, 1995). This bulk slowing of replication is achieved through a combination of inhibition of origin firing and regulation of fork progression (Kaufmann and Cleaver, 1981; Kaufmann et al., 1980; Merrick et al., 2004; Falck et al., 2002; Santocanale and Diffley, 1998; Chastain et al., 2006; Seiler et al., 2007; Kumar and Huberman, 2009).

Several studies have hinted that regulation of forks is perhaps the most crucial function of the intra-S checkpoint and yet there seems to be no clear answer to the exact role of the checkpoint in regulating forks encountering DNA damage (Paciotti et al., 2001; Tercero et al., 2003; Tercero and Diffley, 2001; Jossen and Bermejo, 2013; Cortez, 2015). A separation-of-function checkpoint mutant in which origin regulation is disrupted, is not sensitive to DNA damaging drugs, unlike a checkpoint null allele, suggesting that fork regulation is the more crucial role of the checkpoint (Tercero et al., 2003; Paciotti et al., 2001). Although origin regulation by the checkpoint has been worked out in great details, regulation of forks by the checkpoint has remained largely elusive (Santocanale and Diffley, 1998; Shirahige et al., 1998; Kaufmann et al., 1980; Merrick et al., 2004; Falck et al., 2001; Falck et al., 2002; Chastain et al., 2006; Seiler et al., 2007; Kumar and Huberman, 2009; Luciani et al., 2004). A long-standing question in the field is whether fork progression is regulated by the checkpoint and if so, how?

To understand the regulation of forks by the checkpoint, we decided to use DNA combing, a single-molecule based technique for visualizing replication fork dynamics, to unequivocally monitor the regulation of individual forks in response to different kinds of lesions. This dissertation describes the development of sequential analog labeling in fission yeast to study the regulation of forks at single-molecule level by DNA combing (Chapter II) (Iyer et al., in press). Further, using a novel analytic approach we have identified fork stalling events in our

combing datasets (Chapter II). Using three different damaging drugs - 4NQO, MMS and bleomycin - we have studied the behavior of individual forks in response to different kinds of lesions during S phase (Chapter III). Finally we have also studied the consequences of aberrations in chromosome number on replication kinetics by combing (Chapter IV).

In this introductory chapter, I will discuss the mechanism of activation of the intra-S checkpoint, regulation of origins and forks by the checkpoint in response to DNA damage, and finally discuss the methodologies used over the years to study replication kinetics and end with the advantages of using a single-molecule approach to study the regulation of replication kinetics by the checkpoint.

1. The Intra-S Checkpoint – why, what and how?

1.1 Need for an S phase Checkpoint

"The dream of every cell is to become two cells" is the basic tenet of cell cycle, as stated by Francois Jacob in 1965 (Monod, 1971). In order to achieve this dream, cells need to faithfully duplicate their genetic material without aberrations. Genetic material is constantly subject to insults by both intrinsic and extrinsic factors such as free radicals and UV light (Zhou and Elledge, 2000; Hoeijmakers, 2009; Lindahl and Barnes, 2000). DNA damage checkpoints safeguard the genome against these insults and ensure its faithful transmission across generations. Once activated, these checkpoints block cell cycle progression and ensure that the DNA is fully repaired before allowing progression to the next

phase of the cell cycle (Hartwell and Weinert, 1989). However, even though the cell has checkpoints and repair pathways dedicated to DNA damage repair in G1, it is impossible to guarantee that cells will enter S phase with a perfect template. Further, damage could occur during S phase itself. Therefore, the cell must be prepared to encounter damaged DNA during S phase (Bartek et al., 2004; Ciccia and Elledge, 2010; Livneh et al., 2016).

1.2 Sources of Damage

1.2.1 Intrinsic Sources of Damage

Intrinsic sources of damage include reactive oxygen species (ROS) generated as a by-product of cellular metabolism, which can cause oxidative damage to DNA (Cooke et al., 2003). Other toxic metabolites include reactive aldehydes generated via alcohol metabolism, which can crosslink DNA (Burcham, 1999; Brooks and Theruvathu, 2005). Apart from toxic by-products of metabolism, ribonucleotides can pose a threat, too (Dalgaard, 2012). Despite the specificity of DNA polymerases for deoxyribonucleotides over ribonucleotides, recent studies have shown that more than 10,000 ribonucleotides may be incorporated into the *Saccharomyces cerevisiae* genome during replication and can cause genomic stress if not actively removed. In unperturbed cells, ribonucleotides are removed from the genome using a combination of ribonuclease H (RNaseH) activity and post-replication repair pathways (Nick McElhinny et al., 2010; Lazzaro et al., 2012). Replication stress can also be caused by intrinsically difficult to replicate sequences in the genome, such as G-quadruplexes and

repeats, which can lead to replication fork slippage and chromosomal breaks (Pearson et al., 2005; Valton and Prioleau, 2016; Kim and Mirkin, 2013). Another natural impediment to the replication fork is the transcriptional machinery. Collision between the replication and the transcription machinery leads to fork stalling, R-loop formation, and topological stress, which may trigger DNA damage and recombination (Bermejo et al., 2012b; Helmrich et al., 2013). Cells have active mechanisms to constrain the deleterious effects of all these aberrations, so as to curtail their impact on the genome.

1.2.2 Extrinsic Sources of Damage

Extrinsic factors that damage DNA include ultra-violet light (UV) and IR, and chemicals such as methyl-methane sulfonate (MMS), mitomycin C, cisplatin, psoralen, camptothecin (CPT), and etoposide, to list a few of the well-known DNA damaging agents. These damaging agents cause different kinds of lesions, from simple alkylation of bases by MMS, to the more complex pyrimidine dimers by UV, topoisomerase-DNA covalent complexes by CPT, and inter-strand and intra-strand crosslinks by cisplatin and psoralen (Wyatt and Pittman, 2006; Cadet et al., 2005; Liu et al., 2000a; Deans and West, 2011). Cells have evolved various pathways to specifically detect and repair different kinds of lesions. The repair pathways include base excision repair (BER), which targets modified bases, nucleotide excision repair (NER), which targets more complex modifications such as pyrimidine dimers. Inter-strand crosslinks are repaired using inter-strand crosslink repair pathway, which involves a combination of

repair pathways consisting of NER, homologous recombination (HR), translesion synthesis (TLS), and Fanconi anemia (FA) repair pathways. Finally, double strand breaks (DSB) are repaired by non-homologous end-joining (NHEJ) and HR pathways (Hoeijmakers, 2009; Ciccia and Elledge, 2010; Wyatt and Pittman, 2006; Deans and West, 2011; Lindahl and Wood, 1999; Sancar et al., 2004; Marteijn et al., 2014; Jackson, 2002; Mehta and Haber, 2014).

1.3 The Main Players of Intra-S Checkpoint

Despite having specific repair pathways dedicated to each kind of DNA lesion, the cell relies on a single checkpoint to mediate the DNA damage response during S phase. The cell has two main checkpoint kinases, Ataxia Telangiectasia Mutated (ATM) and ATM and Rad3-related (ATR), both of which are critical for maintaining genomic integrity. Of the two, ATR is the more crucial mediator of intra-S checkpoint responses since it is activated in response to diverse lesions. ATM (Tel1 in budding and fission yeast) mainly responds to double strand breaks, while ATR (Mec1 in budding yeast, Rad3 in fission yeast) is activated in response to a variety of genotoxins such as UV, MMS, hydroxyurea (HU), aphidicolin, and psoralen. ATR also functions in every unperturbed S phase, where it regulates origin firing (Shechter et al., 2004b; Syljuåsen et al., 2005; Petermann et al., 2010; Sørensen et al., 2003; Sørensen et al., 2004; Marheineke and Hyrien, 2004). Since several different pathways activate ATR in response to diverse lesions, it has been suggested that the checkpoint is activated by a common repair intermediate (Cimprich and Cortez, 2008;

Cimprich, 2007; Paulsen and Cimprich, 2007; Cortez, 2005; Flynn and Zou, 2011; Maréchal and Zou, 2013; Shechter et al., 2004a).

1.4 Detection of Lesion During S phase

The first step key to all repair pathways is the detection of the lesion itself. Detection of a lesion can be a challenge in the vast pool of undamaged template (Livneh et al., 2016; Sancar et al., 2004). Furthermore, individual damaged bases must be detected in the context of DNA complexed with protein and condensed into chromatin (Peterson and Côté, 2004). Depending on the severity of lesions, certain aberrations may be detected only during the act of replication itself. The replication fork is a sensitive detector of lesions, since it has to interact with every base in the genome during replication. Several studies have shown that lesions caused by UV and MMS activate the checkpoint only during S phase (Tercero and Diffley, 2001; Tercero et al., 2003; Lupardus et al., 2002; Stokes et al., 2002; Callegari et al., 2010; Takeda and Dutta, 2005). Studies in *S. cerevisiae* have shown that, if replication initiation is blocked using conditional alleles of initiation factors such as Cdc6, or Cdc45, or Cdc7, then cells undergo nuclear division without replicating DNA or activating the checkpoint even when treated with 0.033% MMS, demonstrating that this level of damage is not recognized outside of S phase (Tercero et al., 2003). However, during S phase, as little as 0.005% MMS is sufficient to activate the checkpoint, suggesting that the replication fork is a highly sensitive and efficient activator of the checkpoint (Tercero et al., 2003). Similarly, in *Xenopus* extracts, prevention of replication by addition of geminin

blocks checkpoint activation in response to UV and MMS induced lesions (Lupardus et al., 2002; Stokes et al., 2002). In human cells too, ATR activation in response to UV requires replication (Ward et al., 2004).

UV- and MMS-induced lesions at high concentrations can activate the DNA damage checkpoint outside S phase. Such activation relies on repair pathways such as BER in the case of MMS-induced lesions and NER in the case of UV-induced lesions to generate intermediate structures capable of activating the checkpoint (Pellicioli et al., 1999; Sidorova and Breeden, 1997; Sun et al., 1996; Marini et al., 2006; Giannattasio et al., 2010; Hanasoge and Ljungman, 2007). Thus, the checkpoint can be activated by stalled replication forks as well as intermediate structures generated by repair pathways in response to diverse lesions caused by different agents such as UV, MMS, and aphidicolin (Cimprich, 2007).

2. Intra-S Checkpoint Activation

2.1 The Structure Necessary for Checkpoint Activation

The fact that ATR is activated in response to different kinds of genotoxins suggests that the activation might occur not through recognition of damage itself but a common intermediate generated in response to any lesion that perturbs replication. Several studies indicate that the common intermediate necessary for checkpoint activation is replication protein A (RPA)–single-stranded DNA (ssDNA) complex (Longhese et al., 1996; Garvik et al., 1995; Kim and Brill, 2001; Zou and Elledge, 2003; Byun et al., 2005; Paulsen and Cimprich, 2007; Cortez,

2005). Replicative polymerases tend to stall in response to lesions while the helicase continues to unwind the DNA ahead of the lesion. Such uncoupling of the helicase and the polymerase leads to generation of ssDNA, which gets coated with the ssDNA binding protein RPA (Zou and Elledge, 2003; Byun et al., 2005; Paulsen and Cimprich, 2007; Cortez, 2005). This common intermediate comprised of stalled replicative polymerase allows for a simple mode of checkpoint activation by diverse lesions (Paulsen and Cimprich, 2007; Cortez, 2005). In the cases of double-strand breaks and inter-strand crosslinks—which do not directly produce ssDNA—lesion processing creates ssDNA, as described below.

2.2 The Factors Necessary for Checkpoint Activation

Several studies have shown that RPA coated ssDNA is essential for activation of the S-phase checkpoint kinase, ATR (Longhese et al., 1996; Zou and Elledge, 2003; Byun et al., 2005; Costanzo et al., 2003; Ball et al., 2007). ATR is a highly-conserved checkpoint kinase, which responds to various kinds of lesions that block DNA replication (Melo and Toczyski, 2002; Zeman and Cimprich, 2014). RPA bound ssDNA interacts with ATR-interacting protein (ATRIP) (Ddc2 in budding yeast, Rad26 in fission yeast), which binds ATR, leading to its recruitment to sites of DNA damage (Table 1) (Zou and Elledge, 2003; Ball et al., 2007; Paciotti et al., 2000; Rouse and Jackson, 2002).

Table 1: List of key proteins involved in intra-S checkpoint activation conserved across species

	S. cerevisiae	*S. pombe*	Mammals
Checkpoint kinase	Mec1	Rad3	ATR
	Ddc2	Rad26	ATRIP
	Rad24	Rad17	Rad17
Sensors	Ddc1	Rad9	Rad9
	Mec3	Hus1	Hus1
	Rad17	Rad1	Rad1
	Dpb11	Cut5	TopBP1
Adaptors	Mrc1	Mrc1	Claspin
	Tof1	Swi1	Tim
	Csm3	Swi3	Tipin
Effector kinase	Rad53	Cds1	Chk1

The stalled fork junction composed of ssDNA-RPA complex and dsDNA further recruits Rad17-RFC complex, which loads a trimeric ring-shaped complex Rad9-Rad1-Hus1 (9-1-1) at sites of damage, although it is unclear if Rad17-RFC recognizes the 3'ds/ssDNA junction, perhaps after polymerase release or a 5'ds/ssDNA junction, which would be created by repriming ahead of a stalled polymerase on either the leading or lagging strand (Figure 1.1) (MacDougall et al., 2007; Zou et al., 2003). 9-1-1 complex in turn recruits DNA topoisomerase II binding protein 1 (TopBP1) (Dpb11 in budding yeast, Cut5 in fission yeast), which further stimulates ATR activity (Zou et al., 2003; Bonilla et al., 2008; Kumagai et al., 2006; Navadgi-Patil and Burgers, 2009; Majka et al., 2006; Bermudez et al., 2003; Parrilla-Castellar and Karnitz, 2003; Ellison and Stillman, 2003; Mordes et al., 2008; Delacroix et al., 2007). Rad17-RCF and 9-1-1, together with regulators Claspin (Mrc1 in budding and fission yeast) and Tim/Tipin (Tof1/Csm3 in budding yeast, Swi1/Swi3 in fission yeast), are essential for activation of checkpoint kinase 1 (Chk1), which is the main target of ATR and the effector kinase in the checkpoint pathway in metazoan (Figure 1.1) (Foss, 2001; Chou and Elledge, 2006; Noguchi et al., 2003; Noguchi et al., 2004; Bartek and Lukas, 2003; Osborn and Elledge, 2003; Yoo et al., 2004; Liu et al., 2006; Yoshizawa-Sugata and Masai, 2007; Unsal-Kaçmaz et al., 2007).

Figure 1.1 Intra-S checkpoint activation

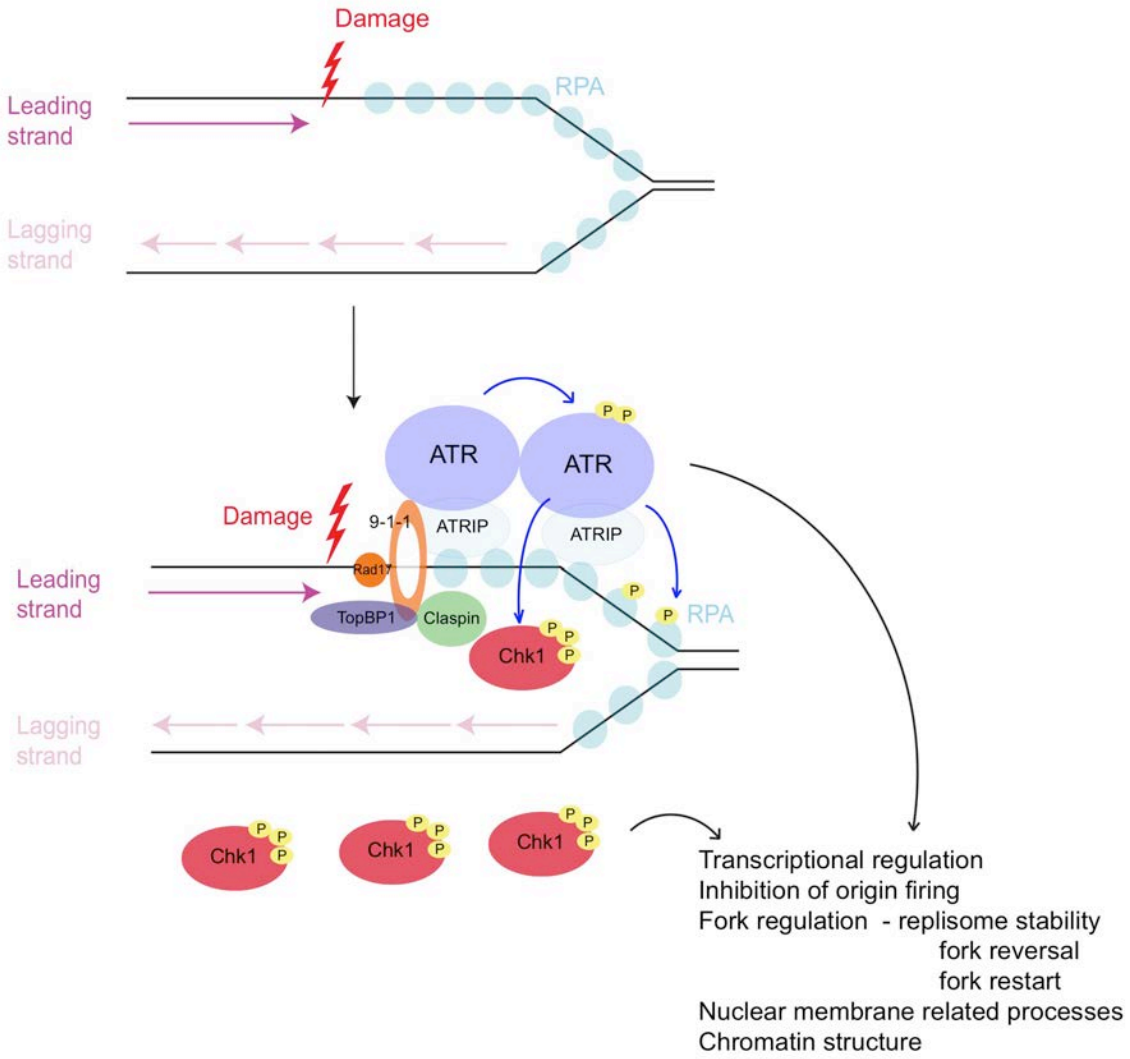

Figure 1.1 Intra-S checkpoint activation. Fig1.1 depicts how a stalled fork generates RPA-ssDNA, which subsequently recruits ATR-ATRIP, Rad17/9-1-1, TopBP1 leading to ATR activation. Rad17/9-1-1 complex further recruits adaptors like Claspin which leads to transduction of the signal to the effector kinase Chk1. Chk1 and ATR phosphorylate a wide range of substrates affecting several aspects of cellular physiology in response to damage such as transcription, replication kinetics, modulation of nuclear membrane processes and alteration of chromatin structure.

2.3 Downstream Effectors of Checkpoint Activation

ATR and ATM activate two effector kinases, Chk1 and Chk2, in response to damage to relay the checkpoint signal across the cell. In mammals, Chk1 and Chk2 play overlapping roles. Although Chk1 is primarily activated by ATR in response to various kinds of lesions and Chk2 by ATM in response to DSBs, there is substantial cross-talk between the two pathways making it difficult to unambiguously assign Chk1 and Chk2 to a single checkpoint pathway (Zhao and Piwnica-Worms, 2001; Rhind, 2009; Shiotani and Zou, 2009; Bartek and Lukas, 2001; Bartek et al., 2004; Bartek et al., 2001; Shiloh, 2001; Bartek and Lukas, 2003; Zhang and Hunter, 2014). The roles played by Chk1 and Chk2 also vary substantially across species (Rhind and Russell, 2000b). In budding and fission yeasts, Rad53 and Cds1 are homologs of mammalian Chk2, respectively. However, they are functionally equivalent to mammalian Chk1. In budding yeast Rad53 is required for the intra-S checkpoint as well as G2/M checkpoint responses, while Cds1 in fission yeast acts only during S phase (Melo and Toczyski, 2002; Sanchez et al., 1999; Lindsay et al., 1998; Rhind and Russell, 1998; Boddy and Russell, 1999).

Inter-strand crosslinks also activate ATR, even though they do not generate RPA-ssDNA in the canonical way by uncoupling helicase and the polymerase. To activate ATR, inter-strand crosslinks rely on the FA pathway. Processing of the inter-strand crosslink by the FA pathway leads to generation of ssDNA-RPA, which in turn activates ATR. Inhibition of the FA pathway using chemical inhibitor

DDN or by immunodepletion of FANCD2, greatly diminishes Chk1 activation in response to inter-strand crosslinks (Pichierri and Rosselli, 2004; Ben-Yehoyada et al., 2009).

2.4 Strength of Checkpoint Activation

Replication initiation involves melting of DNA, which produces RPA-coated ssDNA, the structure necessary for checkpoint activation. Therefore, one complication of checkpoint activation via RPA-ssDNA complex is that it is a common intermediate generated even during an unperturbed S phase. Several studies indicate that the checkpoint functions in every S phase even in the absence of damage. The importance of this function is suggested by the fact that inhibition of Chk1 during unperturbed S phase leads to unrestrained origin firing, which is detrimental to genomic stability (Shechter et al., 2004b; Syljuåsen et al., 2005; Petermann et al., 2010; Sørensen et al., 2003; Sørensen et al., 2004; Marheineke and Hyrien, 2004). The effect of the checkpoint during unperturbed replication can also be seen in *Xenopus* extracts, where the rate of replication decreases with increasing concentration of template in a checkpoint-dependent manner (Shechter et al., 2004b; Walter and Newport, 1997). Therefore, it appears that the ssDNA-RPA structures of many unperturbed replication forks are capable of collectively activating the checkpoint, even in the absence of damage.

Even though the checkpoint is activated in every S phase, there is a quantitative difference between level of activation during an unperturbed S phase and level required to be induced by DNA damage to activate a full-strength checkpoint response. The level of Chk1 activation is tightly correlated with the amount of ssDNA generated. In the presence of fork stalling lesions the helicase becomes uncoupled from the polymerase leading to generation of longer stretches of ssDNA than present in an unperturbed fork (Byun et al., 2005). The excess ssDNA-RPA complex formed in response to DNA damage leads to robust activation of the checkpoint. Titration experiments with plasmids of varying sizes in *Xenopus* extracts show that the amount of ssDNA generated determines the strength of Chk1 activation (Byun et al., 2005). Along similar lines, the number of active forks determine the activation of Rad53 in response to DNA damage in *S. cerevisiae* (Shimada et al., 2002).

Although double strand breaks primarily activate ATM, resection of their ends leads to ssDNA generation leading to subsequent activation of ATR (Shiotani and Zou, 2009; Jazayeri et al., 2006; Myers and Cortez, 2006; Adams et al., 2006; Mantiero et al., 2007; Rhind, 2009). The strength of checkpoint activation and subsequent cell cycle delay in response to DSB is regulated by both the number of DSBs generated and the amount of ssDNA generated at each DSB (Mantiero et al., 2007; Lee et al., 1998; Nakada et al., 2004). Thus, checkpoint activation can be quantitatively modulated by the amount of ssDNA generated in response to different kinds of lesions.

2.5 Downstream Targets

Unlike ATR, which mainly phosphorylates substrates on chromatin, the S-phase effector kinases transduce the signal to many targets across the cell (Bermejo et al., 2011; Bermejo et al., 2012a; Smolka et al., 2007; Randell et al., 2010; Chen et al., 2010; Rodriguez and Tsukiyama, 2013; Willis et al., 2016). Activation of Chk1 in metazoans and Rad53 and Cds1 in yeast in response to replication stress leads to regulation of replication kinetics via inhibition of origin firing and regulation of replication forks, and to transcriptional reprogramming.

3. Regulation of Replication Kinetics by the Checkpoint

3.1 Origin Regulation

3.1.1 Inhibition of Origin Firing

Replication of the genome occurs in a temporally ordered manner with different parts of the genome replicating at specific times in S phase (Rhind and Gilbert, 2013). In the presence of damage, the early origins fire regardless of the presence of lesions, since the forks established by early origins are the ones, which sense the lesions and activate the checkpoint. Once the checkpoint is activated, it suppresses firing of late origins (Santocanale and Diffley, 1998; Shirahige et al., 1998; Kaufmann et al., 1980; Merrick et al., 2004; Falck et al., 2001; Falck et al., 2002; Chastain et al., 2006; Seiler et al., 2007; Kumar and Huberman, 2009; Luciani et al., 2004). In *S. cerevisiae*, Rad53 phosphorylates the origin activation factors Sld3 and Dbf4 in response to replication stress to

prevent subsequent origin firing (Lopez-Mosqueda et al., 2010; Zegerman and Diffley, 2010). Sld3 is a replication-fork assembly factor required during early steps of replication initiation; Dbf4 is the regulatory subunit of Dbf4-dependent kinase (DDK), which is required for origin firing and fork progression (Kamimura et al., 2001; Kanemaki and Labib, 2006; Jackson et al., 1993). In mammals, Chk1 targets multiple substrates to block origin firing. In response to IR, Chk1 phosphorylates Cdc25A, targeting it for ubiquitin-mediated degradation. Cdc25A is a phosphatase necessary for Cdk2-CyclinE activity, which is required for binding of Cdc45 to the pre-replicative complex (pre-RC) and initiating replication (Sørensen et al., 2003; Falck et al., 2001). Chk1 also phosphorylates Treslin, the metazoan homolog of Sld3, to prevent loading of Cdc45 onto chromatin (Guo et al., 2015). Further studies in *Xenopus* and mammalian cells suggest that Chk1 also targets DDK in response to UVC and etoposide treatments (Costanzo et al., 2003; Heffernan et al., 2007; Matsuoka et al., 2007). Inhibition of origin firing prevents new forks from encountering damage and stalling. Although reduction in origin firing leads to slowing of replication, it does not significantly contribute to maintenance of cell viability, at least not in *S. cerevisiae* (Tercero et al., 2003).

3.1.2 Activation of Dormant Origins

Although checkpoint activation inhibits origin firing globally, several reports suggest that it might allow dormant origins to fire locally in response to replication stress (Yekezare et al., 2013; McIntosh and Blow, 2012). Cells license origins during G1 phase of the cell cycle and activate them throughout S phase (Blow

and Dutta, 2005; Diffley, 2011; Masai et al., 2010; Tanaka and Araki, 2011). In an unperturbed S phase, a cell fires only about 10% of its licensed origins. Most of the remaining origins are licensed but not fired and hence referred to as dormant origins. During unperturbed replication, dormant origins are passively replicated. However, in the event of replication stress, forks from early origins stall and the dormant origins remain un-replicated. Under such conditions, the dormant origins fire and help complete replication in the vicinity of stalled forks and thereby mitigate the consequences of fork stalling. Reduction of dormant origin firing via depletion of mini-chromosome maintenance (MCM) complex makes the cell hypersensitive to replication perturbation, highlighting the importance of dormant origins (Ge and Blow, 2010; Ge et al., 2007; Woodward et al., 2006; Anglana et al., 2003). At this point, it is unclear how the checkpoint could suppress origin firing globally but permit activation of dormant origins in response to replication stress. A possible explanation is that the checkpoint reduces origin firing globally, but that even so dormant origin firing increases due to the reduction in passive replication or that the dormant origins fire before the checkpoint is fully activated and thus escape inhibition (Yekezare et al., 2013; McIntosh and Blow, 2012).

3.2 Fork regulation

3.2.1 Importance of fork regulation

Several studies suggest that the regulation of replication forks in response to replication stress is the crucial function of the intra-S checkpoint. The first hint of the importance of fork regulation came from the discovery of a separation of

function mutant in budding yeast called *mec1-100* (Paciotti et al., 2001). *mec1-100* cells cannot suppress origin firing in response to stress, but are not hypersensitive to MMS, unlike *mec1*Δ cells (Tercero et al., 2003; Paciotti et al., 2001). Presumably fork regulation is intact in *mec1-100*, hinting that fork regulation is more critical for cell viability in response to MMS than origin firing inhibition. Consistent with this conclusion, Tercero et al. have shown that forks progress slowly but stably in *mec1-100* to complete replication in response to MMS (Tercero et al., 2003). In contrast, in *mec1*Δ and *rad53*Δ cells treated with HU or MMS, forks collapse irreversibly leading to large stretches of un-replicated DNA (Tercero and Diffley, 2001; Lopes et al., 2001). Experiments in which Rad53 expression is suppressed during HU treatment but induced after release from HU arrest show that the checkpoint is necessary at the time of fork stalling to maintain the replication fork in a restart competent manner. Expression of Rad53 after release from HU arrest is not sufficient to maintain viability (Tercero et al., 2003). Along similar lines in mammals, *ATR-/-* and *CHK1-/-* are embryonic lethal in mice and inactivation of ATR during replication stress greatly hampers fork progression and cell viability (Couch et al., 2013; Brown and Baltimore, 2000; Liu et al., 2000b). Collectively, these studies suggest that the checkpoint is essential for preventing fork collapse in response to replication stress. The mechanism by which the checkpoint accomplishes fork stabilization and maintains cell viability is not understood.

3.2.2 Regulation of Fork Speed

A consistent observation is that forks slow in response to DNA damage (Tercero and Diffley, 2001; Szyjka et al., 2008; Unsal-Kaçmaz et al., 2007; Seiler et al., 2007; Conti et al., 2007). Whether slowing of forks in the presence of damage is checkpoint-dependent or simply due to the physical presence of lesions is not clear (Tercero and Diffley, 2001; Szyjka et al., 2008; Unsal-Kaçmaz et al., 2007; Seiler et al., 2007; Conti et al., 2007). Initial work in budding yeast showed that replication forks in checkpoint mutant and wild-type cells were slowed to the same extent in the presence of damage, suggesting that slowing is checkpoint-independent (Tercero and Diffley, 2001). However, subsequent work showed that checkpoint activation inhibited replication of damaged DNA, suggesting an active role in the slowing of replication forks (Szyjka et al., 2008). Furthermore, work in mammalian cells showed a role for checkpoint signaling in DNA-damage-dependent slowing of replication forks (Unsal-Kaçmaz et al., 2007; Seiler et al., 2007; Conti et al., 2007). Thus, so far it is unclear whether the checkpoint regulates the progression of forks through the damaged template or not.

3.2.3 Regulation of Number of Forks

In response to replication stress, suppression of late firing origins limits the generation of an excess number of stalled forks. Unrestrained firing of origins in the presence of replication stress might overwhelm the capacity of the checkpoint to attenuate the consequences of stalled forks. Supporting this idea, Toledo et al. observed that in the absence of ATR activity, excess firing of origins in response to HU depletes the nuclear pool of RPA leading to DSB generation (Toledo et al.,

2013). Therefore, the critical role of the checkpoint may not be to regulate the fork per se but to curtail origin firing in response to replication stress so as to avoid generation of an excess number of stalled forks. However, it is yet to be determined whether replication forks from ATR inhibited cells supplemented with excess RPA are capable of stably progressing and completing replication when released from HU arrest. Furthermore, HU treatment in the absence of a checkpoint leads to excessive unwinding and generation of longer stretches of ssDNA as compared to cells in which the checkpoint activity is intact (Sogo et al., 2002). Therefore, RPA may have a more critical role under excessive unwinding, as seen in checkpoint mutants, than in wild-type cells.

3.2.4 Maintenance of Replisome Stability

The most controversial role of the checkpoint at stalled forks is the maintenance of replisome stability (Jossen and Bermejo, 2013; Cortez, 2015). Replisome stability refers to the physical association of the replisome factors with the stalled replication fork (Figure 1.2.a). Several chromatin immuno-precipitation (ChIP) studies done in budding yeast have suggested that, in response to HU, polymerases and helicases tend to dissociate from the stalled fork in the absence of an active checkpoint (Cobb et al., 2003; Cobb et al., 2005; Cotta-Ramusino et al., 2005; Lucca et al., 2004; Naylor et al., 2009). Similarly, studies in *Xenopus* and mammalian cells have shown that several components of the replisome are lost from forks stalled in response to prolonged treatment with aphidicolin in the absence of ATR (Trenz et al., 2006; Ragland et al., 2013;

Hashimoto et al., 2011). However, contrary to these studies, De Piccoli et al. have shown—using genome-wide ChIP-seq—that the replisome components remain stably associated with forks stalled in HU even in the absence of Rad53 or Mec1 in budding yeast (De Piccoli et al., 2012). Perhaps the discrepancy between these reports can be explained by the differences between their ChIP assays. The former focused on early origins with ChIP PCR probes designed at close proximity to the early origins as opposed to genome-wide ChIP-seq by the latter, which gives a more comprehensive picture. The latter work shows that, in the absence of checkpoint, forks from early origins continue to replicate longer and hence stall replisome components further downstream than they would in wild-type cells. Thus, by ChIP-PCR with probes designed at close proximity to the early origins, the replisome components appear to be intact in wild-type and depleted in the checkpoint mutant (De Piccoli et al., 2012). However, at this point, it remains a matter of debate whether the checkpoint affects the physical association of the replisome components or only regulates their functionality in response to replication stress (Cortez, 2015).

Most studies trying to understand the role of checkpoint in maintaining replisome stability have focused on forks stalled for a prolonged duration (20 to 60 min) in response to HU arrest. Stalling forks in the order of tens of minutes in response to HU might be biologically very different than fork pausing briefly in response to MMS-induced lesions. It is not clear whether stability of the replisome components is affected if the fork stalls are short-lived as compared to

that in a HU arrest. Therefore, the mechanism by which Rad53 allows the forks to progress slowly but stably and complete replication of the whole genome in response to MMS remains unclear.

Figure 1.2 Regulation of forks in response to damage

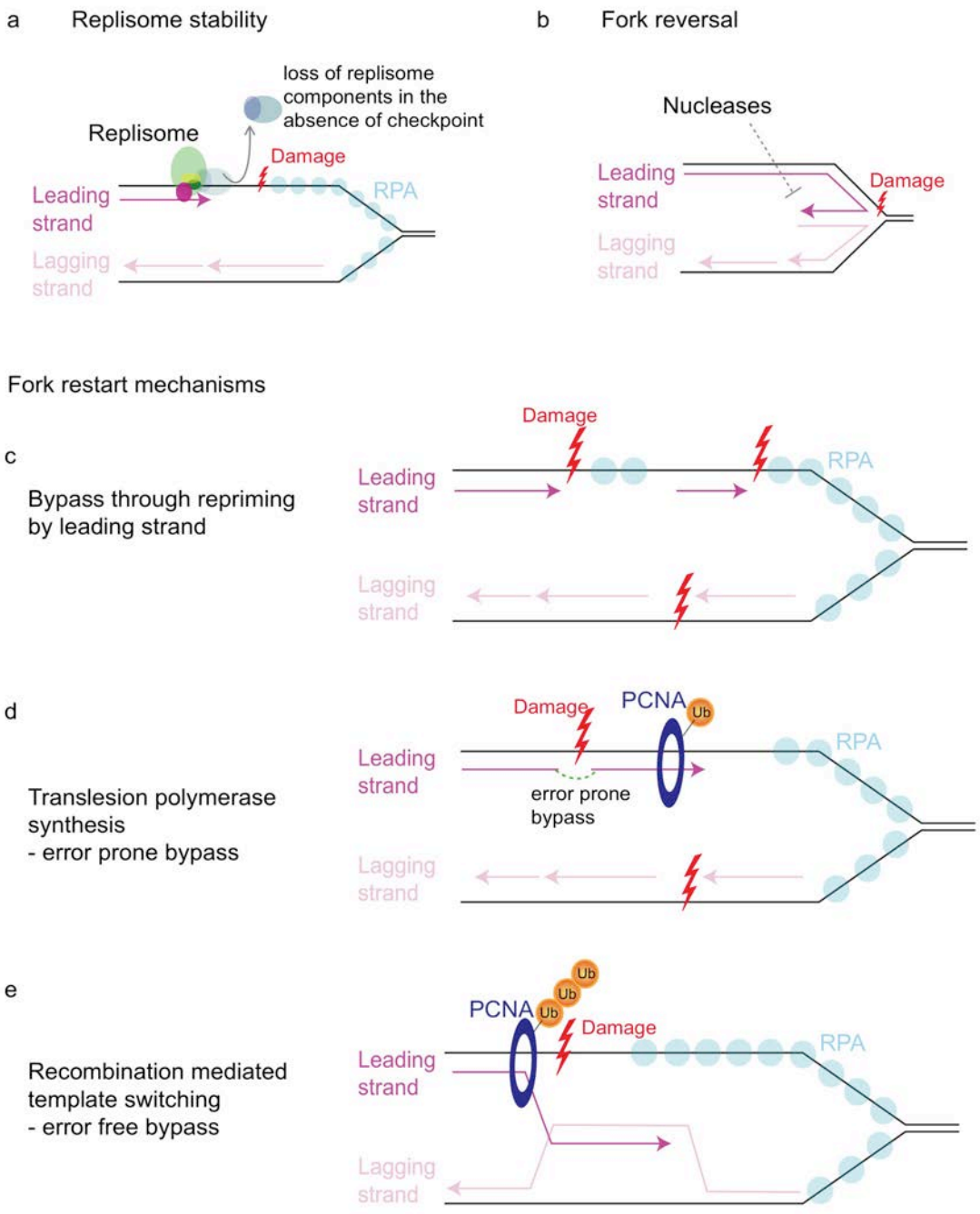

Figure 1.2 Regulation of forks in response to damage. (a) Replisome stability pertains to stable association of replisome components; (b) Fork reversal in response to damage, wherein the leading strand anneals with the lagging strand to form a four-way structure. Fork reversal is opposed by nucleases such as Exo1, Dna2; (c) Downstream repriming. Leading strand can bypass damage by repriming downstream of the stalled fork; (d) Translesion polymerase based synthesis. A stalled fork can bypass damage by recruiting translesion ploymerase in an error prone manner. Recruitment of translesion polymerase requires mono-ubiquitination of PCNA; (e) Template switching. A stalled fork can bypass damage by using the lagging strand as a template instead of the damaged parental strand. Template switching requires poly-ubiquitination of PCNA.

3.2.5 Fork Reversal

Regardless of whether the checkpoint affects replisome stability or not, it prevents accumulation of pathological structures at stalled replication forks. *rad53* mutants accumulate structures similar to those obtained by destabilizing replisome components as monitored by 2D gels (Lopes et al., 2001). Similarly, electron microscopy (EM) studies have shown that HU treatment of *rad53*Δ cells leads to excessive unwinding and generation of longer stretches of ssDNA as compared to wild-type cells (Sogo et al., 2002). Furthermore, *rad53*Δ cells accumulate reversed forks wherein the leading strand is unwound and anneals with the lagging strand to form a four-way structure (Figure 1.2.b) (Sogo et al., 2002; Cotta-Ramusino et al., 2005). Whether reversed forks are a pathological structure or productive repair intermediates is uncertain. In yeast, fork reversal is mainly observed in the absence of checkpoint and therefore appears to be pathological. However, in metazoans, fork reversal appears to be a part of DNA damage tolerance mechanism (Neelsen and Lopes, 2015). Chaudhuri et al. have shown that in mammalian cells, *Xenopus* extracts, and yeast cells, low doses of CPT treatment lead to fork reversal. In mammals, reversal of forks is mediated by poly (ADP-ribose) polymerase 1 (PARP1) (Ray Chaudhuri et al., 2012). Depletion of PARP1 prevents fork reversal and leads to double strand break formation (Ray Chaudhuri et al., 2012). Furthermore, Rad51 dependent fork reversal is seen in human cells in response to a variety of genotoxins (Zellweger et al., 2015). Thus, in mammals, fork reversal appears to

play a protective role. However, in the absence of checkpoint, nucleases such as Mus81 and Slx4 can improperly process reversed forks leading to genomic instability (Couch et al., 2013; Neelsen et al., 2013; Froget et al., 2008). Thus, fork reversal itself may not be pathological, but its regulation by the checkpoint may prevent deleterious outcomes. *In vitro* biochemical studies have identified several helicases and translocases such as Rad54, WRN, BLM, HLTF, FANCM, FBH1, SMARCAL1, and ZRANB3 capable of regressing forks (Bugreev et al., 2011; Bétous et al., 2012; Bétous et al., 2013; Yusufzai and Kadonaga, 2008; Yusufzai and Kadonaga, 2010; Gari et al., 2008; Ciccia et al., 2012; Blastyák et al., 2007; Blastyák et al., 2010; Kile et al., 2015; Fugger et al., 2015; Machwe et al., 2006; Machwe et al., 2011). However, of all these factors, only Rad51 and FBH1 have been shown to be required for fork regression *in vivo* (Zellweger et al., 2015; Fugger et al., 2015). Furthermore, how helicases and translocases may be regulated by the checkpoint at stalled forks is not known.

3.2.6 Regulation of Nucleases

There is mounting evidence that the checkpoint plays a role in protecting forks from aberrant activity of nucleases. Support for this idea comes from Segurado and Diffley, who show that deletion of *EXO1* rescues *rad53*Δ sensitivity to the genotoxins UV, MMS, and IR, although not HU (Segurado and Diffley, 2008). Phospho-proteomic screens have also identified Exo1 as a target of Rad53 and this phosphorylation has been shown to negatively regulate Exo1's activity (Smolka et al., 2007; Morin et al., 2008). Furthermore, EM studies in budding

yeast have shown that Exo1 creates ssDNA intermediates of reversed forks and drives fork collapse in the absence of Rad53 (Cotta-Ramusino et al., 2005). However, deletion of *EXO1* alone is not sufficient for fork stabilization. Forks are unable to restart when released from HU arrest even in a *rad53*Δ*exo1*Δ background, as is the case for *rad53*Δ cells (Segurado and Diffley, 2008). Thus, Rad53 has Exo1-independent functions at maintaining fork integrity.

In fission yeast, Cds1 phosphorylates and activates Dna2, a helicase/nuclease, which prevents accumulation of reversed forks (Hu et al., 2012). In human cells, DNA2 is involved in the processing and restart of reversed forks (Thangavel et al., 2015; Duxin et al., 2012). These observations further support the notion that the checkpoint modulates fork reversal by activating or inhibiting nucleases.

3.2.7 Restart of Stalled Forks

The ultimate question of how the checkpoint restores progression of stalled forks is just being uncovered. As mentioned above, stalled forks can undergo fork reversal even in the presence of checkpoint. In human cells, reversed forks are restarted in a RECQ1 and DNA2 dependent manner (Thangavel et al., 2015; Berti et al., 2013). Mus81-Eme1, a structure specific endonuclease, is normally active only during mitosis due to the requirement of phosphorylation by CDK1 and Polo-like kinase 1 (Plk1) for activation (Matos et al., 2011; Matos et al., 2013;

Szakal and Branzei, 2013). However, several recent studies suggest that Mus81 could also play a role in fork restart mechanisms during S phase by creating double strand breaks and promoting recombination (Dehé et al., 2013; Pepe and West, 2014b; Whitby et al., 2003; Pepe and West, 2014a; Amangyeld et al., 2014; Shimura et al., 2008; Regairaz et al., 2011; Fugger et al., 2013; Hanada et al., 2007). In human cells, fork cleavage and restart of stalled forks in S phase is governed by Mus81-Eme2, while the G2/M functions of Mus81 are guided by Mus81-Eme1 complex (Pepe and West, 2014b; Pepe and West, 2014a; Amangyeld et al., 2014). SMARCAL1 may also be an important candidate, as it possesses both fork reversal as well as fork restoration activities, and is regulated by ATR (Couch et al., 2013; Bétous et al., 2012; Bétous et al., 2013). However, its exact function at stalled forks *in vivo* is yet to be determined.

In the case of stalled forks that have not reversed, restart or restoration of fork progression occurs mainly in three ways: by repriming (Figure 1.2.c), by translesion-polymerase-based synthesis (TLS) (Figure 1.2.d), or by template switching (Figure 1.2.e) (Branzei and Szakal, 2016; Branzei and Foiani, 2007; Branzei and Foiani, 2009; Ulrich and Walden, 2010; García-Rodríguez et al., 2016; Sale, 2012; Ulrich, 2009). Lesions on the lagging strand can be easily bypassed due to the discontinuous nature of lagging-strand synthesis. However, lesions on the leading strand must be actively bypassed using various mechanisms in order to continue DNA synthesis. The first evidence that lesion bypass via repriming downstream could be employed in the case of leading

strand comes from studies done in bacteria. Bacterial replisomes are capable of repriming and re-initiating replication in response to UV-induced lesions (Figure 1.2.c) (Heller and Marians, 2006; Yeeles and Marians, 2011). Recent discovery of similar activity by PrimPol in human cells shows that repriming downstream may be an evolutionarily widespread approach. PrimPol, which has primase as well as translesion polymerase activity, allows repriming of stalled forks in response to UV as well as dNTP depletion (Bianchi et al., 2013; Mourón et al., 2013; Helleday, 2013). Furthermore, EM studies suggest that repriming activities on leading strand in response to UV occurs in budding yeast, too, although it must be via a distinct mechanism, because PrimPol is not conserved in yeast (Lopes et al., 2006; Rudd et al., 2014).

The TLS and template switching mechanisms of fork restart are regulated by ubiquitination of the proliferating cell nuclear antigen (PCNA) (Hoege et al., 2002; Frampton et al., 2006; Lee and Myung, 2008). ssDNA generated in response to replication stress recruits Rad18, which, along with Rad6, monoubiquitinates PCNA at K164 (Hoege et al., 2002; Davies et al., 2008). Monubiquitination of PCNA allows recruitment of translesion polymerases, which have low fidelity, allowing the fork to replicate across damaged bases (Figure 1.2.d) (Kannouche et al., 2004; Watanabe et al., 2004; Stelter and Ulrich, 2003). Although translesion polymerases permit replication across damaged template, the bypass occurs in an error prone manner. PCNA can also be polyubiquitinated at K164 by Rad5 along with Mms-Ubc13 (Hoege et al., 2002; Ulrich and Jentsch, 2000;

Parker and Ulrich, 2009). Polyubiquitination of PCNA promotes template switching (Figure 1.2.e) (Zhang and Lawrence, 2005; Hishida et al., 2009; Branzei et al., 2004; Chiu et al., 2006). Template switching involves usage of the undamaged sister chromatid for bypass of lesions and usually occurs in an error free manner. Inhibition of polyubiquitination increases TLS-based mutations suggesting competition between TLS and template switching pathways (Chiu et al., 2006). SUMOylation at K164 of PCNA also affects template switching (Papouli et al., 2005; Pfander et al., 2005; Branzei et al., 2008). The exact role of polyubiquitination of PCNA and how it leads to recruitment of the recombination factors necessary for template switching are not known (Branzei and Szakal, 2016; Ulrich and Walden, 2010; Lee and Myung, 2008; Moldovan et al., 2007). Regulation and crosstalk between various modifications on PCNA and the role of checkpoint in mediating lesion bypass are also poorly understood. Furthermore, PCNA functions as a tri-mer at the replication fork. Therefore, at a single stalled fork, individual copies of PCNA may harbor different modifications and the tri-mer collectively may regulate the mechanism of lesion bypass (Branzei and Szakal, 2016; Ulrich and Walden, 2010; Sale, 2012; Moldovan et al., 2007).

4. Tools to look at replication kinetics

4.1 Bulk methods used to study replication kinetics in response to damage

Some of the earliest methods looking at slowing of replication in response to irradiation involved measuring ^{32}P, ^{14}C or ^{3}H incorporation rates into DNA (Ord

and Stocken, 1956; Ord and Stocken, 1958; Lajtha et al., 1958; Painter, 1967). At the time, the program of replication was not known and thus the net effect on replication rate via scintillation counting was the only way to study the effect of damage on DNA replication rate.

4.1.1 Flow Cytometry – a rapid approach to look at slowing of replication

A more rapid method to look at net slowing of replication in a large population of cell was made feasible with the development of flow cytometry to analyze DNA content and thereby define the distribution of cells across different phases of cell cycle (Holm and Cram, 1973; Imray and Kidson, 1983). Eventually slowing of DNA replication was characterized by flow cytometry in mammalian cells, budding and fission yeasts (Lavin et al., 1989; Lindsay et al., 1998; Rhind and Russell, 1998; Paulovich and Hartwell, 1995}.

By 1960's the mechanism of eukaryotic replication was beginning to be understood. Some of the key discoveries on the mechanism of replication, which were critical for understanding the regulation of replication kinetics was that the mammalian DNA was organized in the form of "long fibers" and the fibers replicated in "fork-like growing points" (Cairns, 1966; Huberman and Riggs, 1966; Sasaki and Norman, 1966). Furthermore these "fork-like growing points" originated at several sections on the fiber and the pairs of them tended to move in opposite directions (Huberman and Riggs, 1968). Thus with the discovery of the mechanism of replication it became important to understand how origins and forks are regulated in response to damage.

4.1.2 Density gradient centrifugation distinguishes between effects on initiation v. elongation rates

Initial studies aimed at understanding the regulation of origins and forks involved labeling cells with ^{3}H-thymidine and separating the newly replicated fragments of DNA by alkaline sucrose density gradient centrifugation. Several studies initially found that irradiation only led to repression of initiation of replication (Walters and Hildebrand, 1975; Painter and Young, 1975; Makino and Okada, 1975; Painter and Young, 1976; Dahle et al., 1979). However later studies using higher doses of irradiation found that initiation of replication as well as chain elongation (fork speed), both were affected. In conclusion, initiation of replication was highly sensitive to inhibition even at low doses, while fork rates were affected only at high doses of damage (Watanabe, 1974; Makino and Okada, 1974; Cleaver et al., 1983; Painter and Young, 1980; Painter, 1981; Young and Painter, 1989).

4.1.3 2D-gels – studying the effect of damage one origin at a time

Once again advances in the understanding of replication program generated further questions about the regulation of replication in response to damage. Specifically it was realized that replication of the genome occurs in a temporal manner (Hatton et al., 1988; McCarroll and Fangman, 1988; Fangman et al., 1983; Fangman and Brewer, 1992; Reynolds et al., 1989). Studies were carried out to understand how the intra-S checkpoint regulates the temporal program of origin firing. 2D-gels were employed to study specific loci in the genome to understand the impact of damage-induced checkpoint activity on origin firing

(Larner et al., 1994). By late 1990's several origins of replication were mapped in *S. cerevisiae* along with their replication timings. This knowledge allowed a systematic comparison of the checkpoint effects on early v. late-firing origins. It was discovered that the checkpoint preferentially inhibited the late-firing origins in response to DNA damage (Santocanale and Diffley, 1998; Shirahige et al., 1998).

4.2 Why use single-molecule approach to study replication kinetics?

Caveats of bulk methods

Labeling cells with ^{3}H and separating newly synthesized DNA by density gradient centrifugation allows one to compare the effect of damage on initiation v. elongation rates. A reduction in origin firing rate is inferred from the absence of small fragments in the irradiated sample (Walters and Hildebrand, 1975; Painter and Young, 1975; Makino and Okada, 1975; Painter and Young, 1976; Dahle et al., 1979; Painter and Young, 1980). However absence of small fragments could be due to two reasons – reduction in origin firing rate or reduction in cells entering S phase. Using synchronized cultures a later study found that loss of small fragments was a combination of cells arresting in G1 phase as well as inhibition of origin firing in cells already in S phase (Lee et al., 1997). Thus density gradient results in isolation cannot give the complete picture.

2D-gels can be employed to distinguish between the effects on origins and forks in response to damage, however the analysis is limited to one origin at a time and is suitable for only defined and highly efficient origins. Studies over the

last decade have highlighted that although distinct domains of the genome replicate at defined times during S phase, the replication of each domain itself is achieved using a different cohort of origins in each cell (Lebofsky et al., 2006; Cayrou et al., 2011; Hamlin et al., 2008; Bechhoefer and Rhind, 2012; Farkash-Amar et al., 2008; Ryba et al., 2010; Yaffe et al., 2010; Xu et al., 2012; Dileep et al., 2015). This cell-to-cell variability in the usage of origin is due to the presence of inefficient origins, which fail to fire in every cell cycle (Patel et al., 2006; Czajkowsky et al., 2008; Hawkins et al., 2013). Particularly higher organisms tend to have many inefficient origins making 2D-gels an intractable approach to study the effects of DNA damage on origin regulation (Lebofsky et al., 2006; Cayrou et al., 2011; Hamlin et al., 2008; Bechhoefer and Rhind, 2012; Farkash-Amar et al., 2008; Ryba et al., 2010; Yaffe et al., 2010; Xu et al., 2012; Hamlin et al., 2008; Rhind and Gilbert, 2013; Dileep et al., 2015).

4.3 Single-molecule approaches

4.3.1 DNA fiber autoradiography

DNA fiber autoradiography was the first single-molecule method, applied to DNA replication, which allowed several seminal discoveries to be made. Replicating cells were first labeled with ^{3}H-thymidine, and then chased with ^{3}H-thymidine of higher activity or with cold thymidine. After labeling, cells were lysed and DNA fibers were spread on a surface and autoradiographed. The replicated DNA is observed as silver grains on an autoradiogram. Since the cells are first labeled

with ^{3}H-thymidine, followed by cold or ^{3}H-thymidine of a different activity, the direction of replication could be ascertained (Hand, 1975; Liapunova, 1994). This technique led to the discovery of the bi-directional movement of forks in *Escherichia coli* (Cairns, 1963; Masters and Broda, 1971; Prescott and Kuempel, 1972). Later this technique was employed by Huberman and Riggs to discover that in mammalian cells the DNA fiber replicates by initiating replication at several loci called origins and the forks from each origin move in a bi-directionally opposite manner (Huberman and Riggs, 1968). Further since the length of the tracks could be estimated and divided by the length of the labeling period, the approach allowed for a quantitative estimation of parameters such as fork rate as well as distances between origins. DNA fiber autoradiography studies by Watanbe in 1974 provided the first direct proof that chain elongation (fork rate) is affected at high doses of irradiation (Watanabe, 1974).

Despite the wealth of knowledge gained from DNA fiber autoradiography the technique had several limitations (Liapunova, 1994). The resolution was limited by the size and continuity of the silver grains. Moreover only the replicated regions could be visualized by autoradiography while the un-replicated regions had to be guessed. The size of the replicated regions could be vastly overestimated due to merging of tracks or bundling of fibers. Further the stretching of the DNA fibers was very unpredictable. Therefore a quantitative estimation of replicated regions was difficult. It was also difficult to isolate long

fibers reproducibly. Finally the exposure times were often in the order of several months making the whole process very time consuming.

4.3.2 DNA Combing

Several issues with fiber autoradiography were overcome with the development of fluorescence fiber techniques. Briefly cells are lysed on glass slides and the DNA fibers are stretched by the flow of the buffer across a tilted slide. Fibers are visualized by hybridizing fluorescently labeled probes complementary to specific regions in the genome (Parra and Windle, 1993). Fluorescence fiber studies of replication were first enabled with the development of antibodies specific to thymidine analogs such as 5-bromo-2'-deoxyuridine (BrdU) (Gratzner, 1982). Development of specific antibodies towards two different thymidine analogs, 5-chloro-2'-deoxyuridine and 5-iodo-2'-deoxyuridine made it possible to study the temporal dynamics of replication (Aten et al., 1992). However a major drawback was still the lack of reproducibility of stretched fibers. These difficulties were overcome with the invention of dynamic molecular combing (Bensimon et al., 1994; Allemand et al., 1997; Michalet et al., 1997).

In combing, a silanized coverslip is dipped into a DNA solution and slowly withdrawn at constant rate to get reproducibly high density of uniformly stretched (1 μm ≈ 2 kb), linear, single molecules of DNA. The high density of molecules permits statistical sampling of parameters. The technique has been employed to study replication kinetics, map genes, detect micro-deletions or amplifications, as

well as rearrangements such as inversions, and translocations (Herrick et al., 2000; Lebofsky and Bensimon, 2003; Herrick and Bensimon, 1999a; Herrick and Bensimon, 1999b; Herrick and Bensimon, 2009).

Studying perturbations of replication kinetics by DNA combing has several advantages (Herrick and Bensimon, 1999a). Combing allows for detection of individual origins and forks on a global scale (Jackson and Pombo, 1998; Iyer et al., in press; Gallo et al., 2016a; Gallo et al., 2016b; Bianco et al., 2012). Briefly cells are labeled in vivo with thymidine analogs and DNA is isolated, combed and immuno-stained with antibodies against the thymidine analogs. Sequential labeling with two different analogs allows for determination of the direction and speed of replication of labeled tracks on a fiber(Jackson and Pombo, 1998; Iyer et al., in press). Further, combing can be supplemented with FISH to study specific regions of interest. Because combing reveals the behavior of individual replication origins and forks, it allows for unambiguous study of the effect of checkpoint on origin firing and fork rates. In particular, it allows one to measure the heterogeneity of fork rates and determine if all forks respond the same way to lesions. The importance of measuring the heterogeneity of fork rates can be illustrated in a case where some forks pass lesions without slowing, but others stop at the lesion and do not resume replication for the duration of the experiment, a condition we refer to as fork stalling (Chapter II and III).

Finally using combing we can distinguish whether the regulation of forks is a global or local effect. A fundamental question about the regulation of fork

progression in response to DNA damage is whether it is a global or local effect (Iyer and Rhind, 2013). The effect of checkpoint on origins is inherently a global response because origins distant to sites of damage are blocked from firing. However slowing of forks could be a local or a global effect. If all forks are slowed by checkpoint activation, irrespective of whether they encounter damage or not, then slowing is a global effect. On the other hand, if forks are slowed only when they encounter a lesion, then it is a local effect (Iyer and Rhind, 2013). Analysis of individual forks by combing should allow us to decipher whether fork regulation by checkpoint is global or local.

Conclusion

In conclusion, studying regulation of forks is critical to understand how the intra-S checkpoint contributes to maintenance of genomic stability. Important insight into the role of fork regulation comes from EM studies, which have helped us uncover the structural alterations observed at stalled forks, and from *in vitro* biochemical studies with fork components and artificial templates, which have allowed us to decipher their catalytic functions. However, how the fate of a stalled fork is determined by the interplay of various factors *in vivo* is unclear. Specifically how the checkpoint regulates the various factors to mediate stable progression of forks through a damaged template is unknown. Thus, to understand the regulation of individual forks on a global scale by the checkpoint at single-molecule level we have used DNA combing (Chapter II and III). Specifically we have studied the behavior of forks in response to three different DNA damaging

drugs and the role of checkpoint in regulating the fork responses as discussed in greater detail in Chapter III.

Chapter II

Materials and Methods:

Analysis of DNA Replication in Fission Yeast by Combing

A part of Chapter II is compiled from the methods paper, which was written by Nick Rhind and me. Shankar Das is also a contributing author in this methods paper for his efforts in initial trouble-shooting of the technique. The methods paper has been accepted at *Cold Spring Harbor Protocols* (Iyer et al., in press). Chapter II also contains a part of the manuscript written by Nick Rhind and me. This manuscript is currently under review at *PLOS Genetics* (Iyer and Rhind).

Introduction

DNA replication studies based on population experiments give an average estimate of replication kinetics from many cells. This average replication profile masks the stochastic nature of origin firing in eukaryotes, which is revealed by using single-molecule techniques, such as DNA combing. The analysis of replication kinetics by DNA combing involves isolating DNA from cells that have been pulse-labeled with thymidine analogs and stretching it on a silanized coverslip. The analog-labeled patches on the stretched DNA fibers can then be detected using fluorescent antibodies against the analog. Each fiber represents a part of the genome from a single cell; therefore, it is possible to study the variation in behavior of individual origins and forks from one cell to another. Furthermore, each DNA fiber is uniformly stretched, making it possible to measure distances accurately at kilobase resolution. It is also possible to stretch a high density of fibers on coverslips allowing for statistical sampling of replication parameters.

In order to study the effect of DNA damage on replication kinetics at single molecule level, we implemented a sequential analog labeling approach in fission yeast. Sequential analog labeling is necessary to ascertain the directionality of replication and thus distinguish between origins and forks. This chapter describes in detail the protocol developed for sequential analog labeling in fission yeast during S phase. Further it describes an in-depth analysis of every permutation of replication pattern observed in a tri-color combing dataset. Finally using a novel

analytic approach we have developed a probabilistic approach to rigorously determine the rate of fork stalling in a tri-color combing dataset.

1. General methods

All experiments were done in fission yeast. Uptake of the thymidine-analog label requires yeast cells integrated with human equilibrative nucleoside transporter 1 (hENT1) and herpes simplex virus thymidine kinase (tk) (Hodson et al., 2003; Sivakumar et al., 2004). hENT1 is a nucleoside transporter that allows uptake of exogenous nucleosides into cell and tk phosphorylates them so that it can be incorporated into DNA (Griffiths et al., 1997; Lengronne et al., 2001; McNeil and Friesen, 1981; Vernis et al., 2003). The following strain used in this study was created by standard methods and grown in YES at 25°C (Forsburg and Rhind, 2006): yFS940 (*h+ leu-32 ura4-D18 his7-366 cdc10-M17 leu1::pFS181 (leu1 adh1:hENT1) pJL218 (his7 adh1:tk)).*

2. S phase progression assay by flow cytometry

2.1 Time course

Cells were synchronized in G1 phase using *cdc10-M17* temperature sensitive allele combined with centrifugal elutriation, which selects cells that have been arrested in G1 for as little time as possible (Willis and Rhind, 2011). Cells were grown to mid log phase at 25°C and arrested at 35°C for 2 hours followed by centrifugal-elutriation-based size selection at 35°C to collect cells that had most

recently arrested in G1. The cells were then immediately released into S phase by shifting them to 25°C.

2.2 Flow Cytometry

S-phase progression was followed by flow cytometry using a nuclei isolation protocol, as previously described (Willis and Rhind, 2011) with the following minor modifications.

- 0.6 O.D. of cells were pelleted every 20 minutes for 2 hours after release into S phase.
- Pelleted cells were fixed by resuspension in 70% ethanol and stored overnight at 4°C.
- Fixed cells were washed once with 0.6M KCl and spheroplasted at 37°C for 1 hour in 0.6 M KCl with 1 mg/ml Lysing enzyme (Sigma # L1412) and 0.5 mg/ml Zymolyase 20T (Sunrise Science Products # N0766391).
- Cells were then washed with 0.1 M KCl containing 0.1% Triton X-100 followed by 20 mM Tris-HCl, 5 mM EDTA, pH 8.0.
- The cells were then resuspended in 20 mM Tris-HCl, 5 mM EDTA, pH 8.0 containing 250 µg/ml RNaseA and incubated at 37°C overnight.
- Cells were pelleted, chilled and sonicated for 7 seconds with a Sonifier (Branson Sonifier 450) equipped with a micro tip at power 5 and constant duty cycle to release nuclei.

- Nuclei were mixed with equal amount of 1x PBS containing 2 μM Sytox Green and analyzed by flow cytometry (Figure 2.1A). S-phase progression values were obtained from the histograms as previously described (Figure 2.1B) (Willis and Rhind, 2011).

Figure 2.1 S phase progression by FACS in wild-type

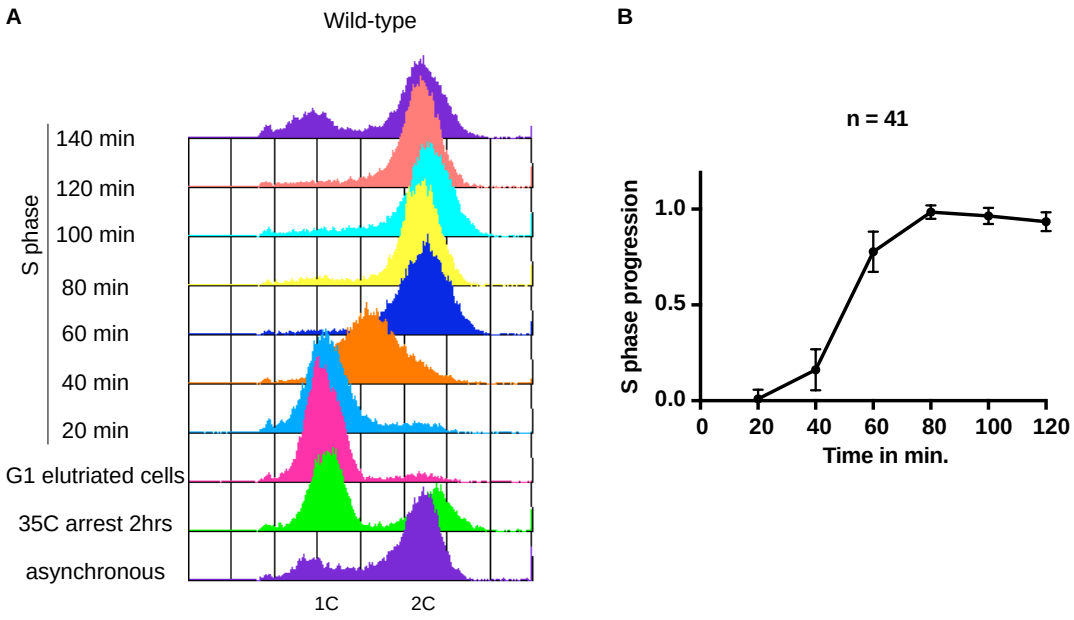

Figure 2.1 S phase progression by FACS in wild-type. A) yFS940 cells were synchronized in G1 phase using *cdc10-M17* temperature sensitive allele followed by elutriation. Elutriated G1 cells were released into permissive temperature. Progression of S phase was monitored by collecting samples for FACS. B) S phase progression values were obtained from histograms of DNA content as described in Willis and Rhind, 2011. Error bars represent standard deviation.

3. DNA Combing

3.1 Cell labeling

Cells were pulse labeled with 2 µM or 5 µM CldU for 5 minutes and chased with 20 µM IdU for 10 minutes at 45, 50 or 55 minutes into S phase time course, which corresponds to mid S phase. Analog labeling was stopped by adding sodium azide to a final concentration of 0.1% and cooling the cells on ice. 10 O.D. of cells were pelleted for combing, frozen in liquid N_2 and stored at -80°C.

The effect of analog addition on replication kinetics

Addition of analog early in S phase causes slowing of bulk replication, probably due to checkpoint-dependent origin inhibition (Figure 2.2A). Therefore, we have labeled cells in a manner so as to incur minimal effect on S phase progression due to analog addition (Figure 2.2B). By adding analogs at different time points across S phase and examining the effect on S phase progression by FACS, we chose to add analog at 50 minutes after release and harvest cells for combing by 65 minutes after release for wild-type (Figure 2.2B).

Figure 2.2 Effect of analog addition on replication kinetics

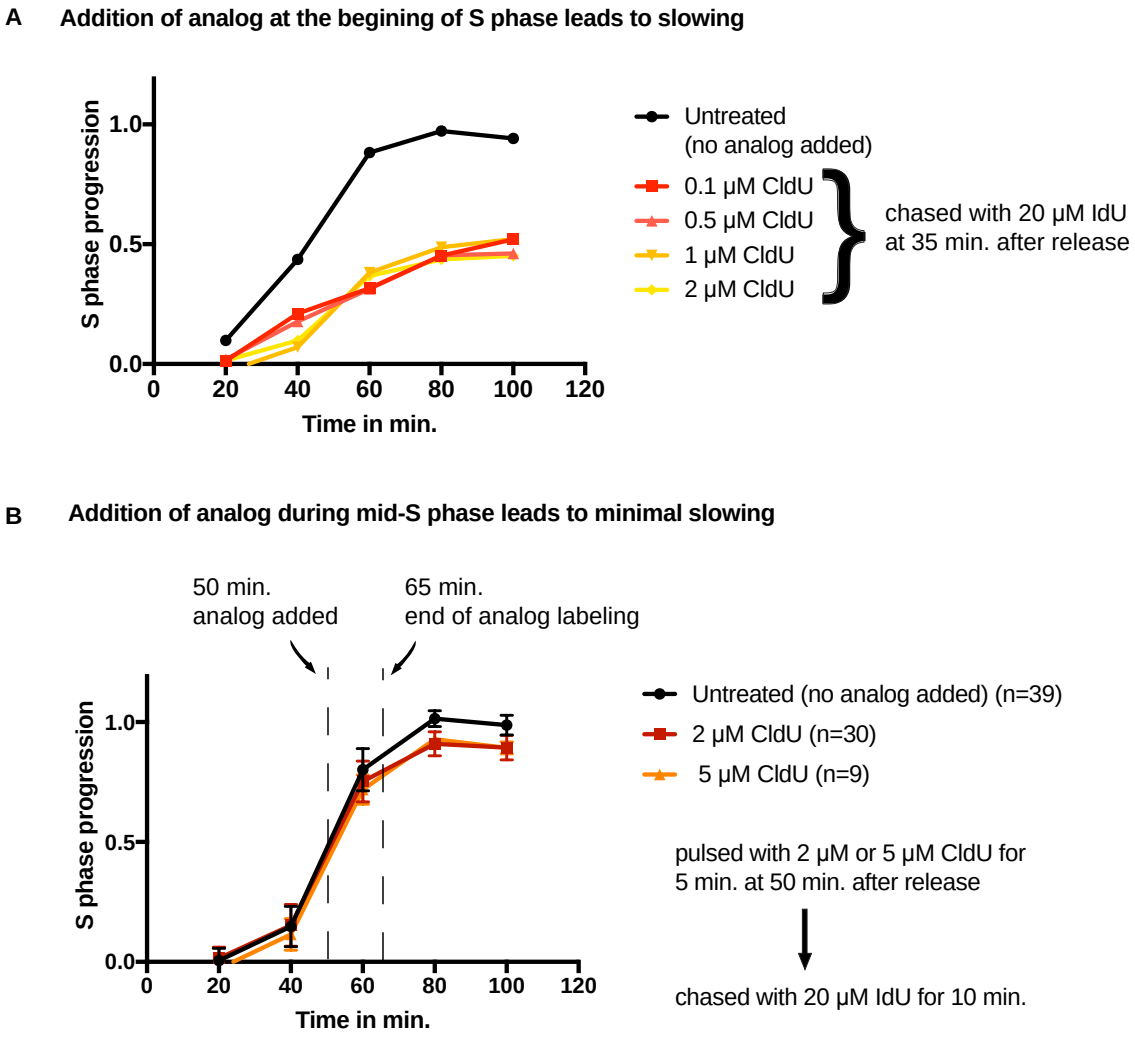

Figure 2.2 Effect of analog addition on replication kinetics. A) Wild-type cells were synchronized and released into S phase with analog added at different concentrations—0.1 μM, 0.5 μM, 1 μM, 2 μM CldU—and chased with 20 μM IdU at 35 minutes after release or without any analog. B) The S-phase progression of cultures with and without analog addition used for combing experiments. 2 μM or 5 μM CldU analog was added at 50 minutes after release for 5 minutes and chased with 20 μM IdU for 10 minutes and the cells were harvested for combing at 65 minutes after release so as to have minimal effects of analog addition on replication kinetics.

3.2 Plug preparation and digestion

- The pellet was washed twice with 1ml spheroplasting buffer (20mM Citrate phosphate pH 5.6, 50mM EDTA pH 8.0, 1M Sorbitol) in a 2ml round-bottomed microcentrifuge tube. To wash, the cells were re-suspended gently with a pipette, and centrifuged at 5000g for 1min, at room temperature.
- The pellet was then re-suspended in 150 µL of DNA combing enzyme mix (spheroplasting buffer with 0.4 mg/ml Zymolyase 20T, 0.5mg/ml Lysing enzyme (Sigma # L1412), 0.5% β-mercaptoethanol) and incubated at 37°C for 5 minutes.
- The re-suspended cells were mixed with 150 µL of 1.5% low-melting agarose (1.5% in spheroplasting buffer, dissolved by boiling at 95°C and cooled to 42°C) using a cut-off 200 µL tip. The cells were mixed well with agarose and 150 µL was dispensed into each well of plug mold (two wells per sample) and left to solidify for 20 – 30 minutes at 4°C.
- Plugs from each sample (two) were placed in a single round-bottomed tube with 1 ml of DNA combing plug solution (spheroplasting buffer with 10mg/ml Zymolyase 20T, 12mg/ml Lysing enzyme, 1% β-mercaptoethanol). The plugs were digested with DNA combing plug solution for at least 6 hours or up to 9 hours.

3.3 Proteinase K treatment

The plugs were transferred to a new round-bottomed tube and digested with 1ml Proteinase K buffer (50mM EDTA pH 8.0, 1% SDS, 0.5mg/ml Proteinase K enzyme (10mM Tris pH 8.0, 1mM $CaCl_2$, 30% glycerol, 20mg/ml Proteinase K)) in a 50°C water bath overnight. The Proteinase K buffer was replaced roughly every 12 hours. The Proteinase K digestion was done for a total of 60 hours with 5 changes of freshly made buffer.

3.4 TE washes

After Proteinase K treatment the plugs were transferred to a 15ml conical bottom tube and washed twice for 2 hours each with 10ml TE buffer (10mM Tris, 1mM EDTA) + 1ml of 0.5M EDTA pH 8.0 at room temperature with gentle rocking. The plugs were then washed twice for 2 hours each with 10ml TE buffer at room temperature with gentle rocking. The plugs were stored at 4°C in TE until needed.

3.5 Melting plugs

- One-half or one plug was placed in a 2 mL round bottomed microcentrifuge tube. To the plug 500 µL TE/YOYO (0.4 µM YOYO-1 Iodide (ThermoFisher # Y3601) in TE), 480 µL 0.5 M MES pH 5.35* and up to 1.4 mL H_2O was added.

(*The pH of MES is extremely critical for combing. It determines the density of DNA that will stick to coverslips and their degree of stretching. Titrate the pH of MES using λ DNA. Prepare several combing solutions of λ DNA with MES buffer

of varying pH. Add 200 ng λ DNA to 500 µL TE/YOYO and 480 µL 0.5M MES of pH varying between 5.2 and 6.5 in a final volume of 1.4 mL. Comb the λ DNA and check for density of fibers and their stretching as described below. With 200 ng of DNA, the coverslip should be densely covered with fibers. Use very small increments of pH for standardization (e.g., 0.05). Once the pH is standardized, use the optimum pH for melting sample plugs. Combing can vary substantially between pH 5.30 and pH 5.35; a more basic pH gives fewer, but longer fibers on the coverslip and a more acidic pH allows more DNA of shorter length to stick on the coverslip but allows more stretching. Higher pH of MES (6.25 or 6.35) was used for combing instead of pH 5.4 to isolate longer fibers (Kaykov and Nurse, 2015).)

- The plug was incubated for 20 minutes at 65°C. If the plug had not fully melted then the incubation was extended by another 10 minutes.
- The plug was transferred to 42°C and incubated for 30 minutes.
- 40 µL β-agarase mix (4 µL 10× NEB buffer, 4 µL β-agarase, 32 µL sterile H_2O) was added to the tube**. The plug was digested overnight at 42°C.

(**Do not mix after adding β-agarase. Gently swirl with a tip if needed. After digestion the samples should appear very clear. Usually, a small amount of wispy, thread-like agarose remnant is seen but there should be very few, if any, agarose clumps. If clumps are present, remelt the plug at 65°C and digest again with β-agarase mix. Improper cell wall digestion will make the plugs appear very

cloudy and the β-agarase digestion will not occur optimally leading to poor DNA recovery.)

- The melted plug was centrifuged at 800g for 5 min at room temperature. The tubes were handled with extreme care to avoid any damage to DNA fibers.
- The supernatant was transferred directly into the Teflon reservoir of a DNA Combing instrument or, if the sample is to be stored for latter processing, into a new round-bottomed tube using a cut off 1 mL tip***.

(***This supernatant is the DNA combing solution and there should be hardly any pellet. Use extreme care while transferring the supernatant to avoid DNA fiber breakage. The combing solution can be stored at 4°C. However, with time the DNA fibers break; therefore, avoid storing for >1 mo.)

3.6 Preparation of silanized coverslips

Coverslips were cleaned in a plasma cleaner such as a Harrick basic plasma cleaner. Liquid-based cleaning protocols can be used if a plasma cleaner is not available (Demczuk and Norio, 2009; Marheineke et al., 2009).

3.6.1 Plasma cleaning of coverslips

- Ceramic coverslip holders were washed with water and then with ethanol and allowed to dry.
- The coverslips (22 x 22 mm, No. 1) were placed in ceramic holders

without touching the flat surfaces of the coverslips. The coverslips were cleaned according to the instructions of the plasma cleaner manufacturer. The coverslips were quickly transferred to the desiccator for silanization.

(After plasma cleaning, proceed immediately to silanization. Exposure of the coverslip to oxygen will lead to poor silanization.)

3.6.2 Silanization and storage of coverslips

- A 25 mL beaker was placed in the center of the desiccator chamber. (Use a fresh beaker each time.)
- 1 mL octenyltrichlorosilane mixture of isomers 96% (Sigma 539279) was added to the beaker.(Open the silane bottle, quickly take 1 mL and immediately close the bottle to minimize silane oxidization.)
- The air was evacuated from the desiccator by connecting it to a vacuum pump. The silane will boil after vacuum is established. The desiccator was evacuated for 2 min.
- The desiccator was sealed and silane coating was allowed to occur overnight.
- The seal was broken and the beaker containing remaining silane was removed. The desiccator was resealed using vacuum.
- The coverslips were stored under vacuum until needed but used within 1 week.

3.7 DNA Combing

This protocol is based upon the DNA Combing System instrument from Genomic Vision, although other surface- coating systems should work (Marheineke et al., 2009; Kaykov et al., 2016). Over 50 coverslips can be combed using the combing solution from one-half of a plug.

- The DNA combing solution was transferred very carefully (to avoid DNA breakage) into a Teflon reservoir. To avoid breakage of DNA, after spinning the melted plug, the supernatant can be transferred using a cut off 1 mL tip directly into the Teflon reservoir, instead of transferring it into a new tube and then into the reservoir.
- A silanized coverslip was attached to the instrument holder and dipped into the reservoir for 5 min.
- The coverslip was withdrawn at a constant speed of 500 µM/sec to allow DNA molecules to stretch.
- The density of fibers and stretching on the coverslips was checked by epifluorescence using a GFP filter set and a 100× objective to visualize YOYO-1 stained DNA fibers. Coverslips with well- stretched fibers of appropriate density were selected for further analysis. Usually 5–10 coverslips will be suitable for further analysis. The coverslips can be easily viewed with an inverted microscope. An upright microscope can also be used, but a coverslip holder is required to hold the coverslip DNA-side down while it is being viewed. Such a holder can be made by cutting a square hole in a thin piece of stiff plastic.

- The immersion oil was aspirated away from the coverslip. A drop of super glue was placed on a slide and the coverslip was placed oil-side down on the glue and the slide was labeled using pencil.
- The slide was incubated for 2 h at 65°C or overnight. Baking robustly attaches DNA strands to the cover slip.

3.8 Immuno-staining of stretched DNA fibers

- The slides were cooled at room temperature for 5 min. The slides were placed in a Coplin jar. The slides were denatured with freshly prepared 0.5 N NaOH or 2.5 N HCl for 30 min; acid or alkali was added and the jar was placed on a rocking platform.

The choice of denaturing agent, either HCl or NaOH, depends on the batch of coverslips. Test the coverslip batch for optimal staining using spare labeled DNA before proceeding with test samples. Typically, CldU is best visualized using HCl denaturation. However, IdU staining does not work well with HCl denaturation. IdU is best visualized using NaOH denaturation, while CldU staining is moderate. At low concentrations, CldU staining is quite punctate, which can complicate analysis. At high CldU concentrations, NaOH gives good results.

- The slides were transferred to a fresh Coplin jar and washed with 0.1× PBS three times for 5 min each on a rocking platform.
- The slides were placed in a humid chamber (box containing wet paper

towels).

- The coverslips were blocked with 1% BSA (1% BSA fraction V in 0.1x PBS with 0.05% Tween-20) by adding 50 µL of solution per coverslip. A second coverslip was placed on top of each to spread out the solution and to prevent evaporation. Incubate the box for 25 min at 37°C. Fresh top coverslips were applied as described in this step for all subsequent antibody incubations.
- The top coverslip was removed by dipping the slide horizontally in a wide chamber containing 0.1× PBST (0.1x PBS with 0.05% Tween-20). The slides were washed with 0.1× PBST twice for 2 min each. The top coverslips were removed as described in this step for all subsequent washes. In most cases the top coverslip will float off easily; however, it may be necessary to gently ease it off using a micropipette tip.
- 50 µL CldU (rat) and IdU (mouse) primary antibodies were added to each coverslip (prepare all Ab dilutions in blocking agent; see Table 2 for dilutions). The coverslips were incubated for 1 h at 37°C.
- The slides were washed with 0.1× PBST twice for 3 min each.
- Anti-rat 594 or Cy5 and anti-mouse 488 or Cy 3.5 antibodies were added to each coverslip. The coverslips were incubated for 30 min at 37°C.
- The slides were washed with 0.1× PBST twice for 3 min each.
- Rabbit anti-ssDNA primary antibody was added to each coverslip. The coverslips were incubated for 1 h at 37°C.

- The slides were washed with 0.1× PBST twice for 3 min each.
- Anti-rabbit 350 or BV480 was added to each coverslip. The coverslips were incubated for 30 min at 37°C.
- The slides were washed with 0.1× PBST twice for 3 min each.
- Excess 0.1× PBST was drained off. 18 µL of anti-fade mounting medium was added per coverslip. A coverslip was placed on top of each and sealed with nail polish. The nail polish was allowed to dry before visualization. If using ProLong Gold Antifade, allow the slides to cure for 24 h at room temperature before sealing with nail polish.
- The slides were kept at −20°C for long-term storage.

Table2.1: Antibody dilutions (all dilutions were prepared in blocking agent)

	Antibody	Detection	Dilution
1	Mouse anti-BrdU (BD Biosciences 347580)	IdU and BrdU	1:20
2	Rabbit anti-ssDNA (IBL 18731)	ssDNA	1:50
3	Rat anti-BrdU (Abcam ab 6326)	CldU and BrdU	1:50
4	Alexa fluor 488 goat anti-mouse IgG (H+L), highly cross-adsorbed (Invitrogen A-11029)	Mouse BrdU Ab	1:100
5	Alexa fluor 350 goat anti-rabbit IgG (H+L), highly cross-adsorbed (Invitrogen A-21068)	Rabbit ssDNA Ab	1:100
6	Alexa fluor 594 goat anti-rat IgG (H+L) (Invitrogen A-11007)	Rat BrdU Ab	1:100
7	Goat anti-mouse IgG H&L Cy3.5 preadsorbed (Abcam ab6946)	Mouse BrdU Ab	1:50
8	BV480 Goat anti-rabbit IgG polyclonal (BD Biosciences 564879)	Rabbit ssDNA Ab	1:10
9	Goat anti-rat IgG H&L Cy5 preadsorbed (Abcam ab6565)	Rat BrdU Ab	1:50

3.9 Imaging

Fibers stained with secondary antibodies Alexa Fluor 488, 350, and 594 were visualized using a Zeiss Axioskop 2 Plus epifluorescence microscope with 100X Plan-NEOFLUAR oil objective and standard DAPI (Ex:360/40 DC:400 Em:460/50), GFP(Ex:470/40 DC:495 Em:525/50), and Texas red (Ex:560/60 DC:600 Em:615) filter sets and imaged using SPOT monochrome cooled-CCD camera. Fibers stained with secondary antibodies Cy3.5, BV480 and Cy5 were imaged using the FiberVision® scanner in collaboration with Genomic Vision, France.

3.10 Data collection

Fibers were measured in pixels using Image J (Schneider et al., 2012). Pixels were converted to kb using λ DNA as a standard. Only fibers longer than 120 kb were analyzed. For images acquired in collaboration with Genomic Vision, the fibers were manually measured using FiberStudio® software. About 25 Mb of DNA was collected for each dataset. For each fiber, the length of each green, red and unlabeled track was manually measured. Analysis of this data was automated using MATLAB scripts.

4. Data Analysis

We pulsed cells in S phase with 5-chloro-2'-deoxyuridine (CldU) for 5 minutes and chased it with 5-iodo-2'-deoxyuridine (IdU) for 10 minutes, isolated and combed DNA, and visualized the CldU and IdU analogs with red and green

antibodies, respectively. Figure 2.3 shows a sample fiber from the dataset. The fiber contains a rightward moving fork (red-green [RG]), an origin that fired during IdU labeling (green [G]), and three origins that fired during CldU labeling (green-red-green [GRG]). Further replication patterns observed in our combing dataset are shown with an interpretation of each pattern. The patterns observed were most simply interpreted as a leftward fork (green-red [GR]), a rightward fork (RG), origins that fired during CldU (GRG) or IdU (G), and terminations during IdU (red-green-red [RGR]) or CldU (red [R]). However, a more sophisticated analysis allowing the possibility of fork stalling reveals that many of these patterns—in particular termination during CldU (R)—are ambiguous, as described below (Figure 2.6). For each experiment we collected about 25 Mb of DNA, which is about twice the size of the fission yeast genome, ensuring representation of most genomic loci in our analysis. From the combing data we estimated four parameters: origin firing rate, fork density, fork rate and fork stalling frequency

Figure 2.3 Visualization of replication fork progression

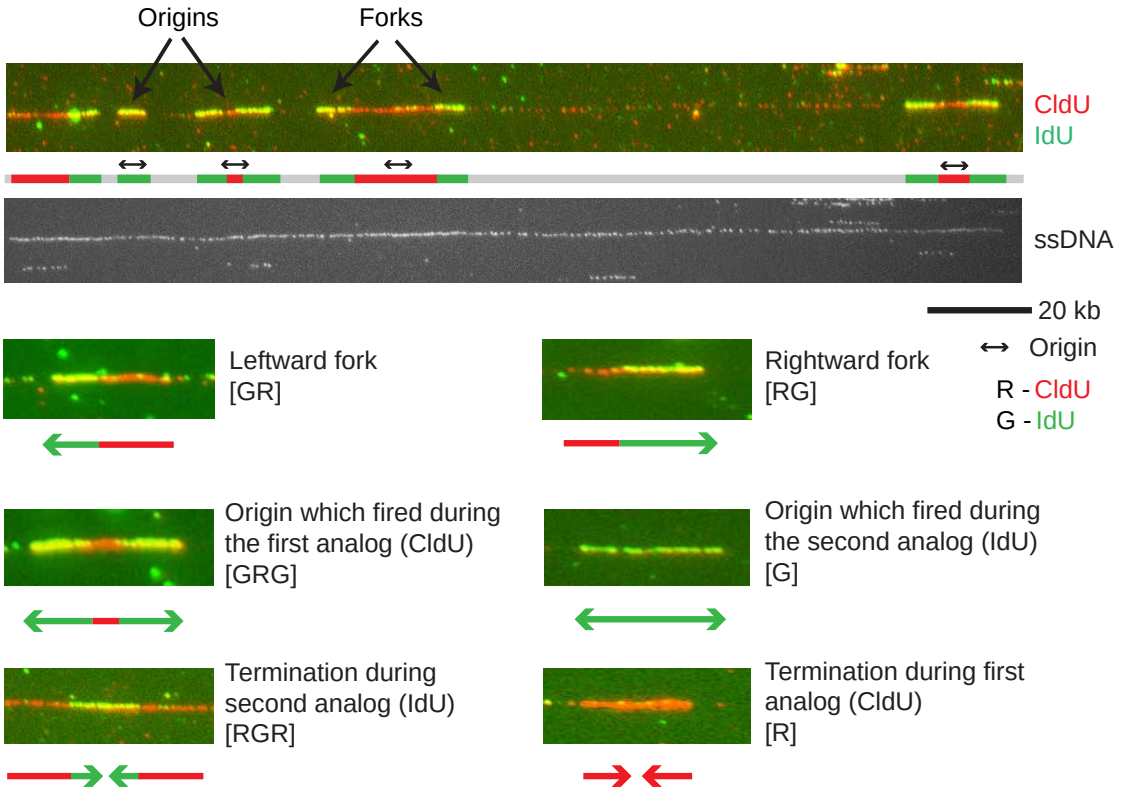

Figure 2.3 Visualization of replication fork progression. Wild-type cells (yFS940) were G1 synchronized and pulse labeled at 50 minutes after release into S phase with CldU (visualized using red antibody) for 5 minutes, and chased with IdU (visualized using green antibody) for 10 minutes. Shown are a sample fiber from the wild-type dataset and the various replication patterns observed in the dataset with their simplest interpretations. See Figure 2.6 for other possible interpretations of ambiguous patterns.

4.1 Fork rate measurement

Green tracks (containing IdU, the second analog added) continuing from red tracks (containing CldU, the first analog added) were used to determine fork rate. The length of the green track was measured from green-red (GR), red-green (RG) and green-red-green (GRG) events and divided by the length of the chase time (10 minutes). For each dataset the fork rate distribution was plotted as a histogram and was fit to a Gaussian curve (Figure 2.4). The mean fork rate was obtained from the fit.

We also considered that there could be a lag between the addition of analog and its incorporation into the DNA, which might lead to an underestimation of the actual fork rate. To estimate the lag we labeled the cells as previously described with 2μM CldU for 5 minutes and chased it with 20μM IdU but collected samples after different lengths of IdU incubation: 3, 4, 5, 6, 7, 8, 10, 14 and 16 minutes. However we did not find any lag in analog incorporation by plotting the lengths of IdU labeled forks across different lengths of time after IdU addition (Figure 2.5).

Fork rate was also analyzed by excluding forks occurring at the ends of the fiber, as broken forks may lead to an under-estimation of the actual fork rate. However, excluding the forks occurring at the ends of the fiber does not significantly affect fork rate estimations, consistent with the observation that only 6% of the forks in our dataset occur at the end of a fiber.

Figure 2.4 Fork rate distribution in wild-type sample

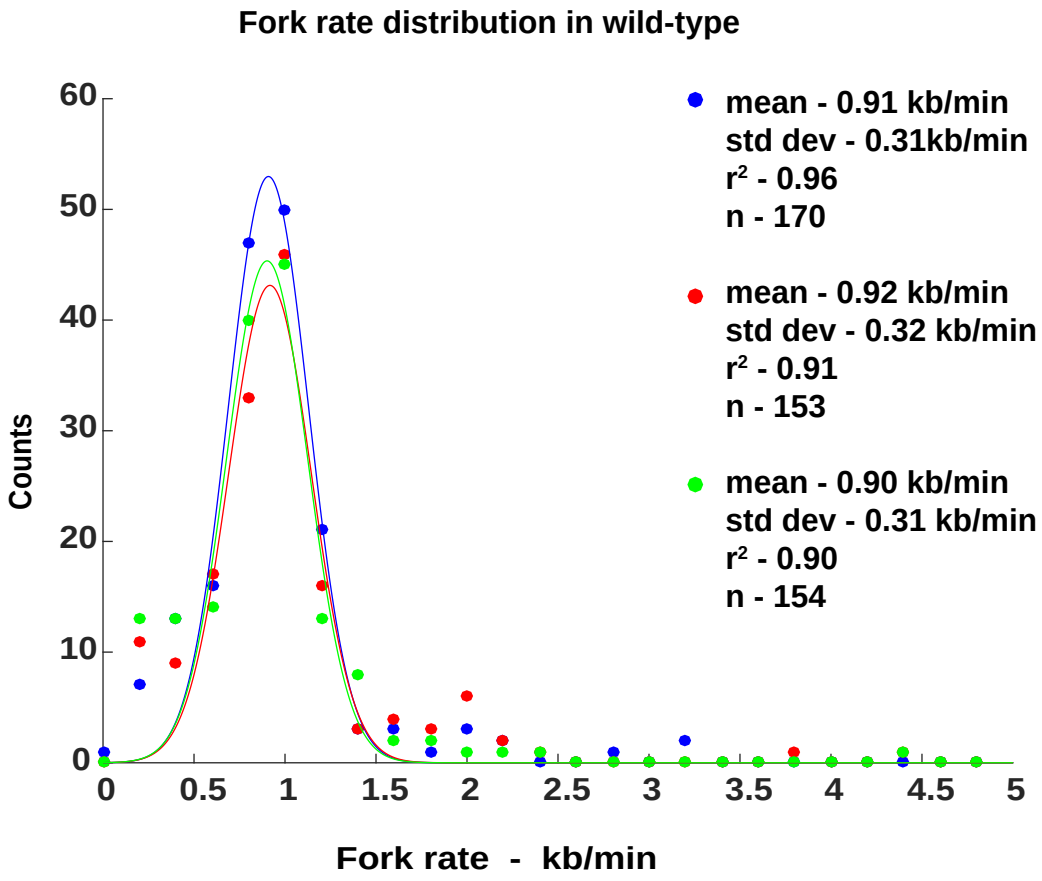

Figure 2.4 Fork rate distribution in wild-type sample. Fork rate distribution from wild-type sample from three different time-courses (blue, red, green). Each distribution was fit to a Gaussian curve. Mean fork rate and standard deviation was obtained from the fit.

Figure 2.5 Estimation of lag in analog incorporation

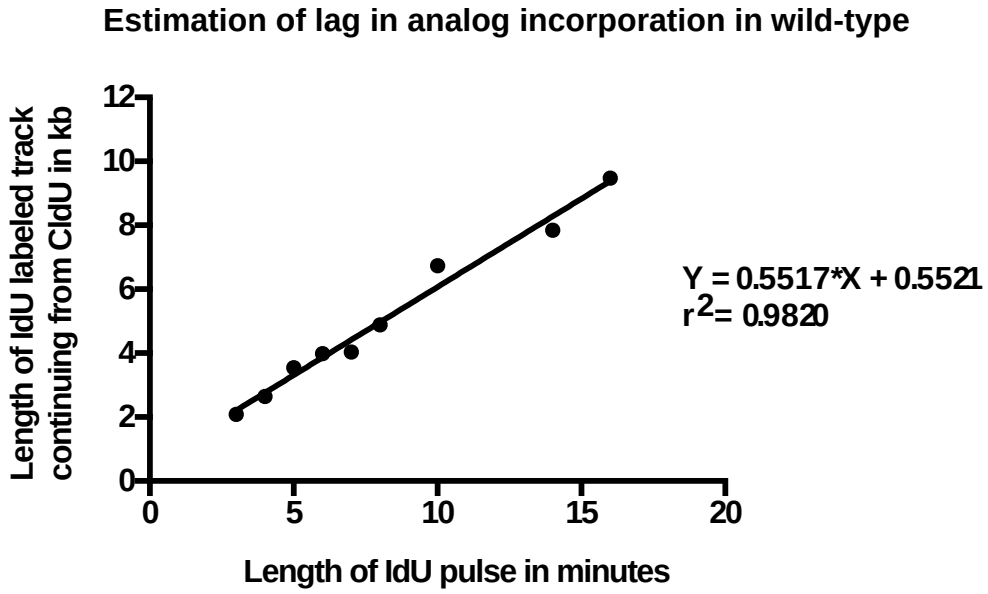

Figure 2.5 Estimation of lag in analog incorporation. Cells were pulse labeled with 2 µM CldU for 5 minutes and chased with 20 µM IdU for varying lengths of time: 3, 4, 5, 6, 7, 8, 10, 14, 16 minutes. At least 100 forks were collected for each time point except for 3 and 4 minutes of IdU labeling for which only 11 and 44 forks were measured, respectively, due to lack IdU labeled forks at such short lengths of labeling period.

4.2 Origin firing rate measurement

To estimate the rate of origin firing, the total number of origin firing events in each fiber was divided by the length of the unreplicated DNA of that fiber and by the total length of the analog pulses (15 minutes). The total number of origins firing in the fiber is the sum of origins that fire during the first and the second analog. Origins that fire during the first analog are identified as GRG events. Origins that fire during the second analog are identified as isolated green events. However, origins that fire in the first analog will appear as GRG only if both its forks progress into the second analog labeling. In the event of a unidirectional fork stall during the first analog pulse, origins that fire will appear as GR or RG. An origin may also appear as an isolated red event if both its forks stall during the first analog pulse. Therefore, the origin firing rates were corrected by accounting for the probability of forks stalling during the first analog pulse which would have disrupted GRG events, based on the measured fork stall rate (see below for stall rate calculation).

4.3 Fork density measurement

Origin firing rate captures the origins that fire during the course of the analog pulses. However, the rate of origin firing prior to labeling influences the density of forks during the pulses and provides a parallel measure of origin activity. Therefore, we measured fork density to assess origin firing rate during the period prior to our S-phase labeling pulses. Fork density, the total number of forks in each fiber was divided by the length of the unreplicated DNA of that fiber, and

was calculated independently for the two labeling pulses. The basic strategy for measuring the fork density during either analog pulse is straight-forward. For the first pulse, it is done by counting the following events in each fiber and dividing by the length of the unreplicated DNA of that fiber: the number of origins firing (GRG) and terminations (R and RGR) during the first pulse multiplied by two, since each origin or termination comprises two forks, and the unidirectional forks (GR and RG) counted once. Likewise, for the second analog pulse it is done by counting the following events in each fiber and dividing by the length of the unreplicated DNA of that fiber: the number of origin firing during the second pulse (G), forks from origins firing in the first pulse (GRG) and terminations during the second pulse (RGR) multiplied by two, and the unidirectional forks (GR and RG) counted once. We also calculated the total fork density for each fiber, which is done by counting following events in each fiber and dividing by the length of the unreplicated DNA of that fiber: number of origins firing during each analog (GRG and G) and terminations (R and RGR) multiplied by two, and the unidirectional forks (GR and RG) counted once. However, these calculations are confounded by forks that stall during the first pulse, leading to the misclassification of events (Figure 2.6). To account for such stalling events, we took a probabilistic approach, in which the measured stall rate is used to more accurately estimate fork density, as described below.

4.4 Fork stall rate measurement

Difficulty in identifying fork stalling events in combing data arises from the fact that stalls during the first pulse can result in ambiguous analog incorporation patterns (Figure 2.6A) (Técher et al., 2013). For instance, an isolated first analog event is open to any of the following three interpretations: an unidirectional elongating fork that stalled, or an origin firing event for which both forks stalled, or a termination event (Figure 2.6A). Therefore, we cannot use first-pulse events alone as rigorous evidence for stalled forks. However, using double-labeled combing data we can unambiguously identify fork stalling. In particular, two apparently unidirectional forks moving in the same direction on a fiber must have had the fork in between them stall (Figure 2.6B). Such unambiguous stall events leave signature red-unlabeled-green (RUG) or green-unlabeled-red (GUR) patterns (Figure 2.6B & 2.7). On the other hand the signature for two unstalled forks is green-unlabeled-green (GUG) (Figure 2.7). Thus, a red-unlabeled-green (RUG) or green-unlabeled-red (GUR) pattern is diagnostic of a fork stall. Since the fibers in our datasets average over 400 kb, we observed many neighboring forks, allowing us to robustly measure fork stalling. We can estimate the fork stall rate only during the first analog pulse. Stalls occurring during the second analog pulse simply reduce the length of the second analog incorporation track and thus get interpreted as a reduction in fork rate.

Figure 2.6 Identification of stalled forks using the context of neighboring forks

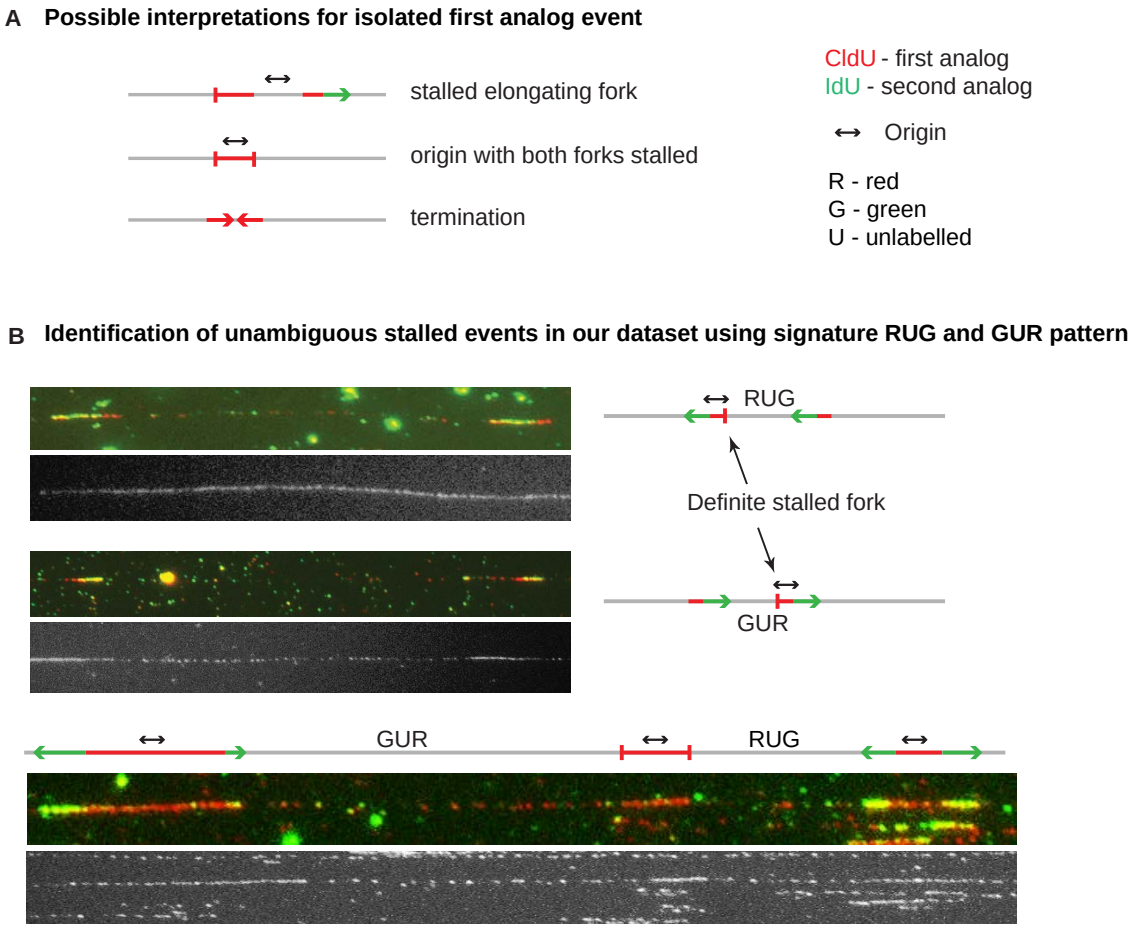

Figure 2.6 Identification of stalled forks using the context of neighboring forks (A) Ambiguity in interpreting isolated first analog events. Possible interpretations of isolated first analog event based on the neighboring event are listed. (B) The signature we have used to identify definite stalled forks: RUG (red-unlabeled-green) and GUR (green-unlabeled-red). Two forks moving in the same direction indicate that the fork moving in between them in the opposite direction must have stalled.

Calculation of stall rate from unambiguous events

To estimate the apparent stall rate in the dataset we counted every RUG and GUR event and divided it by the sum of GUR, RUG and GUG events (Figure 2.7). The GUR and RUG events are included in the denominator because every stall event represents a loss of one fork. For example, consider an origin (GRG) on a fiber. If one of its fork is stalled then it will appear as GR or RG and we would calculate the stall rate as 50% since one fork is stalled but ideally there should be two (one fork which we can visualize and one which is stalled).

Calculation of stall rate from all events (unambiguous as well as ambiguous events)

Although the unambiguous events allow us to determine the stall rate with certainty, not every isolated first analog event is flanked by second analog events to help us determine whether it is stalled or not. For example consider Figure 2.8, which shows two forks moving away from one another (RUR pattern). It can be interpreted as forks moving away from a single origin or as two origins with stalled forks on their inner side.

Figure 2.7 Calculation of apparent stall rate (for unambiguous events only).

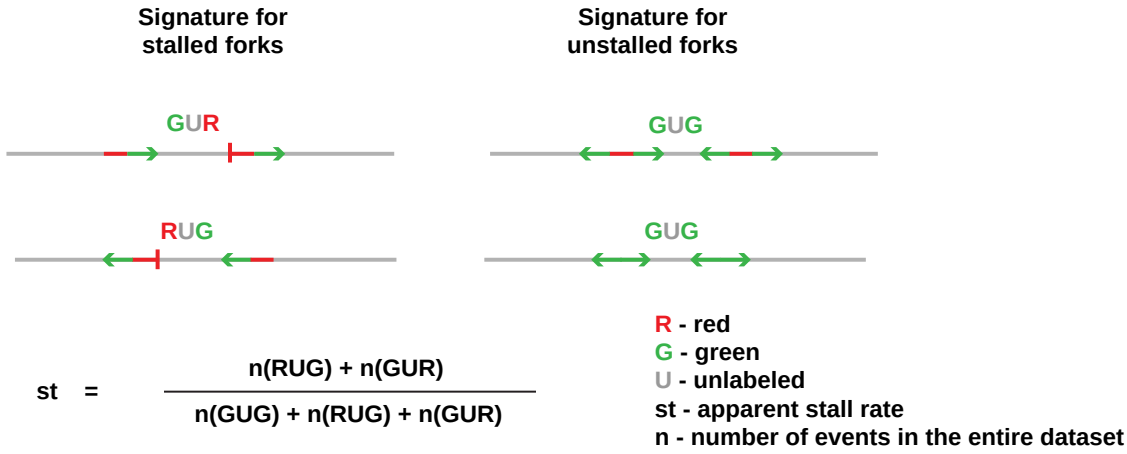

Figure 2.7 Calculation of apparent stall rate (for unambiguous events only). Apparent stall rate was estimated by dividing the number of RUG and GUR events by summation of GUG, RUG, and GUR events.

Figure 2.8 Ambiguous events in the dataset

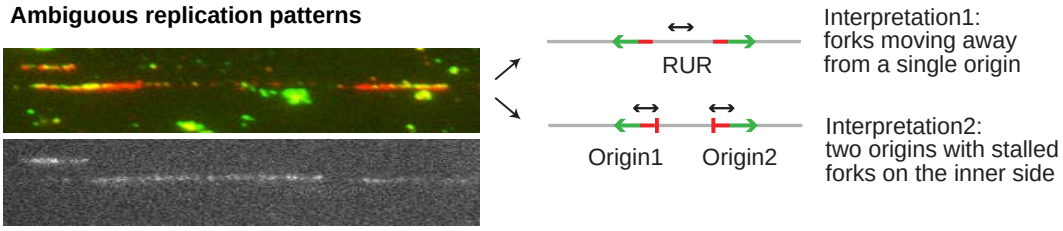

Figure 2.8 Ambiguous events in the dataset. Ambiguous events such as RUR (red-unlabeled-red) and their possible interpretations.

To estimate the stall rate across the ambiguous events we used a probabilistic approach. We considered all combinations in which ambiguous events could occur (e.g. UR, RU, RUR, GRU, URG, GRUR, RURG, URUR, RURU, RURUR etc.) (Figure 2.9). Figure 2.9 shows a schematic representation of all the permutations in which a red track can occur and their possible interpretations.

Figure 2.9 Permutations in which a red track can occur.

Permutation 1: red track is an origin with a stalled fork

Permutation 2: red track could be an origin with a stalled leftward fork or just an elongating rightward fork

Permutation 3:elongating forks from an origin in the center or two origins whose inner forks have stalled

Permutation 4: red track is an origin with a stalled rightward fork

Permutation 5: red track could be an origin with a stalled rightward fork or just an elongating leftward fork

Permutation 6: elongating forks from an origin in the center or two origins whose inner forks have stalled

Permutation 7: red track could be an elongating fork with a stalled leftward fork or an origin with two stalls

Permutation 8:red track could be an elongating fork with a stalled rightward fork or an origin with two stalls

Permutation 9: red track could be a termination event or an origin with two stalls or an elongating fork with stall on either side

Permutation 10: red track could be a termination event or an origin with two stalls or an elongating fork with stall on either side

Permutation 11: red track could be a termination event or an origin with two stalls or an elongating fork with stall on either side

Permutation 12: red track could be an elongating fork with a stalled rightward fork or could be an origin with two stalls

Permutation 13: red track could be an elongating fork with a stalled leftward fork or could be an origin with two stalls

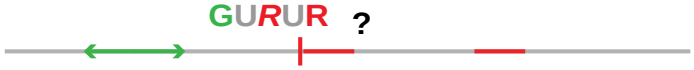

Permutation 14: red track is an origin with both its forks stalled

Permutation 15: red track could be a termination event or an origin with two stalls or an elongating fork with stall on either side

Permutation 16: red track is an origin with two forks

R - red
G - green
U - unlabeled
? - ambiguous red track

Figure 2.9 Permutations in which a red track can occur. A schematic representation of all the permutations in which a red track can occur and their possible interpretations. The red track of interest is italicized in each case.

The ambiguous events were assigned a probability of being either stalled or not, using the apparent stall rate as the probability of a fork stalling (Table 2.2). For example, consider red-unlabeled-red (RUR) event represented in Figure 2.8, if the leftward moving fork is interpreted as an origin with stalled rightward fork then it automatically implies that the rightward moving fork on the fiber is also an origin with stalled leftward moving fork. Therefore the probability of both the events being considered as origins with a stalled fork, is the product of two stall events occurring at the same time i.e. square of the apparent stall rate. If the apparent stall rate is 10%, then RUR events are assigned a 1% probability of as having two stalled forks. The probabilistic interpretation of the ambiguous events also changes the absolute number of forks in the dataset. For example according to interpretation 1 in Figure 2.8 there is only one origin with two elongating forks on the fiber. However according to interpretation 2 there are two origins with a total of 4 expected and 2 apparent forks. To estimate the stalls per kb for each fiber the unambiguous stall events (RUG and GUR) in each fiber were combined with the fraction of the ambiguous events that were predicted to be stalled and this total was divided by the length of the un-replicated DNA. To estimate the stall rate per fiber the unambiguous stall events (RUG and GUR) in each fiber were combined with the fraction of the ambiguous events that were predicted to be stalled and this total was divided by the total number of ongoing forks in the first analog, which was calculated as the sum of GR, RG, and R

events (counted once or twice based on whether they were interpreted as elongating forks or as an origin with a stalled fork) plus two forks for each GRG.

Table 2.2 Probability of stalling assigned to each permutation listed in Figure 2.9

R - red
G - green
U - unlabeled
st - apparent stall rate
n - number of events in the entire dataset

Permutation	Probability of the red track having a stalled fork	Probability of the red track being an origin with two stalled forks	Total number of stalled forks	Total number of unstalled forks	Total number of ongoing forks
1	1	-	n(GURG)	n(GURG)	2*n(GURG)
2	st	-	n(URG)*st	n(URG)*(1-st)	n(URG)*(1-st) + 2*st*n(URG)
3	st^2	-	n(RURG)*st^2	n(RURG)*(1-st^2)	n(RURG)*(1-st^2) + 2*st^2*n(RURG)
4	1	-	n(GRUG)	n(GRUG)	2*n(GRUG)
5	st	-	n(GRU)*st	n(GRU)*(1-st)	n(GRU)*(1-st) + 2*st*n(GRU)
6	st^2	-	n(GRUR)*st^2	n(GRUR)*(1-st^2)	n(GRUR)*(1-st^2) + 2*st^2*n(GRUR)
7	1-st	st	n(GURU)*(1-st) + 2*n(GURU)*st	-	n(GURU)*(1-st) + 2*n(GURU)*st
8	1-st	st	n(URUG)*(1-st) +	-	n(URUG)*(1-st) + 2*n(URUG)*st

			2*n(URUG)*st		
9	$st + st^2 - 2*st^3$	st^3	$n(RURU)*(st + st^2 - 2*st^3) + 2*n(RURU)*st^3$	$2*n(RURU)*(1 - st - st^2 + st^3)$	$n(RURU)*(st + st^2 - 2*st^3) + 2*n(RURU)*st^3 + 2*n(RURU)*(1 - st - st^2 + st^3)$
10	$st + st^2 - 2*st^3$	st^3	$n(URUR)*(st + st^2 - 2*st^3) + 2*n(URUR)*st^3$	$2*n(URUR)*(1 - st - st^2 + st^3)$	$n(URUR)*(st + st^2 - 2*st^3) + 2*n(URUR)*st^3 + 2*n(URUR)*(1 - st - st^2 + st^3)$
11	$2*(st^2 - st^4)$	st^4	$2*n(RURUR)*(st^2 - st^4) + 2*n(RURUR)*st^4$	$2*n(RURUR)*(1 - 2*st^2 + st^4)$	$2*n(RURUR)*(st^2 - st^4) + 2*n(RURUR)*st^4 + 2*n(RURUR)*(1 - 2*st^2 + st^4)$
12	$1-st^2$	st^2	$n(RURUG)*(1-st^2) + 2*n(RURUG)*st^2$	-	$n(RURUG)*(1-st^2) +2*n(RURUG)*st^2$
13	$1-st^2$	st^2	$n(GURUR)*(1-st^2) + 2*n(GURUR)*st^2$	-	$n(GURUR)*(1-st^2) + 2*n(GURUR)*st^2$
14	-	1	2*n(GURUG)	-	2*n(GURUG)
15	$2*(st - st^2)$	st^2	$2*n(URU)*(st - st^2) + 2*n(URU)*st^2$	$2*n(URU)*(1 - 2*st + st^2)$	$2*n(URU)*(st - st^2) + 2*n(URU)*st^2 + 2*n(URU)*(1 - 2*st + st^2)$
16	-	-	-	2*n(GRG)	2*n(GRG)

$$\text{stall rate} = \frac{\text{total number of stalled forks per fiber}}{\text{total number of ongoing forks per fiber}}$$

Conclusion

Bulk assays of replication kinetics, such as the quantitation of radioactive thymidine incorporation or flow cytometry, provide only an average profile of replication kinetics, convolving the effects of origin firing and fork progression and obscuring any heterogeneity in fork slowing. The effects of DNA damage on specific origins and on forks replicating specific loci can be analyzed by gel- or sequence-based methods (Santocanale and Diffley, 1998; Shirahige et al., 1998; Tercero and Diffley, 2001; Kumar and Huberman, 2009; Szyjka et al., 2008), but these techniques still only reveal the average response to DNA damage. Such approaches lack the single-molecule resolution necessary to identify heterogeneity in response to damage and to distinguish, for instance, if all forks pause briefly at all lesions or if only a fraction of forks stall, but for a longer time.

Therefore, to investigate the effect of polymerase blocking lesions on individual origins and forks on a global scale, we have implemented a double-analog labeled, single-molecule DNA combing assay in fission yeast. Sequential analog labeling allows us to distinguish between origins and forks and thus study their regulation in response to damage. Further, we have developed an in-depth analysis of every permutation of labeled track found in a tri-color combing dataset to rigorously study the effect of damage on origins v forks. Finally, using the context of neighboring events we have identified fork stalling events in tri-color combing dataset. Detection of fork stalling events is complicated due to lack of consensus on how to identify them in the DNA fiber datasets (Técher et al.,

2013). Generally, signal from the first (red) analog alone on a fiber (a unlabeled-red-unlabeled [URU] event) is presumed to be either an elongating fork that stalled or an origin that fired in the first pulse followed by stalling of both its forks (Figure 2.6A) (Técher et al., 2013; Scorah and McGowan, 2009; Wilsker et al., 2008; Merrick et al., 2004; Conti et al., 2010). Alternatively the events from the first analog alone can be interpreted as terminations (Figure 2.6A) (Técher et al., 2013; Anglana et al., 2003; Courbet et al., 2008; Letessier et al., 2011). However, both interpretations rely on heuristic arguments and are unable to quantitate ambiguous signals, such as URU. Therefore we developed a new, rigorous way of quantitating stalled forks in double-labeled data. We have used the context in which the first analog event occurs to define it as a stalled fork or not. As discussed in greater detail in the data analysis section we have used RUG and GUR patterns as a diagnostic for fork stall event occurring during the first analog (Figure 2.6B and 2.7). We then used a probabilistic approach to quantitate the frequency of stall events in the ambiguous patterns in order to determine the net fork stall rate for the entire dataset (Figure 2.8 and 2.9, Table 2.2). It should be noted that we can detect a stall only if it occurs during the first (red) analog pulse and persists throughout the second (green) analog pulse.

Thus using the approach we have developed we can study the behavior of individual forks and understand their regulation by checkpoint in response to damage (Chapter III). We can ascertain whether regulation of forks is global or

local, that is do all forks show uniform or heterogeneous behavior in response to damage (Chapter III)(Iyer and Rhind, 2013).

Chapter III

Replication fork slowing and stalling are distinct, checkpoint-independent consequences of replicating damaged DNA

Chapter III is mainly from the manuscript written by Nick Rhind and me and is currently under review at *PLOS Genetics* (Iyer and Rhind, submitted).

Introduction

In response to DNA damage during the G1 or G2 phase of the cell cycle, DNA damage checkpoints block cell cycle progression, giving cells time to repair damage before proceeding to the next phase of the cell cycle (Hartwell and Weinert, 1989; Rhind and Russell, 2012). The response to DNA damage during S phase is more complicated, because repair has to be coordinated with ongoing DNA replication (Bartek et al., 2004). DNA damage during S phase activates the intra-S DNA damage checkpoint, which does not completely block S-phase progression, but rather slows DNA replication, presumably allowing for replication-coupled repair (Rhind and Russell, 2000a). Lack of the intra-S DNA damage checkpoint predisposes cells to genomic instability (Zhou and Elledge, 2000). Nonetheless, the mechanisms by which replication is slowed, and the roles of checkpoint-dependent and -independent regulation in the S-phase DNA damage response, are not well understood.

The slowing of S phase in response to damage involves both inhibition of origin firing and reduction in fork rate (Kaufmann et al., 1980; Merrick et al., 2004; Falck et al., 2002; Santocanale and Diffley, 1998; Chastain et al., 2006; Seiler et al., 2007; Kumar and Huberman, 2009). The effect of the checkpoint on origin firing has been characterized in budding yeast and mammalian cells. The checkpoint prevents activation of late origins by targeting initiation factors required for origin firing. In mammals, checkpoint kinase 1 (Chk1) inhibits origin firing by targeting the replication kinases, cyclin-dependent kinase (CDK) and

Dbf4-dependent kinase (DDK) (Zhao and Piwnica-Worms, 2001; Falck et al., 2001; Sørensen et al., 2003). In budding yeast, Rad53 targets Sld3, an origin initiation factor, and Dbf4, the regulatory subunit of DDK (Zegerman and Diffley, 2010; Lopez-Mosqueda et al., 2010).

Although checkpoint inhibition of origin firing is conserved from yeast to mammals, the contribution of origin regulation to damage tolerance is not clear. For instance, budding yeast mutants such as *mec1-100, SLD3-m25 and dbf4-m25*, which cannot block origin firing in response to damage, are not sensitive to damaging agents such as methyl methanesulfonate (MMS) (Zegerman and Diffley, 2010; Lopez-Mosqueda et al., 2010; Tercero et al., 2003; Paciotti et al., 2001) suggesting that checkpoint regulation of origin firing is not as critical as the checkpoint's contribution to damage tolerance via fork regulation.

The effect of checkpoint activation on replication forks is less well understood. Because many DNA damage lesions block the replicative polymerases, in order for forks to pass leading-strand lesions, they must have some way to reestablish leading-strand synthesis downstream of the lesion. Recruitment of trans-lesion polymerases, template switching and leading-strand repriming have all been proposed to be involved in the fork by-pass of lesions, but which is actually used *in vivo* and how the checkpoint may affect that choice, is unclear (Branzei and Foiani, 2009; Branzei and Foiani, 2005; Ulrich, 2012; Daigaku et al., 2010; Sale, 2012; Lee and Myung, 2008).

DNA damage leads to slowing of fork progression. However, whether slowing of forks is checkpoint dependent or independent is controversial (Tercero and Diffley, 2001; Szyjka et al., 2008; Unsal-Kaçmaz et al., 2007). Bulk assays (2D-gels) provide only an average snapshot of fork behavior. To understand the regulation of individual forks on a global scale we have used single-molecule DNA combing assay. Sequential analog labeling allows us to distinguish between origins and forks and thus allows us to get a detailed snapshot of behavior of individual forks in response to damage.

Here, we have assayed checkpoint-dependent slowing of S phase in fission yeast in response to three DNA damaging drugs that activate the checkpoint at significantly different densities of lesions: methyl methanesulfonate (MMS), which mainly methylates purines and creates a relatively small adduct, 4-nitroquinoline 1-oxide (4NQO), which adds a quinoline group to purines resulting in a bulkier adduct (Sikora et al., 2010; Galiègue-Zouitina et al., 1985; Galiègue-Zouitina et al., 1986) and bleomycin, which mainly creates single strand and double strand DNA breaks (Chen and Stubbe, 2005). MMS and 4NQO create polymerase-stalling lesions and have been shown to activate the intra-S checkpoint (Friedberg et al., 1995; Larson et al., 1985; Minca and Kowalski, 2011; Lopez-Mosqueda et al., 2010; Willis and Rhind, 2009; Lindsay et al., 1998). The standard dose of 3.5 mM (0.03%) MMS causes about one lesion every 1 kb whereas a physiologically similar dose of 1 µM 4NQO causes one lesion about every 25 kb and 16.5 µM of bleomycin causes about 5 double-strand breaks per

haploid yeast genome (Lundin et al., 2005; Snyderwine and Bohr, 1992; Ma et al., 2008; Asaithamby and Chen, 2009). Although these are only rough approximations of lesion density, they show that forks will encounter many more MMS lesions than 4NQO lesions or bleomycin-induced double-strand breaks. This wide disparity in lesion density allows us to address differences in global and local effects of the checkpoint. In case of 4NQO, since the lesions are rare, we expect few forks to encounter lesions. Therefore, if all forks slow in response to 4NQO then we can conclude that fork regulation by checkpoint is global in nature. On the contrary, if fork regulation is a local effect then only the very few forks that actually encounter lesion will slow. Similarly since the double-strand breaks caused by bleomycin are infrequent we expect very few forks to be affected by the breaks unless the checkpoint actively regulates all forks. In case of MMS, since the lesions are frequent we expect all forks to encounter lesions, and thus to slow regardless of whether slowing is a local or global effect. By comparing the effects of these three drugs, we can differentiate between global and local effects on fork regulation by the checkpoint. We find that fork slowing is a local, checkpoint-independent effect, but that persistent fork stalling plays a more significant role in replication kinetics than previously appreciated.

Results

MMS, bleomycin and 4NQO-induced DNA damage show a similar effect on the overall replication rate

To determine the effect of MMS, bleomycin, and 4NQO—three compounds that activate the checkpoint at very different densities of lesions—on the replication rate at a population level, we analyzed cells response to them by flow cytometry. G1 synchronized cells were released into S phase with or without DNA damage, using the commonly used dose of 3.5 mM (0.03%) MMS or a dose of 1 μM 4NQO or 16.5 μM bleomycin chosen to produce a similar slowing of bulk replication (Figure 3.16). These doses of MMS, 4NQO and bleomycin cause lesions about once every 1 kb, 25 kb, and 3000 kb respectively (Lundin et al., 2005; Snyderwine and Bohr, 1992; Ma et al., 2008; Asaithamby and Chen, 2009). By flow cytometry, control cells completed replication by 80 minutes, while in the presence of either drug cells slowed replication, reaching only about 60% replicated by the end of the time course (Figures 3.1A and 3.2A).

Figure 3.1 Slowing of S phase progression in response to damage by FACS.

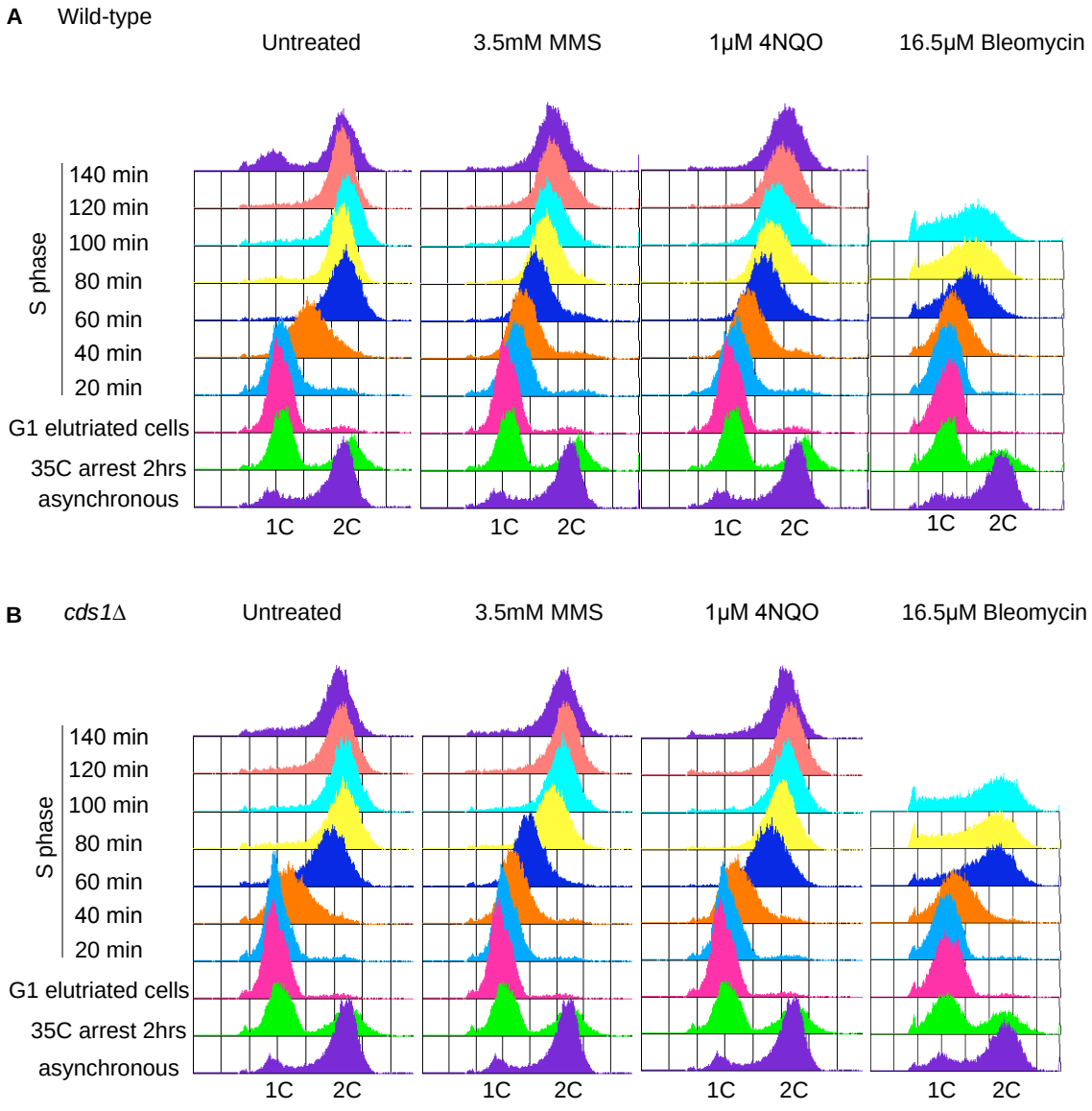

Figure 3.1 Slowing of S phase progression in response to damage by FACS. Wild-type (yFS940) (A) and *cds1*Δ (yFS941) (B) cells were synchronized

in G1 phase using cdc10-M17 temperature sensitive allele followed by elutriation. Elutriated G1 cells were released into permissive temperature untreated or treated with 3.5 mM MMS or 1 µM 4NQO or 16.5 µM Bleomycin. S phase progression was followed by taking samples for FACS.

Figure 3.2 MMS-, 4NQO and bleomycin-induced DNA damage show a similar effect on the overall replication rate

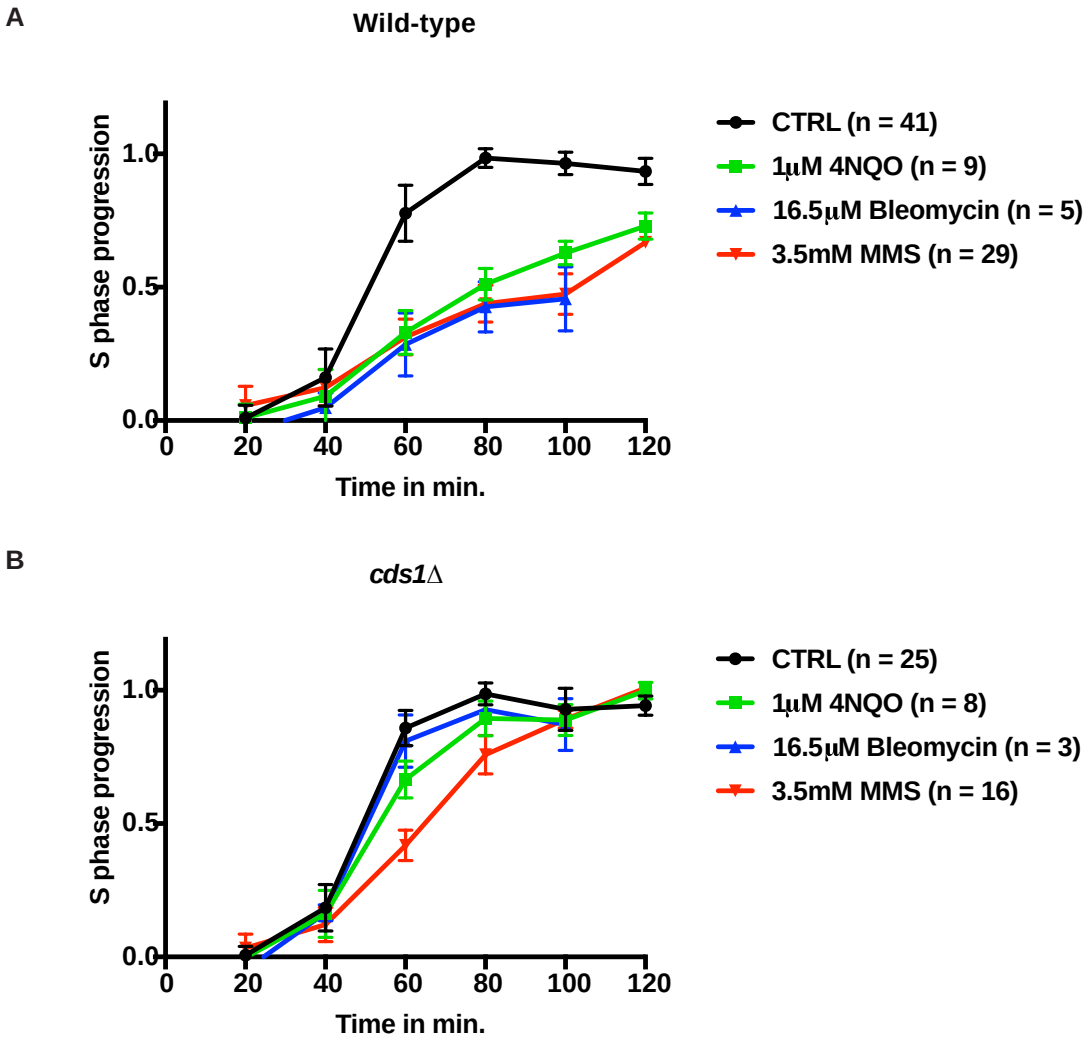

Figure 3.2 MMS-, 4NQO and bleomycin-induced DNA damage show a similar effect on the overall replication rate (A) Wild-type cells (yFS940) show similar slowing of replication in response to 3.5 mM (0.03%) MMS, 1 µM 4NQO, and 16.5 µM bleomycin by flow cytometry. (B) Slowing in response to damage is largely checkpoint dependent by bulk assay. Wild-type (yFS940, A) and *cds1*Δ

(yFS941, B) cells were synchronized in G1 and released into S phase in the presence or absence of 3.5 mM MMS, or 1µM 4NQO, or 16.5 µM bleomycin. S-phase progression values were obtained from histograms of Figure 3.1. The error bars represent standard deviation.

Thus, despite the disparity in the number of lesions created by MMS, 4NQO and bleomycin, all three drugs led to a similar extent of replication slowing at the doses used. In all cases, the slowing in response to DNA damage was largely checkpoint-dependent. In the absence of the Cds1 checkpoint kinase, cells completed replication by 100 minutes even in the presence of damage, as reported previously (Figure 3.1B and 3.2B) (Lindsay et al., 1998; Rhind and Russell, 1998). Although the three drugs appeared to have similar extent of slowing in wild-type, their effects in *cds1*Δ cells differed, with *cds1*Δ cells showing more checkpoint-independent slowing in MMS than in 4NQO or bleomycin (Figure 3.2B). We therefore examined if there is a difference in the mechanism by which DNA replication is slowed in response to MMS, 4NQO and bleomycin.

Inhibition of origin firing is immediate in response to 4NQO and Bleomycin, but delayed in the case of MMS

As shown in Figure 3.2A we see similar levels of bulk slowing for all three damage treatments at 60 minutes in S phase (Figure 3.2A and 3.3A). We first analyzed the effect of DNA damage on origin firing. To measure the rate of origin firing, we directly measured the number of new origins fired during the CldU pulse (green-red-green (GRG) patches) or IdU pulse (isolated green patches). The overall origin firing rate was calculated as the total number of origin firing events in each fiber normalized to total length of un-replicated DNA of that fiber and to the length of the analog pulse (Figure 3.3B). Additionally, the

origin firing rate during first analog and second analog was determined separately (Figure 3.4A, B, C). In untreated controls, the rate of origin firing in the first analog was 2.3±0.7 origins per Mb per minute, similar to previous estimates of origin firing rates (Table 3.1) (Goldar et al., 2009).

Table 3.1 Summary of all the combing datasets with the total and analog specific origin firing rate and fork density for each sample.

				Origin firing rate per Mb per min			Fork density per Mb		
Strain no.	**Expt**	**Dataset No**	**Drug**	**Total**	**CldU**	**IdU**	**Total**	**CldU**	**IdU**
yFS940	WT	WT1-N	Untreated	0.84	1.75	0.38	28.53	20.87	24.78
yFS940	WT	WT1-N	4NQO	0.35	0.88	0.08	13.82	12.19	9.66
yFS940	WT	WT2-M	Untreated	0.81	1.92	0.26	28.43	23.19	24.75
yFS940	WT	WT2-M	MMS	0.72	1.96	0.09	24.96	23.12	15.79
yFS940	WT	WT3-M	Untreated	1.33	3.18	0.41	44.26	36.13	41.12
yFS940	WT	WT3-M	MMS	0.86	2.28	0.16	30.25	27.13	24.83
yFS940	WT	WT4-M	Untreated	1.28	2.25	0.80	43.88	27.80	40.54
yFS940	WT	WT4-M	MMS	1.06	2.23	0.47	36.53	27.05	31.15
yFS940	WT	WT5-M	Untreated	1.18	2.52	0.51	39.36	29.14	36.35
yFS940	WT	WT5-M	MMS	1.09	2.63	0.32	39.63	33.24	30.29
yFS940	WT	WT6-M	Untreated	1.06	2.21	0.49	39.07	29.35	34.96
yFS940	WT	WT6-M	MMS	0.78	1.82	0.25	31.86	26.82	22.57
yFS940	WT	WT7-N	Untreated	0.97	1.58	0.66	38.59	25.39	32.37
yFS940	WT	WT7-N	4NQO	0.50	0.99	0.25	19.52	14.49	15.95
yFS940	WT	WT8-B	Untreated	1.15	1.65	0.90	42.48	24.50	36.88
yFS940	WT	WT8-B	Bleomycin	0.77	1.56	0.38	29.07	21.53	23.24
yFS940	WT	WT9-B	Untreated	1.53	3.51	0.54	62.58	51.84	52.06
yFS940	WT	WT9-B	Bleomycin	0.95	2.02	0.42	36.37	28.07	28.26
yFS941	*cds1*Δ	cds1-1-N	Untreated	1.24	3.28	0.22	41.25	36.81	37.00
yFS941	*cds1*Δ	cds1-1-N	4NQO	1.03	2.63	0.23	35.58	30.90	29.42
yFS941	*cds1*Δ	cds1-2-M	Untreated	1.43	3.35	0.47	47.49	38.02	44.57
yFS941	*cds1*Δ	cds1-2-M	MMS	1.66	3.33	0.83	57.13	40.57	49.54
yFS941	*cds1*Δ	cds1-3-M	Untreated	1.54	3.29	0.66	49.10	35.86	46.45
yFS941	*cds1*Δ	cds1-3-M	MMS	1.81	3.94	0.75	60.98	45.91	55.83
yFS941	*cds1*Δ	cds1-4-M	Untreated	1.53	3.06	0.76	51.89	36.76	47.72
yFS941	*cds1*Δ	cds1-4-M	MMS	1.59	3.50	0.64	54.82	41.94	49.99
yFS941	*cds1*Δ	cds1-5-N	Untreated	1.62	3.00	0.93	63.93	45.24	52.43
yFS941	*cds1*Δ	cds1-5-N	4NQO	1.77	2.20	1.56	61.33	30.22	55.85
yFS941	*cds1*Δ	cds1-6-B	Untreated	1.83	4.61	0.44	69.17	60.34	56.25
yFS941	*cds1*Δ	cds1-6-B	Bleomycin	1.53	3.50	0.55	58.95	47.98	41.93
yFS941	*cds1*Δ	cds1-7-B	Untreated	1.75	3.67	0.79	68.94	53.20	51.88
yFS941	*cds1*Δ	cds1-7-B	Bleomycin	1.36	2.70	0.69	53.40	39.55	41.09

Figure 3.3 4NQO, MMS and bleomycin slow S phase by reducing origin firing rate.

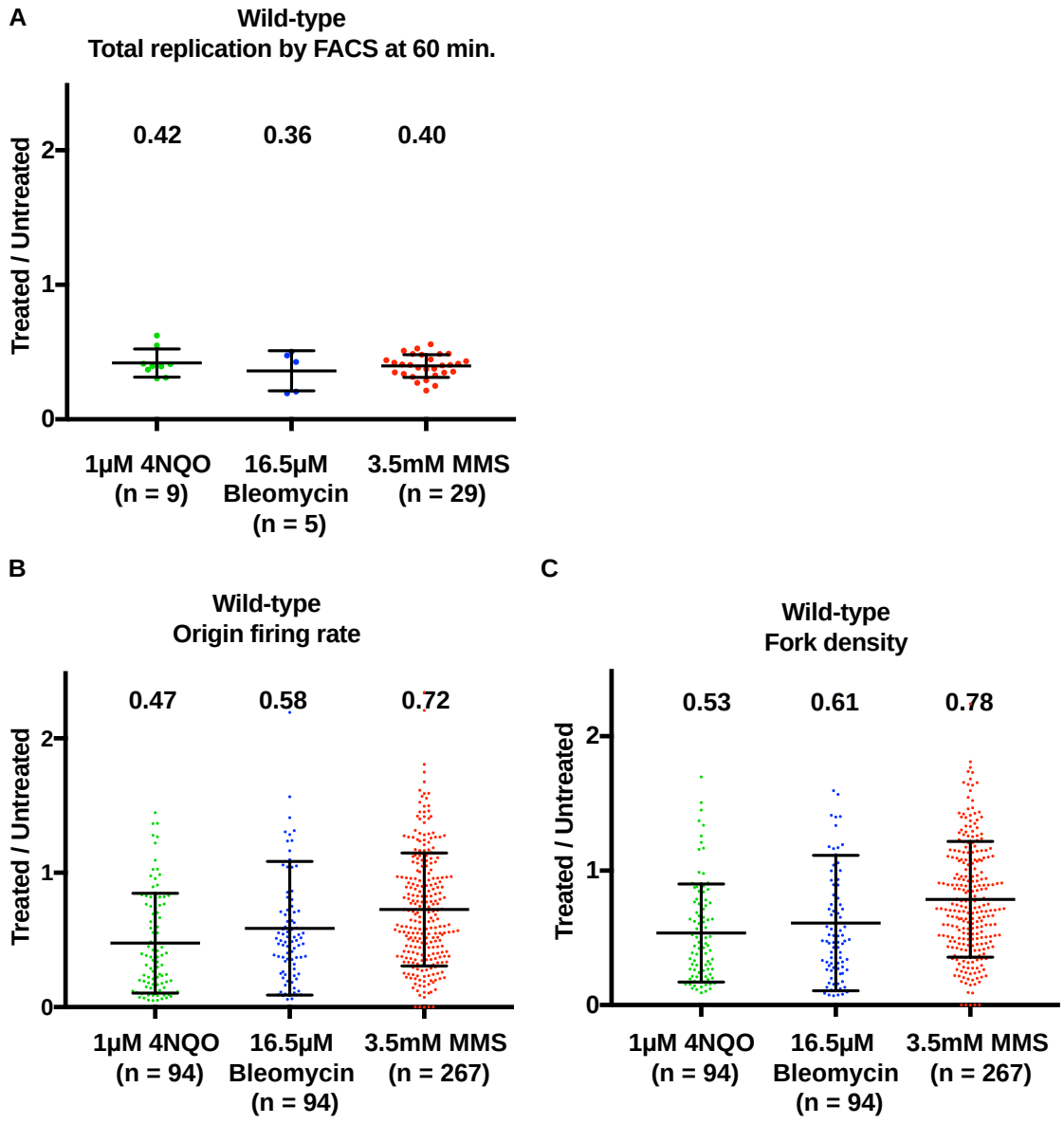

Figure 3.3 4NQO, MMS and bleomycin slow S phase by reducing origin firing rate. Wild-type cells (yFS940) were synchronized in G1 and released into

S phase untreated, or treated with 3.5 mM MMS, or 1µM 4NQO, or 16.5 µM bleomycin. Cells were labeled at mid-S phase with CldU followed by IdU for DNA combing. All parameters are represented as a ratio of treated v. untreated sample. (A) 4NQO, bleomycin and MMS slow S phase to similar extent by flow cytometry. Total replication by FACS was calculated at 60 minutes after release, which is close to the mid-point of analog labeling. (B) and (C) 4NQO, bleomycin and MMS show differing levels of reduction in origin firing rate and fork density. For calculations of origin firing rate and fork density refer to Chapter II. For each sample of each experiment, about 25Mb of DNA was collected. All error bars represent SD.

In the presence of 4NQO, the origin firing rate in wild-type cells decreased to 47% of the untreated control ($p=5.17x10^{-12}$, t tests were used for all statistical tests) (Figure 3.3B and Table 3.1). Since, the origin firing rate only measures the origins that fired during the analog pulses, we also measured the density of active forks in the datasets in order to estimate the effect on origin firing prior to the analog pulses (see Chapter II for details). Fork density in 4NQO-treated cells was 64% of the untreated control ($p=1.28x10^{-6}$) during the first analog pulse and 44% ($p=3.08x10^{-13}$) in the second, consistent with the trend seen in origin firing rates (Figure 3.4A). Thus, the response to 4NQO included an immediate reduction in origin firing rate. We see a similar trend for bleomycin treated sample. The origin firing rate decreases to 58% ($p=7.45x10^{-5}$) and the fork density decreases to 61% ($p=1.33x10^{-5}$) (Figure 3.3B and 3.3C). Analog specific estimation shows that bleomycin treatment leads to reduction in the origin firing rate in the first analog as well as second analog to 69% ($3.91x10^{-4}$) and shows a corresponding decrease in fork density during the first (77%, $p=7.65x10^{-4}$) and the second analog (55%, $p=8.54x10^{-7}$) (Figure 3.4B).

Figure 3.4 Inhibition of origin firing is immediate in response to 4NQO and Bleomycin, but delayed in the case of MMS

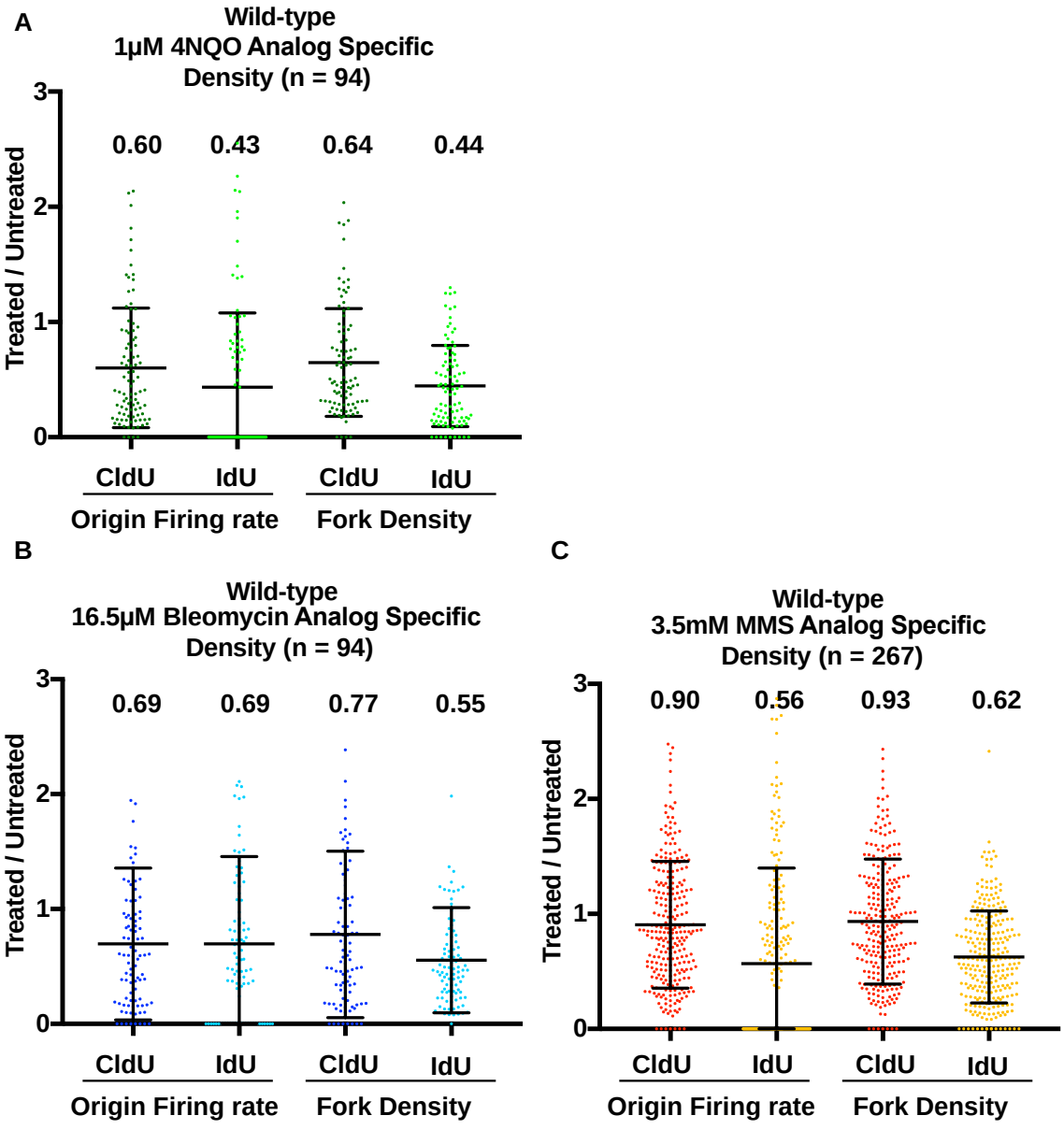

Figure 3.4 Inhibition of origin firing is immediate in response to 4NQO and Bleomycin, but delayed in the case of MMS (A), (B), (C) Analog specific estimations of origin firing rate and fork density for 4NQO, bleomycin and MMS respectively. 4NQO and bleomycin treatment leads to immediate reduction in origin firing rate in the first analog while in MMS the reduction is apparent only during the second analog. For calculations of origin firing rate and fork density refer to Chapter II. For each sample of each experiment, about 25Mb of DNA was collected. All error bars represent SD.

In case of MMS, the overall origin firing rate was reduced to 72% ($p=1.18x10^{-6}$) (Figure 3.3B). Analyzing origin firing during the first and second pulse separately, we saw no statistically significant reduction in the first analog (90%, p=0.0748) followed by a stronger reduction to 56% ($p=7.15x10^{-11}$) in the second analog (Figure 3.4C). Therefore, the effect of MMS on origin firing rate is delayed. This conclusion was supported by two observations. Firstly, the average fork density across both analogs in MMS showed a modest reduction to 78% ($p=2.59x10^{-5}$) as compared to 53% ($p=5.7x10^{-12}$) in 4NQO (Figure 3.3C). Second, the analog-specific fork density estimations for MMS followed a similar trend as the origin firing rate showing a greater reduction during the second analog (0.93 v. 0.62, Figure 3.4C). Hence, the effect of MMS-induced damage on origin firing is only manifest late in S-phase, after significant bulk slowing has already occurred, whereas 4NQO- and bleomycin-induced damage inhibit origin firing immediately in early S phase.

Fork rate declines in response to MMS but not 4NQO or bleomycin

Since 4NQO and MMS both create polymerase-blocking lesions (Friedberg et al., 1995; Larson et al., 1985; Minca and Kowalski, 2011; Lopez-Mosqueda et al., 2010), we next studied how these drugs affect fork speed. We measured fork rate in the combing data as the length of the green track (second analog) continuing from a red track (first analog), divided by the length of the chase time (10 minutes). The average fork rate in our untreated samples was 0.91±0.02

kb/minute, which is within the range of previous estimates (Conti et al., 2007; Conti et al., 2010; Técher et al., 2013; Petermann et al., 2008; Petermann et al., 2010).

In MMS, the fork rate decreases to 76% of the untreated control ($p=6.13x10^{-38}$) (Figure 3.5A and Table 3.2). The reduction in fork rate was expected since the lesions are so frequent that every fork encounters about ten of lesions during the 10 minutes pulse. In case of 4NQO, the lesions are significantly less common, so only about half of the forks should encounter a lesion during the second pulse. Consistent with the low density of lesions, fork rates in 4NQO treated cells were similar to untreated cells (Figure 3.5A). In fact, the fork rate showed a 27% increase in the presence of 4NQO as compared to untreated cells ($p=5.75x10^{-4}$). The dose of bleomycin used should create only 5 breaks per haploid yeast genome and therefore should not affect fork rates. Consistently we do not see any statistically significant reduction in fork rate for bleomycin treated sample as compared to untreated sample ($p=0.3138$) (Figure 3.5A).

Figure 3.5 Fork rate decreases in response to MMS and fork stall rate increases in response to damage

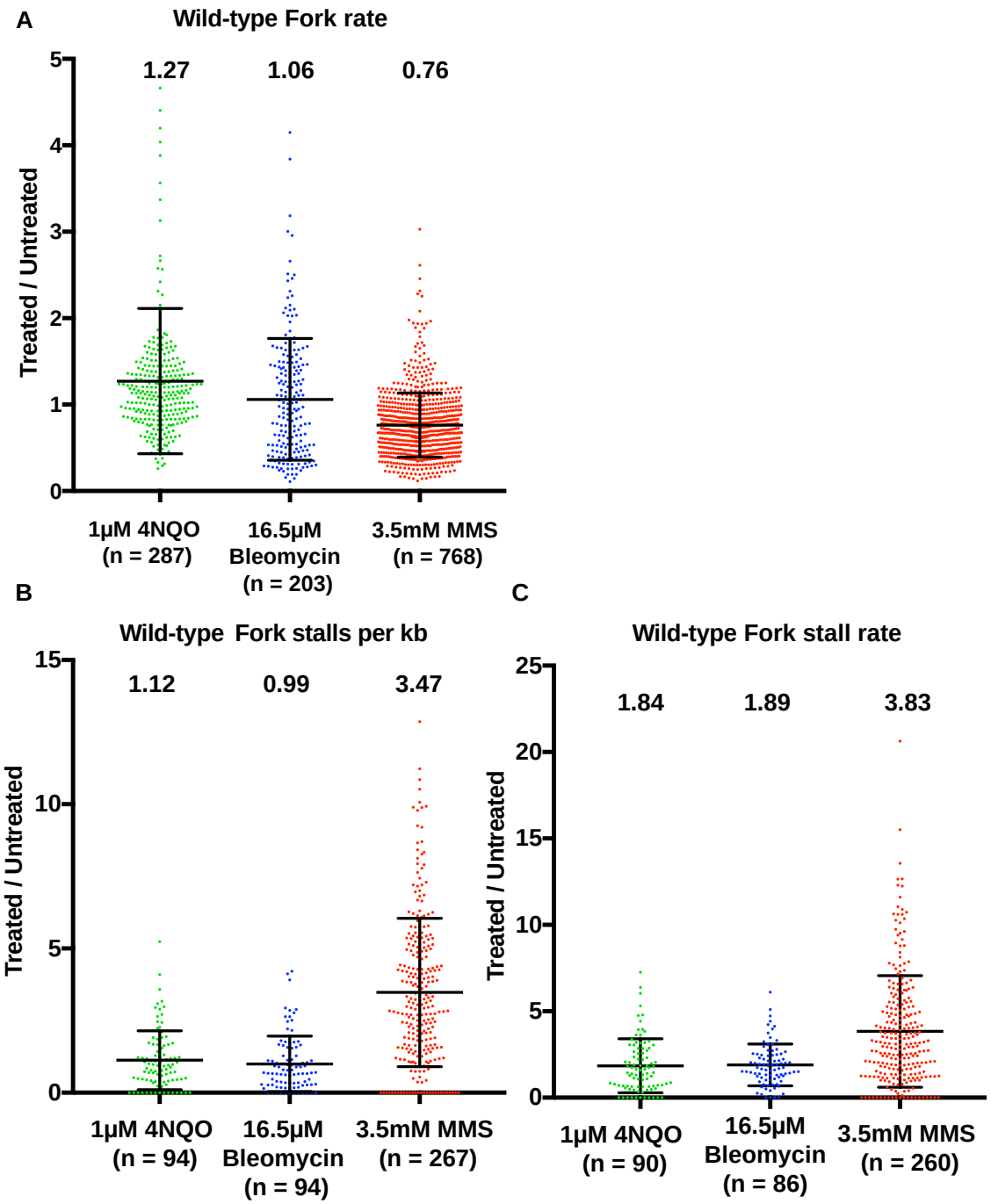

Figure 3.5 Fork rate decreases in response to MMS and fork stall rate increases in response to damage (A) Fork rate decreases in response to MMS, but not in response to 4NQO or bleomycin. (B) Fork stalls per kb increases in response to MMS, but not in response to 4NQO or bleomycin (C) Fork stall rate increases in response to MMS, 4NQO and bleomycin. For calculations of fork rate, fork stalls per kb and fork stall rate refer to Chapter II. All error bars represent SD.

Table 3.2 Summary of all the combing datasets with the fork rate for each sample.

Strain no.	Expt	Dataset No.	Drug	Fork rate kb/min	pH of combing buffer
yFS940	WT	WT1-N	Untreated	0.67	6.35
yFS940	WT	WT1-N	4NQO	0.75	6.35
yFS940	WT	WT2-M	Untreated	0.67	6.35
yFS940	WT	WT2-M	MMS	0.53	6.35
yFS940	WT	WT3-M	Untreated	0.60	6.35
yFS940	WT	WT3-M	MMS	0.43	6.35
yFS940	WT	WT4-M	Untreated	0.92	6.25
yFS940	WT	WT4-M	MMS	0.66	6.25
yFS940	WT	WT5-M	Untreated	0.91	6.25
yFS940	WT	WT5-M	MMS	0.6	6.25
yFS940	WT	WT6-M	Untreated	0.89	6.25
yFS940	WT	WT6-M	MMS	0.57	6.25
yFS940	WT	WT7-N	Untreated	0.85	6.2
yFS940	WT	WT7-N	4NQO	0.88	6.2
yFS940	WT	WT8-B	Untreated	0.65	6.2
yFS940	WT	WT8-B	Bleomycin	0.62	6.2
yFS940	WT	WT9-B	Untreated	0.48	6.2
yFS940	WT	WT9-B	Bleomycin	0.47	6.2
yFS941	*cds1* Δ	cds1-1-N	Untreated	0.42	6.35
yFS941	*cds1* Δ	cds1-1-N	4NQO	0.48	6.35
yFS941	*cds1* Δ	cds1-2-M	Untreated	0.61	6.25
yFS941	*cds1* Δ	cds1-2-M	MMS	0.27	6.25
yFS941	*cds1* Δ	cds1-3-M	Untreated	0.76	6.25
yFS941	*cds1* Δ	cds1-3-M	MMS	0.43	6.25
yFS941	*cds1* Δ	cds1-4-M	Untreated	0.75	6.25
yFS941	*cds1* Δ	cds1-4-M	MMS	0.35	6.25
yFS941	*cds1* Δ	cds1-5-N	Untreated	0.61	6.2
yFS941	*cds1* Δ	cds1-5-N	4NQO	0.58	6.2
yFS941	*cds1* Δ	cds1-6-B	Untreated	0.58	6.2
yFS941	*cds1* Δ	cds1-6-B	Bleomycin	0.51	6.2
yFS941	*cds1* Δ	cds1-7-B	Untreated	0.52	6.2
yFS941	*cds1* Δ	cds1-7-B	Bleomycin	0.52	6.2

Fork stalling increases in response to MMS, 4NQO and bleomycin

In case of MMS treated sample, we only see a modest reduction in fork density as compared to 4NQO and bleomycin (Figure 3.3C). In particular, there is no statistically significant reduction in fork density in the MMS treated sample during the first analog (93%, p=0.1951) (Figure 3.4C). However by bulk assay we see the same kinetics of slowing for all three damage treatments (Figure 3.2A and 3.3A). A possible explanation for this discrepancy is that forks stall during the first pulse in response to damage and thus are not observed during the second pulse (Chapter II, Figure 2.6). We therefore interrogated our combing data for evidence of fork stalling.

We first determined the absolute number of stalls per kb for each dataset (see Chapter II for details). The absolute number of stalls per kb determines the contribution of stalled forks towards total replication slowing. In MMS treated sample we see a 3.47-fold increase in the number of stalls as compared to untreated ($p=6.23x10^{-27}$), while we see no significant increase in stalling in response to 4NQO (1.12, p=0.604) and bleomycin (0.99, p=0.346) (Figure 3.5B). Thus an increase in the total number of stalls per kb in response to MMS helps explain the slowing of total replication to similar levels as compared to 4NQO and bleomycin despite having a delayed effect on origin firing rate.

Next we estimated the fork stall rate. We define the fork stall rate as the total number of stall events per fiber during the first analog pulse divided by the total number of ongoing forks in that fiber during the first analog. Although the

absolute number of stalls per kb in response to 4NQO and bleomycin treatment is similar to the wild-type untreated sample, the treated samples have far fewer origins firing as compared to untreated sample (Figure 3.3B and 3.5B). Therefore the rate of stalling normalized to the origin firing rate is higher in the treated sample (Figure 3.5C). The average stall rate per fiber in the untreated sample was 14%. The fork stall rate showed 1.8-fold increase in response to 4NQO ($p=1.2x10^{-4}$) and a 1.9-fold increase in response to bleomycin ($p=2.26x10^{-7}$), whereas MMS caused a 3.8-fold increase relative to untreated cells ($p=1.55x10^{-26}$) (Figure 3.5C). Combining our stall-rate data with estimates of lesion density, we estimate that forks stall at 1.3% of 4NQO lesions and at 0.5% of MMS lesions, consistent with the fact that 4NQO creates a bulkier lesion than MMS. The stall rate per lesion is more complicated to interpret for bleomycin. Since the stalls we detect are not at the ends for our fibers, they cannot be at the sites of bleomycin-induced double-strand breaks. However, bleomycin creates about a 20-fold excess of single-strand nicks to double strand breaks, which, at the dose we used should produce one nick about every 150 kb (Chen and Stubbe, 2005). In the absence of repair, forks would stall at 8.1% of bleomycin-induced nicks. If nicks are repaired, that rate of stalling at the remaining unrepaired nicks could be much higher. Although the stall events seem to be infrequent relative to lesion density, approximately 53% of forks in MMS-treated cells and 25% of forks in 4NQO- and bleomycin-treated cells stalled, contributing significantly to slowing, and ensuring that all treated cells had many stalled forks.

Inhibition of origin firing is checkpoint dependent

To determine the role of the intra-S checkpoint in the observed DNA-damage dependent changes in replication kinetics, we repeated our combing experiments in checkpoint-deficient *cds1*Δ cells. In the presence of 4NQO, wild-type cells replicated 42% ($p=5.55x10^{-16}$) as much as untreated cells, as assayed by flow cytometry at 60 minutes after release, whereas, in the absence of checkpoint, *cds1*Δ 4NQO treated cells replicated 77% as compared to untreated cells (p=5.82x10-8) (Figure 3.6A). 4NQO did not significantly reduce origin firing in *cds1*Δ cells (89%, p=0.206), as opposed to 47% in wild-type cells ($p=5.17x10^{-12}$) (Figure 3.6B).

Figure 3.6 Reduction in origin firing rate is checkpoint dependent

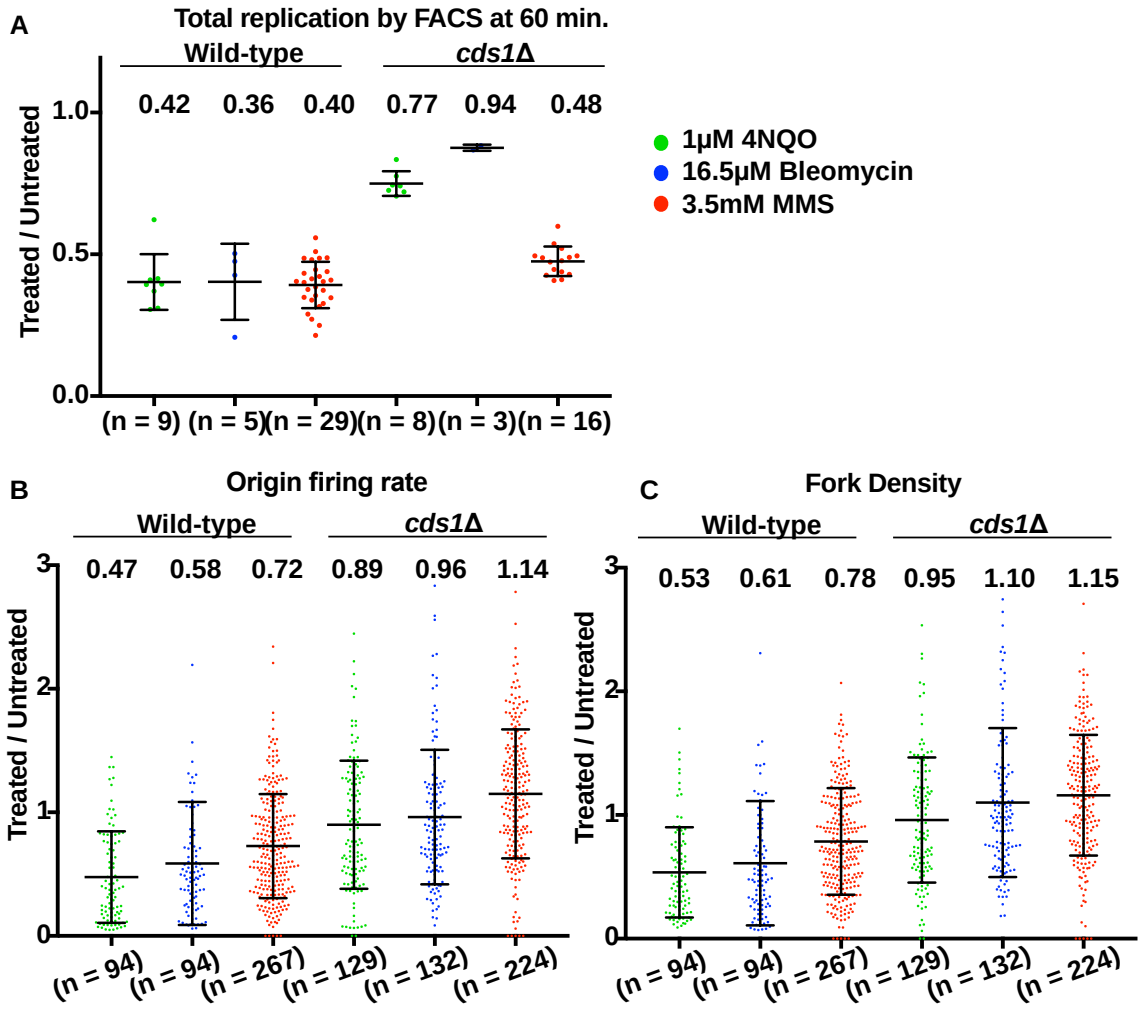

Figure 3.6 Reduction in origin firing rate is checkpoint dependent. *cds1*Δ cells (yFS941) were synchronized in G1 and released into S phase untreated, or treated with 3.5 mM MMS, or 1μM 4NQO, or 16.5 μM bleomycin. Cells were labeled at mid-S phase with CldU followed by IdU for DNA combing. All parameters from combing data of *cds1*Δ are represented as a ratio of treated v. untreated. Wild-type dataset is plotted alongside *cds1*Δ for comparison. (A) Total replication by FACS was calculated at 60 minutes after release, which is close to the mid-point of analog labeling. (B) and (C) Reduction in origin firing

and fork density is checkpoint dependent for 4NQO, bleomycin and MMS. For calculations of origin firing rate and fork density refer to Chapter II. For each sample of each experiment, about 25Mb of DNA was collected. All error bars represent SD.

Thus, the inhibition of origin firing in response to 4NQO is checkpoint-dependent (Figures 3.3B and 3.6B). Analog specific origin density and fork density followed similar trends as the total origin firing rate data (Figure 3.7A). During both the analog pulses, *cds1*Δ cells had a higher origin firing rate and fork density than wild-type cells (Figure 3.7A).

Likewise, inhibition of origin firing in response to bleomycin and MMS is checkpoint-dependent (Figure 3.6B, 3.6C, 3.7B and 3.7C). In wild-type cells, the overall origin firing rate was reduced to 58% by bleomycin ($p=7.45x10^{-5}$) and 72% by MMS ($p=1.18x10^{-6}$) treatment (Figures 3.3B and 3.6B). In contrast, *cds1*Δ cells showed no significant decrease in origin firing relative to untreated cells when treated with bleomycin (96%, p=0.389) or MMS (114%, p=0.011) (Figure 3.6B). Analog specific estimation of fork density and origin firing rate in *cds1*Δ treated with bleomycin or MMS showed a similar trend (Figure 3.7B and 3.7C). *cds1*Δ cells had higher fork density and origin firing rate in response to bleomycin and MMS than wild-type cells for both analog pulses (Figure 3.7B and 3.7C).

Figure 3.7 Reduction in origin firing rate in response to damage during each analog is checkpoint dependent

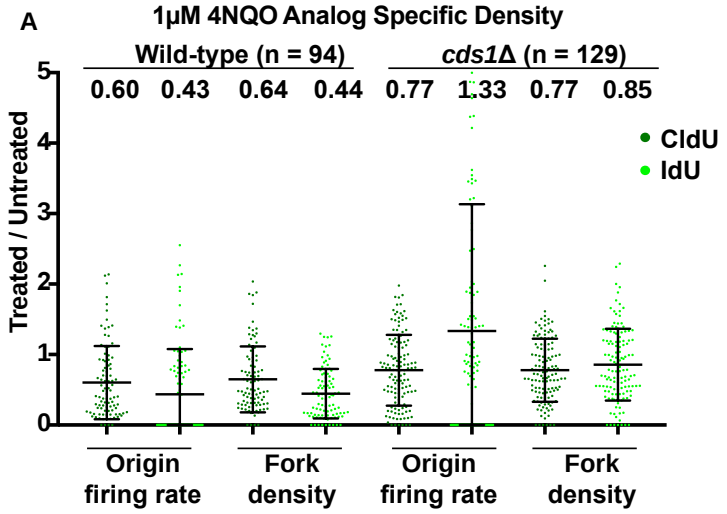
A
1μM 4NQO Analog Specific Density
Wild-type (n = 94)
cds1Δ (n = 129)
0.60 0.43 0.64 0.44 0.77 1.33 0.77 0.85
CldU
IdU
Treated / Untreated
0
1
2
3
4
5
Origin firing rate
Fork density
Origin firing rate
Fork density

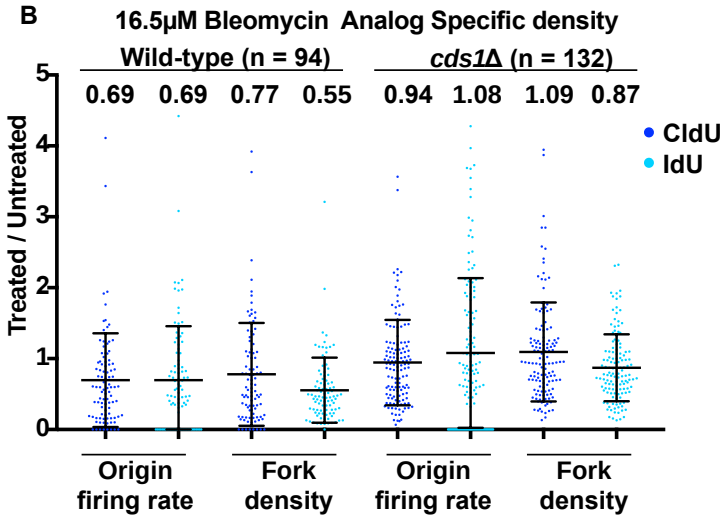
B
16.5μM Bleomycin Analog Specific density
Wild-type (n = 94)
cds1Δ (n = 132)
0.69 0.69 0.77 0.55 0.94 1.08 1.09 0.87
CldU
IdU
Treated / Untreated
0
1
2
3
4
5
Origin firing rate
Fork density
Origin firing rate
Fork density

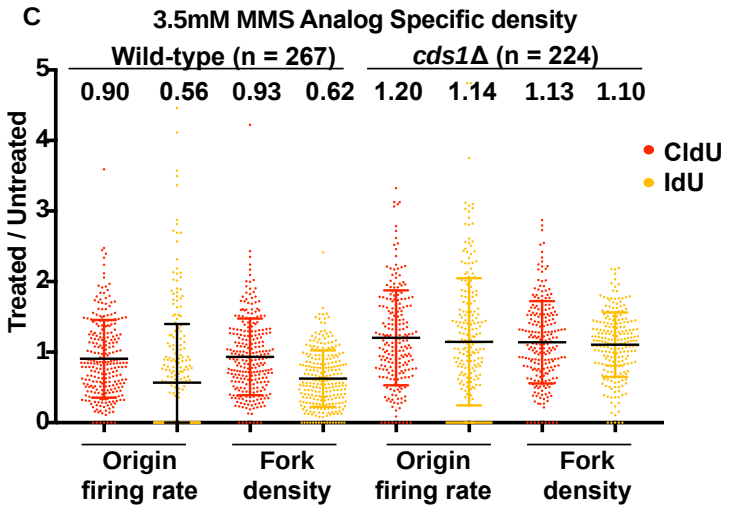
C
3.5mM MMS Analog Specific density
Wild-type (n = 267)
cds1Δ (n = 224)
0.90 0.56 0.93 0.62 1.20 1.14 1.13 1.10
CldU
IdU
Treated / Untreated
0
1
2
3
4
5
Origin firing rate
Fork density
Origin firing rate
Fork density

Figure 3.7 Reduction in origin firing rate in response to damage during each analog is checkpoint dependent. (A, B, C) Analog specific estimations of origin firing rate and fork density for 4NQO, bleomycin and MMS respectively shows higher values in *cds1*Δ than wild-type. For calculations of origin firing rate and fork density refer to Chapter II. For each sample of each experiment, about 25Mb of DNA was collected. All error bars represent SD.

In the absence of DNA damage, the lack of Cds1 caused a 51% increase in the rate of origin firing (3.5±0.6 v. 2.3±0.6 origins firing/Mb/minute, Table 3.1), consistent with previous reports in other systems of checkpoint inhibition of origin firing in unperturbed S phase (Petermann et al., 2010; Shechter et al., 2004b). Nonetheless, loss of Cds1 increases origin firing in damaged cells to the same level as in undamaged cells, showing that there is no checkpoint independent inhibition of origin firing (Figure 3.8).

Figure 3.8 *cds1*Δ cells have a higher origin firing rate as compared to wild-type in untreated as well as treated samples.

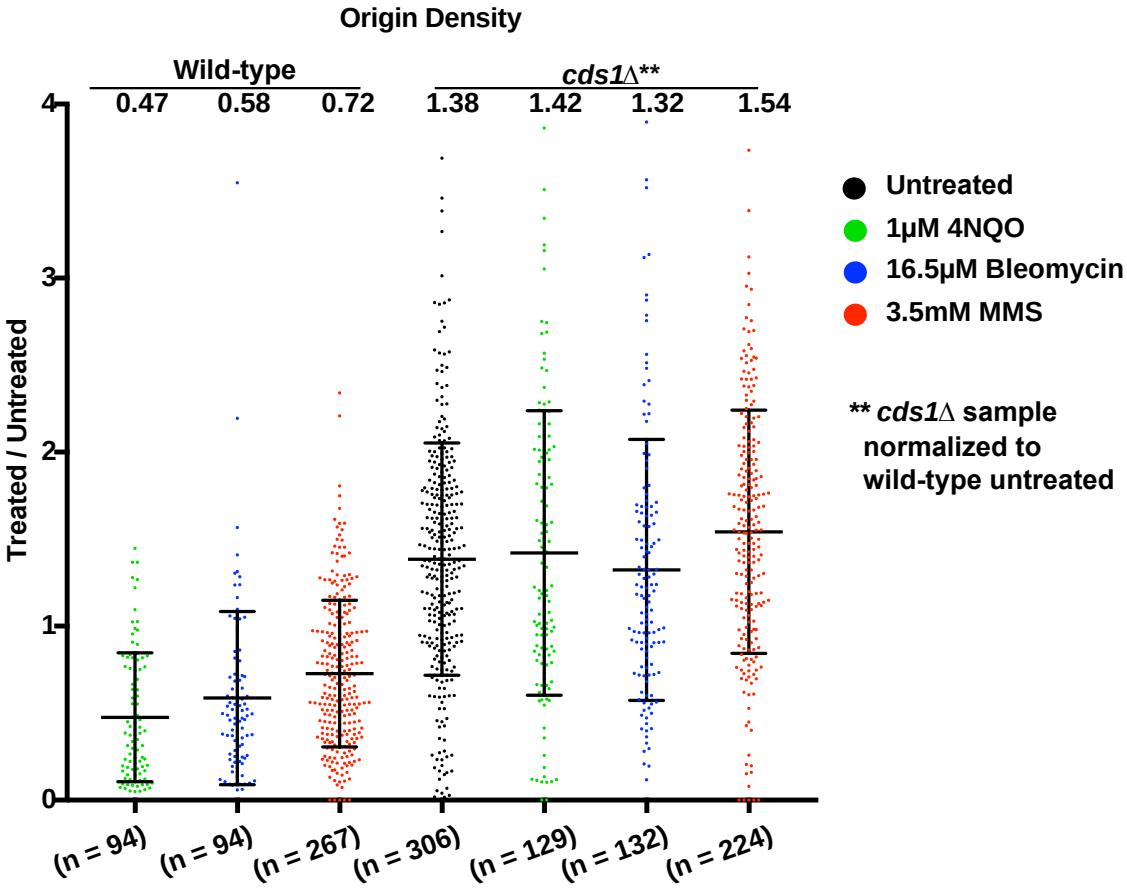

Figure 3.8 *cds1*Δ cells have a higher origin firing rate as compared to wild-type in untreated as well as treated samples. Origin firing rate from *cds1*Δ untreated and treated samples, and wild-type treated samples were normalized to wild-type untreated sample.

Reduction in fork rate is checkpoint independent

In MMS-treated wild-type cells, fork rate was reduced to 76% of the untreated cells ($p=6.14x10^{-38}$) (Figures 3.5A and 3.9A). This effect was not checkpoint-dependent. In fact, at 61% ($p=6.13x10^{-66}$), *cds1*Δ cells showed a greater reduction in fork rate than seen in wild-type cells in response to MMS (Figure 3.9A). Thus, the observed reduction in fork rate in response to MMS seems to be due to the physical presence of the lesions and the checkpoint activation may facilitate efficient by-pass of the lesions.

Figure 3.9 Reduction in fork rate and increase in fork stalling is checkpoint independent.

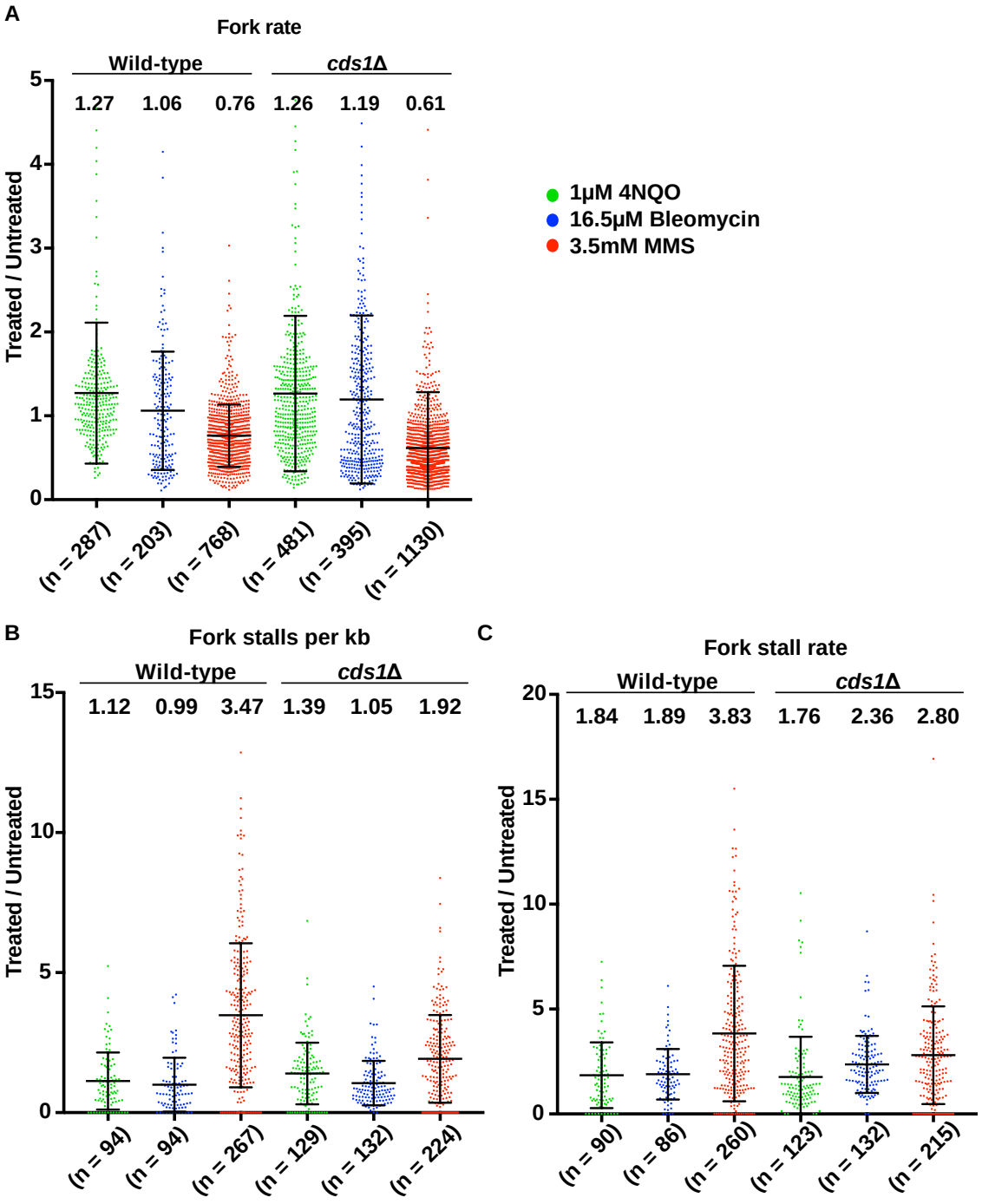

Figure 3.9 Reduction in fork rate and increase in fork stalling is checkpoint independent. (A) Fork rate, (B) fork stalls per kb and (C) fork stall rate data for

*cds1*Δ (yFS941) treated with 4NQO, bleomycin and MMS. Both parameters are represented as a ratio of treated v. untreated. Wild-type dataset is plotted alongside *cds1*Δ for comparison. See Chapter II for calculation of fork rate, fork stall per kb and fork stall rate.

Fork rates showed similar increase in *cds1*Δ cells treated with 4NQO (126%, $p=1.17x10^{-5}$) as they did in wild-type cells (127%, $p=5.75x10^{-4}$) (Figures 3.5A and 3.9A). Although the lack of Cds1 does not seem to have an effect on the relative fork rate between untreated and 4NQO-treated cells, it does have a significant effect on the absolute fork rate in untreated cells. Forks moved significantly slower in untreated *cds1*Δ cells than in wild-type cells (0.72 v 0.91 kb/min, $p < 10^{-9}$, Table 3.2). This difference may be an indirect effect of the higher origin firing rate and fork density in *cds1*Δ cells (Table 3.1). Several groups working in different systems have made the similar observation that fork rate is inversely correlated to the number of active forks, perhaps due to constrains on a limiting factor required for replication, such as the dNTP pool (Herrick and Sclavi, 2007; Poli et al., 2012; Herrick and Bensimon, 2008).

Fork stalling in response to damage is largely checkpoint independent

Similar to wild-type cells, we see an increase in fork stalls per kb in response to MMS treatment in *cds1*Δ but not in case of 4NQO and bleomycin (Figure 3.5B and 3.9B). The fork stalls per kb shows a 1.9-fold increase in response to MMS as compared to untreated ($p=4.42x10^{-10}$) *cds1*Δ cells. Fork stalls per kb does not change significantly between 4NQO (1.39, p=0.987) and bleomycin (1.05, p=0.839) treated *cds1*Δ cells as compared to untreated *cds1*Δ (Figure 3.9B).

In wild-type cells, the fork stalling rate was increased 1.8-fold by 4NQO ($p=1.2x10^{-4}$), 1.9-fold by bleomycin ($p=2.26x10^{-7}$) and 3.8-fold ($p=1.55x10^{-26}$) by

MMS treatment, relative to untreated cells (Figures 3.5C and 3.9C). In *cds1*Δ cells, we saw a 1.7-, 2.3- and 2.8-fold increase of the stall rate in 4NQO ($p=2.59x10^{-4}$), bleomycin ($p=7.96x10^{-13}$) and MMS ($p=2.93x10^{-15}$) treated cells respectively as compared to untreated cells (Figure 3.9C). This increase in stall rate is slightly lower in MMS-treated *cds1*Δ cells than in wild-type cells (2.8 fold v 3.8 fold, $p=9.86x10^{-5}$), showing that there are checkpoint-dependent and -independent contributions to stalling in response to MMS, however the difference in stall rates for *cds1*Δ treated with 4NQO (1.7 fold v 1.8 fold, p=0.746) and bleomycin (2.3 fold v 1.89 fold, p=0.01) as compared to wild-type are not as significant. Therefore the bulk of fork stalling events appears to be checkpoint-independent (Figure 3.9C).

Delayed Inhibition of Origin Firing by MMS Correlates with Delayed Checkpoint Kinase Activation

To test the possibility that the later inhibition of origin firing seen in response to MMS (Figure 3.3C and 3.4C) is due to delayed checkpoint activation, and to confirm that the doses of the various damaging agents we use cause comparable checkpoint activation, we assayed activation of the Cds1 S-phase checkpoint kinase in response to MMS, 4NQO and bleomycin. Cells with an HA-tagged Cds1 were synchronized in G1 and released into DNA damage (Figure 3.10).

Figure 3.10 S phase progression of time-courses used for kinase activity measurement

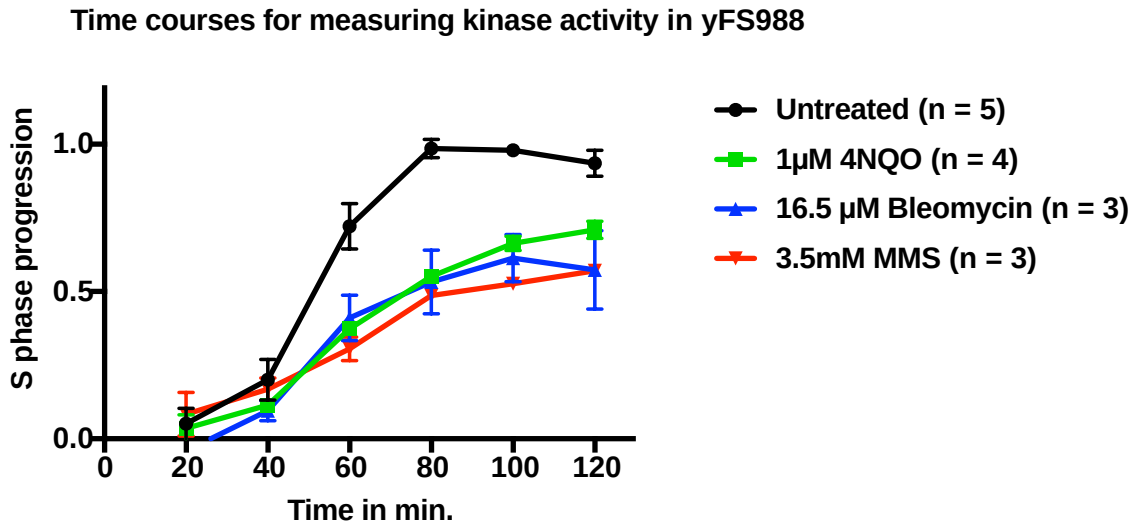

Figure 3.10 S phase progression of time-courses used for kinase activity measurement. *cds1*-HA (yFS988) cells were synchronized in G1 phase using cdc10-M17 temperature sensitive allele followed by elutriation. Elutriated G1 cells were released into permissive temperature untreated or treated with 3.5 mM MMS or 1 µM 4NQO or 16.5 µM Bleomycin. S phase progression was followed by taking samples for FACS.

Cells were harvested throughout S phase and Cds1 was immunopurified and split into two portions. One-half was used to estimate the amount of Cds1 pulled down by western blot and the second half was used to perform *in vitro* kinase assays. Kinase assay reactions were run on SDS-PAGE gel normalized to the amount of pull down in each lane (Figure 3.11). Average kinetics of kinase activity from all time courses is shown in Fig 3.11A and results from individual time courses are shown in Fig 3.11B (Figure 3.11A and 3.11B). We observe a significant and reproducible delay of Cds1 activation in response to MMS, relative to both 4NQO and bleomycin (Figure 3.11A). These results are consistent with MMS taking longer to disrupt a sufficient number of replication forks to trigger a robust checkpoint response.

Figure 3.11: Delayed Inhibition of Origin Firing by MMS Correlates with Delayed Checkpoint Kinase Activation.

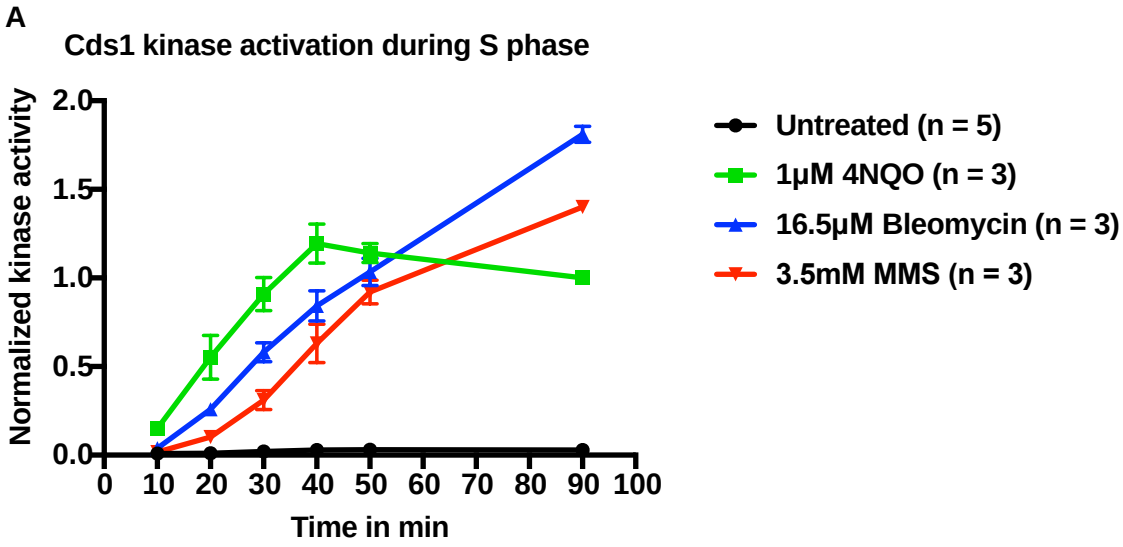

B

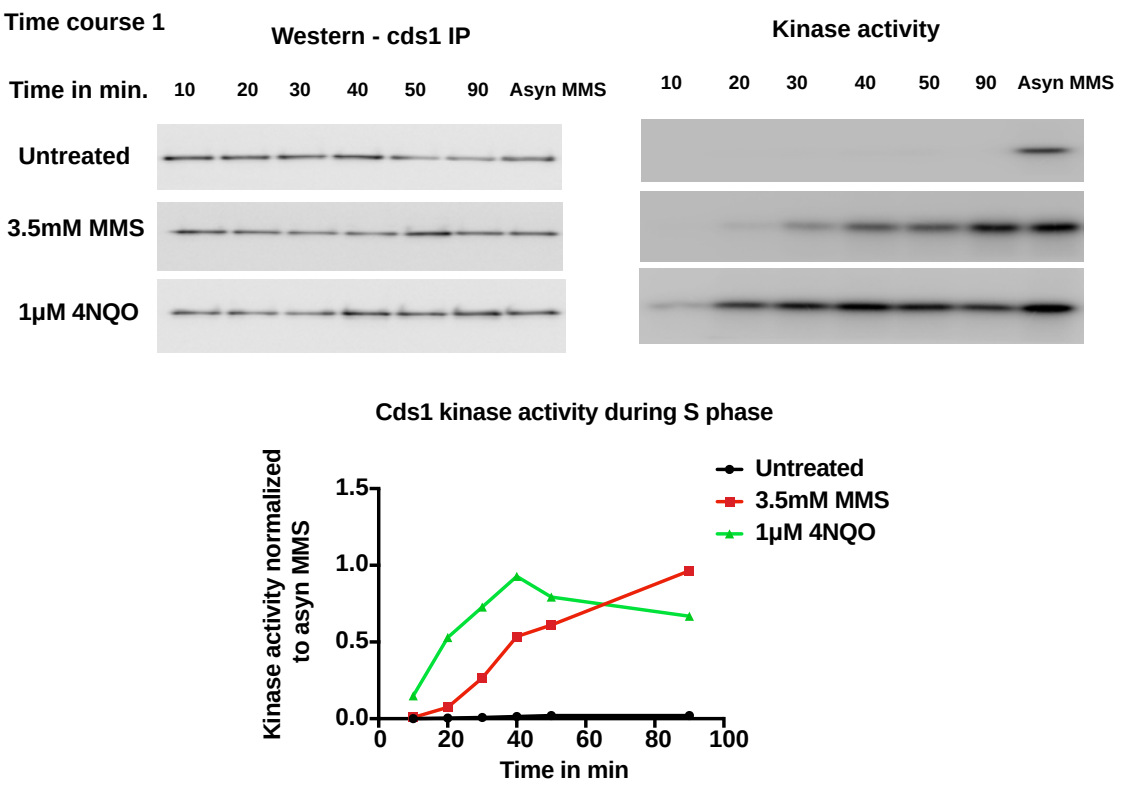
Time course 1
Western - cds1 IP
Kinase activity
Time in min.
10
20
30
40
50
90
Asyn MMS
Untreated
3.5mM MMS
1µM 4NQO
Cds1 kinase activity during S phase
Kinase activity normalized to asyn MMS
1.5
1.0
0.5
0.0
0
20
40
60
80
100
Time in min
Untreated
3.5mM MMS
1µM 4NQO

Time course 2

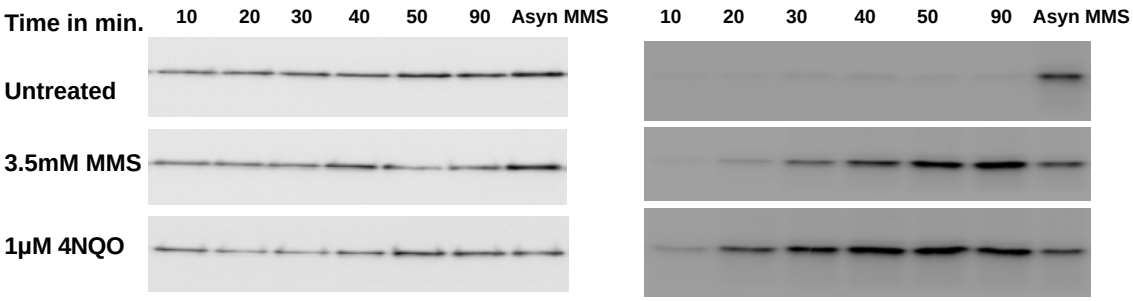

Cds1 kinase activity during S phase

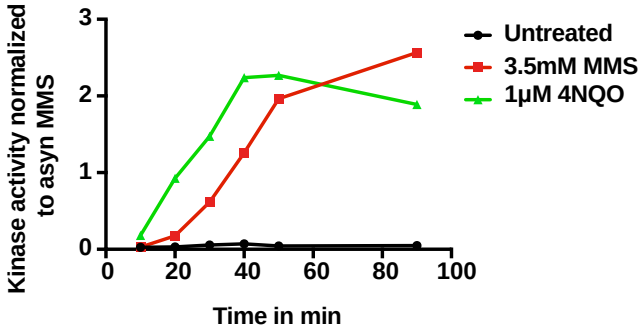

Time course 3

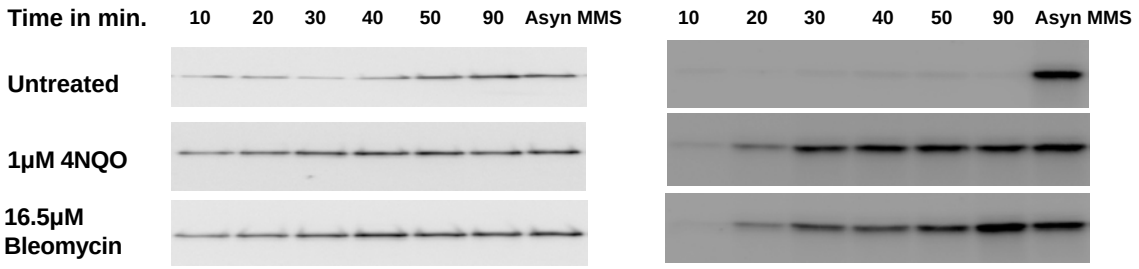

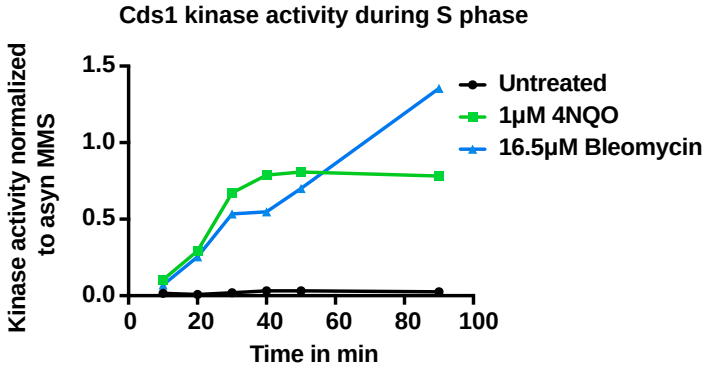

Time course 4

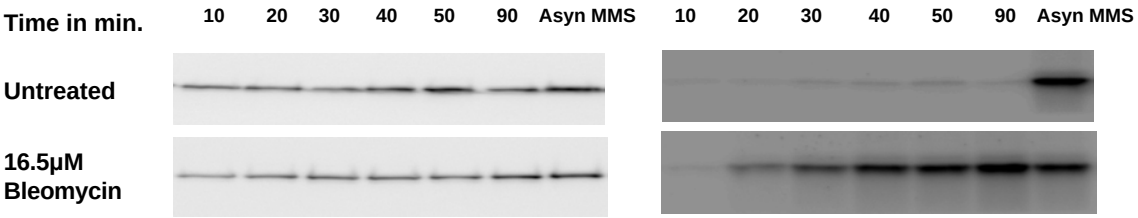

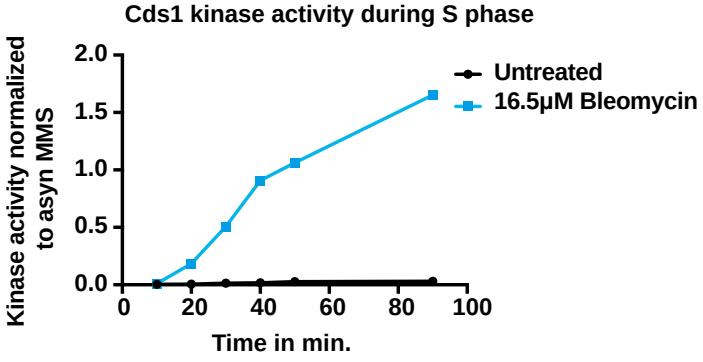

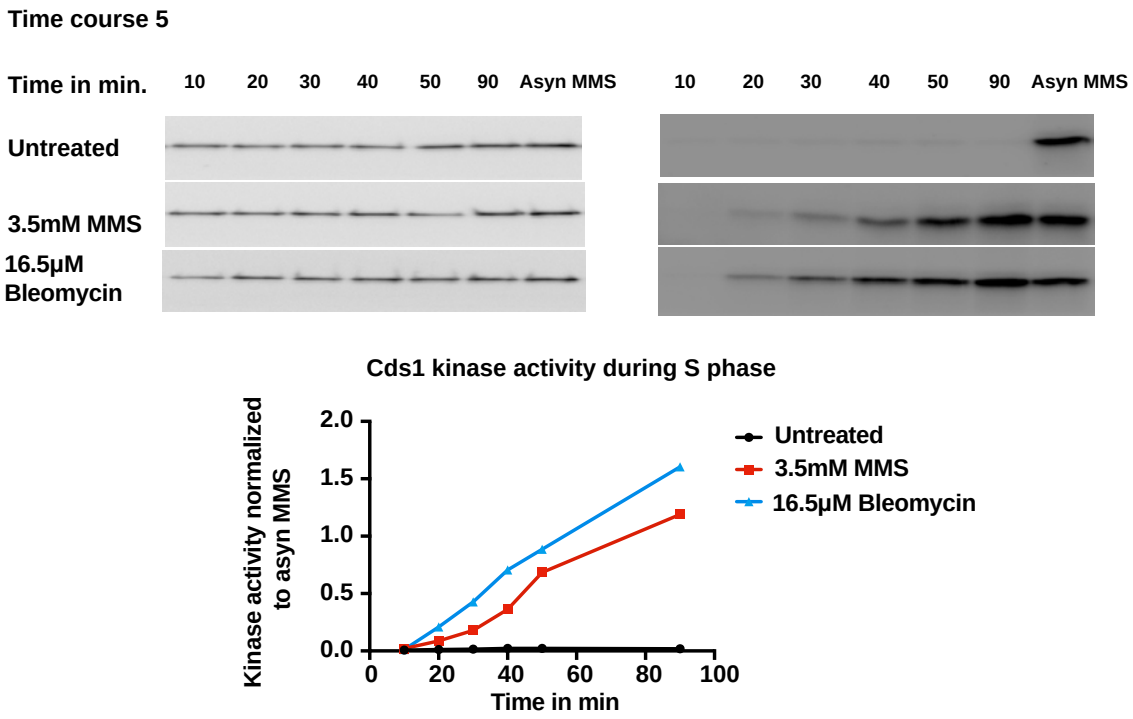

Figure 3.11: Delayed Inhibition of Origin Firing by MMS Correlates with Delayed Checkpoint Kinase Activation. (A) Wild-type cells with an HA-tagged Cds1 (yFS988) were G1 synchronized, released into S phase is the presence of 1μM 4NQO, 16.5 μM bleomycin or 3.5 mM MMS, harvested at the indicated times and processed for Cds1 IP kinase assays. Average signal normalized to the 4NQO 90-minute time point is plotted ± standard error of the mean. (B) Kinase assay to measure Cds1 activation in 5 time courses. For each time course, Cds1 western was done to estimate the amount of Cds1 pulled down in each condition. Kinase assay reactions were run normalized to the amount of Cds1 pull down. Signal from each lane of the kinase assay gel was normalized to the asynchronous MMS sample to get the normalized kinase activity.

Accumulation of RPA foci in response to 4NQO and MMS

To investigate the relationship between the fork stalling that we measured by DNA combing and the fate of forks in living cells, we visualized replication protein A (RPA)-GFP foci, which mark the accumulation of single-stranded DNA (ssDNA), in cells treated with MMS or 4NQO. Because RPA-coated single-stranded DNA is a trigger for the activation of the intra-S checkpoint (Zou and Elledge, 2003; Cimprich and Cortez, 2008; Byun et al., 2005; Xu et al., 2008; Wu et al., 2005), we hypothesized that stalls that accumulate substantial amounts of RPA are likely to correlate with checkpoint activation, but that stalls that lead to less RPA accumulation may be checkpoint silent.

We analyzed 100 cells for each sample and sorted them into three categories based on the intensity and number of foci: strong foci, weak foci or no foci (see Methods for details). 21% of untreated wild-type cells have some foci, consistent with previous reports (Sabatinos and Forsburg, 2015), but the majority of these are weak foci, consistent with the hypothesis that weak foci do not activate the checkpoint (Figure 3.12A). In the presence of damage, we saw distinctly different responses to MMS and 4NQO. In the presence of MMS, 36% of cells had strong foci (Figure 3.12A). Since all MMS-treated cells have stalled forks (Table 3.3), we conclude that only a minority of MMS-induced stalls accumulate substantial ssDNA. On the contrary, essentially all 4NQO-treated cells had strong foci, suggesting a qualitatively different nature of 4NQO-induced fork stalls, in which the majority of 4NQO-induced lesions accumulated

substantial ssDNA (Figure 3.12A). As previously reported (Sabatinos et al., 2012), RPA did not accumulate at HU-stalled forks in checkpoint-proficient cells.

Figure 3.12: Accumulation of RPA foci in response to 4NQO and MMS.

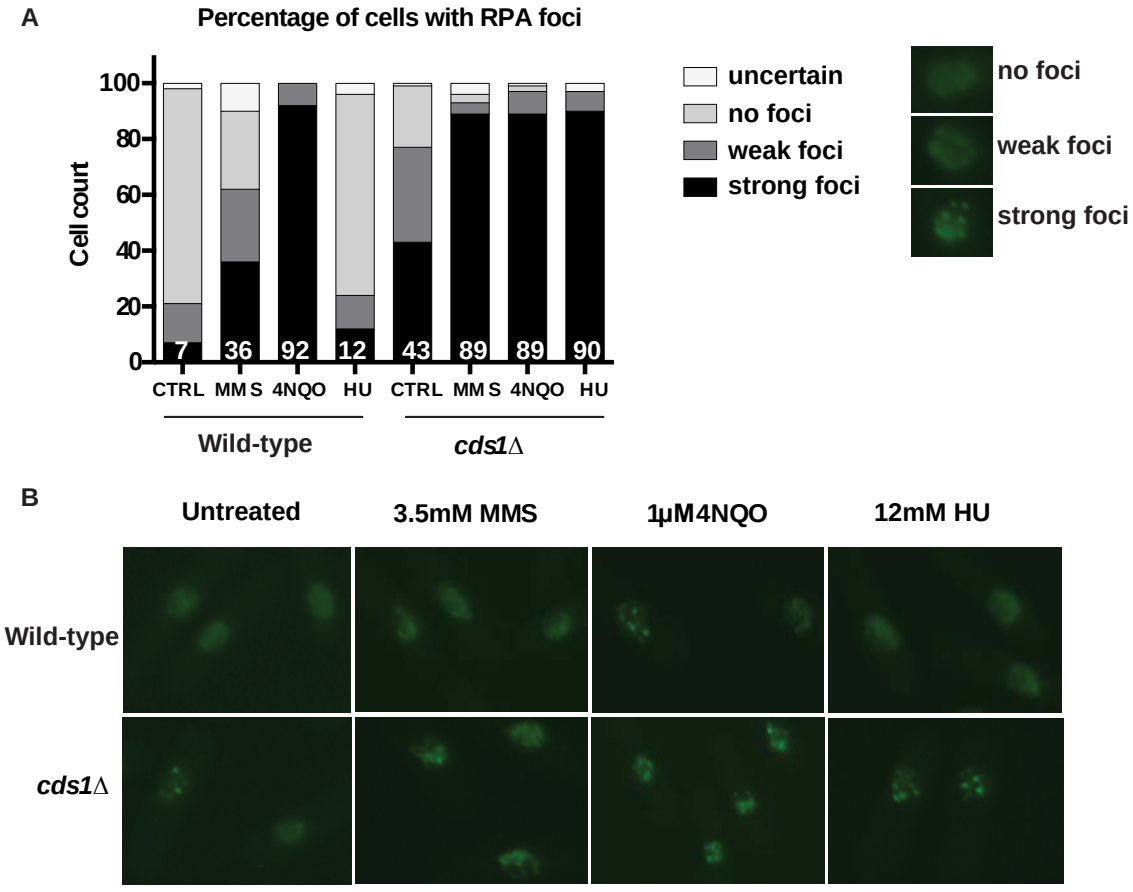

Figure 3.12: Accumulation of RPA foci in response to 4NQO and MMS. (A) Percentage of cells with RPA foci in each sample with the numbers on the bars indicating the percentage of cells with strong foci. Wild-type (yFS956) and *cds1*Δ (yFS957) cells were synchronized and released into S phase in the presence of 3.5 mM MMS,1 μM 4NQO or 12 mM HU or left untreated. Samples were collected for microscopy at 100 minutes after release. Cells were fixed and stained with DAPI and imaged in the DIC, GFP and DAPI channels. For each sample 100 cells were blinded and scored independently by two individuals. (B) Representative images for all samples quantified in (A).

Table 3.3 Summary of all the combing datasets with the fork stall rate for each sample.

Strain no.	Expt.	Dataset No.	Drug	Stalling Rate	Stalls per Mb of total DNA
yFS940	WT	WT1-N	Untreated	0.16	2.451
yFS940	WT	WT1-N	4NQO	0.28	2.988
yFS940	WT	WT2-M	Untreated	0.13	2.239
yFS940	WT	WT2-M	MMS	0.41	9.165
yFS940	WT	WT3-M	Untreated	0.09	3.099
yFS940	WT	WT3-M	MMS	0.25	6.762
yFS940	WT	WT4-M	Untreated	0.14	3.308
yFS940	WT	WT4-M	MMS	0.24	6.027
yFS940	WT	WT5-M	Untreated	0.15	3.254
yFS940	WT	WT5-M	MMS	0.30	9.959
yFS940	WT	WT6-M	Untreated	0.12	3.079
yFS940	WT	WT6-M	MMS	0.34	8.543
yFS940	WT	WT7-N	Untreated	0.26	6.209
yFS940	WT	WT7-N	4NQO	0.30	4.282
yFS940	WT	WT8-B	Untreated	0.26	5.92
yFS940	WT	WT8-B	Bleomycin	0.31	6.529
yFS940	WT	WT9-B	Untreated	0.23	10.75
yFS940	WT	WT9-B	Bleomycin	0.33	8.471
yFS941	*cds1* Δ	cds1-1-N	Untreated	0.12	3.795
yFS941	*cds1* Δ	cds1-1-N	4NQO	0.23	5.916
yFS941	*cds1* Δ	cds1-2-M	Untreated	0.07	2.821
yFS941	*cds1* Δ	cds1-2-M	MMS	0.23	8.482
yFS941	*cds1* Δ	cds1-3-M	Untreated	0.11	3.571
yFS941	*cds1* Δ	cds1-3-M	MMS	0.15	6.564
yFS941	*cds1* Δ	cds1-4-M	Untreated	0.14	4.27
yFS941	*cds1* Δ	cds1-4-M	MMS	0.17	6.644
yFS941	*cds1* Δ	cds1-5-N	Untreated	0.25	11.443
yFS941	*cds1* Δ	cds1-5-N	4NQO	0.26	7.638
yFS941	*cds1* Δ	cds1-6-B	Untreated	0.23	13.266
yFS941	*cds1* Δ	cds1-6-B	Bleomycin	0.38	18.358
yFS941	*cds1* Δ	cds1-7-B	Untreated	0.32	15.906
yFS941	*cds1* Δ	cds1-7-B	Bleomycin	0.31	11.707

In the absence of checkpoint all treated samples displayed strong foci in about 90% of cells. In particular, in MMS and HU treated cells we saw a large increase in the number of cells with strong foci in *cds1*Δ as compared to wild-type, suggesting that in response to MMS treatment the checkpoint plays a role in preventing accumulation of excess ssDNA at stalled forks, as it does in HU (Sogo et al., 2002; Sabatinos et al., 2012) (Figure 3.12A).

Discussion

The regulation of DNA replication in response to DNA damage involves both inhibition of origin firing and reduction of fork speed, but relative contributions of the two effects have been unclear. Furthermore, although genetic evidence has suggested that the checkpoint regulation of fork progression is critical for genomic stability, it has been unclear if the checkpoint regulates fork speed, *per se*, and, if so, whether the regulation is at a global or local level (Seiler et al., 2007; Unsal-Kaçmaz et al., 2007; Wang et al., 2004; Szyjka et al., 2008; Iyer and Rhind, 2013). One of the reasons that these questions have persisted is that bulk methods, such as gel- or sequence-based approaches, provide an average profile of checkpoint regulation of origins and forks in response to damage and often convolve origin and fork dynamics. We have used DNA combing in fission yeast to systematically look at the effect of the checkpoint on individual origins and forks at a global scale and hence to capture the heterogeneity in response to damage. To understand the behavior of the checkpoint at a global and local

scale we have used three different types of lesion inducing agents at vastly differing concentrations—3.5mM (0.03%) for MMS, 1μM for 4NQO and 16.5 μM bleomycin—which thus produce very different densities of lesions—1000 per Mb for MMS, 40 per Mb for 4NQO and 0.35 per Mb for bleomycin (Lundin et al., 2005; Snyderwine and Bohr, 1992; Ma et al., 2008; Asaithamby and Chen, 2009)—but nonetheless have very similar effects on bulk replication kinetics (Figures 3.2A and 3.16). We find that the inhibition of origin firing is a checkpoint-dependent response, but one that develops more slowly in response to the many fork encounters with MMS than the less frequent but more severe fork interactions with 4NQO lesions or in response to repair of bleomycin-induced double-strand breaks. The slowing of fork progression, in contrast, is checkpoint-independent and therefore a local effect in which forks only slow when they encounter DNA damage (Figure 3.13). Finally, we discover that fork stalling, an event in which a fork stops and does not resume for the duration of the experiment, plays a significant role, with as many as 50% of forks stalling in response to DNA damage caused by MMS.

Figure 3.13 Summary of results

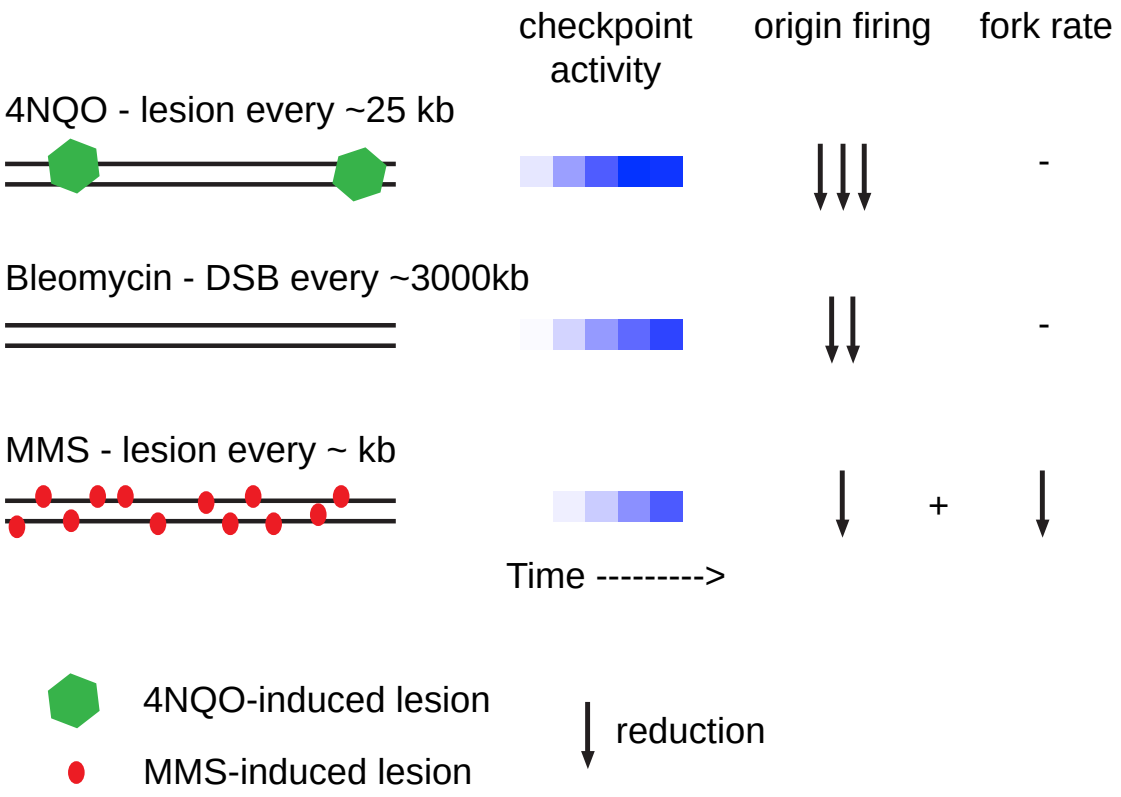

Figure 3.13 Summary of results. 4NQO causes 1 lesion every ~25 kb and bleomycin causes 1 DSB every ~3000 kb. Although the lesions are rare, 4NQO- and bleomycin-induced lesions are severe and thus lead to rapid activation of the checkpoint and a strong reduction in origin firing rate. MMS causes 1 lesion every ~ 1kb. Since the MMS-induced lesions are minor as compared to 4NQO or bleomycin the checkpoint activation is delayed and correspondingly there is a modest reduction in origin firing rate. However, since MMS-induced lesions are more frequent than those caused by 4NQO or bleomycin there is a reduction in fork rate only in response to MMS. Thus reduction in origin firing is checkpoint-dependent while reduction in fork rate is checkpoint-independent and simply due to the physical presence of the lesions.

Inhibition of origin firing is a global, checkpoint-dependent response to interactions of forks with DNA damage

Consistent with previous studies from *S. cerevisiae* (Santocanale and Diffley, 1998) and human cells (Falck et al., 2002; Sørensen et al., 2003; Merrick et al., 2004) reduction in origin firing in response to 4NQO, bleomycin and MMS is checkpoint-dependent. By flow cytometry, 4NQO, bleomycin and MMS lead to similar extent of slowing, however the combing data reveals important differences in the regulation of origin firing in response to the two drugs. In case of 4NQO reduction in origin firing is robust and immediate. The fork density during the first analog, which is a proxy for origin firing occurring prior to analog labeling, decreases to 64% ($p=1.28x10^{-6}$) in case of 4NQO and 77% ($p=7.65x10^{-4}$) in case of bleomycin, as compared to untreated cells (Figure 3.4A and 3.4B). Therefore, origin firing inhibition starts early in S phase in response to 4NQO bleomycin. On the contrary, in the case of MMS, fork density in the first analog is not significantly reduced (93%, p=0.074) suggesting no significant reduction in origin firing during early S phase (Figure 3.4C). Furthermore, even during the second analog, the fork density is 40% higher in MMS than in 4NQO (62% v. 44%, Figure 3.4A and C). Therefore reduction of origin firing in MMS is delayed and modest as compared to 4NQO.

The disparity in origin firing inhibition response can be explained by the observation that a certain threshold of damage has to be met for the activation of the intra-S checkpoint. A certain number of arrested forks are necessary for

checkpoint activation during S phase (Shimada et al., 2002). Therefore robust reduction in origin firing in response to 4NQO in early S phase suggests that 4NQO lesions, although less frequent than MMS lesion at the concentrations used in our studies, have more severe effects on forks and hence are more efficient at activating the checkpoint than MMS. Consistent with this interpretation, 4NQO lesions lead to a 2.6- fold higher rate of fork stalls per lesion than MMS (1.3% v. 0.5%) as detected by combing. The low density of stalls per lesion in response to MMS suggests that MMS takes longer to induce sufficient fork stalls to activate a checkpoint signal, and explains why the checkpoint mainly inhibits origin firing later in S phase. Our analysis of RPA accumulation is also consistent with this interpretation, showing that 4NQO-induced lesions accumulate RPA to a much greater extent than MMS-induced lesions (Figure 3.12).

Reduction in fork rate is a local checkpoint-independent response to interactions of forks with DNA damage

The fork rate in wild-type cells is reduced in response to MMS to 76% ($p=6.14x10^{-38}$) (Figure 3.5A). The fork rate is also reduced to 61% in *cds1*Δ cells treated with MMS ($p=6.13x10^{-66}$) (Figure 3.9A) consistent with previous reports (Tercero and Diffley, 2001). Thus, reduction in fork rate is checkpoint-independent and seems to be simply due to the physical presence of the lesions. In fact, by combing we see a slower fork rate in response to MMS in *cds1*Δ cells

than in wild-type cells as compared to untreated (61% v. 76%, Figure 3.9A). The previously discussed correlation between fork rate and fork density in undamaged cells notwithstanding (Herrick and Bensimon, 2008), we do not believe this effect in MMS-treated *cds1*Δ cells is an indirect consequence of the increased origin firing, because we do not see a similar decrease in fork rate in the 4NQO-treated cells, which show much greater increase in origin firing and fork density in *cds1*Δ cells relative to wild-type cells (Figures 3.9A, 3.7A and 3.7C). Instead, we prefer the interpretation that the checkpoint facilitates fork progression across a damaged template. Recent work shows that even in the absence of the checkpoint, the replisome is intact at stalled forks (De Piccoli et al., 2012). Therefore, it has been speculated that the checkpoint does not affect the stability of the replisome *per se*, but instead helps maintain the replisome in a replication competent state at sites of DNA damage (Segurado and Diffley, 2008), a possibility supported by our data. In contrast, previous studies have reported similar extent of slowing in both wild-type and the checkpoint mutants in response to MMS (Tercero and Diffley, 2001; Szyjka et al., 2008). One explanation for the discrepancy could be that the previous methods—density transfer approach and BrdU-IP-seq—offer an average profile at lower resolution and mask the difference between wild-type and checkpoint-deficient cells.

Reduction of fork rate in response to MMS but not to 4NQO supports the model that slowing of forks is simply due to a transient physical slowing of forks at each lesion encountered and is not due to a global checkpoint-dependent

effect on fork progression rates. Consistent with this model, we do not see a reduction in fork rate in response to bleomycin treatment (1.06, p=0.31), which activates the checkpoint robustly (Figure 3.5A and 3.11). This result is consistent with our previous observations that slowing is dependent on MMS dose (Willis and Rhind, 2009) and occurs in response to frequent UV-induced lesions, but not rare IR-induced double-strand breaks (Rhind and Russell, 1998). Since the lesions induced by 4NQO and bleomycin are 25 and 3000 times rarer than those caused by MMS, the forks are less likely to encounter damage and slow down in 4NQO-treated cells. The corollary to this conclusion is that activation of the checkpoint does not slow replication forks, as demonstrated by the fact that forks in 4NQO- and bleomycin-treated cells fail to slow despite the strong Cds1 activation and checkpoint-dependent inhibition of origin function.

Fork stalling is a qualitatively different response to damage than fork slowing

The interaction of a fork with a DNA lesion is a first step towards recognition of damaged template during S phase and is a critical mechanism for checkpoint activation (Zou and Elledge, 2003). Activation of the intra-S checkpoint by stalled forks allows the cell to activate repair pathways, tolerate damage and prevent genomic instability (Cimprich and Cortez, 2008). Although it is believed that forks can pass polymerase-blocking lesions on the leading strand using translesion polymerases, leading-strand repriming or recombinational lesion bypass, the role

of the checkpoint in such responses is unclear (Branzei and Foiani, 2009; Branzei and Foiani, 2005; Ulrich, 2012; Daigaku et al., 2010; Sale, 2012; Lee and Myung, 2008).

Here we show that forks can bypass both MMS- and 4NQO-induced lesions and that the checkpoint is not required for that bypass. However, in the case of MMS-induced lesion, the checkpoint seems to facilitate bypass, since forks move past lesions more slowly in *cds1*Δ cells as compared to wild-type (0.61% v. 0.76%, Figure 3.9A). We also show that, whereas forks can bypass most lesions efficiently, at a small fraction of lesions—0.5% of MMS-induced lesions, 1.3% of 4NQO-induces lesions and 8.1% of bleomycin-induced breaks—forks stall for the duration of the experiment. Given the large number of lesions throughout the genome, even these small numbers lead to a large number of stalled forks: 50% in MMS-treated cells and 25% in 4NQO- and bleomycin-treated cells.

Fork stalling does not appear to be simply an extreme example of the transient fork pausing that leads to observed fork slowing. If it were, we would expect to see a continuum of fork pause lengths from very short pauses to full stalls. Such heterogeneity would lead to a greater variation in apparent fork speeds and, in particular an increase in the asymmetry of rates in fork pairs, neither of which we see (Figure 3.14, 3.15).

Figure 3.14 Fork rate distribution in MMS treated samples does not show wider range as compared to untreated samples.

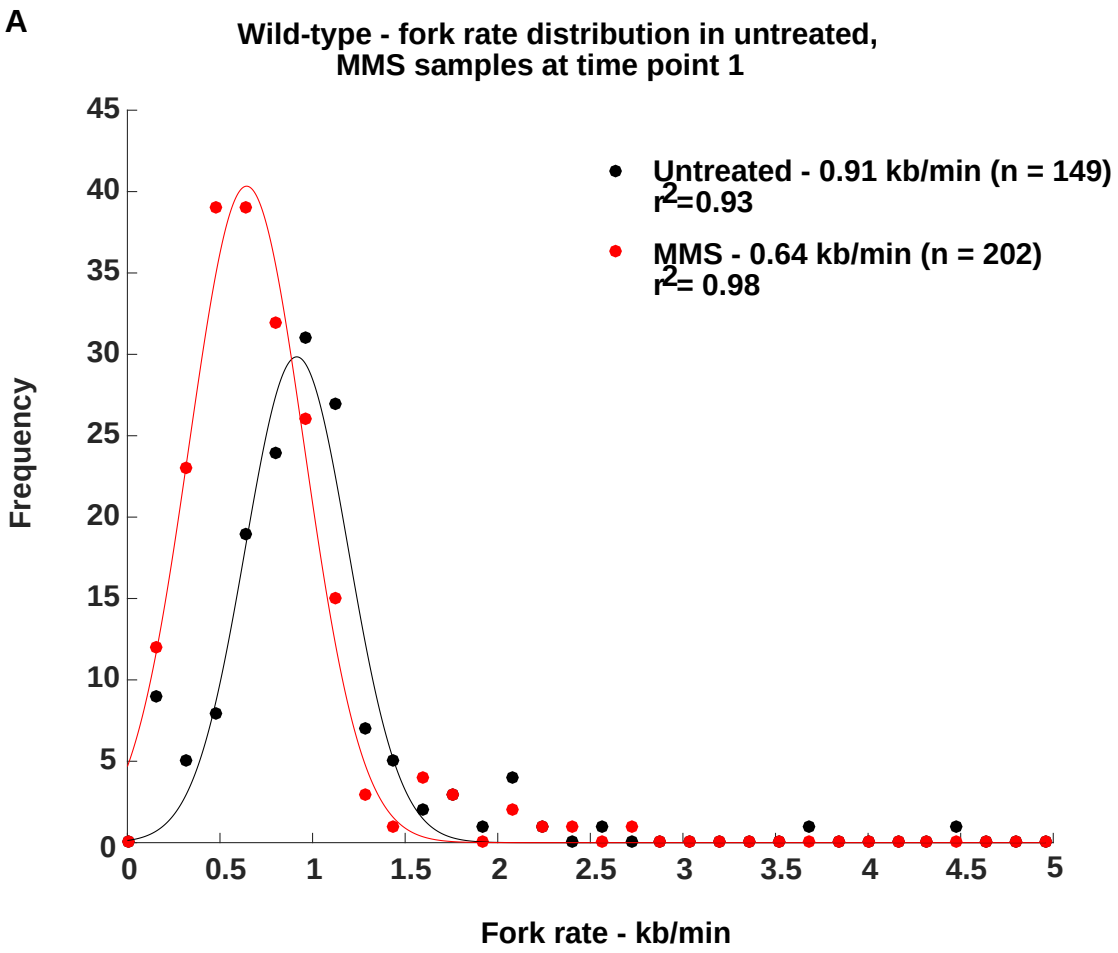

B

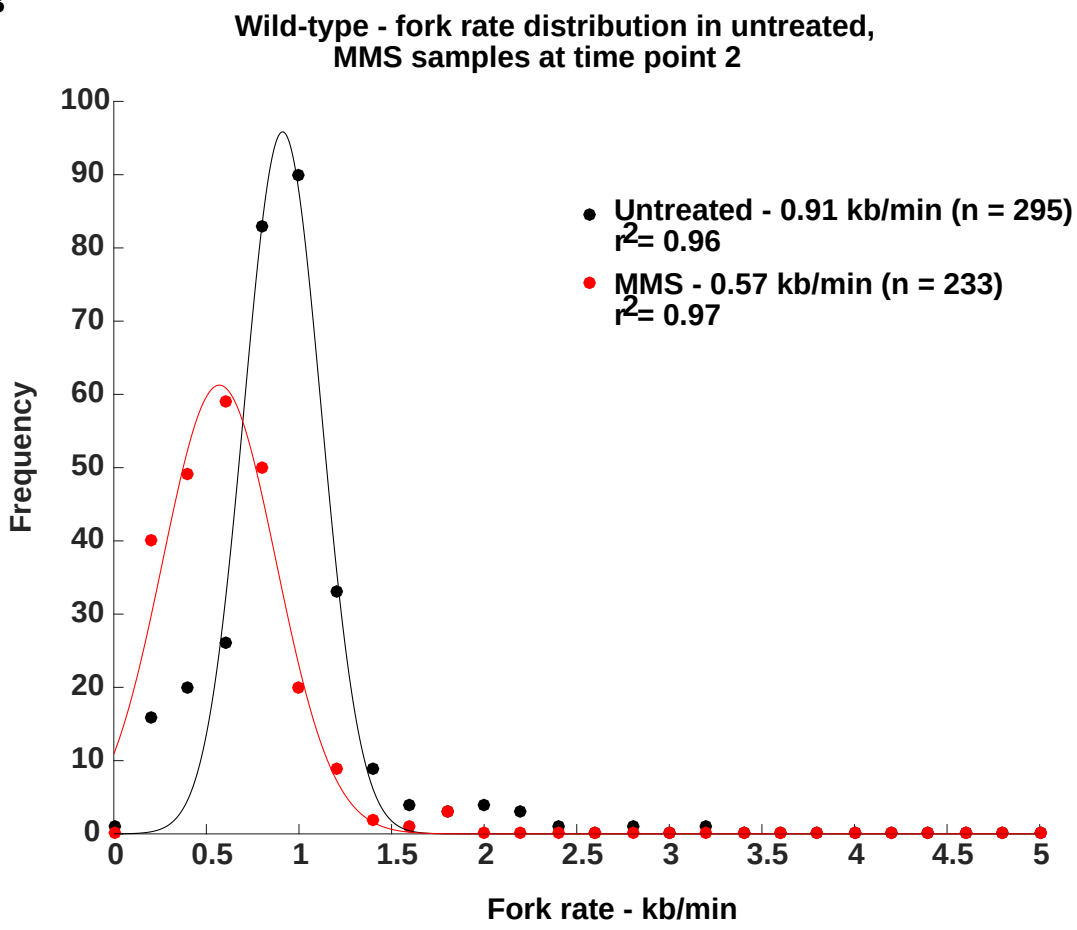
Wild-type - fork rate distribution in untreated, MMS samples at time point 2
Frequency
Fork rate - kb/min
Untreated - 0.91 kb/min (n = 295)
r2= 0.96
MMS - 0.57 kb/min (n = 233)
r2= 0.97
0
10
20
30
40
50
60
70
80
90
100
0
0.5
1
1.5
2
2.5
3
3.5
4
4.5
5

C

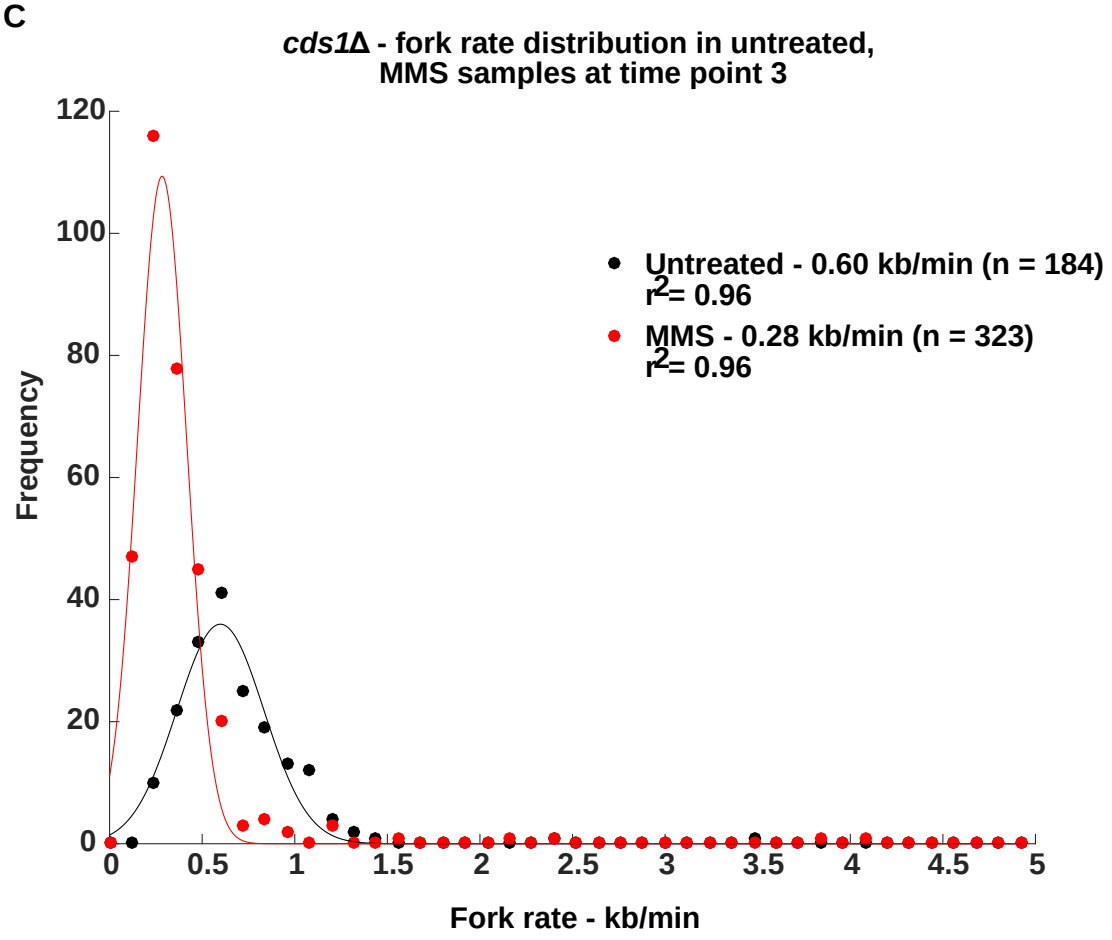
cds1Δ - fork rate distribution in untreated, MMS samples at time point 3
Frequency
Fork rate - kb/min
Untreated - 0.60 kb/min (n = 184) r2= 0.96
MMS - 0.28 kb/min (n = 323) r2= 0.96
0
20
40
60
80
100
120
0
0.5
1
1.5
2
2.5
3
3.5
4
4.5
5

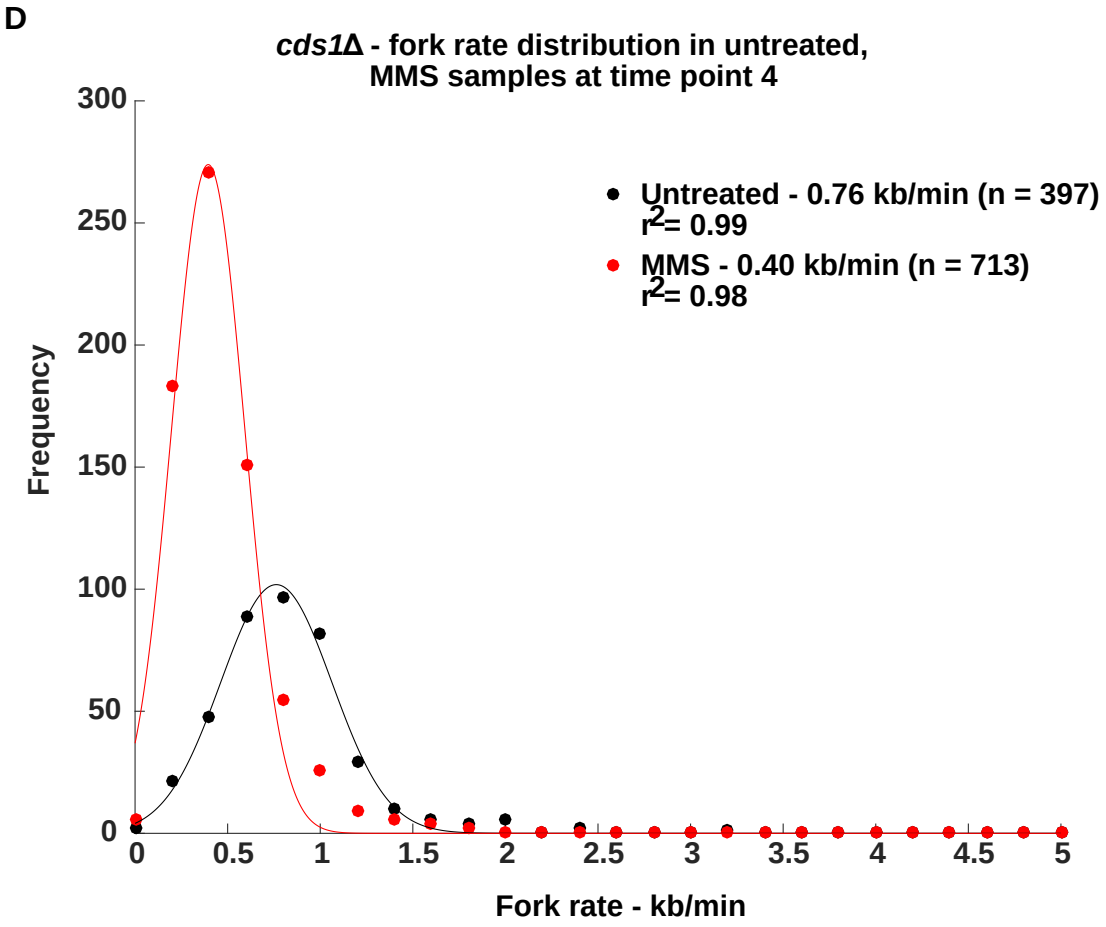

Figure 3.14 Fork rate distribution in MMS treated samples does not show wider range as compared to untreated samples. Fork rate distribution in wild-type and *cds1*Δ cells untreated or treated with MMS from a single experiment at time points 1 and 3, respectively (A and C) and from two experiments at time points 2 and 4, respectively (B and D). For the exact timings refer to Table 3.4. Each distribution of fork rate was fit to a Gaussian curve. Mean fork rate was obtained from the fit.

Figure 3.15 Comparing fork rates of left and right fork pairs in wild-type (yFS940)

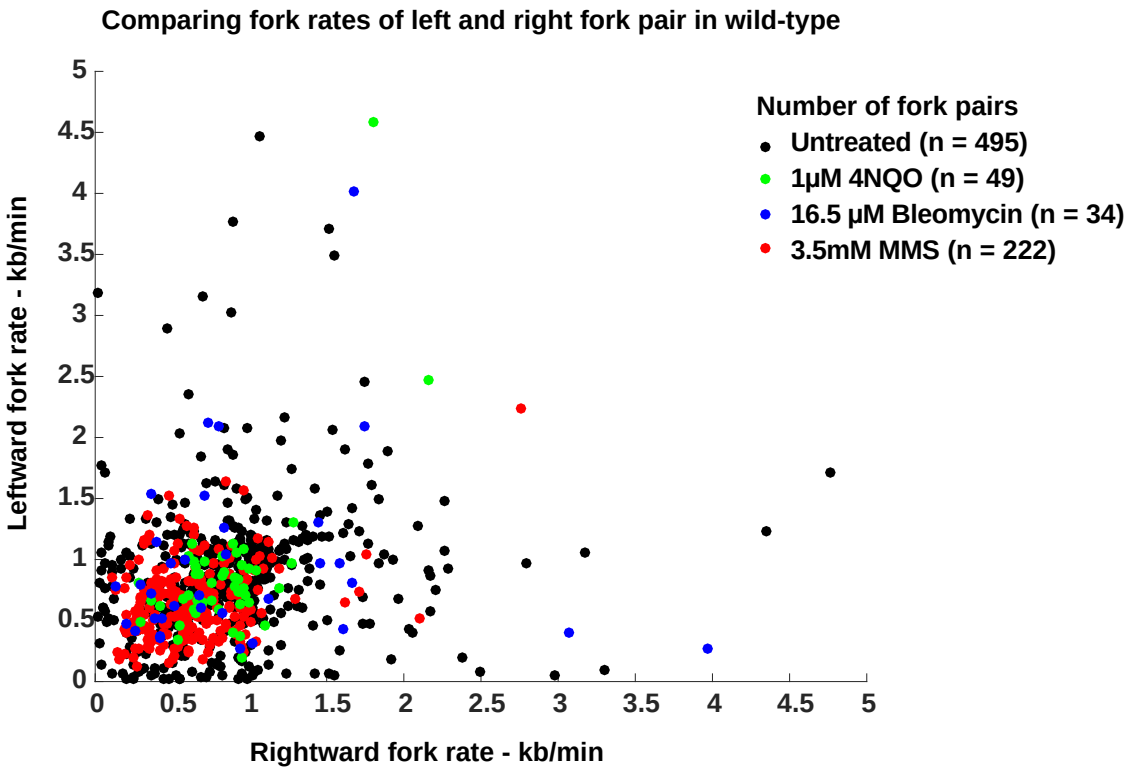

Figure 3.15 Comparing fork rates of left and right fork pairs in wild-type (yFS940) does not show a greater asymmetry in treated samples as compared to an untreated sample.

Therefore, we conclude that there are two distinct possible fate for a fork that encounters damage. It can pause briefly as it bypasses the lesion or it can stall permanently. A permanent stall does not appear to be a catastrophic event, as a majority of MMS-treated cells, which all have many stalls (Table 3.3), do not have strong RPA foci (Figure 3.12A). However, such stalls do appear to require the checkpoint to restrain ssDNA accumulation. 4NQO-induced lesions appear to cause more severe stalls, since 4NQO-treated cells have many more strong RPA foci, even though they have fewer stalls (Table 3.3 and Figure 3.12A).

The replication fork dynamics that we observe in response to MMS- and 4NQO-induced DNA damage demonstrate that forks interact with DNA damage largely in a checkpoint-independent manner. Forks are able to bypass lesions that stall the replicative polymerases with only a modest reduction in speed (Figure 3.9A) and are no more prone to stall at lesions in the absence of checkpoint (Figure 3.9B and 3.9C). However, stalled forks do appear to accumulate more ssDNA in the absence of the checkpoint (Figure 3.12). These results suggest that the major role of the checkpoint is not to regulate the interaction of replication forks with DNA damage, *per se*, but to mitigate the consequences of fork stalling when forks are unable to successfully navigate DNA damage on their own.

Material and Methods

General methods

The following strains used in this study were created by standard methods and grown in YES at 25°C (Forsburg and Rhind, 2006): yFS940 (*h+ leu-32 ura4-D18 his7-366 cdc10-M17 leu1::pFS181 (leu1 adh1:hENT1) pJL218 (his7 adh1:tk))*, yFS941 (*h- leu-32 his7-366 cdc10-M17 cds1::kanMX leu1::pFS181(leu1 adh1:hENT1) pJL218 (his7 adh1:tk)),* yFS956 (*h+ leu1-32 ura4-D18 cdc10-M17 rpa1-GFP::hph-MX6*), yFS957 (*h+ leu1-32 ura4-D18 cdc10-M17 cds1::ura4 rpa1-GFP::hph-MX6*), yFS988 (*h- leu1-32 ura4-D18 ade-? cdc10-M17 cds1-6his2HA(int)*)

S phase progression assay by flow cytometry

Cells were synchronized in G1 phase using *cdc10-M17* temperature sensitive allele combined with centrifugal elutriation, which selects cells that have been arrested in G1 for as little time as possible (Willis and Rhind, 2011). Cells were grown to mid log phase at 25°C and arrested at 35°C for 2 hours followed by centrifugal-elutriation-based size selection at 35°C to collect cells that had most recently arrested in G1. The cells were then immediately released into S phase by shifting them to 25°C, untreated or treated with 3.5mM MMS or 1 µM 4NQO or 16.5 µM bleomycin. S-phase progression was followed by flow cytometry using a nuclei isolation protocol, as previously described (Willis and Rhind, 2011) with some minor modifications (Chapter II). In case of MMS, 3.5mM or 0.03% concentration was used, which is the standard dose used in DNA damage field.

The concentration of 4NQO and bleomycin was titrated to get similar levels of bulk slowing as seen in case of MMS (Figure 3.16A and 3.16B).

Figure 3.16 Titration of 4NQO and Bleomycin

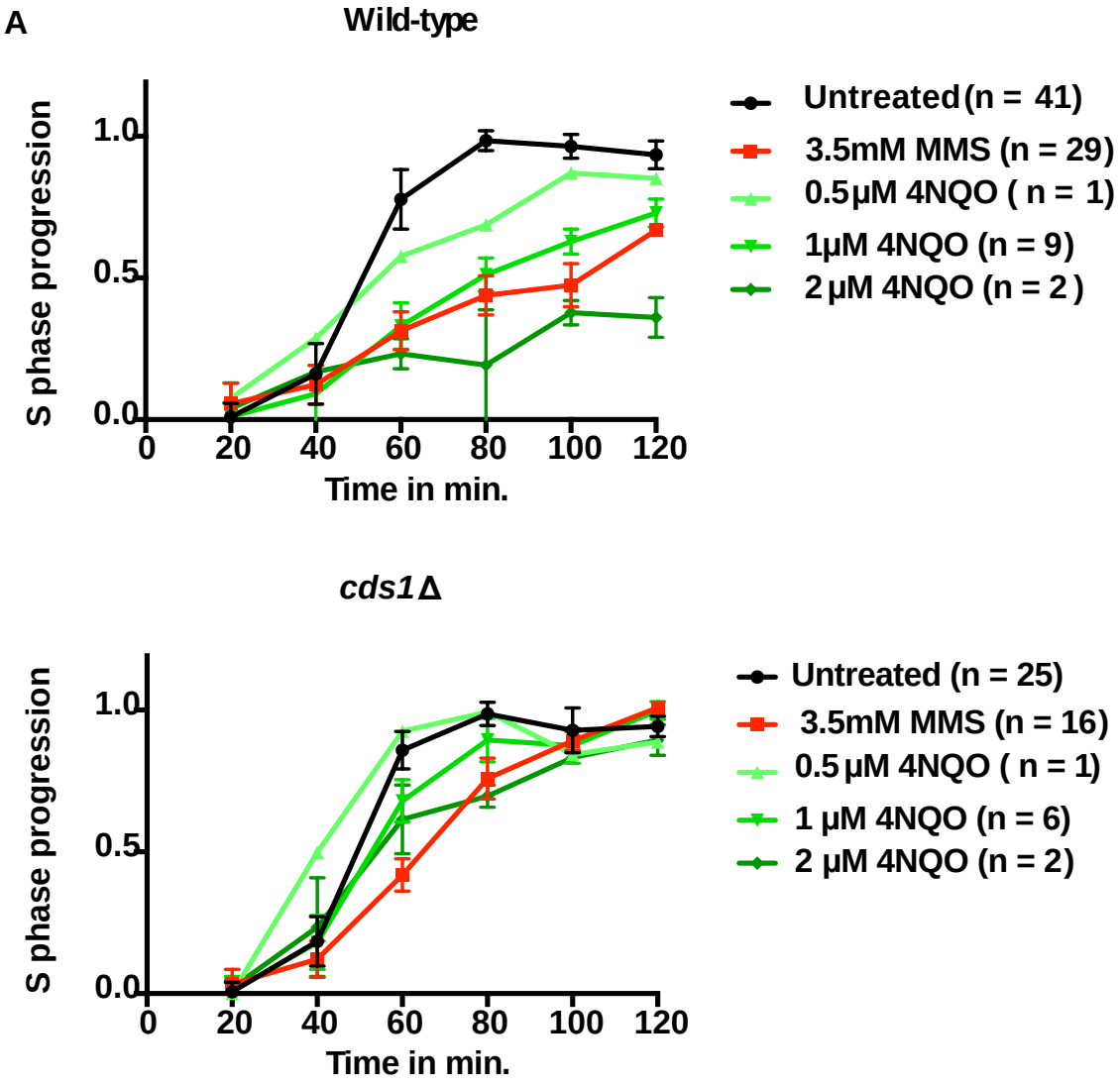

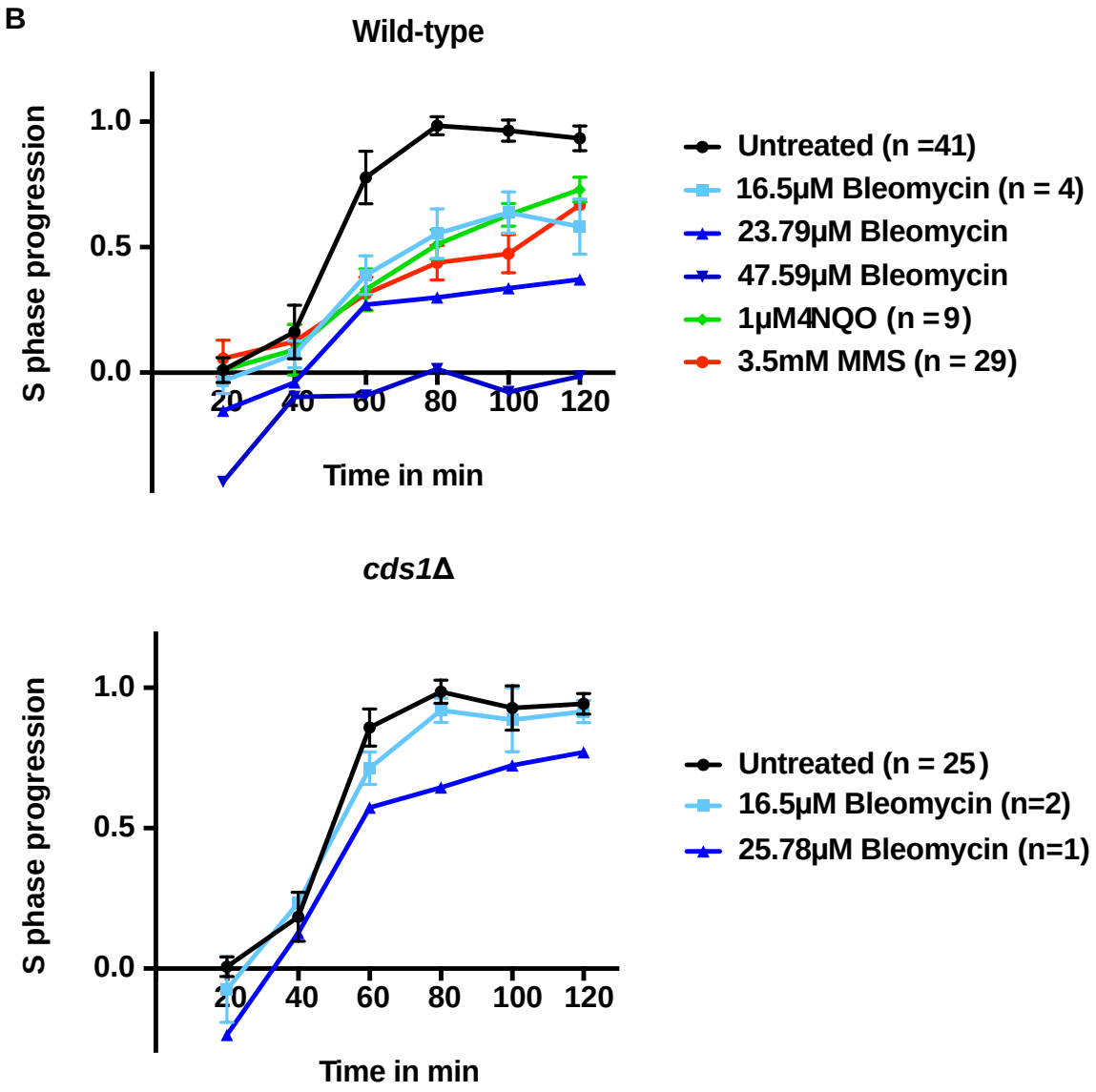

Figure 3.16 Titration of 4NQO and Bleomycin. (A) Titration of 4NQO. Wild-type (yFS940) and *cds1*Δ (yFS941) cells were synchronized and released into S phase with 3.5 mM MMS, 0.5 μM, 1 μM, 2 μM 4NQO or left untreated (B) Titration of Bleomycin. Wild-type (yFS940) and *cds1*Δ (yFS941) cells were synchronized and released into S phase with different concentrations of bleomycin 16.5 μM, 23.79 μM, 47.9 μM or left untreated. S phase progression was monitored by taking samples every 20 minutes for flow cytometry.

We have used three different drugs (3.5mM MMS, 1 μM 4NQO and 16.5 μM bleomycin) to create significantly differing lesion densities (of 1 every 1 kb, 25 kb or 3000 kb, respectively) in order to differentiate between global v. local regulation of forks. Conceivably, variable lesion density could be achieved by just titrating one of the drugs. However, we cannot achieve a 25-fold difference in lesion density (let alone a 3000-fold difference) by just titrating either drug alone. In case of 4NQO, increasing dose concentration to even 2 μM 4NQO almost inhibits replication, while decreasing MMS dose below 3.5mM to 0.875mM greatly reduces the effect of damage on replication kinetics (Figure 3.16A) (Willis and Rhind, 2009).

DNA Combing

Cell labeling and plug preparation

Cells were pulse labeled with 2 μM CldU for 5 minutes and chased with 20 μM IdU for 10 minutes. For the second replicate of 4NQO dataset in wild-type and *cds1*Δ cells and all the bleomycin datasets, cells were labeled with 5 μM CldU for 5 minutes and chased with 20 μM IdU for 10 minutes. For MMS, experiments were done 5 times in wild-type cells and 3 times in *cds1*Δ cells; 4NQO and bleomycin experiments were done twice in each wild-type and *cds1*Δ cells. Cells were pulse labeled at different time points across S phase for both wild-type and *cds1*Δ, however they gave similar results and hence have been combined and

represented together in the figures for simplicity. Refer to Table 3.4 for the exact timing of analog labeling during S phase for the various replicates.

Table 3.4 Summary of all the combing datasets with the time at which analog was added, temperature at which Proteinase K treatment was done, and the pH of MES buffer used for combing.

Strain no.	Expt	Dataset No.	Drug	Time point # (see Methods)	Time of analog addition	pH of combing buffer	Proteinase K temperature
yFS940	WT	WT1-N	Untreated	Time point 1	50 min.	6.35	50°C
yFS940	WT	WT1-N	4NQO	Time point 1	50 min.	6.35	50°C
yFS940	WT	WT2-M	Untreated	Time point 1	50 min.	6.35	50°C
yFS940	WT	WT2-M	MMS	Time point 1	50 min.	6.35	50°C
yFS940	WT	WT3-M	Untreated	Time point 1	50 min.	6.35	37°C
yFS940	WT	WT3-M	MMS	Time point 1	50 min.	6.35	37°C
yFS940	WT	WT4-M	Untreated	Time point 1	50 min.	6.25	37°C
yFS940	WT	WT4-M	MMS	Time point 1	50 min.	6.25	37°C
yFS940	WT	WT5-M	Untreated	Time point 2	55 min.	6.25	37°C
yFS940	WT	WT5-M	MMS	Time point 2	55 min.	6.25	37°C
yFS940	WT	WT6-M	Untreated	Time point 2	55 min.	6.25	37°C
yFS940	WT	WT6-M	MMS	Time point 2	55 min.	6.25	37°C
yFS940	WT	WT7-N	Untreated	Time point 1	50 min.	6.2	50°C
yFS940	WT	WT7-N	4NQO	Time point 1	50 min.	6.2	50°C
yFS940	WT	WT8-B	Untreated	Time point 1	50 min.	6.2	50°C
yFS940	WT	WT8-B	Bleomycin	Time point 1	50 min.	6.2	50°C
yFS940	WT	WT9-B	Untreated	Time point 1	50 min.	6.2	50°C
yFS940	WT	WT9-B	Bleomycin	Time point 1	50 min.	6.2	50°C
yFS941	*cds1* Δ	cds1-1-N	Untreated	Time point 1	50 min.	6.35	50°C
yFS941	*cds1* Δ	cds1-1-N	4NQO	Time point 1	50 min.	6.35	50°C
yFS941	*cds1* Δ	cds1-2-M	Untreated	Time point 3	45 min.	6.25	37°C
yFS941	*cds1* Δ	cds1-2-M	MMS	Time point 3	45 min.	6.25	37°C
yFS941	*cds1* Δ	cds1-3-M	Untreated	Time point 4	50 min.	6.25	37°C
yFS941	*cds1* Δ	cds1-3-M	MMS	Time point 4	55 min.	6.25	37°C
yFS941	*cds1* Δ	cds1-4-M	Untreated	Time point 4	50 min.	6.25	37°C
yFS941	*cds1* Δ	cds1-4-M	MMS	Time point 4	55 min.	6.25	37°C
yFS941	*cds1* Δ	cds1-5-N	Untreated	Time point 1	50 min.	6.2	50°C
yFS941	*cds1* Δ	cds1-5-N	4NQO	Time point 1	50 min.	6.2	50°C
yFS941	*cds1* Δ	cds1-6-B	Untreated	Time point 1	50 min.	6.2	50°C
yFS941	*cds1* Δ	cds1-6-B	Bleomycin	Time point 1	50 min.	6.2	50°C
yFS941	*cds1* Δ	cds1-7-B	Untreated	Time point 1	50 min.	6.2	50°C
yFS941	*cds1* Δ	cds1-7-B	Bleomycin	Time point 1	50 min.	6.2	50°C

Analog labeling was stopped by adding sodium azide to a final concentration of 0.1% and cooling the cells on ice. 10 O.D. of cells were pelleted for combing, frozen in liquid N_2 and stored at -80°C. Cells were processed as previously described with minor modifications (Chapter II) (Iyer et al., in press). For MMS experiments the plugs were digested with proteinase K at 37°C instead of 50°C to facilitate isolation of longer fibers based on the observation that MMS creates heat-labile DNA damage (Table 3.4)(Lundin et al., 2005). Higher pH of MES (6.25 or 6.35) was used for combing instead of pH 5.4 to isolate longer fibers (Table 3.4) (Kaykov and Nurse, 2015). Combing and immuno-staining of samples were done as previously described (Chapter II) (Iyer et al., in press). For the second replicate of 4NQO dataset in wild-type and *cds1*Δ cells, and for all the bleomycin datasets, data collection was done in collaboration with Genomic Vision, France. Data collection and analysis was done as described in detail in Chapter II. For distribution of fiber lengths refer to Figure 3.17 and Table 3.5.

Figure 3.17 Fiber length distribution

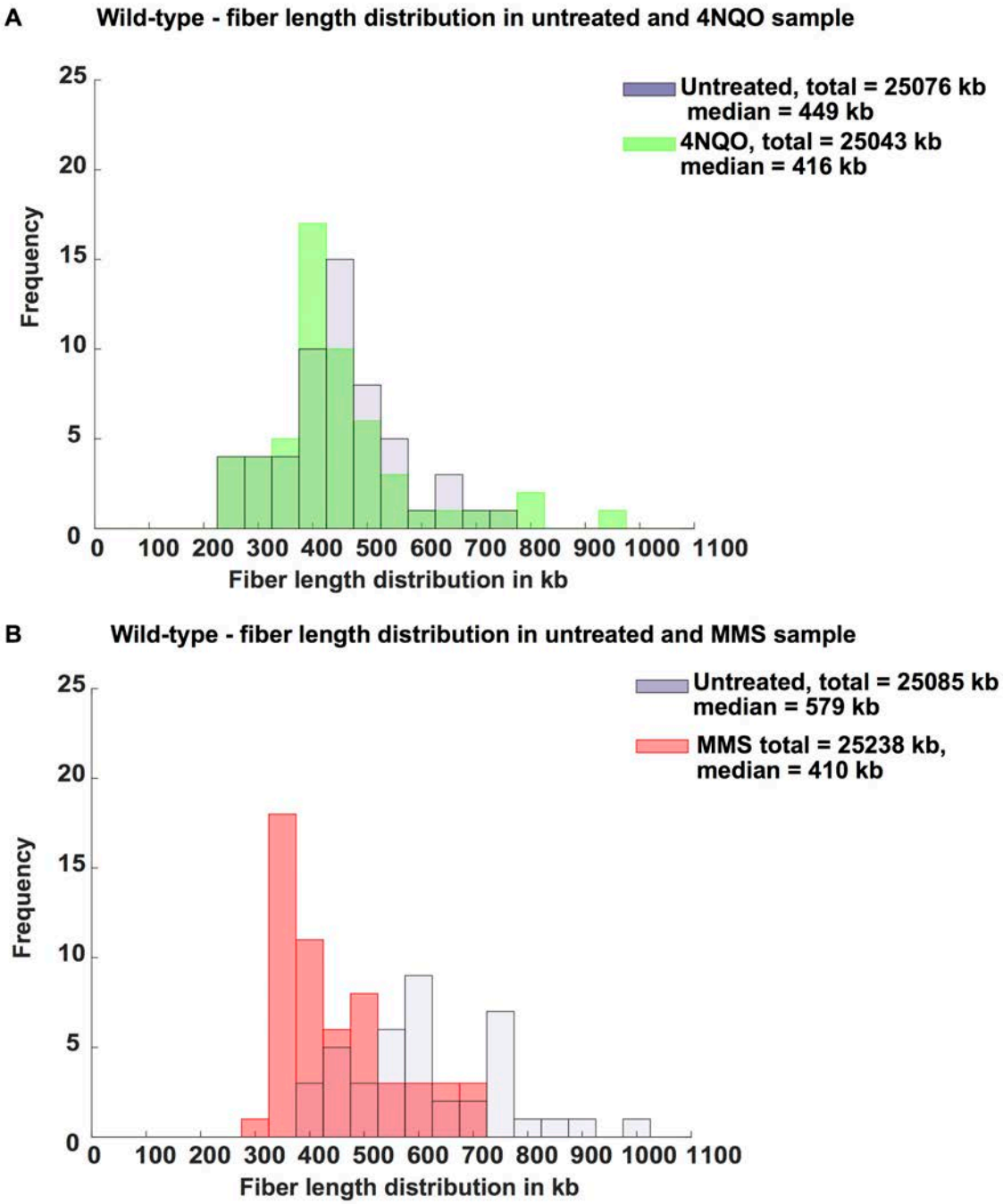

Figure 3.17 Fiber length distribution. Length of fibers from wild-type 4NQO (A) and MMS (B) samples from a single experiment. Approximately 25 Mb of total DNA was collected for each sample (Table 3.5).

Table 3.5 Summary of all combing datasets with total DNA measured, maximum, minimum, median, and standard deviation of fiber lengths for each dataset.

Strain no.	Expt	Dataset No.	Drug	Total Fiber Length (Mb)	Max. fiber Length (kb)	Min. fiber Length (kb)	Median fiber Length (kb)	Standard Dev. (kb)
yFS940	WT	WT1-N	Untreated	25.11	744.59	234.61	375.21	97.02
yFS940	WT	WT1-N	4NQO	25.27	710.73	197.34	355.49	100.15
yFS940	WT	WT2-M	Untreated	25.53	958.11	292.80	504.67	148.24
yFS940	WT	WT2-M	MMS	25.23	490.24	186.47	239.17	52.55
yFS940	WT	WT3-M	Untreated	9.81	1220.10	295.16	383.56	198.90
yFS940	WT	WT3-M	MMS	9.34	686.20	342.61	426.18	112.81
yFS940	WT	WT4-M	Untreated	25.09	1002.70	391.83	578.93	140.03
yFS940	WT	WT4-M	MMS	25.24	709.70	320.85	409.88	108.80
yFS940	WT	WT5-M	Untreated	25.43	1041.07	362.80	543.91	156.67
yFS940	WT	WT5-M	MMS	12.03	489.21	171.04	262.82	69.55
yFS940	WT	WT6-M	Untreated	25.27	1161.17	335.90	463.26	141.31
yFS940	WT	WT6-M	MMS	24.94	656.86	251.81	339.72	85.47
yFS940	WT	WT7-N	Untreated	24.84	1293.50	416.02	636.30	186.11
yFS940	WT	WT7-N	4NQO	24.73	1288.80	165.90	485.87	231.67
yFS940	WT	WT8-B	Untreated	24.58	1360.30	363.55	580.56	201.69
yFS940	WT	WT8-B	Bleomycin	25.08	828.12	206.87	437.54	120.18
yFS940	WT	WT9-B	Untreated	25.23	1521.10	429.79	658.65	257.08
yFS940	WT	WT9-B	Bleomycin	24.42	1004.30	291.86	435.38	147.10
yFS941	*cds1* Δ	cds1-1-N	Untreated	25.03	585.50	203.60	308.20	76.09
yFS941	*cds1* Δ	cds1-1-N	4NQO	25.27	469.64	170.98	261.11	63.08
yFS941	*cds1* Δ	cds1-2-M	Untreated	25.08	1426.07	403.80	588.80	210.95
yFS941	*cds1* Δ	cds1-2-M	MMS	24.99	715.53	248.00	354.10	101.79
yFS941	*cds1* Δ	cds1-3-M	Untreated	25.18	1474.83	300.62	478.76	172.51
yFS941	*cds1* Δ	cds1-3-M	MMS	23.47	450.52	176.62	230.62	54.79
yFS941	*cds1* Δ	cds1-4-M	Untreated	25.35	1607.26	413.59	497.38	189.87
yFS941	*cds1* Δ	cds1-4-M	MMS	23.42	509.38	208.27	287.28	66.72
yFS941	*cds1* Δ	cds1-5-N	Untreated	24.72	1027.80	330.62	549.59	160.81
yFS941	*cds1* Δ	cds1-5-N	4NQO	24.3	1225.40	308.95	510.19	225.41
yFS941	*cds1* Δ	cds1-6-B	Untreated	24.73	2139.40	393.45	720.47	401.47
yFS941	*cds1* Δ	cds1-6-B	Bleomycin	24.08	839.32	124.53	331.86	147.39
yFS941	*cds1* Δ	cds1-7-B	Untreated	25.25	1983.1	237.1	578.69	337.99
yFS941	*cds1* Δ	cds1-7-B	Bleomycin	22.94	588.37	138.17	327.4	100.25

Variation in absolute fork rate values

We note that the fork rate for wild-type untreated samples varies across different replicates (0.65±0.4 kb/min for the first three replicates v. 0.91±0.2 kb/min for the last three replicates, Table 3.2). We ascribe this variation to the pH of MES (6.35) used for combing the first three replicates, which we used to facilitate isolation of longer fibers. We have concluded that the stretching factor estimated from lambda DNA at 6.35 is not reliable. Hence we switched to a lower pH of 6.25 for further combing experiments. We believe that the values obtained at pH 6.25 are more reliable, since we have obtained 0.9 kb/min fork rate value from wild-type untreated samples stretched at pH 5.4, which is close to the standard pH used in most combing experiments (Figure 3.18) (Michalet et al., 1997; Allemand et al., 1997; Herrick and Bensimon, 1999b; Bianco et al., 2012). Despite the variation in the absolute fork rate values the relative trend observed between treated and untreated sample holds true across both pH. For example consider experiments WT3-M and WT4-M, which are similar except for the pH of the combing solution used (Table 3.2). The absolute value of wild-type untreated fork rate differs between the experiments (0.60 kb/min v. 0.92 kb/min, Table 3.2). However the change in fork rate in treated v. untreated sample is 0.72 for both the experiments.

Figure 3.18 Wild-type fork rate distribution in untreated sample combed using MES buffer pH 5.4

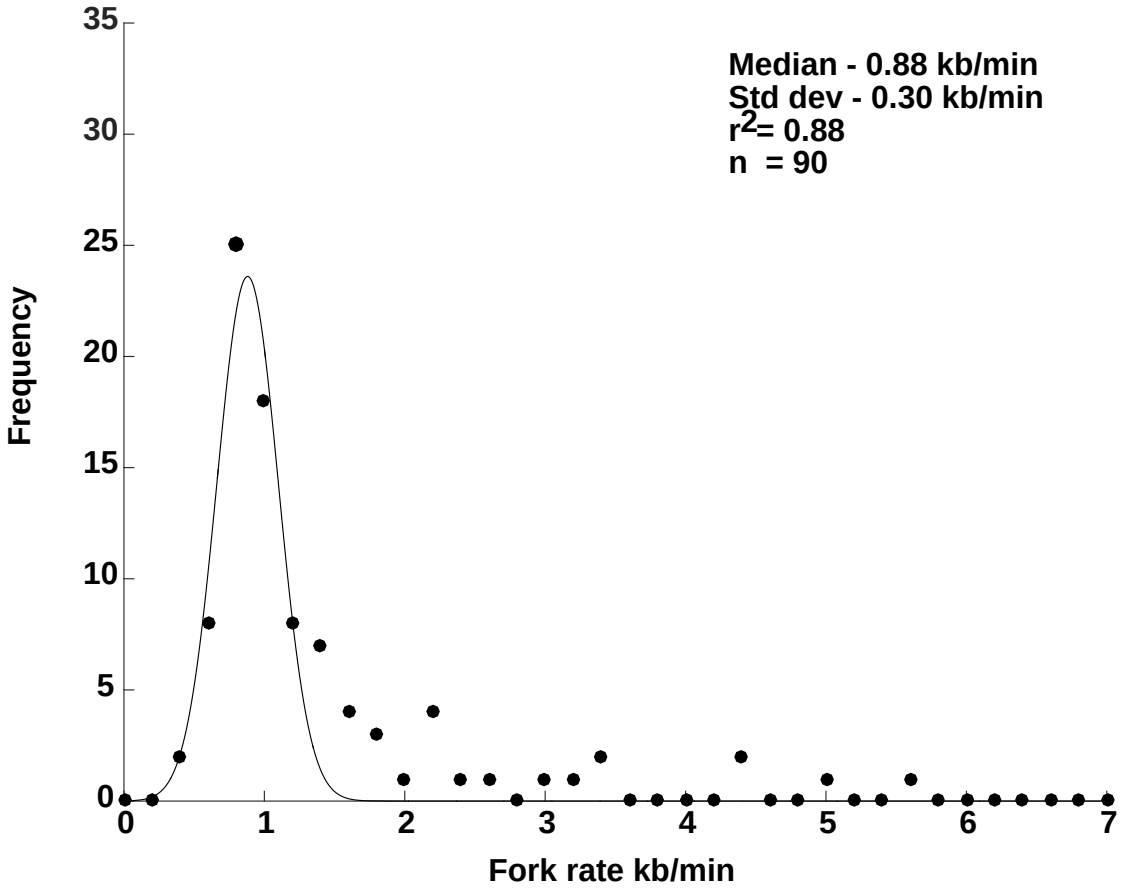

Figure 3.18 Fork rate distribution in wild-type untreated sample combed using MES buffer pH 5.4. Fork rate value was estimated from the second analog track continuing from the first analog as explained in Chapter II.

High fork stall rate in untreated sample

The fork stall rate in untreated wild-type and *cds1*Δ cells is about 15% (Table 3.3). This result reveals an unexpectedly high rate of spontaneous fork stalling. To exclude the possibility that the high stall rate is a result of previously identified combing artifacts (Demczuk and Norio, 2009), we re-analyzed our dataset, excluding the labeled events occurring at the ends of the fibers, where such artifacts can occur. However the stall rate estimations remain unchanged after re-analysis (Figure 3.19). We cannot rule out the possibility that the observed fork stall rate is increased by the thymidine analogs used to label the DNA. Nonetheless, since we normalize our quantitation of fork-stalling to an untreated sample, our results are internally controlled. Furthermore, double-labeled combing studies done in mammalian cells show similar rate of fork stalling in the untreated sample (Merav Socolovsky, personal communication).

Figure 3.19 Re-estimation of stall rate accounting for potential artifacts yields minimal variation

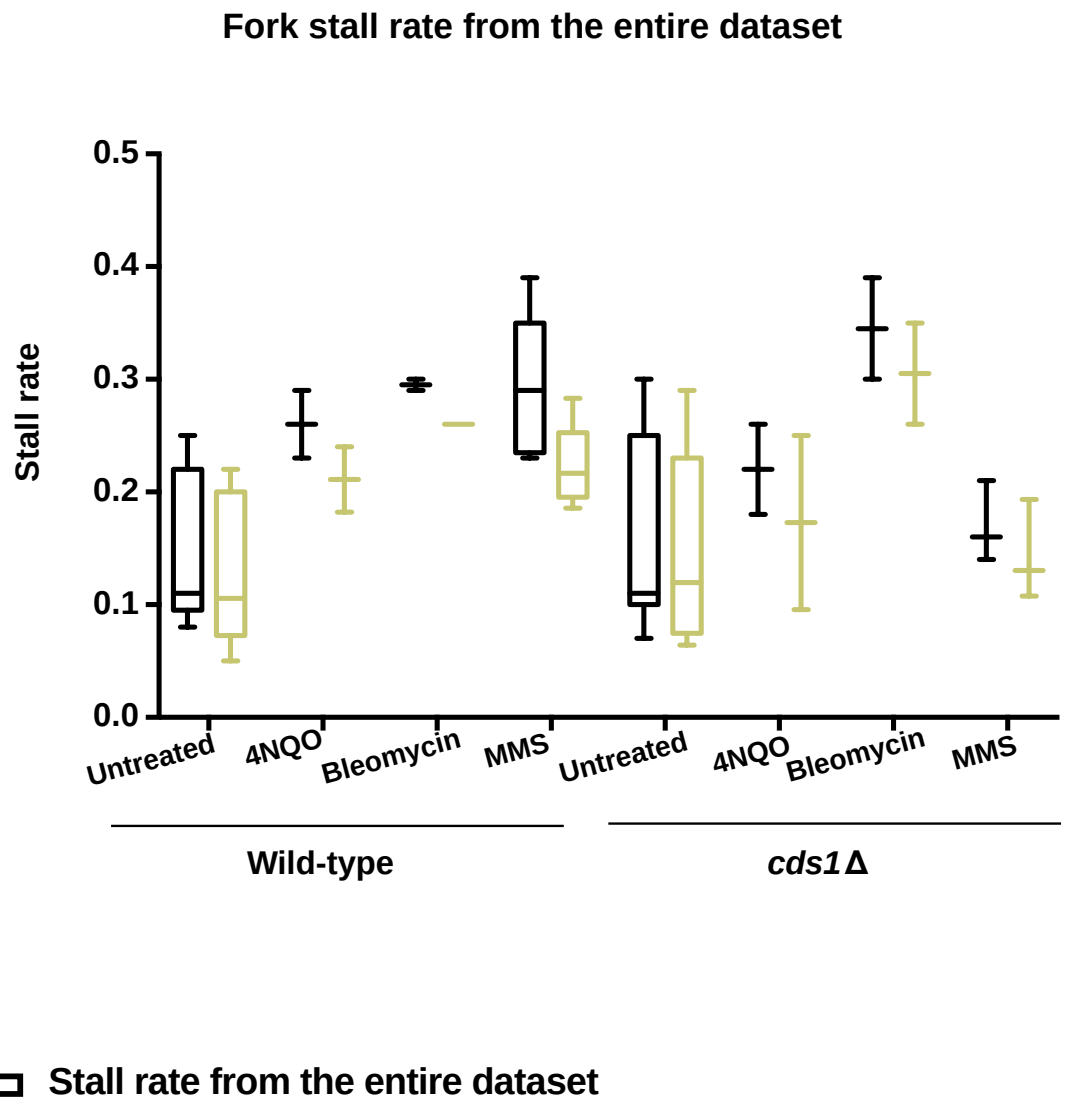

Figure 3.19 Re-estimation of stall rate accounting for potential artifacts yields minimal variation. We re-analyzed the fibers considering stretching artifacts, which may lead to incorrect interpretation of analog incorporation

patterns (Demczuk and Norio, 2009). Ends of the fiber are most susceptible to such stretching artifacts and hence we ignored the labeled events occurring at the ends of the fiber and re-calculated the stall rate. However we do not see a significant change between the stall rate calculated from the whole fiber or after ignoring the labeled events occurring at the ends of the fiber.

Cds1 kinase assay

To estimate the Cds1 kinase activity S phase progression assay was done in triplicate as described earlier in response to 3.5 mM MMS, 1 µM 4NQO, and 16.5 µM bleomycin in yFS988 strain. Approximately 10 OD of cells were pelleted at 10, 20, 30, 40, 50, and 90 minutes in S phase for measuring Cds1 activity. Cells were lysed by bead beating in 400µl ice-cold lysis buffer (150 mM NaCl, 50 mM Tris pH 8.0, 5 mM EDTA pH 8.0, 10% Glycerol, 1%IGEPAL CA630, 50 mM NaF, freshly added 1 mM Na_3VO_4 and protease inhibitor cocktail (Sigma 11836170001)) for 15 minutes at 4°C. Lysate was cleared by centrifuging at 1000g, 5 minutes and combined with anti-HA Ab conjugated agarose beads (Pierce 26181) and incubated with constant mixing at 4°C for 4 hours. Beads were washed twice with lysis buffer and twice with kinase buffer (5 mM HEPES pH 7.5, 37.5 mM KCl, 2.5 mM $MgCl_2$, 1 mM DTT). The sample was then split into two portions, one was used to estimate the amount of Cds1 pulled down by western blot and the other was processed to estimate the kinase activity. For western, the Cds1 was eluted off the beads by boiling in 2x SDS PAGE gel loading dye. Cds1 was detected by using rabbit anti-Cds1 Ab at 1:1000 and anti-rabbit HRP conjugated secondary Ab at 1:10000. For kinase assay, the beads were re-suspended in 10 µl 2x kinase buffer, 0.5 µl 10 µCi/µl γP32-ATP, 2 µl 1 mM ATP, 5 µl 1 mg/ml myelin basic protein and incubated at 30°C for 15 minutes. The reaction was quenched by adding SDS PAGE gel loading buffer and boiling at 95°C for 5 minutes. Kinase reactions were run on a 15% gel

normalized to the amount of Cds1 pulled down in each lane. The gel was dried under vacuum and exposed to phosphorimager screen for 48 hours. The screen was scanned on Typhoon FLA-9000 and quantitated using ImageJ (Schneider et al., 2012). Asynchronous culture of yFS988 treated with 3.5 mM MMS for 4 hours was used as a control to normalize across gels and blots.

RPA foci estimation

In order to estimate RPA foci formation due to damage, S-phase progression assays were performed as described above with strains expressing GFP-tagged Rpa1 (yFS956 and yFS957). Cells were collected at 100 minutes after release from untreated, 3.5 mM MMS, 1 µM 4NQO and 12 mM HU treated cultures and fixed in ice-cold 100% methanol and stored at -20°C for at least 20 minutes. Fixed cells were washed thrice with 1x PBS and re-suspended in 10 µl Vectashield mounting medium with DAPI at 2 µg/ml. Cells were visualized using a Zeiss Axioskop 2 Plus epifluorescence microscope with 100X Plan-NEOFLUAR oil objective and imaged using SPOT monochrome cooled-CCD camera. Images were analyzed using ImageJ and Microsoft Excel. Image of each nuclei in the GFP channel was cut and pasted into cells in an excel file. The nuclei were then blinded, randomly sorted and scored independently by two individuals. 100 nuclei were analyzed for each sample. The nuclei were scored into three categories: uncertain, foci negative, and foci positive. Foci positive cells were further characterized into nuclei with few weak foci (1 or 2) or containing many weak foci, strong foci or a combination of strong and weak foci.

Chapter IV

Aneuploidy causes replication defects

(This work was done in collaboration with Angelika Amon's lab at MIT. The experiments were designed by AA, SS and DI. The cells were prepared by SS. Sample processing, combing and analysis was performed by DI. This work is published as part of a larger study(Santaguida et al., 2017))

Introduction

What is aneuploidy?

The term ‘ploidy’ refers to the chromosomal content of a cell. Most mammalian cells tend to have two copies of each set of chromosome, a condition referred to as diploidy (Orr et al., 2015). Although diploid is the preferred state in mammals, other species such as plants and amphibians tend to have more than two sets of chromosomes (polyploidy) with stable genomes (Comai, 2005). In fact, being polyploid confers adaptive advantages to the species (Paquin and Adams, 1983; Zerulla and Soppa, 2014; Selmecki et al., 2015). Thus having multiple (more than 2) sets of chromosomes is well tolerated, so long as all the genes on different chromosomes are equally represented. This condition of having an exact multiple of the haploid chromosomal content is called euploidy (Comai, 2005; Orr et al., 2015; Siegel and Amon, 2012). In contrast, aneuploidy is a condition of having an unbalanced karyotype involving loss or gain of whole chromosomes or parts of a chromosome. In humans, having one chromosome less (monosomy) or extra (trisomy) is mostly lethal. In the few cases where trisomy is tolerated (trisomy 13, 18, 21) the individuals tend to have severe developmental abnormalities. Thus having a balanced number of chromosomes is essential for the survival and fitness of the organism (Hassold and Hunt, 2001; Nagaoka et al., 2012; Potapova et al., 2013; Orr et al., 2015). Consistently, aneuploidy is rare amongst somatic tissues (Knouse et al., 2014).

Aneuploidy and cancer

Although aneuploidy is mostly detrimental for cell survival, oddly it is also a hallmark of a disease involving unrestrained growth - cancer, with 90% of solid tumors and 50% of blood cancers being aneuploid (Holland and Cleveland, 2012; Mitelman et al., 2017). Chromosomal instability associated with aneuploidy promotes genomic instability and thus leads to heterogeneity amongst the population of tumor cells, which in turn provides genetic diversity, from which cells refractory to treatment can be selected. Aneuploidy in tumors is linked to metastasis and poor prognosis (Gordon et al., 2012; McGranahan et al., 2012; Gerlinger and Swanton, 2010; Lee et al., 2011; Walther et al., 2008). Thus to understand the effects of aneuploidy on cell behavior, we looked at the immediate consequences of mis-segregation of chromosomes. The goal of this project is to understand how mis-segregation and the resulting aneuploidy affect the progression of cells through the subsequent phases of cell cycle.

Generation of aneuploid cells

A common method used to generate aneuploid cells involves destabilizing the mitotic spindle with small molecule spindle poisons such as colchicine, taxol, nocodazole or monastrol, which is an inhibitor of Eg5, a kinesin required for bi-polar spindle establishment (Lampson and Kapoor, 2006). Destabilization of the spindle leads to activation of the spindle assembly checkpoint (SAC), which leads to mitotic arrest. The SAC is a quality control mechanism, which ensures that each kinetochore from a pair of sister chromatids are attached to microtubule

spindles originating from the opposite poles, a phenomenon called as bi-orientation. Bi-orientation of sister chromatids ensures that during cell division, each daughter cell receives an equal complement set of chromosomes (Musacchio and Salmon, 2007). Perturbation of the mitotic spindle with poisons and subsequent mitotic delay favor merotelic kinetochore attachment, wherein a single kinetochore is attached to microtubules originating from both the poles (Cimini et al., 1999; Cimini et al., 2001; Knowlton et al., 2006). Mis-attachment of kinetochores hampers the fidelity of chromosome segregation leading to lagging chromosomes during anaphase culminating in generation of aneuploid daughter cells (Thompson and Compton, 2008).

Recently, studies have found that aneuploidy induced by using spindle poisons leads to p53 activation and subsequent arrest in G1 phase and thus making it difficult to study cell cycle progression in aneuploid cells (Thompson and Compton, 2010; Hinchcliffe et al., 2016; Li et al., 2010). Interestingly, Uetake and Sluder found that the p53-dependent arrest is linked to the duration spent in pro-metaphase rather than mis-segregation of chromosomes. If cells spent more than 1.5 hours in pro-metaphase then they arrested in the subsequent G1 phase regardless of whether chromosomes mis-segregated or not (Uetake and Sluder, 2010). Thus aneuploidy itself does not activate p53, but rather prolonged duration of arrest in pro-metaphase does (Uetake and Sluder, 2010; Orth et al., 2012; Hayashi et al., 2012).

With this result in mind Santaguida et al., generated aneuploid cells by using the exact opposite approach, that is by inhibiting SAC rather than activating it (Santaguida et al., 2010; Santaguida et al., 2015; Hewitt et al., 2010; Colombo et al., 2010). Since SAC ensures bi-orientation and proper segregation of chromosomes, its inhibition allows for mitosis to occur even when the chromosomes are mis-attached thus generating aneuploid daughter cells. Aneuploid cells are generated by faster progression through mitosis in the presence of mis-attached chromosomes rather than a delay and thus avoid G1 arrest. By generating aneuploid cells by inhibiting SAC, we could look at how aneuploidy affects the subsequent progression through cell cycle. Specifically we studied how subsequent S phase progression is affected by DNA combing (Santaguida et al., 2017).

Results

Examining S phase by DNA combing in human aneuploid cells

To study the effect of aneuploidy on S phase progression we induced mis-segregation in non-transformed human retinal pigment epithelial cells immortalized with human telomerase reverse transcriptase (RPE-1 hTERT). The cells were treated for 24 hours with vehicle control or 2 μM AZ3146, an inhibitor of Mps1, to generate aneuploidy (Hewitt et al., 2010). Mps1 is a kinase that localizes to the kinetochores and is necessary for activation and maintenance of the SAC (Liu and Winey, 2012). Inhibition of Mps1 leads to mis-

segregation of a few chromosomes in a majority of cells (Santaguida et al., 2015). Each chromosome was found to be mis-segregated in 6-8% of mitoses (Santaguida et al., 2015; Santaguida et al., 2017). Following mis-segregation the cells were synchronized in G1 phase using mimosine and released into S phase. 3 hours into S phase the cells were pulsed with 25 μM IdU for 1 hr. followed by 200 μM CldU for 1 hr. The cells were processed for combing as before except the cell wall digestion step was skipped. IdU was visualized using green antibody and CldU was visualized using red antibody. Figure 4.1 shows a representative fiber from each sample with an interpretation for each labeled track below it. The combing experiment was done twice. The second replicate was done in collaboration with Genomic Vision, France. For euploid cells we collected a total of 47 and 54 Mb of DNA and for the aneuploid cells we collected 33 and 38 Mb of DNA in the first and the second replicate respectively.

Figure 4.1 Representative fibers from euploid and aneuploid cells.

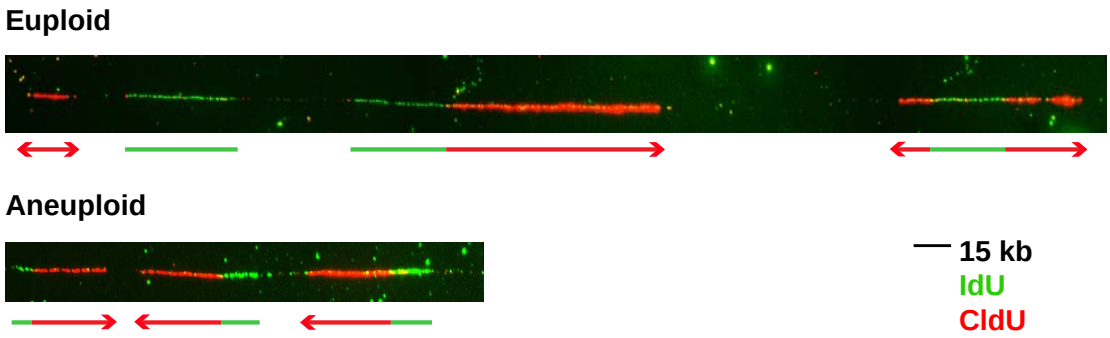

Figure 4.1 Representative fibers from euploid and aneuploid cells. RPE-1 hTERT cells were treated with Mps1 inhibitor to induce aneuploidy. Following mis-segregation cells were synchronized in G1 phase and pulsed with IdU and CldU in the subsequent S phase. Figure 4.1 shows a fiber from each euploid and aneuploid cells with IdU labeled in green and CldU in red.

Aneuploidy causes an increase in origin firing rate

We first examined the effect of aneuploidy on origin firing. As explained in greater detail in Chapter II we calculated origin firing rate and fork density for both analogs combined as well as separately for each analog per fiber per kb. We normalized the values obtained from the aneuploid cells to that from the euploid cells. We find that the total origin firing rate is higher by 2-fold ($p=1.5x10^{-34}$) in the aneuploid cells as compared to euploid cells (Figure 4.2A). Analog specific origin firing estimations also show 2- and 1.5- fold higher origin firing during first ($p=2.27x10^{-36}$) and second ($p=0.03$) analog in aneuploid cells as compared to euploid cells (Figure 4.2A). It should be noted that the increase in origin density seen in the second analog in aneuploid cells as compared to euploid cells is not reflected in the total origin density because, there were far fewer second analog origins than the first analog origins in the majority of fibers. Fork density also shows a similar pattern. We see a 1.7-fold increase in total ($p=7.46x10^{-13}$) as well as first ($p=1.22x10^{-19}$) and second ($p=4.71x10^{-11}$) analog specific fork densities in aneuploid cells as compared to euploid cells (Figure 4.2A).

Figure 4.2 Aneuploidy causes replication defects.

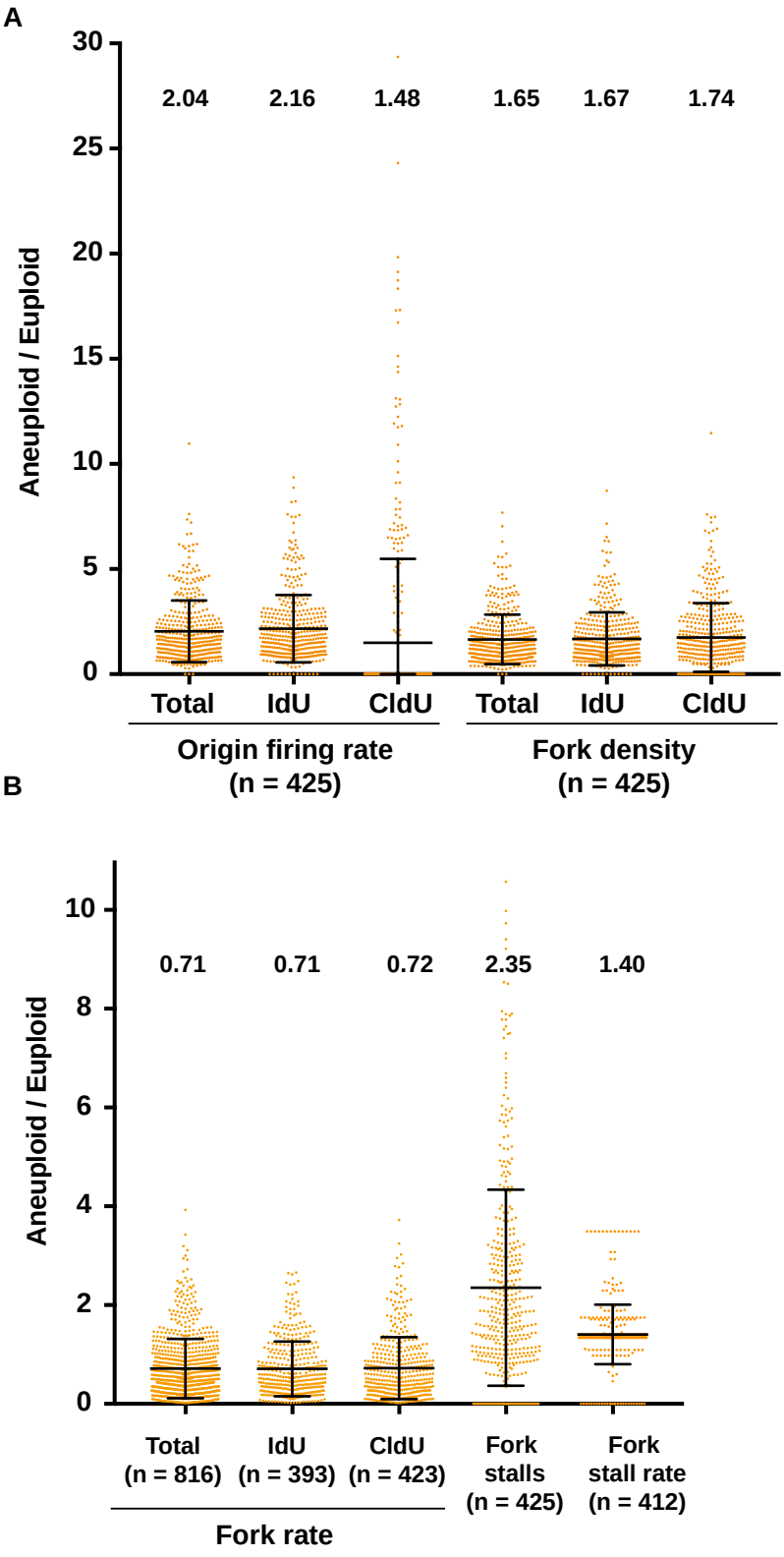
A
Aneuploid / Euploid
30
25
20
15
10
5
0
2.04
2.16
1.48
1.65
1.67
1.74
Total
IdU
CldU
Total
IdU
CldU
Origin firing rate
(n = 425)
Fork density
(n = 425)
B
Aneuploid / Euploid
10
8
6
4
2
0
0.71
0.71
0.72
2.35
1.40
Total
(n = 816)
IdU
(n = 393)
CldU
(n = 423)
Fork
stalls
(n = 425)
Fork
stall rate
(n = 412)
Fork rate

Figure 4.2 Aneuploidy causes replication defects. (A) Aneuploidy causes an increase in origin firing rate. Total and analog specific origin firing rate and fork densities were estimated for aneuploid cells from 2 replicates and normalized to that from the euploid cells. (B) Aneuploidy causes reduction in fork rate and an increase in fork stalls and fork stalling rate. Fork rate from all forks, or IdU forks, or CldU forks, fork stalls, and fork stall rate were estimated for aneuploid cells from 2 replicates and normalized to that from the euploid cells. See Chapter II for calculations.

Aneuploidy causes reduction in fork rate and an increase in fork stalls

We calculated fork rate values from both IdU (green [G]) and CldU (red [R]) tracks. For IdU, fork rate values were obtained from RG and GR elongating forks as well as GRG termination events. For CldU, fork rates were obtained from RG, GR, and RGR (origins). Overall we see a reduction of 29% in fork rates ($p=2.21x10^{-16}$) from aneuploid cells as compared to euploid cells (Figure 4.2B). Fork rate during IdU ($p=4.46x10^{-10}$) and CldU ($p=2.89x10^{-8}$) also show 29 and 28% reduction respectively in aneuploid as compared to euploid cells (Figure 4.2B).

Next, we calculated fork stalls as well as fork stall rate per fiber per kb. We see a 2.35-fold increase ($p=2.93x10^{-33}$) in absolute number of fork stalls per kb in aneuploid cells as compared to euploid cells (Figure 4.2B). Since the origin firing rate is higher in aneuploid cells as compared to euploid population, we normalized the absolute number of stalls to the number of ongoing forks to get the fork stall rate. We see a 1.4-fold increase ($p=7.71x10^{-23}$) in fork stall rate in aneuploid cells as compared to euploid cells (Figure 4.2B).

Discussion

In this study we have looked at the immediate consequences of aneuploidy on S phase progression. Although aneuploidy is frequently associated with genomic instability and poor outcomes in tumor therapy, the exact mechanism by which aneuploidy induces genomic instability or whether it is merely a consequence of

genomic instability has been difficult to tease apart (Storchova and Pellman, 2004; Santaguida and Amon, 2015; Gordon et al., 2012; Weaver and Cleveland, 2006; Siegel and Amon, 2012). To understand the immediate consequences of aneuploidy on cell cycle progression we took a novel approach to generate aneuploid cells. Briefly, we used an SAC inhibitor rather than an activator to generate aneuploid cells, which usually triggers a mitotic delay. The absence of mitotic delay prevents p53 dependent G1 arrest, allowing us to study the immediate consequences of aneuploidy on cell cycle progression.

By DNA combing we find that there is a discernable effect on the subsequent S phase progression following mis-segregation in mitosis. Fork progression is slowed and origin firing rate increased in aneuploid cells as compared to euploid cells. The reduced fork progression may prevent passive replication of less efficient origins and thus increase the probability of them firing leading to increased origin firing rate in aneuploid cells (Yekezare et al., 2013; Rhind et al., 2010). Reduction in fork rate and increase in origin firing in response to aneuploidy was recently also reported in human pluripotent stem cells (Lamm et al., 2016). Thus it appears to be a conserved response to aneuploidy across cell types. Finally we also see an increase in fork stalling events in aneuploid cells as compared to euploid cells.

What is the source of replication defects in aneuploid cells?

A recent study has found evidence that addition of even a single extra chromosome causes a reduction in the levels of MCM2, 3, 7 subunits. Specifically, less MCM complexes were loaded on the chromatin in aneuploid cells as compared to euploid cells (Passerini et al., 2016). Several studies have shown that reduced MCM levels causes replication defects (Ge and Blow, 2010; Ge et al., 2007; Woodward et al., 2006). Decrease in MCM levels was found to be consistent, regardless of which extra copy of chromosome was added (chromosome 3, 5, 8, 12 or 21) to HCT116 or RPE-1 cells. Finally Passerini et al., were able to mitigate the accumulation of DNA damage markers such as 53BP1 foci by over-expressing MCM7 subunit in aneuploid cells (Passerini et al., 2016). Thus, perturbations of replication components could be a source of replication stress in aneuploid cells.

Based on the combing results Santaguida et al. carried out further investigation of immediate effects of aneuploidy on cell cycle progression (Santaguida et al., 2017). They found that replication defects during S phase furthers genomic instability as assessed by accumulation of 53BP1 and γ-H2AX foci, and DNA bridges during the subsequent anaphase. Mitosis of such aneuploid cells further exacerbates the genome imbalance with a larger percentage of cells harboring complex karyotypes during the second round of cell division. Thus mis-segregation and generation of aneuploidy during one round of mitosis leads to replication stress and exacerbates the chromosomal imbalance

during the second round of mitosis leading to generation of cells with complex karyotypes.

Chapter V

Discussion

Discussion

The intra-S checkpoint plays a critical role in protecting the integrity of genome. ATR deletion is lethal and hypomorphic mutations lead to severe developmental abnormalities, resulting in Seckel Syndrome in humans (Brown and Baltimore, 2000; O'Driscoll et al., 2003). Depletion of ATR in adult mice leads to replication stress, genomic instability and premature onset of age-related degeneration of tissues, emphasizing the importance of the intra-S checkpoint (Ruzankina et al., 2007; Murga et al., 2009). Thus, understanding the role of intra-S checkpoint is critical.

The overall goal of this project is to understand the regulation of forks by the checkpoint in response to DNA damage. Several studies have hinted that regulation of forks is the most crucial function of intra-S checkpoint in response to damage (Chapter I). However the role of the checkpoint at replication forks encountering damage has remained largely elusive. A major hurdle to studying fork progression has been lack of techniques to measure fork rates at single-molecule resolution on a global scale. To address this issue we implemented sequential analog labeling in fission yeast to measure replication fork rates by DNA combing (Chapter II). We also developed a detailed analysis of every permutation of labeled track found in a tri-color combing dataset. This analysis has helped us rigorously identify and measure fork stall rates as a distinct response from fork slowing in response to DNA damage (Chapter III). Further, by combing we also saw a distinct response to DNA damage caused by different

kinds of lesions at different densities. To summarize, inhibition of origin firing is checkpoint dependent, while reduction in fork rate is checkpoint independent. However the checkpoint may facilitate progression of forks through a damaged template.

Finally we also looked at how aneuploidy affects S phase progression in collaboration with Angelika Amon's lab at MIT. We find that aneuploidy leads to decrease in fork rate, increase in origin firing and fork stall rate.

In this chapter, I'll discuss the implications of our results (Chapter III) and avenues for future research.

Fork slowing is checkpoint independent

Although several different groups have reported slowing of forks in response to DNA damage, whether the response is checkpoint dependent or not has been controversial (Tercero and Diffley, 2001; Szyjka et al., 2008; Unsal-Kaçmaz et al., 2007; Seiler et al., 2007; Conti et al., 2007). Therefore, we addressed this issue by using three different DNA damaging drugs – 4NQO, MMS and bleomycin at very different lesions densities. We find that fork rate reduces only in response to MMS, which causes the highest lesion density at the concentrations used in our study as compared to 4NQO and bleomycin. Even though 4NQO and bleomycin activate the checkpoint we don't see any reduction in fork rate. Consistently, we see reduction in fork rate only in *cds1*Δ cells treated with MMS. Thus we have conclusively shown that reduction in fork rate is

checkpoint independent and depends on the physical presence of the lesions at a sufficiently high frequency (Chapter III).

How does the checkpoint facilitate fork progression across a damaged template?

We see a greater reduction in fork rate in *cds1*Δ cells as compared to wild-type cells treated with MMS (Chapter III). This result indicates that the checkpoint may facilitate replication through a damaged template. It would be interesting to identify the factors at the replication fork that facilitate replication across a damaged template in a checkpoint dependent manner. One approach could be using isolation of proteins on nascent DNA (iPOND), which involves labeling cells with 5-ethynyl-2'-deoxyuridine (EdU), conjugating biotin to EdU using click chemistry, and purifying nascent replicated regions using biotin-streptavidin affinity purification (Sirbu et al., 2012; Dungrawala and Cortez, 2015; Sirbu et al., 2013; Dungrawala et al., 2015). When combined with mass-spectrometry, iPOND allows identification of proteins at nascent replication forks (Sirbu et al., 2012). Comparing the proteins or the post-translational modification they harbor in the presence and absence of checkpoint in response to damage may shed light on the role of checkpoint in facilitating replication across a damaged template. Further it would be interesting to quantitatively identify the modifications on PCNA in the presence and absence of the checkpoint. Such an approach may shed light on the regulation of mono-, poly-ubiquitination, and sumoylation of PCNA by the checkpoint in response to damage.

Another approach could be to try combing with mutants implicated in fork restart to see whether we can recapitulate the phenotype of *cds1*Δ. Candidates of interest could be Mus81 and Dna2 (Chapter I).

Fate of stalled forks

A major finding from our combing data is that fork slowing and fork stalling are two distinct responses to DNA damage with different contribution towards bulk slowing (Chapter III). This finding opens a lot of questions regarding fork progression through a damaged template. What is the kinetics of fork progression across a damaged template? What is the kinetics of fork stalling? Do forks stall only at complex lesions or is stalling a stochastic response to lesions? Are the fork stalls different between 4NQO and MMS? What is the fate of the forks that stall (at least throughout the duration of our experiment)? Further, we see a high percentage (15%) of forks stalling even in unperturbed conditions (Chapter III). What is the source of stalling under unperturbed conditions? Is it sequence specific?

A major limitation of combing is that it provides a snapshot rather than a dynamic picture of replication. The questions listed above can be addressed by monitoring real-time fork progression through a damaged template as discussed below.

Real-time analysis of forks

Several tools recently developed in the field of replication offer great promise for elucidation of fork regulation. The three main advances are – the first - development of *in vitro* purified system for regulated eukaryotic replication, the second - ‘DNA curtains’ to look at protein-DNA interaction at single–molecule level in a high-throughput manner, and the third - a novel approach termed ‘PhADE’ to look at single molecules of labeled protein in action (Yeeles et al., 2017; Yeeles et al., 2015; Kurat et al., 2017; Yardimci et al., 2012; Loveland et al., 2012; Greene et al., 2010; Duzdevich et al., 2014).

The Diffley lab has made great advances in the field of replication by purifying and defining the minimal components necessary for eukaryotic chromosomal replication (Yeeles et al., 2017; Yeeles et al., 2015; Kurat et al., 2017). This system could potentially be used to understand the roles of individual proteins in fork regulation identified from iPOND as well as other studies (Chapter I).

Although the reconstituted system will allow us to identify the role of new factors at the fork, ensemble studies mask heterogeneity and short-lived interactions. DNA curtains, is a powerful approach to study protein-DNA interactions at single-molecule level in a high-throughput fashion (Greene et al., 2010; Collins et al., 2014). Briefly, flow cells with slides containing nanobarriers are created manually or using nanofabrication techniques. The slide is coated with lipid bilayer and one end of the λ-DNA is conjugated to the lipid bilayer using

biotin-streptavidin interaction. The DNA molecules are aligned, by flowing buffer into the flow cell. The lipid molecules flow in the direction of buffer until they hit a nanobarrier, which is designed to be perpendicular to the direction of the flow. This approach leads to alignment of thousands of DNA molecules parallel to one another. The slide can be modified so that the second end of the DNA is also tethered. By flowing in a fluorescently labeled protein of interest we can study the dynamics of protein-DNA interaction at several molecules of DNA simultaneously using total internal reflection fluorescence (TIRF) microscopy (Sternberg et al., 2014; Redding et al., 2015; Wang et al., 2013; Qi et al., 2015; Gorman et al., 2012; Finkelstein et al., 2010; Collins et al., 2014).

A major obstacle to studying protein function at single-molecule level in real-time is the ability to image fluorescently labeled protein at physiological concentrations. This obstacle was overcome by the development of a novel approach termed 'PhADE' (*Ph*oto*A*ctivation, *D*iffusion, *E*xcitation) by Loveland from the Walter lab (Loveland et al., 2012). Briefly, replication is visualized on λ-DNA immobilized in a flow cell supplemented with *Xenopus* egg extract (Yardimci et al., 2012). In the egg extract, a protein of interest is tagged with a photo-activatable fluorescent protein and allowed to flow in and bind to the immobilized DNA. The labeled molecules of the protein of interest close to the surface are converted by using TIRF illumination, so that they fluoresce at a different wavelength than the protein molecules that are not illuminated. The converted molecules of protein bound on the DNA can be easily visualized by TIRF

excitation. The converted protein molecules that are not bound to DNA but are close to the surface are in constant equilibrium with the non-illuminated protein molecules in the extract, which are in far greater excess. Thus the unbound converted protein molecules easily diffuse away minimizing the noise in this TIRF imaging system (Loveland et al., 2012).

DNA curtains could be potentially combined with the purified reconstituted system developed by the Diffley lab to study the role of individual factors in action at the replication forks in real-time at single-molecule resolution. The PhADE approach could be implemented with DNA curtains if a protein of interest must be used at high concentration for optimal activity. While combing only gives us static information regarding fork stalling, using real-time monitoring will allow us to detect the kinetics of fork stalling. We will be able to address whether fork stalling is programmed or stochastic. We could potentially create λ-DNA molecules harboring different kinds of MMS-induced lesions, to characterize which lesions predominantly cause fork stalling. Further it will also allow us to clarify whether reduction of forks observed by combing is due to uniform slowing or frequent stalls leading to less replication in response to damage.

Why does 4NQO activate the checkpoint faster than MMS?

We estimate that the lesions caused by 4NQO are 25-fold rarer than those caused by MMS at the concentrations used in our study (Snyderwine and Bohr, 1992; Lundin et al., 2005). Yet 4NQO appears to activate the checkpoint faster

than MMS and leads to similar levels of bulk slowing as assessed by flow cytometry (Chapter III). Lesions caused by 4NQO are repaired by NER and MMS-induced lesions are repaired by BER (Wyatt and Pittman, 2006; Jones et al., 1989; Fujiwara, 1989; Edwards et al., 1987; Ikenaga et al., 1977). The kinetics of repair of the lesions caused by the two drugs could be different. It would be interesting to ascertain how their repair efficiencies affect the checkpoint response. One approach could be to use radioactive 4NQO and MMS to estimate the lesion densities achieved in the S phase time course, although such reagents are not commercially available. It may be interesting to see whether the checkpoint activation occurs faster or slower in NER and BER repair deficient mutants as opposed to wild-type. Finally a quantitative detection of formation of ssDNA in response to 4NQO and MMS as described below may help us understand why 4NQO is better at activating the checkpoint.

Bypass of lesions in *cds1*Δ cells

*cds1*Δ cells show greater reduction in fork rate than wild-type in response to MMS, yet they manage to complete replication by 100 minutes as seen by flow cytometry (Chapter III). We wanted to understand how forks are able to bypass lesions and complete replication in *cds1*Δ cells treated with MMS. As mentioned in Chapter I, restart of forks encountering lesions is thought to rely on repriming, translesion-polymerase-based synthesis and/or recombination-mediated template switching. To see which of the above mechansims are used in *cds1*Δ cells to bypass lesions, we deleted all the translesion polymerases as well

recombination factors *swi5* and *rad51* (Chapter VI, Appendix). Surprisingly even in the absence of translesion polymerases as well as recombination factors, *cds1*Δ cells still manage to replicate in the presence of MMS nearly to the levels seen in wild-type (Figure 6.2B). Perhaps lesion bypass in the absence of translesion polymerase as well as recombination occurs via repriming. Repriming of forks on the leading strand should leave ssDNA gaps (Figure 6.2B). One approach could be to look for ssDNA gaps by electron microscopy (Lopes et al., 2006). Another approach to detect ssDNA could be, to do a pull-down for ssDNA regions in the genome using an antibody against ssDNA binding protein followed by strand-specific sequencing (Zhou et al., 2013).

Conclusion

In summary, we have studied the regulation of replication in response to damage using a single-molecule approach in *S pombe*. Using three different damaging drugs at different densities we find that reduction in forks in response to damage is checkpoint independent. However the checkpoint may facilitate fork progression through a damaged template. Using a novel approach we have rigorously quantified fork stall events in a tri-color combing dataset and find that they contribute significantly towards bulk slowing.

For future work, it would be interesting to look at the kinetics of fork stalling using real-time monitoring of fork progression as well identifying factors that

mediate checkpoint-dependent progression of forks through a damaged template.

Chapter VI

Appendix

Bypass of lesions in *cds1*Δ cells

Unpublished results

Bypass of lesions in *cds1*Δ cells

*cds1*Δ cells fail to suppress origin firing and show a greater reduction in fork rate than wild-type in response to MMS. By bulk assay, *cds1*Δ cells complete replication in the presence of MMS by 100 minutes. We were interested in understanding the mechanism by which *cds1*Δ cells bypass lesions and complete replication in the presence of MMS. As mentioned in Chapter I the mechanisms by which forks restart include repriming, translesion-polymerase-based synthesis, and template switching. We were interested in understanding which of the above three pathways are employed in *cds1*Δ cells to bypass MMS-induced lesions. To this end, we deleted all the four translesion polymerases as well as recombination factors *swi5* and *rad51* in a *cds1*Δ background in *S. pombe*. We performed the S phase progression assay in response to MMS and 4NQO.

Results

To examine the progression of S phase in *cds1*Δ cells lacking translesion-polymerase-based synthesis and recombination-mediated template switching we built *cds1*Δ*swi5*Δ*rad51*Δ*rev3*Δ*rev1*Δ*mug40*Δ*eso1-D147N* (yDI157) strain. The *eso1* gene in fission yeast encodes a fusion protein of two domains with one domain coding for DNA polymerase η and the other domain coding for an essential sister chromatid cohesion protein, Eco1/Ctf7 (Tanaka et al., 2000). The point mutant (147 aspartate to asparagine) of Eso1 abolishes the catalytic activity of the polymerase domain (Callegari et al., 2010). We performed the S phase

progression assay as mentioned before. We found that in yDI157 replication in the untreated sample itself is slightly slower than in the *cds1*Δ cells. In the presence of MMS or 4NQO, yDI157 cells replicate slower and do not complete replication even by 180 minutes (Figure 6.1 A). The extent of slowing in yDI157 is quite similar to what we observe in wild-type in response to 4NQO or MMS, albeit a little less (Figure 6.1 B).

We also looked at S phase slowing in *cds1*Δ*swi5*Δ*rev3*Δ*rev1*Δ*mug40*Δ*eso1-D147N* (yDI132) *or cds1*Δ*swi5*Δ*rev3*Δ*rev1*Δ*mug40*Δ*rad30*Δ*nmt41*::*eso1* (yDI131). *rad30*Δ*nmt41::eso1* is an allele in which the polymerase domain of *eso1* is deleted and the *eso1* is overexpressed under the *nmt41* promoter. In yDI131 and yDI132, the TLS pathway is completely compromised however the rad51-dependent recombination pathway is only partially compromised. In *S. pombe* the Rad51-dependent recombination depends on two sets of mediators, Swi5/Sfr1 and Rhp55/57 (Akamatsu et al., 2003; Akamatsu et al., 2007). Therefore deletion of *swi5* only compromises the recombination pathway partially. In yDI131 or yDI132 the phenotype in response to MMS is very similar to that of *cds1*Δ (Figure 6.1C). Only at 120 minutes we see slightly less replication in yDI131 or yDI132 as compared to *cds1*Δ treated with MMS (Figure 6.1C). Thus recombination may play a bigger role than TLS pathway in bypass of lesions in the absence of *cds1* (Figure 6.1).

Figure 6.1 Replication of damaged DNA in *cds1*Δ is partially dependent on translesion polymerases and recombination.

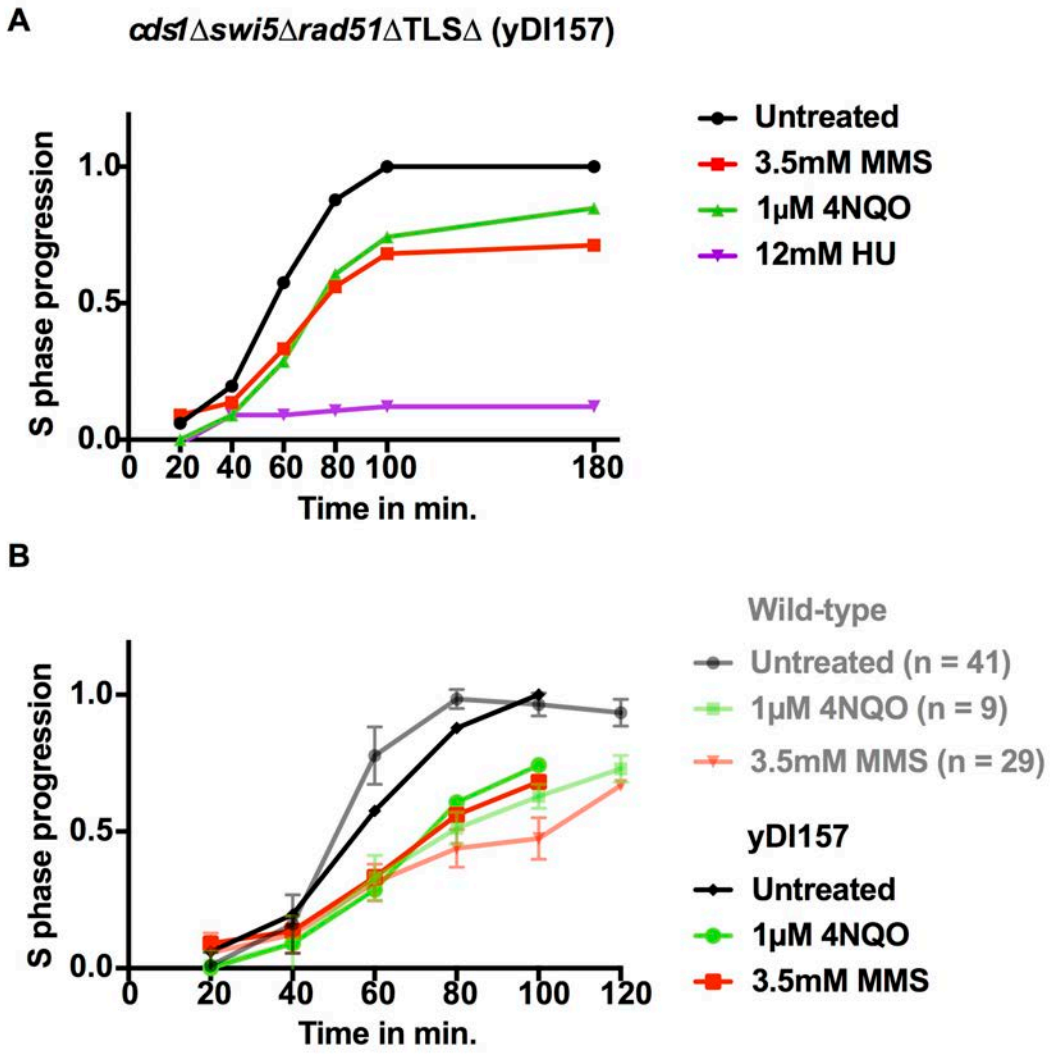

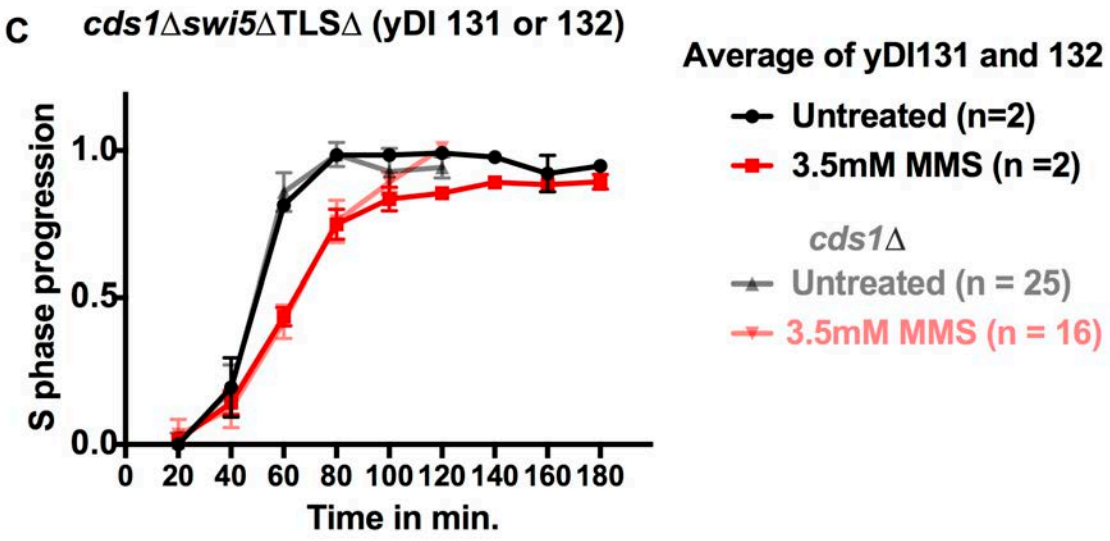

Figure 6.1 Replication of damaged DNA in *cds1*Δ is partially dependent on translesion polymerases and recombination. (A) yDI157 cells were synchronized in G1 phase using cdc10-M17 temperature sensitive allele followed by elutriation. Elutriated G1 cells were released into permissive temperature untreated or treated with 3.5 mM MMS or 1 µM 4NQO or 12mM HU. S phase progression was followed by taking samples for FACS. (B) S phase progression in yDI157 is overlayed with wild-type for comparison. (C) Average S phase progression of yDI131 and132 overlayed with *cds1*Δ. Error bars represent standard deviation. TLSΔ = *rev3*Δ*rev1*Δ*mug40*Δ*eso1-D147N or rev3*Δ*rev1*Δ*mug40*Δ*rad30*Δ*nmt41::eso1.*

Discussion

The goal of this experiment was to understand how forks bypass damage-induced lesions to complete replication in *cds1*Δ cells. To address this question we deleted all the translesion polymerases and recombination factors in *cds1*Δ cells. We find that the bypass of lesion and continued progression of fork relies on translesion-polymerase-based synthesis as well as recombination-mediated template switching. Recombination may contribute more to bypass of lesions than the translesion polymerases in the absence of *cds1*. Despite the lack of translesion polymerases and recombination, the yDI157 cells still manage to replicate nearly as much as seen in wild-type cells in response to MMS. We hypothesize that some forks may still bypass lesions using downstream repriming as a mechanism (Figure 6.2). It would be interesting to test this hypothesis by looking for ssDNA gaps.

Figure 6.2 Schematic representation of ssDNA gaps left behind by repriming on the leading strand.

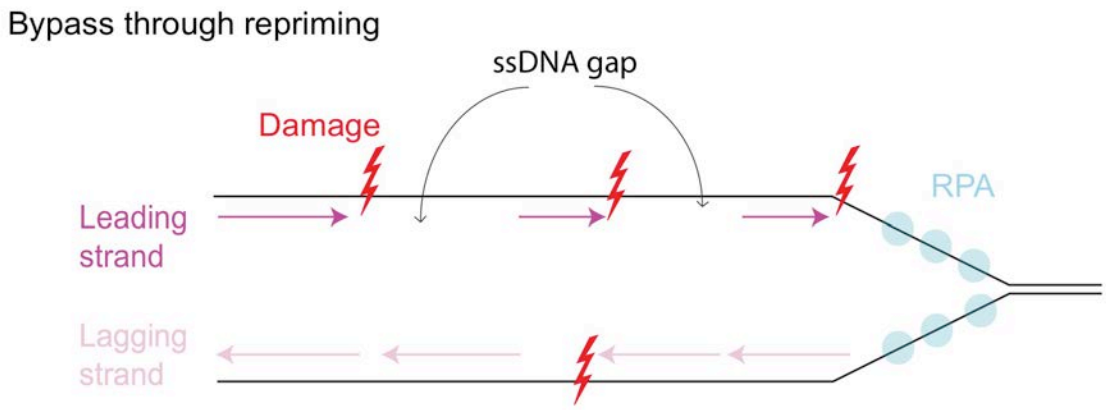

Figure 6.2 Schematic representation of ssDNA gaps left behind by repriming on the leading strand.

Materials and Methods

Strains

yDI157 (*h- leu1-32 ura4-D18 cdc10-M17 cds1::ura4+ rad51::natR swi5::his3 rev3::kanMX6 rev1::ura4 mug40::hyg eso1-D147N-kanMX rad11-GFP::hph-MX6*)

yDI131 (*h- leu1-32 ura4-D18 cdc10-M17 cds1::ura4+ swi5::his3 rev3::kanMX6 rev1::ura4 mug40::hyg rad30::kanMX::nmt41:eso1*)

yDI132 (*h- leu1-32 ura4-D18 cdc10-M17 cds1::ura4+ swi5::his3 rev3::kanMX6 rev1::ura4 mug40::kanMX eso1-D147N-kanMX*)

S phase progression by flow cytometry.

yDI157, 131, and 132 were grown to mid log phase at 25°C and arrested at 35°C for 2 hours followed by centrifugal-elutriation-based size selection at 35°C to collect cells that had most recently arrested in G1. The cells were then immediately released into S phase by shifting them to 25°C, untreated or treated with 3.5mM MMS or 1 μM 4NQO or 12mM HU. S-phase progression was followed by flow cytometry using a nuclei isolation protocol, as previously described (Willis and Rhind, 2011) with some minor modifications (Chapter II).

References

Adams, K. E., Medhurst, A. L., Dart, D. A., and Lakin, N. D. (2006). Recruitment of ATR to sites of ionising radiation-induced DNA damage requires ATM and components of the MRN protein complex. Oncogene *25*, 3894-3904.

Akamatsu, Y., Dziadkowiec, D., Ikeguchi, M., Shinagawa, H., and Iwasaki, H. (2003). Two different Swi5-containing protein complexes are involved in mating-type switching and recombination repair in fission yeast. Proc Natl Acad Sci U S A *100*, 15770-15775.

Akamatsu, Y., Tsutsui, Y., Morishita, T., Siddique, M. S., Kurokawa, Y., Ikeguchi, M., Yamao, F., Arcangioli, B., and Iwasaki, H. (2007). Fission yeast Swi5/Sfr1 and Rhp55/Rhp57 differentially regulate Rhp51-dependent recombination outcomes. EMBO J *26*, 1352-1362.

Allemand, J. F., Bensimon, D., Jullien, L., Bensimon, A., and Croquette, V. (1997). pH-dependent specific binding and combing of DNA. Biophys J *73*, 2064-2070.

Amangyeld, T., Shin, Y. K., Lee, M., Kwon, B., and Seo, Y. S. (2014). Human MUS81-EME2 can cleave a variety of DNA structures including intact Holliday junction and nicked duplex. Nucleic Acids Res *42*, 5846-5862.

Anglana, M., Apiou, F., Bensimon, A., and Debatisse, M. (2003). Dynamics of DNA replication in mammalian somatic cells: nucleotide pool modulates origin choice and interorigin spacing. Cell *114*, 385-394.

Asaithamby, A., and Chen, D. J. (2009). Cellular responses to DNA double-strand breaks after low-dose gamma-irradiation. Nucleic Acids Res *37*, 3912-3923.

Aten, J. A., Bakker, P. J., Stap, J., Boschman, G. A., and Veenhof, C. H. (1992). DNA double labelling with IdUrd and CldUrd for spatial and temporal analysis of cell proliferation and DNA replication. Histochem J *24*, 251-259.

Ball, H. L., Ehrhardt, M. R., Mordes, D. A., Glick, G. G., Chazin, W. J., and Cortez, D. (2007). Function of a conserved checkpoint recruitment domain in ATRIP proteins. Mol Cell Biol *27*, 3367-3377.

Bartek, J., Falck, J., and Lukas, J. (2001). CHK2 kinase--a busy messenger. Nat Rev Mol Cell Biol *2*, 877-886.

Bartek, J., Lukas, C., and Lukas, J. (2004). Checking on DNA damage in S phase. Nat Rev Mol Cell Biol *5*, 792-804.

Bartek, J., and Lukas, J. (2001). Mammalian G1- and S-phase checkpoints in response to DNA damage. Curr Opin Cell Biol *13*, 738-747.

Bartek, J., and Lukas, J. (2003). Chk1 and Chk2 kinases in checkpoint control and cancer. Cancer Cell *3*, 421-429.
Bechhoefer, J., and Rhind, N. (2012). Replication timing and its emergence from stochastic processes. Trends Genet *28*, 374-381.
Ben-Yehoyada, M., Wang, L. C., Kozekov, I. D., Rizzo, C. J., Gottesman, M. E., and Gautier, J. (2009). Checkpoint signaling from a single DNA interstrand crosslink. Mol Cell *35*, 704-715.
Bensimon, A., Simon, A., Chiffaudel, A., Croquette, V., Heslot, F., and Bensimon, D. (1994). Alignment and sensitive detection of DNA by a moving interface. Science *265*, 2096-2098.
Bermejo, R., Capra, T., Jossen, R., Colosio, A., Frattini, C., Carotenuto, W., Cocito, A., Doksani, Y., Klein, H., Gómez-González, B., Aguilera, A., Katou, Y., Shirahige, K., and Foiani, M. (2011). The replication checkpoint protects fork stability by releasing transcribed genes from nuclear pores. Cell *146*, 233-246.
Bermejo, R., Kumar, A., and Foiani, M. (2012a). Preserving the genome by regulating chromatin association with the nuclear envelope. Trends Cell Biol *22*, 465-473.
Bermejo, R., Lai, M. S., and Foiani, M. (2012b). Preventing replication stress to maintain genome stability: resolving conflicts between replication and transcription. Mol Cell *45*, 710-718.
Bermudez, V. P., Lindsey-Boltz, L. A., Cesare, A. J., Maniwa, Y., Griffith, J. D., Hurwitz, J., and Sancar, A. (2003). Loading of the human 9-1-1 checkpoint complex onto DNA by the checkpoint clamp loader hRad17-replication factor C complex in vitro. Proc Natl Acad Sci U S A *100*, 1633-1638.
Berti, M., Ray Chaudhuri, A., Thangavel, S., Gomathinayagam, S., Kenig, S., Vujanovic, M., Odreman, F., Glatter, T., Graziano, S., Mendoza-Maldonado, R., Marino, F., Lucic, B., Biasin, V., Gstaiger, M., Aebersold, R., Sidorova, J. M., Monnat, R. J. J., Lopes, M., and Vindigni, A. (2013). Human RECQ1 promotes restart of replication forks reversed by DNA topoisomerase I inhibition. Nat Struct Mol Biol *20*, 347-354.
Bétous, R., Couch, F. B., Mason, A. C., Eichman, B. F., Manosas, M., and Cortez, D. (2013). Substrate-selective repair and restart of replication forks by DNA translocases. Cell Rep *3*, 1958-1969.
Bétous, R., Mason, A. C., Rambo, R. P., Bansbach, C. E., Badu-Nkansah, A., Sirbu, B. M., Eichman, B. F., and Cortez, D. (2012). SMARCAL1 catalyzes fork regression and Holliday junction migration to maintain genome stability during DNA replication. Genes Dev *26*, 151-162.

Bianchi, J., Rudd, S. G., Jozwiakowski, S. K., Bailey, L. J., Soura, V., Taylor, E., Stevanovic, I., Green, A. J., Stracker, T. H., Lindsay, H. D., and Doherty, A. J. (2013). PrimPol bypasses UV photoproducts during eukaryotic chromosomal DNA replication. Mol Cell *52*, 566-573.

Bianco, J. N., Poli, J., Saksouk, J., Bacal, J., Silva, M. J., Yoshida, K., Lin, Y. L., Tourrière, H., Lengronne, A., and Pasero, P. (2012). Analysis of DNA replication profiles in budding yeast and mammalian cells using DNA combing. Methods *57*, 149-157.

Blastyák, A., Hajdú, I., Unk, I., and Haracska, L. (2010). Role of double-stranded DNA translocase activity of human HLTF in replication of damaged DNA. Mol Cell Biol *30*, 684-693.

Blastyák, A., Pintér, L., Unk, I., Prakash, L., Prakash, S., and Haracska, L. (2007). Yeast Rad5 protein required for postreplication repair has a DNA helicase activity specific for replication fork regression. Mol Cell *28*, 167-175.

Blow, J. J., and Dutta, A. (2005). Preventing re-replication of chromosomal DNA. Nat Rev Mol Cell Biol *6*, 476-486.

Boddy, M. N., and Russell, P. (1999). DNA replication checkpoint control. Front Biosci *4*, D841-8.

Bonilla, C. Y., Melo, J. A., and Toczyski, D. P. (2008). Colocalization of sensors is sufficient to activate the DNA damage checkpoint in the absence of damage. Mol Cell *30*, 267-276.

Branzei, D., and Foiani, M. (2005). The DNA damage response during DNA replication. Curr Opin Cell Biol *17*, 568-575.

Branzei, D., and Foiani, M. (2007). Interplay of replication checkpoints and repair proteins at stalled replication forks. DNA Repair (Amst) *6*, 994-1003.

Branzei, D., and Foiani, M. (2009). The checkpoint response to replication stress. DNA Repair (Amst) *8*, 1038-1046.

Branzei, D., Seki, M., and Enomoto, T. (2004). Rad18/Rad5/Mms2-mediated polyubiquitination of PCNA is implicated in replication completion during replication stress. Genes Cells *9*, 1031-1042.

Branzei, D., and Szakal, B. (2016). DNA damage tolerance by recombination: Molecular pathways and DNA structures. DNA Repair (Amst) *44*, 68-75.

Branzei, D., Vanoli, F., and Foiani, M. (2008). SUMOylation regulates Rad18-mediated template switch. Nature *456*, 915-920.

Brooks, P. J., and Theruvathu, J. A. (2005). DNA adducts from acetaldehyde: implications for alcohol-related carcinogenesis. Alcohol *35*, 187-193.

Brown, E. J., and Baltimore, D. (2000). ATR disruption leads to chromosomal fragmentation and early embryonic lethality. Genes Dev *14*, 397-402.

Bugreev, D. V., Rossi, M. J., and Mazin, A. V. (2011). Cooperation of RAD51 and RAD54 in regression of a model replication fork. Nucleic Acids Res *39*, 2153-2164.

Burcham, P. C. (1999). Internal hazards: baseline DNA damage by endogenous products of normal metabolism. Mutat Res *443*, 11-36.

Byun, T. S., Pacek, M., Yee, M. C., Walter, J. C., and Cimprich, K. A. (2005). Functional uncoupling of MCM helicase and DNA polymerase activities activates the ATR-dependent checkpoint. Genes Dev *19*, 1040-1052.

Cadet, J., Sage, E., and Douki, T. (2005). Ultraviolet radiation-mediated damage to cellular DNA. Mutat Res *571*, 3-17.

Cairns, J. (1963). The bacterial chromosome and its manner of replication as seen by autoradiography. J Mol Biol *6*, 208-213.

Cairns, J. (1966). Autoradiography of HeLa cell DNA. J Mol Biol *15*, 372-373.

Callegari, A. J., Clark, E., Pneuman, A., and Kelly, T. J. (2010). Postreplication gaps at UV lesions are signals for checkpoint activation. Proc Natl Acad Sci U S A *107*, 8219-8224.

Cayrou, C., Coulombe, P., Vigneron, A., Stanojcic, S., Ganier, O., Peiffer, I., Rivals, E., Puy, A., Laurent-Chabalier, S., Desprat, R., and Méchali, M. (2011). Genome-scale analysis of metazoan replication origins reveals their organization in specific but flexible sites defined by conserved features. Genome Res *21*, 1438-1449.

Chastain, P. D., Heffernan, T. P., Nevis, K. R., Lin, L., Kaufmann, W. K., Kaufman, D. G., and Cordeiro-Stone, M. (2006). Checkpoint regulation of replication dynamics in UV-irradiated human cells. Cell Cycle *5*, 2160-2167.

Chen, J., and Stubbe, J. (2005). Bleomycins: towards better therapeutics. Nat Rev Cancer *5*, 102-112.

Chen, S. H., Albuquerque, C. P., Liang, J., Suhandynata, R. T., and Zhou, H. (2010). A proteome-wide analysis of kinase-substrate network in the DNA damage response. J Biol Chem *285*, 12803-12812.

Chiu, R. K., Brun, J., Ramaekers, C., Theys, J., Weng, L., Lambin, P., Gray, D. A., and Wouters, B. G. (2006). Lysine 63-polyubiquitination guards against translesion synthesis-induced mutations. PLoS Genet *2*, e116.

Chou, D. M., and Elledge, S. J. (2006). Tipin and Timeless form a mutually protective complex required for genotoxic stress resistance and checkpoint function. Proc Natl Acad Sci U S A *103*, 18143-18147.

Ciccia, A., and Elledge, S. J. (2010). The DNA damage response: making it safe to play with knives. Mol Cell *40*, 179-204.

Ciccia, A., Nimonkar, A. V., Hu, Y., Hajdu, I., Achar, Y. J., Izhar, L., Petit, S. A., Adamson, B., Yoon, J. C., Kowalczykowski, S. C., Livingston, D. M., Haracska, L., and Elledge, S. J. (2012). Polyubiquitinated PCNA recruits the ZRANB3 translocase to maintain genomic integrity after replication stress. Mol Cell *47*, 396-409.

Cimini, D., Howell, B., Maddox, P., Khodjakov, A., Degrassi, F., and Salmon, E. D. (2001). Merotelic kinetochore orientation is a major mechanism of aneuploidy in mitotic mammalian tissue cells. J Cell Biol *153*, 517-527.

Cimini, D., Tanzarella, C., and Degrassi, F. (1999). Differences in malsegregation rates obtained by scoring ana-telophases or binucleate cells. Mutagenesis *14*, 563-568.

Cimprich, K. A. (2007). Probing ATR activation with model DNA templates. Cell Cycle *6*, 2348-2354.

Cimprich, K. A., and Cortez, D. (2008). ATR: an essential regulator of genome integrity. Nat Rev Mol Cell Biol *9*, 616-627.

Cleaver, J. E., Kaufmann, W. K., Kapp, L. N., and Park, S. D. (1983). Replicon size and excision repair as factors in the inhibition and recovery of DNA synthesis from ultraviolet damage. Biochim Biophys Acta *739*, 207-215.

Cobb, J. A., Bjergbaek, L., Shimada, K., Frei, C., and Gasser, S. M. (2003). DNA polymerase stabilization at stalled replication forks requires Mec1 and the RecQ helicase Sgs1. EMBO J *22*, 4325-4336.

Cobb, J. A., Schleker, T., Rojas, V., Bjergbaek, L., Tercero, J. A., and Gasser, S. M. (2005). Replisome instability, fork collapse, and gross chromosomal rearrangements arise synergistically from Mec1 kinase and RecQ helicase mutations. Genes Dev *19*, 3055-3069.

Collins, B. E., Ye, L. F., Duzdevich, D., and Greene, E. C. (2014). DNA curtains: novel tools for imaging protein-nucleic acid interactions at the single-molecule level. Methods Cell Biol *123*, 217-234.

Colombo, R., Caldarelli, M., Mennecozzi, M., Giorgini, M. L., Sola, F., Cappella, P., Perrera, C., Depaolini, S. R., Rusconi, L., Cucchi, U., Avanzi, N., Bertrand, J. A., Bossi, R. T., Pesenti, E., Galvani, A., Isacchi, A., Colotta, F., Donati, D., and Moll, J. (2010). Targeting the mitotic checkpoint for cancer therapy with NMS-P715, an inhibitor of MPS1 kinase. Cancer Res *70*, 10255-10264.

Comai, L. (2005). The advantages and disadvantages of being polyploid. Nat Rev Genet *6*, 836-846.

Conti, C., Leo, E., Eichler, G. S., Sordet, O., Martin, M. M., Fan, A., Aladjem, M. I., and Pommier, Y. (2010). Inhibition of histone deacetylase in cancer cells slows

down replication forks, activates dormant origins, and induces DNA damage. Cancer Res *70*, 4470-4480.

Conti, C., Seiler, J. A., and Pommier, Y. (2007). The mammalian DNA replication elongation checkpoint: implication of Chk1 and relationship with origin firing as determined by single DNA molecule and single cell analyses. Cell Cycle *6*, 2760-2767.

Cooke, M. S., Evans, M. D., Dizdaroglu, M., and Lunec, J. (2003). Oxidative DNA damage: mechanisms, mutation, and disease. FASEB J *17*, 1195-1214.

Cortez, D. (2005). Unwind and slow down: checkpoint activation by helicase and polymerase uncoupling. Genes Dev *19*, 1007-1012.

Cortez, D. (2015). Preventing replication fork collapse to maintain genome integrity. DNA Repair (Amst) *32*, 149-157.

Costanzo, V., Shechter, D., Lupardus, P. J., Cimprich, K. A., Gottesman, M., and Gautier, J. (2003). An ATR- and Cdc7-dependent DNA damage checkpoint that inhibits initiation of DNA replication. Mol Cell *11*, 203-213.

Cotta-Ramusino, C., Fachinetti, D., Lucca, C., Doksani, Y., Lopes, M., Sogo, J., and Foiani, M. (2005). Exo1 processes stalled replication forks and counteracts fork reversal in checkpoint-defective cells. Mol Cell *17*, 153-159.

Couch, F. B., Bansbach, C. E., Driscoll, R., Luzwick, J. W., Glick, G. G., Bétous, R., Carroll, C. M., Jung, S. Y., Qin, J., Cimprich, K. A., and Cortez, D. (2013). ATR phosphorylates SMARCAL1 to prevent replication fork collapse. Genes Dev *27*, 1610-1623.

Courbet, S., Gay, S., Arnoult, N., Wronka, G., Anglana, M., Brison, O., and Debatisse, M. (2008). Replication fork movement sets chromatin loop size and origin choice in mammalian cells. Nature *455*, 557-560.

Czajkowsky, D. M., Liu, J., Hamlin, J. L., and Shao, Z. (2008). DNA combing reveals intrinsic temporal disorder in the replication of yeast chromosome VI. J Mol Biol *375*, 12-19.

Dahle, D., Griffiths, T. D., and Carpenter, J. G. (1979). Subchromosomal DNA synthesis in X-irradiated V-79 cells. Radiat Res *78*, 542-549.

Daigaku, Y., Davies, A. A., and Ulrich, H. D. (2010). Ubiquitin-dependent DNA damage bypass is separable from genome replication. Nature *465*, 951-955.

Dalgaard, J. Z. (2012). Causes and consequences of ribonucleotide incorporation into nuclear DNA. Trends Genet *28*, 592-597.

Davies, A. A., Huttner, D., Daigaku, Y., Chen, S., and Ulrich, H. D. (2008). Activation of ubiquitin-dependent DNA damage bypass is mediated by replication protein a. Mol Cell *29*, 625-636.

De Piccoli, G., Katou, Y., Itoh, T., Nakato, R., Shirahige, K., and Labib, K. (2012). Replisome stability at defective DNA replication forks is independent of S phase checkpoint kinases. Mol Cell *45*, 696-704.

Deans, A. J., and West, S. C. (2011). DNA interstrand crosslink repair and cancer. Nat Rev Cancer *11*, 467-480.

Dehé, P. M., Coulon, S., Scaglione, S., Shanahan, P., Takedachi, A., Wohlschlegel, J. A., Yates, J. R., Llorente, B., Russell, P., and Gaillard, P. H. (2013). Regulation of Mus81-Eme1 Holliday junction resolvase in response to DNA damage. Nat Struct Mol Biol *20*, 598-603.

Delacroix, S., Wagner, J. M., Kobayashi, M., Yamamoto, K., and Karnitz, L. M. (2007). The Rad9-Hus1-Rad1 (9-1-1) clamp activates checkpoint signaling via TopBP1. Genes Dev *21*, 1472-1477.

Demczuk, A., and Norio, P. (2009). Determining the replication dynamics of specific gene loci by single-molecule analysis of replicated DNA. Methods Mol Biol *521*, 633-671.

Diffley, J. F. (2011). Quality control in the initiation of eukaryotic DNA replication. Philos Trans R Soc Lond B Biol Sci *366*, 3545-3553.

Dileep, V., Rivera-Mulia, J. C., Sima, J., and Gilbert, D. M. (2015). Large-Scale Chromatin Structure-Function Relationships during the Cell Cycle and Development: Insights from Replication Timing. Cold Spring Harb Symp Quant Biol *80*, 53-63.

Dungrawala, H., and Cortez, D. (2015). Purification of proteins on newly synthesized DNA using iPOND. Methods Mol Biol *1228*, 123-131.

Dungrawala, H., Rose, K. L., Bhat, K. P., Mohni, K. N., Glick, G. G., Couch, F. B., and Cortez, D. (2015). The Replication Checkpoint Prevents Two Types of Fork Collapse without Regulating Replisome Stability. Mol Cell *59*, 998-1010.

Duxin, J. P., Moore, H. R., Sidorova, J., Karanja, K., Honaker, Y., Dao, B., Piwnica-Worms, H., Campbell, J. L., Monnat, R. J., and Stewart, S. A. (2012). Okazaki fragment processing-independent role for human Dna2 enzyme during DNA replication. J Biol Chem *287*, 21980-21991.

Duzdevich, D., Redding, S., and Greene, E. C. (2014). DNA dynamics and single-molecule biology. Chem Rev *114*, 3072-3086.

Edwards, S., Fielding, S., and Waters, R. (1987). The response to DNA damage induced by 4-nitroquinoline-1-oxide or its 3-methyl derivative in xeroderma pigmentosum fibroblasts belonging to different complementation groups: evidence for different epistasis groups involved in the repair of large adducts in human DNA. Carcinogenesis *8*, 1071-1075.

Ellison, V., and Stillman, B. (2003). Biochemical characterization of DNA damage checkpoint complexes: clamp loader and clamp complexes with specificity for 5' recessed DNA. PLoS Biol *1*, E33.
Falck, J., Mailand, N., Syljuåsen, R. G., Bartek, J., and Lukas, J. (2001). The ATM-Chk2-Cdc25A checkpoint pathway guards against radioresistant DNA synthesis. Nature *410*, 842-847.
Falck, J., Petrini, J. H., Williams, B. R., Lukas, J., and Bartek, J. (2002). The DNA damage-dependent intra-S phase checkpoint is regulated by parallel pathways. Nat Genet *30*, 290-294.
Fangman, W. L., and Brewer, B. J. (1992). A question of time: replication origins of eukaryotic chromosomes. Cell *71*, 363-366.
Fangman, W. L., Hice, R. H., and Chlebowicz-Sledziewska, E. (1983). ARS replication during the yeast S phase. Cell *32*, 831-838.
Farkash-Amar, S., Lipson, D., Polten, A., Goren, A., Helmstetter, C., Yakhini, Z., and Simon, I. (2008). Global organization of replication time zones of the mouse genome. Genome Res *18*, 1562-1570.
Finkelstein, I. J., Visnapuu, M. L., and Greene, E. C. (2010). Single-molecule imaging reveals mechanisms of protein disruption by a DNA translocase. Nature *468*, 983-987.
Flynn, R. L., and Zou, L. (2011). ATR: a master conductor of cellular responses to DNA replication stress. Trends Biochem Sci *36*, 133-140.
Forsburg, S. L., and Rhind, N. (2006). Basic methods for fission yeast. Yeast *23*, 173-183.
Foss, E. J. (2001). Tof1p regulates DNA damage responses during S phase in Saccharomyces cerevisiae. Genetics *157*, 567-577.
Frampton, J., Irmisch, A., Green, C. M., Neiss, A., Trickey, M., Ulrich, H. D., Furuya, K., Watts, F. Z., Carr, A. M., and Lehmann, A. R. (2006). Postreplication repair and PCNA modification in Schizosaccharomyces pombe. Mol Biol Cell *17*, 2976-2985.
Friedberg, E. C., Walker, G. C., and Siede, W. (1995). DNA Repair and Mutagenesis (Washington, D.C., USA: ASM Press).
Froget, B., Blaisonneau, J., Lambert, S., and Baldacci, G. (2008). Cleavage of stalled forks by fission yeast Mus81/Eme1 in absence of DNA replication checkpoint. Mol Biol Cell *19*, 445-456.
Fugger, K., Chu, W. K., Haahr, P., Kousholt, A. N., Beck, H., Payne, M. J., Hanada, K., Hickson, I. D., and Sørensen, C. S. (2013). FBH1 co-operates with MUS81 in inducing DNA double-strand breaks and cell death following replication stress. Nat Commun *4*, 1423.

Fugger, K., Mistrik, M., Neelsen, K. J., Yao, Q., Zellweger, R., Kousholt, A. N., Haahr, P., Chu, W. K., Bartek, J., Lopes, M., Hickson, I. D., and Sørensen, C. S. (2015). FBH1 Catalyzes Regression of Stalled Replication Forks. Cell Rep

Fujiwara, Y. (1989). Clustered repair of excisable 4-nitroquinoline-1-oxide adducts in a larger fraction of genomic DNA of xeroderma pigmentosum complementation group C cells. Carcinogenesis *10*, 1777-1785.

Galiègue-Zouitina, S., Bailleul, B., Ginot, Y. M., Perly, B., Vigny, P., and Loucheux-Lefebvre, M. H. (1986). N2-guanyl and N6-adenyl arylation of chicken erythrocyte DNA by the ultimate carcinogen of 4-nitroquinoline 1-oxide. Cancer Res *46*, 1858-1863.

Galiègue-Zouitina, S., Bailleul, B., and Loucheux-Lefebvre, M. H. (1985). Adducts from in vivo action of the carcinogen 4-hydroxyaminoquinoline 1-oxide in rats and from in vitro reaction of 4-acetoxyaminoquinoline 1-oxide with DNA and polynucleotides. Cancer Res *45*, 520-525.

Gallo, D., Wang, G., Yip, C. M., and Brown, G. W. (2016a). Analysis of Replicating Yeast Chromosomes by DNA Combing. Cold Spring Harb Protoc *2016*, pdb.prot085118.

Gallo, D., Wang, G., Yip, C. M., and Brown, G. W. (2016b). Single-Molecule Analysis of Replicating Yeast Chromosomes. Cold Spring Harb Protoc *2016*, pdb.top077784.

García-Rodríguez, N., Wong, R. P., and Ulrich, H. D. (2016). Functions of Ubiquitin and SUMO in DNA Replication and Replication Stress. Front Genet *7*, 87.

Gari, K., Décaillet, C., Delannoy, M., Wu, L., and Constantinou, A. (2008). Remodeling of DNA replication structures by the branch point translocase FANCM. Proc Natl Acad Sci U S A *105*, 16107-16112.

Garvik, B., Carson, M., and Hartwell, L. (1995). Single-stranded DNA arising at telomeres in cdc13 mutants may constitute a specific signal for the RAD9 checkpoint. Mol Cell Biol *15*, 6128-6138.

Gatti, R. A., Becker-Catania, S., Chun, H. H., Sun, X., Mitui, M., Lai, C. H., Khanlou, N., Babaei, M., Cheng, R., Clark, C., Huo, Y., Udar, N. C., and Iyer, R. K. (2001). The pathogenesis of ataxia-telangiectasia. Learning from a Rosetta Stone. Clin Rev Allergy Immunol *20*, 87-108.

Ge, X. Q., and Blow, J. J. (2010). Chk1 inhibits replication factory activation but allows dormant origin firing in existing factories. J Cell Biol *191*, 1285-1297.

Ge, X. Q., Jackson, D. A., and Blow, J. J. (2007). Dormant origins licensed by excess Mcm2-7 are required for human cells to survive replicative stress. Genes Dev *21*, 3331-3341.

Gerlinger, M., and Swanton, C. (2010). How Darwinian models inform therapeutic failure initiated by clonal heterogeneity in cancer medicine. Br J Cancer *103*, 1139-1143.

Giannattasio, M., Follonier, C., Tourrière, H., Puddu, F., Lazzaro, F., Pasero, P., Lopes, M., Plevani, P., and Muzi-Falconi, M. (2010). Exo1 competes with repair synthesis, converts NER intermediates to long ssDNA gaps, and promotes checkpoint activation. Mol Cell *40*, 50-62.

Goldar, A., Marsolier-Kergoat, M. C., and Hyrien, O. (2009). Universal temporal profile of replication origin activation in eukaryotes. PLoS One *4*, e5899.

Gordon, D. J., Resio, B., and Pellman, D. (2012). Causes and consequences of aneuploidy in cancer. Nat Rev Genet *13*, 189-203.

Gorman, J., Wang, F., Redding, S., Plys, A. J., Fazio, T., Wind, S., Alani, E. E., and Greene, E. C. (2012). Single-molecule imaging reveals target-search mechanisms during DNA mismatch repair. Proc Natl Acad Sci U S A *109*, E3074-83.

Gratzner, H. G. (1982). Monoclonal antibody to 5-bromo- and 5-iododeoxyuridine: A new reagent for detection of DNA replication. Science *218*, 474-475.

Greene, E. C., Wind, S., Fazio, T., Gorman, J., and Visnapuu, M. L. (2010). DNA curtains for high-throughput single-molecule optical imaging. Methods Enzymol *472*, 293-315.

Griffiths, M., Beaumont, N., Yao, S. Y., Sundaram, M., Boumah, C. E., Davies, A., Kwong, F. Y., Coe, I., Cass, C. E., Young, J. D., and Baldwin, S. A. (1997). Cloning of a human nucleoside transporter implicated in the cellular uptake of adenosine and chemotherapeutic drugs. Nat Med *3*, 89-93.

Guo, C., Kumagai, A., Schlacher, K., Shevchenko, A., Shevchenko, A., and Dunphy, W. G. (2015). Interaction of Chk1 with Treslin negatively regulates the initiation of chromosomal DNA replication. Mol Cell *57*, 492-505.

Hamlin, J. L., Mesner, L. D., Lar, O., Torres, R., Chodaparambil, S. V., and Wang, L. (2008). A revisionist replicon model for higher eukaryotic genomes. J Cell Biochem *105*, 321-329.

Hanada, K., Budzowska, M., Davies, S. L., van Drunen, E., Onizawa, H., Beverloo, H. B., Maas, A., Essers, J., Hickson, I. D., and Kanaar, R. (2007). The structure-specific endonuclease Mus81 contributes to replication restart by generating double-strand DNA breaks. Nat Struct Mol Biol *14*, 1096-1104.

Hanasoge, S., and Ljungman, M. (2007). H2AX phosphorylation after UV irradiation is triggered by DNA repair intermediates and is mediated by the ATR kinase. Carcinogenesis *28*, 2298-2304.

Hand, R. (1975). Regulation of DNA replication on subchromosomal units of mammalian cells. J Cell Biol *64*, 89-97.
Hartwell, L. H., and Weinert, T. A. (1989). Checkpoints: controls that ensure the order of cell cycle events. Science *246*, 629-634.
Hashimoto, Y., Puddu, F., and Costanzo, V. (2011). RAD51- and MRE11-dependent reassembly of uncoupled CMG helicase complex at collapsed replication forks. Nat Struct Mol Biol *19*, 17-24.
Hassold, T., and Hunt, P. (2001). To err (meiotically) is human: the genesis of human aneuploidy. Nat Rev Genet *2*, 280-291.
Hatton, K. S., Dhar, V., Brown, E. H., Iqbal, M. A., Stuart, S., Didamo, V. T., and Schildkraut, C. L. (1988). Replication program of active and inactive multigene families in mammalian cells. Mol Cell Biol *8*, 2149-2158.
Hawkins, M., Retkute, R., Müller, C. A., Saner, N., Tanaka, T. U., de Moura, A. P., and Nieduszynski, C. A. (2013). High-resolution replication profiles define the stochastic nature of genome replication initiation and termination. Cell Rep *5*, 1132-1141.
Hayashi, M. T., Cesare, A. J., Fitzpatrick, J. A., Lazzerini-Denchi, E., and Karlseder, J. (2012). A telomere-dependent DNA damage checkpoint induced by prolonged mitotic arrest. Nat Struct Mol Biol *19*, 387-394.
Heffernan, T. P., Unsal-Kaçmaz, K., Heinloth, A. N., Simpson, D. A., Paules, R. S., Sancar, A., Cordeiro-Stone, M., and Kaufmann, W. K. (2007). Cdc7-Dbf4 and the human S checkpoint response to UVC. J Biol Chem *282*, 9458-9468.
Helleday, T. (2013). PrimPol breaks replication barriers. Nat Struct Mol Biol *20*, 1348-1350.
Heller, R. C., and Marians, K. J. (2006). Replication fork reactivation downstream of a blocked nascent leading strand. Nature *439*, 557-562.
Helmrich, A., Ballarino, M., Nudler, E., and Tora, L. (2013). Transcription-replication encounters, consequences and genomic instability. Nat Struct Mol Biol *20*, 412-418.
Herrick, J., and Bensimon, A. (1999a). Imaging of single DNA molecule: applications to high-resolution genomic studies. Chromosome Res *7*, 409-423.
Herrick, J., and Bensimon, A. (1999b). Single molecule analysis of DNA replication. Biochimie *81*, 859-871.
Herrick, J., and Bensimon, A. (2008). Global regulation of genome duplication in eukaryotes: an overview from the epifluorescence microscope. Chromosoma *117*, 243-260.
Herrick, J., and Bensimon, A. (2009). Introduction to molecular combing: genomics, DNA replication, and cancer. Methods Mol Biol *521*, 71-101.

Herrick, J., Michalet, X., Conti, C., Schurra, C., and Bensimon, A. (2000). Quantifying single gene copy number by measuring fluorescent probe lengths on combed genomic DNA. Proc Natl Acad Sci U S A *97*, 222-227.
Herrick, J., and Sclavi, B. (2007). Ribonucleotide reductase and the regulation of DNA replication: an old story and an ancient heritage. Mol Microbiol *63*, 22-34.
Hewitt, L., Tighe, A., Santaguida, S., White, A. M., Jones, C. D., Musacchio, A., Green, S., and Taylor, S. S. (2010). Sustained Mps1 activity is required in mitosis to recruit O-Mad2 to the Mad1-C-Mad2 core complex. J Cell Biol *190*, 25-34.
Hinchcliffe, E. H., Day, C. A., Karanjeet, K. B., Fadness, S., Langfald, A., Vaughan, K. T., and Dong, Z. (2016). Chromosome missegregation during anaphase triggers p53 cell cycle arrest through histone H3.3 Ser31 phosphorylation. Nat Cell Biol *18*, 668-675.
Hishida, T., Kubota, Y., Carr, A. M., and Iwasaki, H. (2009). RAD6-RAD18-RAD5-pathway-dependent tolerance to chronic low-dose ultraviolet light. Nature *457*, 612-615.
Hodson, J. A., Bailis, J. M., and Forsburg, S. L. (2003). Efficient labeling of fission yeast Schizosaccharomyces pombe with thymidine and BUdR. Nucleic Acids Res *31*, e134.
Hoege, C., Pfander, B., Moldovan, G. L., Pyrowolakis, G., and Jentsch, S. (2002). RAD6-dependent DNA repair is linked to modification of PCNA by ubiquitin and SUMO. Nature *419*, 135-141.
Hoeijmakers, J. H. (2009). DNA damage, aging, and cancer. N Engl J Med *361*, 1475-1485.
Holland, A. J., and Cleveland, D. W. (2012). Losing balance: the origin and impact of aneuploidy in cancer. EMBO Rep *13*, 501-514.
Holm, D. M., and Cram, L. S. (1973). An improved flow microfluorometer for rapid measurement of cell fluorescence. Exp Cell Res *80*, 105-110.
Houldsworth, J., and Lavin, M. F. (1980). Effect of ionizing radiation on DNA synthesis in ataxia telangiectasia cells. Nucleic Acids Res *8*, 3709-3720.
Hu, J., Sun, L., Shen, F., Chen, Y., Hua, Y., Liu, Y., Zhang, M., Hu, Y., Wang, Q., Xu, W., Sun, F., Ji, J., Murray, J. M., Carr, A. M., and Kong, D. (2012). The intra-S phase checkpoint targets Dna2 to prevent stalled replication forks from reversing. Cell *149*, 1221-1232.
Huberman, J. A., and Riggs, A. D. (1966). Autoradiography of chromosomal DNA fibers from Chinese hamster cells. Proc Natl Acad Sci U S A *55*, 599-606.
Huberman, J. A., and Riggs, A. D. (1968). On the mechanism of DNA replication in mammalian chromosomes. J Mol Biol *32*, 327-341.

Ikenaga, M., Takebe, H., and Ishii, Y. (1977). Excision repair of DNA base damage in human cells treated with the chemical carcinogen 4-nitroquinoline 1-oxide. Mutat Res *43*, 415-427.

Imray, F. P., and Kidson, C. (1983). Perturbations of cell-cycle progression in gamma-irradiated ataxia telangiectasia and Huntington's disease cells detected by DNA flow cytometric analysis. Mutat Res *112*, 369-382.

Iyer, D. R., Das, S., and Rhind, N. (in press). Analysis of DNA Replication in Fission Yeast by Combing. In Fission Yeast: A Laboratory Manual, Hagan, I., A. M. Carr, and P. Nurse, eds. (Cold Spring Harbor, NY: Cold Spring Harbor Laboratory Press), pp. 490.

Iyer, D. R., and Rhind, N. Replication Fork Slowing and Stalling are Distinct, Checkpoint-Independent Consequences of Replicating Damaged DNA. re-submitted to PLOS Genetics

Iyer, D. R., and Rhind, N. (2013). Checkpoint regulation of replication forks: global or local. Biochem Soc Trans *41*, 1701-1705.

Iyer, D. R., and Rhind, N. (2017). The Intra-S Checkpoint Responses to DNA Damage. Genes (Basel) *8*,

Jackson, A. L., Pahl, P. M., Harrison, K., Rosamond, J., and Sclafani, R. A. (1993). Cell cycle regulation of the yeast Cdc7 protein kinase by association with the Dbf4 protein. Mol Cell Biol *13*, 2899-2908.

Jackson, D. A., and Pombo, A. (1998). Replicon clusters are stable units of chromosome structure: evidence that nuclear organization contributes to the efficient activation and propagation of S phase in human cells. J Cell Biol *140*, 1285-1295.

Jackson, S. P. (2002). Sensing and repairing DNA double-strand breaks. Carcinogenesis *23*, 687-696.

Jazayeri, A., Falck, J., Lukas, C., Bartek, J., Smith, G. C., Lukas, J., and Jackson, S. P. (2006). ATM- and cell cycle-dependent regulation of ATR in response to DNA double-strand breaks. Nat Cell Biol *8*, 37-45.

Jones, C. J., Edwards, S. M., and Waters, R. (1989). The repair of identified large DNA adducts induced by 4-nitroquinoline-1-oxide in normal or xeroderma pigmentosum group A human fibroblasts, and the role of DNA polymerases alpha or delta. Carcinogenesis *10*, 1197-1201.

Jossen, R., and Bermejo, R. (2013). The DNA damage checkpoint response to replication stress: A Game of Forks. Front Genet *4*, 26.

Kamimura, Y., Tak, Y. S., Sugino, A., and Araki, H. (2001). Sld3, which interacts with Cdc45 (Sld4), functions for chromosomal DNA replication in Saccharomyces cerevisiae. EMBO J *20*, 2097-2107.

Kanemaki, M., and Labib, K. (2006). Distinct roles for Sld3 and GINS during establishment and progression of eukaryotic DNA replication forks. EMBO J *25*, 1753-1763.

Kannouche, P. L., Wing, J., and Lehmann, A. R. (2004). Interaction of human DNA polymerase eta with monoubiquitinated PCNA: a possible mechanism for the polymerase switch in response to DNA damage. Mol Cell *14*, 491-500.

Kaufmann, W. K., and Cleaver, J. E. (1981). Mechanisms of inhibition of DNA replication by ultraviolet light in normal human and xeroderma pigmentosum fibroblasts. J Mol Biol *149*, 171-187.

Kaufmann, W. K., Cleaver, J. E., and Painter, R. B. (1980). Ultraviolet radiation inhibits replicon initiation in S phase human cells. Biochim Biophys Acta *608*, 191-195.

Kaykov, A., and Nurse, P. (2015). The spatial and temporal organization of origin firing during the S-phase of fission yeast. Genome Res *25*, 391-401.

Kaykov, A., Taillefumier, T., Bensimon, A., and Nurse, P. (2016). Molecular Combing of Single DNA Molecules on the 10 Megabase Scale. Sci Rep *6*, 19636.

Kile, A. C., Chavez, D. A., Bacal, J., Eldirany, S., Korzhnev, D. M., Bezsonova, I., Eichman, B. F., and Cimprich, K. A. (2015). HLTF's Ancient HIRAN Domain Binds 3' DNA Ends to Drive Replication Fork Reversal. Mol Cell *58*, 1090-1100.

Kim, H. S., and Brill, S. J. (2001). Rfc4 interacts with Rpa1 and is required for both DNA replication and DNA damage checkpoints in Saccharomyces cerevisiae. Mol Cell Biol *21*, 3725-3737.

Kim, J. C., and Mirkin, S. M. (2013). The balancing act of DNA repeat expansions. Curr Opin Genet Dev *23*, 280-288.

Knouse, K. A., Wu, J., Whittaker, C. A., and Amon, A. (2014). Single cell sequencing reveals low levels of aneuploidy across mammalian tissues. Proc Natl Acad Sci U S A *111*, 13409-13414.

Knowlton, A. L., Lan, W., and Stukenberg, P. T. (2006). Aurora B is enriched at merotelic attachment sites, where it regulates MCAK. Curr Biol *16*, 1705-1710.

Kumagai, A., Lee, J., Yoo, H. Y., and Dunphy, W. G. (2006). TopBP1 activates the ATR-ATRIP complex. Cell *124*, 943-955.

Kumar, S., and Huberman, J. A. (2009). Checkpoint-dependent regulation of origin firing and replication fork movement in response to DNA damage in fission yeast. Mol Cell Biol *29*, 602-611.

Kurat, C. F., Yeeles, J. T., Patel, H., Early, A., and Diffley, J. F. (2017). Chromatin Controls DNA Replication Origin Selection, Lagging-Strand Synthesis, and Replication Fork Rates. Mol Cell *65*, 117-130.

Lajtha, L. G., Oliver, R., Berry, R., and Noyes, W. D. (1958). Mechanism of radiation effect on the process of synthesis of deoxyribonucleic acid. Nature *182*, 1788-1790.

Lamm, N., Ben-David, U., Golan-Lev, T., Storchová, Z., Benvenisty, N., and Kerem, B. (2016). Genomic Instability in Human Pluripotent Stem Cells Arises from Replicative Stress and Chromosome Condensation Defects. Cell Stem Cell *18*, 253-261.

Lampson, M. A., and Kapoor, T. M. (2006). Unraveling cell division mechanisms with small-molecule inhibitors. Nat Chem Biol *2*, 19-27.

Larner, J. M., Lee, H., and Hamlin, J. L. (1994). Radiation effects on DNA synthesis in a defined chromosomal replicon. Mol Cell Biol *14*, 1901-1908.

Larson, K., Sahm, J., Shenkar, R., and Strauss, B. (1985). Methylation-induced blocks to in vitro DNA replication. Mutat Res *150*, 77-84.

Lazzaro, F., Novarina, D., Amara, F., Watt, D. L., Stone, J. E., Costanzo, V., Burgers, P. M., Kunkel, T. A., Plevani, P., and Muzi-Falconi, M. (2012). RNase H and postreplication repair protect cells from ribonucleotides incorporated in DNA. Mol Cell *45*, 99-110.

Lebofsky, R., and Bensimon, A. (2003). Single DNA molecule analysis: applications of molecular combing. Brief Funct Genomic Proteomic *1*, 385-396.

Lebofsky, R., Heilig, R., Sonnleitner, M., Weissenbach, J., and Bensimon, A. (2006). DNA replication origin interference increases the spacing between initiation events in human cells. Mol Biol Cell *17*, 5337-5345.

Lee, A. J., Endesfelder, D., Rowan, A. J., Walther, A., Birkbak, N. J., Futreal, P. A., Downward, J., Szallasi, Z., Tomlinson, I. P., Howell, M., Kschischo, M., and Swanton, C. (2011). Chromosomal instability confers intrinsic multidrug resistance. Cancer Res *71*, 1858-1870.

Lee, H., Larner, J. M., and Hamlin, J. L. (1997). A p53-independent damage-sensing mechanism that functions as a checkpoint at the G1/S transition in Chinese hamster ovary cells. Proc Natl Acad Sci U S A *94*, 526-531.

Lee, K. Y., and Myung, K. (2008). PCNA modifications for regulation of post-replication repair pathways. Mol Cells *26*, 5-11.

Lee, S. E., Moore, J. K., Holmes, A., Umezu, K., Kolodner, R. D., and Haber, J. E. (1998). Saccharomyces Ku70, mre11/rad50 and RPA proteins regulate adaptation to G2/M arrest after DNA damage. Cell *94*, 399-409.

Lengronne, A., Pasero, P., Bensimon, A., and Schwob, E. (2001). Monitoring S phase progression globally and locally using BrdU incorporation in TK(+) yeast strains. Nucleic Acids Res *29*, 1433-1442.

Letessier, A., Millot, G. A., Koundrioukoff, S., Lachagès, A. M., Vogt, N., Hansen, R. S., Malfoy, B., Brison, O., and Debatisse, M. (2011). Cell-type-specific replication initiation programs set fragility of the FRA3B fragile site. Nature *470*, 120-123.

Li, M., Fang, X., Baker, D. J., Guo, L., Gao, X., Wei, Z., Han, S., van Deursen, J. M., and Zhang, P. (2010). The ATM-p53 pathway suppresses aneuploidy-induced tumorigenesis. Proc Natl Acad Sci U S A *107*, 14188-14193.

Liapunova, N. A. (1994). Organization of replication units and DNA replication in mammalian cells as studied by DNA fiber radioautography. Int Rev Cytol *154*, 261-308.

Lindahl, T., and Barnes, D. E. (2000). Repair of endogenous DNA damage. Cold Spring Harb Symp Quant Biol *65*, 127-133.

Lindahl, T., and Wood, R. D. (1999). Quality control by DNA repair. Science *286*, 1897-1905.

Lindsay, H. D., Griffiths, D. J., Edwards, R. J., Christensen, P. U., Murray, J. M., Osman, F., Walworth, N., and Carr, A. M. (1998). S-phase-specific activation of Cds1 kinase defines a subpathway of the checkpoint response in Schizosaccharomyces pombe. Genes Dev *12*, 382-395.

Liu, L. F., Desai, S. D., Li, T. K., Mao, Y., Sun, M., and Sim, S. P. (2000a). Mechanism of action of camptothecin. Ann N Y Acad Sci *922*, 1-10.

Liu, Q., Guntuku, S., Cui, X. S., Matsuoka, S., Cortez, D., Tamai, K., Luo, G., Carattini-Rivera, S., DeMayo, F., Bradley, A., Donehower, L. A., and Elledge, S. J. (2000b). Chk1 is an essential kinase that is regulated by Atr and required for the G(2)/M DNA damage checkpoint. Genes Dev *14*, 1448-1459.

Liu, S., Bekker-Jensen, S., Mailand, N., Lukas, C., Bartek, J., and Lukas, J. (2006). Claspin operates downstream of TopBP1 to direct ATR signaling towards Chk1 activation. Mol Cell Biol *26*, 6056-6064.

Liu, X., and Winey, M. (2012). The MPS1 family of protein kinases. Annu Rev Biochem *81*, 561-585.

Livneh, Z., Cohen, I. S., Paz-Elizur, T., Davidovsky, D., Carmi, D., Swain, U., and Mirlas-Neisberg, N. (2016). High-resolution genomic assays provide insight into the division of labor between TLS and HDR in mammalian replication of damaged DNA. DNA Repair (Amst) *44*, 59-67.

Longhese, M. P., Neecke, H., Paciotti, V., Lucchini, G., and Plevani, P. (1996). The 70 kDa subunit of replication protein A is required for the G1/S and intra-S DNA damage checkpoints in budding yeast. Nucleic Acids Res *24*, 3533-3537.

Lopes, M., Cotta-Ramusino, C., Pellicioli, A., Liberi, G., Plevani, P., Muzi-Falconi, M., Newlon, C. S., and Foiani, M. (2001). The DNA replication checkpoint response stabilizes stalled replication forks. Nature *412*, 557-561.

Lopes, M., Foiani, M., and Sogo, J. M. (2006). Multiple mechanisms control chromosome integrity after replication fork uncoupling and restart at irreparable UV lesions. Mol Cell *21*, 15-27.

Lopez-Mosqueda, J., Maas, N. L., Jonsson, Z. O., Defazio-Eli, L. G., Wohlschlegel, J., and Toczyski, D. P. (2010). Damage-induced phosphorylation of Sld3 is important to block late origin firing. Nature *467*, 479-483.

Loveland, A. B., Habuchi, S., Walter, J. C., and van Oijen, A. M. (2012). A general approach to break the concentration barrier in single-molecule imaging. Nat Methods *9*, 987-992.

Lucca, C., Vanoli, F., Cotta-Ramusino, C., Pellicioli, A., Liberi, G., Haber, J., and Foiani, M. (2004). Checkpoint-mediated control of replisome-fork association and signalling in response to replication pausing. Oncogene *23*, 1206-1213.

Luciani, M. G., Oehlmann, M., and Blow, J. J. (2004). Characterization of a novel ATR-dependent, Chk1-independent, intra-S-phase checkpoint that suppresses initiation of replication in Xenopus. J Cell Sci *117*, 6019-6030.

Lundin, C., North, M., Erixon, K., Walters, K., Jenssen, D., Goldman, A. S., and Helleday, T. (2005). Methyl methanesulfonate (MMS) produces heat-labile DNA damage but no detectable in vivo DNA double-strand breaks. Nucleic Acids Res *33*, 3799-3811.

Lupardus, P. J., Byun, T., Yee, M. C., Hekmat-Nejad, M., and Cimprich, K. A. (2002). A requirement for replication in activation of the ATR-dependent DNA damage checkpoint. Genes Dev *16*, 2327-2332.

Ma, W., Resnick, M. A., and Gordenin, D. A. (2008). Apn1 and Apn2 endonucleases prevent accumulation of repair-associated DNA breaks in budding yeast as revealed by direct chromosomal analysis. Nucleic Acids Res *36*, 1836-1846.

MacDougall, C. A., Byun, T. S., Van, C., Yee, M. C., and Cimprich, K. A. (2007). The structural determinants of checkpoint activation. Genes Dev *21*, 898-903.

Machwe, A., Karale, R., Xu, X., Liu, Y., and Orren, D. K. (2011). The Werner and Bloom syndrome proteins help resolve replication blockage by converting (regressed) holliday junctions to functional replication forks. Biochemistry *50*, 6774-6788.

Machwe, A., Xiao, L., Groden, J., and Orren, D. K. (2006). The Werner and Bloom syndrome proteins catalyze regression of a model replication fork. Biochemistry *45*, 13939-13946.

Majka, J., Niedziela-Majka, A., and Burgers, P. M. (2006). The checkpoint clamp activates Mec1 kinase during initiation of the DNA damage checkpoint. Mol Cell *24*, 891-901.

Makino, F., and Okada, S. (1974). Comparative studies of the effects of carcinogenic and antitumor agents on the DNA replication of cultured mammalian cells. Mutat Res *23*, 387-394.

Makino, F., and Okada, S. (1975). Effects of ionizing radiation on DNA replication in cultured mammalian cells. Radiat Res *62*, 37-51.

Mantiero, D., Clerici, M., Lucchini, G., and Longhese, M. P. (2007). Dual role for Saccharomyces cerevisiae Tel1 in the checkpoint response to double-strand breaks. EMBO Rep *8*, 380-387.

Maréchal, A., and Zou, L. (2013). DNA damage sensing by the ATM and ATR kinases. Cold Spring Harb Perspect Biol *5*, a012716.

Marheineke, K., Goldar, A., Krude, T., and Hyrien, O. (2009). Use of DNA combing to study DNA replication in Xenopus and human cell-free systems. Methods Mol Biol *521*, 575-603.

Marheineke, K., and Hyrien, O. (2004). Control of replication origin density and firing time in Xenopus egg extracts: role of a caffeine-sensitive, ATR-dependent checkpoint. J Biol Chem *279*, 28071-28081.

Marini, F., Nardo, T., Giannattasio, M., Minuzzo, M., Stefanini, M., Plevani, P., and Muzi Falconi, M. (2006). DNA nucleotide excision repair-dependent signaling to checkpoint activation. Proc Natl Acad Sci U S A *103*, 17325-17330.

Marteijn, J. A., Lans, H., Vermeulen, W., and Hoeijmakers, J. H. (2014). Understanding nucleotide excision repair and its roles in cancer and ageing. Nat Rev Mol Cell Biol *15*, 465-481.

Masai, H., Matsumoto, S., You, Z., Yoshizawa-Sugata, N., and Oda, M. (2010). Eukaryotic chromosome DNA replication: where, when, and how. Annu Rev Biochem *79*, 89-130.

Masters, M., and Broda, P. (1971). Evidence for the bidirectional replications of the Escherichia coli chromosome. Nat New Biol *232*, 137-140.

Matos, J., Blanco, M. G., Maslen, S., Skehel, J. M., and West, S. C. (2011). Regulatory control of the resolution of DNA recombination intermediates during meiosis and mitosis. Cell *147*, 158-172.

Matos, J., Blanco, M. G., and West, S. C. (2013). Cell-cycle kinases coordinate the resolution of recombination intermediates with chromosome segregation. Cell Rep *4*, 76-86.

Matsuoka, S., Ballif, B. A., Smogorzewska, A., McDonald, E. R., Hurov, K. E., Luo, J., Bakalarski, C. E., Zhao, Z., Solimini, N., Lerenthal, Y., Shiloh, Y., Gygi,

S. P., and Elledge, S. J. (2007). ATM and ATR substrate analysis reveals extensive protein networks responsive to DNA damage. Science *316*, 1160-1166.

McCarroll, R. M., and Fangman, W. L. (1988). Time of replication of yeast centromeres and telomeres. Cell *54*, 505-513.

McGranahan, N., Burrell, R. A., Endesfelder, D., Novelli, M. R., and Swanton, C. (2012). Cancer chromosomal instability: therapeutic and diagnostic challenges. EMBO Rep *13*, 528-538.

McIntosh, D., and Blow, J. J. (2012). Dormant origins, the licensing checkpoint, and the response to replicative stresses. Cold Spring Harb Perspect Biol *4*,

McNeil, J. B., and Friesen, J. D. (1981). Expression of the Herpes simplex virus thymidine kinase gene in Saccharomyces cerevisiae. Mol Gen Genet *184*, 386-393.

Mehta, A., and Haber, J. E. (2014). Sources of DNA double-strand breaks and models of recombinational DNA repair. Cold Spring Harb Perspect Biol *6*, a016428.

Melo, J., and Toczyski, D. (2002). A unified view of the DNA-damage checkpoint. Curr Opin Cell Biol *14*, 237-245.

Merrick, C. J., Jackson, D., and Diffley, J. F. (2004). Visualization of altered replication dynamics after DNA damage in human cells. J Biol Chem *279*, 20067-20075.

Michalet, X., Ekong, R., Fougerousse, F., Rousseaux, S., Schurra, C., Hornigold, N., van Slegtenhorst, M., Wolfe, J., Povey, S., Beckmann, J. S., and Bensimon, A. (1997). Dynamic molecular combing: stretching the whole human genome for high-resolution studies. Science *277*, 1518-1523.

Minca, E. C., and Kowalski, D. (2011). Replication fork stalling by bulky DNA damage: localization at active origins and checkpoint modulation. Nucleic Acids Res *39*, 2610-2623.

Mitelman Database of Chromosome Aberrations and Gene Fusions in Cancer (2017). Mitelman F, Johansson B and Mertens F (Eds.) , http://cgap.nci.nih.gov/Chromosomes/Mitelman

Moldovan, G. L., Pfander, B., and Jentsch, S. (2007). PCNA, the maestro of the replication fork. Cell *129*, 665-679.

Monod, J. (1971). Chance and Necessity: An Essay on the Natural Philosophy of Modern Biology (New York: Knopf).

Mordes, D. A., Glick, G. G., Zhao, R., and Cortez, D. (2008). TopBP1 activates ATR through ATRIP and a PIKK regulatory domain. Genes Dev *22*, 1478-1489.

Morin, I., Ngo, H. P., Greenall, A., Zubko, M. K., Morrice, N., and Lydall, D. (2008). Checkpoint-dependent phosphorylation of Exo1 modulates the DNA damage response. EMBO J *27*, 2400-2410.

Mourón, S., Rodriguez-Acebes, S., Martínez-Jiménez, M. I., García-Gómez, S., Chocrón, S., Blanco, L., and Méndez, J. (2013). Repriming of DNA synthesis at stalled replication forks by human PrimPol. Nat Struct Mol Biol *20*, 1383-1389.

Murga, M., Bunting, S., Montaña, M. F., Soria, R., Mulero, F., Cañamero, M., Lee, Y., McKinnon, P. J., Nussenzweig, A., and Fernandez-Capetillo, O. (2009). A mouse model of ATR-Seckel shows embryonic replicative stress and accelerated aging. Nat Genet *41*, 891-898.

Musacchio, A., and Salmon, E. D. (2007). The spindle-assembly checkpoint in space and time. Nat Rev Mol Cell Biol *8*, 379-393.

Myers, J. S., and Cortez, D. (2006). Rapid activation of ATR by ionizing radiation requires ATM and Mre11. J Biol Chem *281*, 9346-9350.

Nagaoka, S. I., Hassold, T. J., and Hunt, P. A. (2012). Human aneuploidy: mechanisms and new insights into an age-old problem. Nat Rev Genet *13*, 493-504.

Nakada, D., Hirano, Y., and Sugimoto, K. (2004). Requirement of the Mre11 complex and exonuclease 1 for activation of the Mec1 signaling pathway. Mol Cell Biol *24*, 10016-10025.

Navadgi-Patil, V. M., and Burgers, P. M. (2009). The unstructured C-terminal tail of the 9-1-1 clamp subunit Ddc1 activates Mec1/ATR via two distinct mechanisms. Mol Cell *36*, 743-753.

Naylor, M. L., Li, J. M., Osborn, A. J., and Elledge, S. J. (2009). Mrc1 phosphorylation in response to DNA replication stress is required for Mec1 accumulation at the stalled fork. Proc Natl Acad Sci U S A *106*, 12765-12770.

Neelsen, K. J., and Lopes, M. (2015). Replication fork reversal in eukaryotes: from dead end to dynamic response. Nat Rev Mol Cell Biol *16*, 207-220.

Neelsen, K. J., Zanini, I. M., Herrador, R., and Lopes, M. (2013). Oncogenes induce genotoxic stress by mitotic processing of unusual replication intermediates. J Cell Biol *200*, 699-708.

Nick McElhinny, S. A., Watts, B. E., Kumar, D., Watt, D. L., Lundström, E. B., Burgers, P. M., Johansson, E., Chabes, A., and Kunkel, T. A. (2010). Abundant ribonucleotide incorporation into DNA by yeast replicative polymerases. Proc Natl Acad Sci U S A *107*, 4949-4954.

Noguchi, E., Noguchi, C., Du, L. L., and Russell, P. (2003). Swi1 prevents replication fork collapse and controls checkpoint kinase Cds1. Mol Cell Biol *23*, 7861-7874.

Noguchi, E., Noguchi, C., McDonald, W. H., Yates, J. R., and Russell, P. (2004). Swi1 and Swi3 are components of a replication fork protection complex in fission yeast. Mol Cell Biol *24*, 8342-8355.

O'Driscoll, M., Ruiz-Perez, V. L., Woods, C. G., Jeggo, P. A., and Goodship, J. A. (2003). A splicing mutation affecting expression of ataxia-telangiectasia and Rad3-related protein (ATR) results in Seckel syndrome. Nat Genet *33*, 497-501.

Ord, M. G., and Stocken, L. A. (1956). The effects of x- and gamma-radiation on nucleic acid metabolism in the rat in vivo and in vitro. Biochem J *63*, 3-8.

Ord, M. G., and Stocken, L. A. (1958). Studies in synthesis of deoxyribonucleic acid; radiobiochemical lesion in animal cells. Nature *182*, 1787-1788.

Orr, B., Godek, K. M., and Compton, D. (2015). Aneuploidy. Curr Biol *25*, R538-42.

Orth, J. D., Loewer, A., Lahav, G., and Mitchison, T. J. (2012). Prolonged mitotic arrest triggers partial activation of apoptosis, resulting in DNA damage and p53 induction. Mol Biol Cell *23*, 567-576.

Osborn, A. J., and Elledge, S. J. (2003). Mrc1 is a replication fork component whose phosphorylation in response to DNA replication stress activates Rad53. Genes Dev *17*, 1755-1767.

Paciotti, V., Clerici, M., Lucchini, G., and Longhese, M. P. (2000). The checkpoint protein Ddc2, functionally related to S. pombe Rad26, interacts with Mec1 and is regulated by Mec1-dependent phosphorylation in budding yeast. Genes Dev *14*, 2046-2059.

Paciotti, V., Clerici, M., Scotti, M., Lucchini, G., and Longhese, M. P. (2001). Characterization of mec1 kinase-deficient mutants and of new hypomorphic mec1 alleles impairing subsets of the DNA damage response pathway. Mol Cell Biol *21*, 3913-3925.

Painter, R. B. (1967). Thymidine incorporation as a measure of DNA-synthesis in irradiated cell cultures. Int J Radiat Biol Relat Stud Phys Chem Med *13*, 279-281.

Painter, R. B. (1981). Radioresistant DNA synthesis: an intrinsic feature of ataxia telangiectasia. Mutat Res *84*, 183-190.

Painter, R. B., and Young, B. R. (1975). X-ray-induced inhibition of DNA synthesis in Chinese hamster ovary, human HeLa, and Mouse L cells. Radiat Res *64*, 648-656.

Painter, R. B., and Young, B. R. (1976). Formation of nascent DNA molecules during inhibition of replicon initiation in mammalian cells. Biochim Biophys Acta *418*, 146-153.

Painter, R. B., and Young, B. R. (1980). Radiosensitivity in ataxia-telangiectasia: a new explanation. Proc Natl Acad Sci U S A *77*, 7315-7317.

Papouli, E., Chen, S., Davies, A. A., Huttner, D., Krejci, L., Sung, P., and Ulrich, H. D. (2005). Crosstalk between SUMO and ubiquitin on PCNA is mediated by recruitment of the helicase Srs2p. Mol Cell *19*, 123-133.

Paquin, C., and Adams, J. (1983). Frequency of fixation of adaptive mutations is higher in evolving diploid than haploid yeast populations. Nature *302*, 495-500.

Parker, J. L., and Ulrich, H. D. (2009). Mechanistic analysis of PCNA poly-ubiquitylation by the ubiquitin protein ligases Rad18 and Rad5. EMBO J *28*, 3657-3666.

Parra, I., and Windle, B. (1993). High resolution visual mapping of stretched DNA by fluorescent hybridization. Nat Genet *5*, 17-21.

Parrilla-Castellar, E. R., and Karnitz, L. M. (2003). Cut5 is required for the binding of Atr and DNA polymerase alpha to genotoxin-damaged chromatin. J Biol Chem *278*, 45507-45511.

Passerini, V., Ozeri-Galai, E., de Pagter, M. S., Donnelly, N., Schmalbrock, S., Kloosterman, W. P., Kerem, B., and Storchová, Z. (2016). The presence of extra chromosomes leads to genomic instability. Nat Commun *7*, 10754.

Patel, P. K., Arcangioli, B., Baker, S. P., Bensimon, A., and Rhind, N. (2006). DNA replication origins fire stochastically in fission yeast. Mol Biol Cell *17*, 308-316.

Paulovich, A. G., and Hartwell, L. H. (1995). A checkpoint regulates the rate of progression through S phase in S. cerevisiae in response to DNA damage. Cell *82*, 841-847.

Paulsen, R. D., and Cimprich, K. A. (2007). The ATR pathway: fine-tuning the fork. DNA Repair (Amst) *6*, 953-966.

Pearson, C. E., Nichol Edamura, K., and Cleary, J. D. (2005). Repeat instability: mechanisms of dynamic mutations. Nat Rev Genet *6*, 729-742.

Pellicioli, A., Lucca, C., Liberi, G., Marini, F., Lopes, M., Plevani, P., Romano, A., Di Fiore, P. P., and Foiani, M. (1999). Activation of Rad53 kinase in response to DNA damage and its effect in modulating phosphorylation of the lagging strand DNA polymerase. EMBO J *18*, 6561-6572.

Pepe, A., and West, S. C. (2014a). Substrate specificity of the MUS81-EME2 structure selective endonuclease. Nucleic Acids Res *42*, 3833-3845.

Pepe, A., and West, S. C. (2014b). MUS81-EME2 promotes replication fork restart. Cell Rep *7*, 1048-1055.

Petermann, E., Helleday, T., and Caldecott, K. W. (2008). Claspin promotes normal replication fork rates in human cells. Mol Biol Cell *19*, 2373-2378.

Petermann, E., Woodcock, M., and Helleday, T. (2010). Chk1 promotes replication fork progression by controlling replication initiation. Proc Natl Acad Sci U S A *107*, 16090-16095.

Peterson, C. L., and Côté, J. (2004). Cellular machineries for chromosomal DNA repair. Genes Dev *18*, 602-616.

Pfander, B., Moldovan, G. L., Sacher, M., Hoege, C., and Jentsch, S. (2005). SUMO-modified PCNA recruits Srs2 to prevent recombination during S phase. Nature *436*, 428-433.

Pichierri, P., and Rosselli, F. (2004). The DNA crosslink-induced S-phase checkpoint depends on ATR-CHK1 and ATR-NBS1-FANCD2 pathways. EMBO J *23*, 1178-1187.

Poli, J., Tsaponina, O., Crabbé, L., Keszthelyi, A., Pantesco, V., Chabes, A., Lengronne, A., and Pasero, P. (2012). dNTP pools determine fork progression and origin usage under replication stress. EMBO J *31*, 883-894.

Potapova, T. A., Zhu, J., and Li, R. (2013). Aneuploidy and chromosomal instability: a vicious cycle driving cellular evolution and cancer genome chaos. Cancer Metastasis Rev *32*, 377-389.

Prescott, D. M., and Kuempel, P. L. (1972). Bidirectional replication of the chromosome in Escherichia coli. Proc Natl Acad Sci U S A *69*, 2842-2845.

Qi, Z., Redding, S., Lee, J. Y., Gibb, B., Kwon, Y., Niu, H., Gaines, W. A., Sung, P., and Greene, E. C. (2015). DNA sequence alignment by microhomology sampling during homologous recombination. Cell *160*, 856-869.

Ragland, R. L., Patel, S., Rivard, R. S., Smith, K., Peters, A. A., Bielinsky, A. K., and Brown, E. J. (2013). RNF4 and PLK1 are required for replication fork collapse in ATR-deficient cells. Genes Dev *27*, 2259-2273.

Randell, J. C., Fan, A., Chan, C., Francis, L. I., Heller, R. C., Galani, K., and Bell, S. P. (2010). Mec1 is one of multiple kinases that prime the Mcm2-7 helicase for phosphorylation by Cdc7. Mol Cell *40*, 353-363.

Ray Chaudhuri, A., Hashimoto, Y., Herrador, R., Neelsen, K. J., Fachinetti, D., Bermejo, R., Cocito, A., Costanzo, V., and Lopes, M. (2012). Topoisomerase I poisoning results in PARP-mediated replication fork reversal. Nat Struct Mol Biol *19*, 417-423.

Redding, S., Sternberg, S. H., Marshall, M., Gibb, B., Bhat, P., Guegler, C. K., Wiedenheft, B., Doudna, J. A., and Greene, E. C. (2015). Surveillance and Processing of Foreign DNA by the Escherichia coli CRISPR-Cas System. Cell *163*, 854-865.

Regairaz, M., Zhang, Y. W., Fu, H., Agama, K. K., Tata, N., Agrawal, S., Aladjem, M. I., and Pommier, Y. (2011). Mus81-mediated DNA cleavage resolves

replication forks stalled by topoisomerase I-DNA complexes. J Cell Biol *195*, 739-749.
Reynolds, A. E., McCarroll, R. M., Newlon, C. S., and Fangman, W. L. (1989). Time of replication of ARS elements along yeast chromosome III. Mol Cell Biol *9*, 4488-4494.
Rhind, N. (2009). Changing of the guard: how ATM hands off DNA double-strand break signaling to ATR. Mol Cell *33*, 672-674.
Rhind, N., and Gilbert, D. M. (2013). DNA replication timing. Cold Spring Harb Perspect Biol *5*, a010132.
Rhind, N., and Russell, P. (1998). The Schizosaccharomyces pombe S-phase checkpoint differentiates between different types of DNA damage. Genetics *149*, 1729-1737.
Rhind, N., and Russell, P. (2000a). Checkpoints: it takes more than time to heal some wounds. Curr Biol *10*, R908-11.
Rhind, N., and Russell, P. (2000b). Chk1 and Cds1: linchpins of the DNA damage and replication checkpoint pathways. J Cell Sci *113*, 3889-3896.
Rhind, N., and Russell, P. (2012). Signaling pathways that regulate cell division. Cold Spring Harb Perspect Biol *4*, a005942.
Rhind, N., Yang, S. C., and Bechhoefer, J. (2010). Reconciling stochastic origin firing with defined replication timing. Chromosome Res *18*, 35-43.
Rodriguez, J., and Tsukiyama, T. (2013). ATR-like kinase Mec1 facilitates both chromatin accessibility at DNA replication forks and replication fork progression during replication stress. Genes Dev *27*, 74-86.
Rouse, J., and Jackson, S. P. (2002). Lcd1p recruits Mec1p to DNA lesions in vitro and in vivo. Mol Cell *9*, 857-869.
Rudd, S. G., Bianchi, J., and Doherty, A. J. (2014). PrimPol-A new polymerase on the block. Mol Cell Oncol *1*, e960754.
Ruzankina, Y., Pinzon-Guzman, C., Asare, A., Ong, T., Pontano, L., Cotsarelis, G., Zediak, V. P., Velez, M., Bhandoola, A., and Brown, E. J. (2007). Deletion of the developmentally essential gene ATR in adult mice leads to age-related phenotypes and stem cell loss. Cell Stem Cell *1*, 113-126.
Ryba, T., Hiratani, I., Lu, J., Itoh, M., Kulik, M., Zhang, J., Schulz, T. C., Robins, A. J., Dalton, S., and Gilbert, D. M. (2010). Evolutionarily conserved replication timing profiles predict long-range chromatin interactions and distinguish closely related cell types. Genome Res *20*, 761-770.
Sabatinos, S. A., and Forsburg, S. L. (2015). Managing Single-Stranded DNA during Replication Stress in Fission Yeast. Biomolecules *5*, 2123-2139.

Sabatinos, S. A., Green, M. D., and Forsburg, S. L. (2012). Continued DNA synthesis in replication checkpoint mutants leads to fork collapse. Mol Cell Biol *32*, 4986-4997.

Sale, J. E. (2012). Competition, collaboration and coordination--determining how cells bypass DNA damage. J Cell Sci *125*, 1633-1643.

Sancar, A., Lindsey-Boltz, L. A., Unsal-Kaçmaz, K., and Linn, S. (2004). Molecular mechanisms of mammalian DNA repair and the DNA damage checkpoints. Annu Rev Biochem *73*, 39-85.

Sanchez, Y., Bachant, J., Wang, H., Hu, F., Liu, D., Tetzlaff, M., and Elledge, S. J. (1999). Control of the DNA damage checkpoint by chk1 and rad53 protein kinases through distinct mechanisms. Science *286*, 1166-1171.

Santaguida, S., and Amon, A. (2015). Short- and long-term effects of chromosome mis-segregation and aneuploidy. Nat Rev Mol Cell Biol *16*, 473-485.

Santaguida, S., Tighe, A., D'Alise, A. M., Taylor, S. S., and Musacchio, A. (2010). Dissecting the role of MPS1 in chromosome biorientation and the spindle checkpoint through the small molecule inhibitor reversine. J Cell Biol *190*, 73-87.

Santaguida, S., Vasile, E., White, E., and Amon, A. (2015). Aneuploidy-induced cellular stresses limit autophagic degradation. Genes Dev *29*, 2010-2021.

Santaguida, S., Richardson, A., Iyer, D. R., M'Saad, O., Zasadil, L., Knouse, K. A., Wong, Y. L., Rhind, N., Desai, A., and Amon, A. Chromosome mis-segregation generates cell cycle-arrested cells with complex karyotypes that are eliminated by the immune system. Dev Cell *41 (6)*, 638-651.e5.

Santocanale, C., and Diffley, J. F. (1998). A Mec1- and Rad53-dependent checkpoint controls late-firing origins of DNA replication. Nature *395*, 615-618.

Sasaki, M. S., and Norman, A. (1966). DNA fibres from human lymphocyte nuclei. Exp Cell Res *44*, 642-645.

Schneider, C. A., Rasband, W. S., and Eliceiri, K. W. (2012). NIH Image to ImageJ: 25 years of image analysis. Nat Methods *9*, 671-675.

Scorah, J., and McGowan, C. H. (2009). Claspin and Chk1 regulate replication fork stability by different mechanisms. Cell Cycle *8*, 1036-1043.

Segurado, M., and Diffley, J. F. (2008). Separate roles for the DNA damage checkpoint protein kinases in stabilizing DNA replication forks. Genes Dev *22*, 1816-1827.

Seiler, J. A., Conti, C., Syed, A., Aladjem, M. I., and Pommier, Y. (2007). The intra-S-phase checkpoint affects both DNA replication initiation and elongation: single-cell and -DNA fiber analyses. Mol Cell Biol *27*, 5806-5818.

Selmecki, A. M., Maruvka, Y. E., Richmond, P. A., Guillet, M., Shoresh, N., Sorenson, A. L., De, S., Kishony, R., Michor, F., Dowell, R., and Pellman, D. (2015). Polyploidy can drive rapid adaptation in yeast. Nature *519*, 349-352.

Shechter, D., Costanzo, V., and Gautier, J. (2004a). Regulation of DNA replication by ATR: signaling in response to DNA intermediates. DNA Repair (Amst) *3*, 901-908.

Shechter, D., Costanzo, V., and Gautier, J. (2004b). ATR and ATM regulate the timing of DNA replication origin firing. Nat Cell Biol *6*, 648-655.

Shiloh, Y. (2001). ATM and ATR: networking cellular responses to DNA damage. Curr Opin Genet Dev *11*, 71-77.

Shimada, K., Pasero, P., and Gasser, S. M. (2002). ORC and the intra-S-phase checkpoint: a threshold regulates Rad53p activation in S phase. Genes Dev *16*, 3236-3252.

Shimura, T., Torres, M. J., Martin, M. M., Rao, V. A., Pommier, Y., Katsura, M., Miyagawa, K., and Aladjem, M. I. (2008). Bloom's syndrome helicase and Mus81 are required to induce transient double-strand DNA breaks in response to DNA replication stress. J Mol Biol *375*, 1152-1164.

Shiotani, B., and Zou, L. (2009). Single-stranded DNA orchestrates an ATM-to-ATR switch at DNA breaks. Mol Cell *33*, 547-558.

Shirahige, K., Hori, Y., Shiraishi, K., Yamashita, M., Takahashi, K., Obuse, C., Tsurimoto, T., and Yoshikawa, H. (1998). Regulation of DNA-replication origins during cell-cycle progression. Nature *395*, 618-621.

Sidorova, J. M., and Breeden, L. L. (1997). Rad53-dependent phosphorylation of Swi6 and down-regulation of CLN1 and CLN2 transcription occur in response to DNA damage in Saccharomyces cerevisiae. Genes Dev *11*, 3032-3045.

Siegel, J. J., and Amon, A. (2012). New insights into the troubles of aneuploidy. Annu Rev Cell Dev Biol *28*, 189-214.

Sikora, A., Mielecki, D., Chojnacka, A., Nieminuszczy, J., Wrzesinski, M., and Grzesiuk, E. (2010). Lethal and mutagenic properties of MMS-generated DNA lesions in Escherichia coli cells deficient in BER and AlkB-directed DNA repair. Mutagenesis *25*, 139-147.

Sirbu, B. M., Couch, F. B., and Cortez, D. (2012). Monitoring the spatiotemporal dynamics of proteins at replication forks and in assembled chromatin using isolation of proteins on nascent DNA. Nat Protoc *7*, 594-605.

Sirbu, B. M., McDonald, W. H., Dungrawala, H., Badu-Nkansah, A., Kavanaugh, G. M., Chen, Y., Tabb, D. L., and Cortez, D. (2013). Identification of proteins at active, stalled, and collapsed replication forks using isolation of proteins on

nascent DNA (iPOND) coupled with mass spectrometry. J Biol Chem *288*, 31458-31467.
Sivakumar, S., Porter-Goff, M., Patel, P. K., Benoit, K., and Rhind, N. (2004). In vivo labeling of fission yeast DNA with thymidine and thymidine analogs. Methods *33*, 213-219.
Smolka, M. B., Albuquerque, C. P., Chen, S. H., and Zhou, H. (2007). Proteome-wide identification of in vivo targets of DNA damage checkpoint kinases. Proc Natl Acad Sci U S A *104*, 10364-10369.
Snyderwine, E. G., and Bohr, V. A. (1992). Gene- and strand-specific damage and repair in Chinese hamster ovary cells treated with 4-nitroquinoline 1-oxide. Cancer Res *52*, 4183-4189.
Sogo, J. M., Lopes, M., and Foiani, M. (2002). Fork reversal and ssDNA accumulation at stalled replication forks owing to checkpoint defects. Science *297*, 599-602.
Sørensen, C. S., Syljuåsen, R. G., Falck, J., Schroeder, T., Rönnstrand, L., Khanna, K. K., Zhou, B. B., Bartek, J., and Lukas, J. (2003). Chk1 regulates the S phase checkpoint by coupling the physiological turnover and ionizing radiation-induced accelerated proteolysis of Cdc25A. Cancer Cell *3*, 247-258.
Sørensen, C. S., Syljuåsen, R. G., Lukas, J., and Bartek, J. (2004). ATR, Claspin and the Rad9-Rad1-Hus1 complex regulate Chk1 and Cdc25A in the absence of DNA damage. Cell Cycle *3*, 941-945.
Stelter, P., and Ulrich, H. D. (2003). Control of spontaneous and damage-induced mutagenesis by SUMO and ubiquitin conjugation. Nature *425*, 188-191.
Sternberg, S. H., Redding, S., Jinek, M., Greene, E. C., and Doudna, J. A. (2014). DNA interrogation by the CRISPR RNA-guided endonuclease Cas9. Nature *507*, 62-67.
Stokes, M. P., Van Hatten, R., Lindsay, H. D., and Michael, W. M. (2002). DNA replication is required for the checkpoint response to damaged DNA in Xenopus egg extracts. J Cell Biol *158*, 863-872.
Storchova, Z., and Pellman, D. (2004). From polyploidy to aneuploidy, genome instability and cancer. Nat Rev Mol Cell Biol *5*, 45-54.
Sun, Z., Fay, D. S., Marini, F., Foiani, M., and Stern, D. F. (1996). Spk1/Rad53 is regulated by Mec1-dependent protein phosphorylation in DNA replication and damage checkpoint pathways. Genes Dev *10*, 395-406.
Syljuåsen, R. G., Sørensen, C. S., Hansen, L. T., Fugger, K., Lundin, C., Johansson, F., Helleday, T., Sehested, M., Lukas, J., and Bartek, J. (2005). Inhibition of human Chk1 causes increased initiation of DNA replication, phosphorylation of ATR targets, and DNA breakage. Mol Cell Biol *25*, 3553-3562.

Szakal, B., and Branzei, D. (2013). Premature Cdk1/Cdc5/Mus81 pathway activation induces aberrant replication and deleterious crossover. EMBO J *32*, 1155-1167.

Szyjka, S. J., Aparicio, J. G., Viggiani, C. J., Knott, S., Xu, W., Tavaré, S., and Aparicio, O. M. (2008). Rad53 regulates replication fork restart after DNA damage in Saccharomyces cerevisiae. Genes Dev *22*, 1906-1920.

Takeda, D. Y., and Dutta, A. (2005). DNA replication and progression through S phase. Oncogene *24*, 2827-2843.

Tanaka, K., Yonekawa, T., Kawasaki, Y., Kai, M., Furuya, K., Iwasaki, M., Murakami, H., Yanagida, M., and Okayama, H. (2000). Fission yeast Eso1p is required for establishing sister chromatid cohesion during S phase. Mol Cell Biol *20*, 3459-3469.

Tanaka, S., and Araki, H. (2011). Multiple regulatory mechanisms to inhibit untimely initiation of DNA replication are important for stable genome maintenance. PLoS Genet *7*, e1002136.

Técher, H., Koundrioukoff, S., Azar, D., Wilhelm, T., Carignon, S., Brison, O., Debatisse, M., and Le Tallec, B. (2013). Replication dynamics: biases and robustness of DNA fiber analysis. J Mol Biol *425*, 4845-4855.

Tercero, J. A., and Diffley, J. F. (2001). Regulation of DNA replication fork progression through damaged DNA by the Mec1/Rad53 checkpoint. Nature *412*, 553-557.

Tercero, J. A., Longhese, M. P., and Diffley, J. F. (2003). A central role for DNA replication forks in checkpoint activation and response. Mol Cell *11*, 1323-1336.

Thangavel, S., Berti, M., Levikova, M., Pinto, C., Gomathinayagam, S., Vujanovic, M., Zellweger, R., Moore, H., Lee, E. H., Hendrickson, E. A., Cejka, P., Stewart, S., Lopes, M., and Vindigni, A. (2015). DNA2 drives processing and restart of reversed replication forks in human cells. J Cell Biol *208*, 545-562.

Thompson, S. L., and Compton, D. A. (2008). Examining the link between chromosomal instability and aneuploidy in human cells. J Cell Biol *180*, 665-672.

Thompson, S. L., and Compton, D. A. (2010). Proliferation of aneuploid human cells is limited by a p53-dependent mechanism. J Cell Biol *188*, 369-381.

Toledo, L. I., Altmeyer, M., Rask, M. B., Lukas, C., Larsen, D. H., Povlsen, L. K., Bekker-Jensen, S., Mailand, N., Bartek, J., and Lukas, J. (2013). ATR prohibits replication catastrophe by preventing global exhaustion of RPA. Cell *155*, 1088-1103.

Trenz, K., Smith, E., Smith, S., and Costanzo, V. (2006). ATM and ATR promote Mre11 dependent restart of collapsed replication forks and prevent accumulation of DNA breaks. EMBO J *25*, 1764-1774.

Uetake, Y., and Sluder, G. (2010). Prolonged prometaphase blocks daughter cell proliferation despite normal completion of mitosis. Curr Biol *20*, 1666-1671.
Ulrich, H. D. (2009). Regulating post-translational modifications of the eukaryotic replication clamp PCNA. DNA Repair (Amst) *8*, 461-469.
Ulrich, H. D. (2012). Ubiquitin and SUMO in DNA repair at a glance. J Cell Sci *125*, 249-254.
Ulrich, H. D., and Jentsch, S. (2000). Two RING finger proteins mediate cooperation between ubiquitin-conjugating enzymes in DNA repair. EMBO J *19*, 3388-3397.
Ulrich, H. D., and Walden, H. (2010). Ubiquitin signalling in DNA replication and repair. Nat Rev Mol Cell Biol *11*, 479-489.
Unsal-Kaçmaz, K., Chastain, P. D., Qu, P. P., Minoo, P., Cordeiro-Stone, M., Sancar, A., and Kaufmann, W. K. (2007). The human Tim/Tipin complex coordinates an Intra-S checkpoint response to UV that slows replication fork displacement. Mol Cell Biol *27*, 3131-3142.
Valton, A. L., and Prioleau, M. N. (2016). G-Quadruplexes in DNA Replication: A Problem or a Necessity. Trends Genet *32*, 697-706.
Vernis, L., Piskur, J., and Diffley, J. F. (2003). Reconstitution of an efficient thymidine salvage pathway in Saccharomyces cerevisiae. Nucleic Acids Res *31*, e120.
Walter, J., and Newport, J. W. (1997). Regulation of replicon size in Xenopus egg extracts. Science *275*, 993-995.
Walters, R. A., and Hildebrand, C. E. (1975). Evidence that x-irradiation inhibits DNA replicon initiation in Chinese hamster cells. Biochem Biophys Res Commun *65*, 265-271.
Walther, A., Houlston, R., and Tomlinson, I. (2008). Association between chromosomal instability and prognosis in colorectal cancer: a meta-analysis. Gut *57*, 941-950.
Wang, F., Redding, S., Finkelstein, I. J., Gorman, J., Reichman, D. R., and Greene, E. C. (2013). The promoter-search mechanism of Escherichia coli RNA polymerase is dominated by three-dimensional diffusion. Nat Struct Mol Biol *20*, 174-181.
Wang, X., Guan, J., Hu, B., Weiss, R. S., Iliakis, G., and Wang, Y. (2004). Involvement of Hus1 in the chain elongation step of DNA replication after exposure to camptothecin or ionizing radiation. Nucleic Acids Res *32*, 767-775.
Ward, I. M., Minn, K., and Chen, J. (2004). UV-induced ataxia-telangiectasia-mutated and Rad3-related (ATR) activation requires replication stress. J Biol Chem *279*, 9677-9680.

Watanabe, I. (1974). Radiation effects on DNA chain growth in mammalian cells. Radiat Res *58*, 541-556.

Watanabe, K., Tateishi, S., Kawasuji, M., Tsurimoto, T., Inoue, H., and Yamaizumi, M. (2004). Rad18 guides poleta to replication stalling sites through physical interaction and PCNA monoubiquitination. EMBO J *23*, 3886-3896.

Weaver, B. A., and Cleveland, D. W. (2006). Does aneuploidy cause cancer. Curr Opin Cell Biol *18*, 658-667.

Whitby, M. C., Osman, F., and Dixon, J. (2003). Cleavage of model replication forks by fission yeast Mus81-Eme1 and budding yeast Mus81-Mms4. J Biol Chem *278*, 6928-6935.

Willis, N., and Rhind, N. (2009). Mus81, Rhp51(Rad51), and Rqh1 form an epistatic pathway required for the S-phase DNA damage checkpoint. Mol Biol Cell *20*, 819-833.

Willis, N., and Rhind, N. (2011). Studying S-phase DNA damage checkpoints using the fission yeast Schizosaccharomyces pombe. Methods Mol Biol *782*, 13-21.

Willis, N. A., Zhou, C., Elia, A. E., Murray, J. M., Carr, A. M., Elledge, S. J., and Rhind, N. (2016). Identification of S-phase DNA damage-response targets in fission yeast reveals conservation of damage-response networks. Proc Natl Acad Sci U S A *113*, E3676-85.

Wilsker, D., Petermann, E., Helleday, T., and Bunz, F. (2008). Essential function of Chk1 can be uncoupled from DNA damage checkpoint and replication control. Proc Natl Acad Sci U S A *105*, 20752-20757.

Woodward, A. M., Göhler, T., Luciani, M. G., Oehlmann, M., Ge, X., Gartner, A., Jackson, D. A., and Blow, J. J. (2006). Excess Mcm2-7 license dormant origins of replication that can be used under conditions of replicative stress. J Cell Biol *173*, 673-683.

Wu, R., Terry, A. V., Singh, P. B., and Gilbert, D. M. (2005). Differential subnuclear localization and replication timing of histone H3 lysine 9 methylation states. Mol Biol Cell *16*, 2872-2881.

Wyatt, M. D., and Pittman, D. L. (2006). Methylating agents and DNA repair responses: Methylated bases and sources of strand breaks. Chem Res Toxicol *19*, 1580-1594.

Xu, J., Yanagisawa, Y., Tsankov, A. M., Hart, C., Aoki, K., Kommajosyula, N., Steinmann, K. E., Bochicchio, J., Russ, C., Regev, A., Rando, O. J., Nusbaum, C., Niki, H., Milos, P., Weng, Z., and Rhind, N. (2012). Genome-wide identification and characterization of replication origins by deep sequencing. Genome Biol *13*, R27.

Xu, X., Vaithiyalingam, S., Glick, G. G., Mordes, D. A., Chazin, W. J., and Cortez, D. (2008). The basic cleft of RPA70N binds multiple checkpoint proteins, including RAD9, to regulate ATR signaling. Mol Cell Biol *28*, 7345-7353.

Yaffe, E., Farkash-Amar, S., Polten, A., Yakhini, Z., Tanay, A., and Simon, I. (2010). Comparative analysis of DNA replication timing reveals conserved large-scale chromosomal architecture. PLoS Genet *6*, e1001011.

Yardimci, H., Loveland, A. B., van Oijen, A. M., and Walter, J. C. (2012). Single-molecule analysis of DNA replication in Xenopus egg extracts. Methods *57*, 179-186.

Yeeles, J. T., Deegan, T. D., Janska, A., Early, A., and Diffley, J. F. (2015). Regulated eukaryotic DNA replication origin firing with purified proteins. Nature *519*, 431-435.

Yeeles, J. T., Janska, A., Early, A., and Diffley, J. F. (2017). How the Eukaryotic Replisome Achieves Rapid and Efficient DNA Replication. Mol Cell *65*, 105-116.

Yeeles, J. T., and Marians, K. J. (2011). The Escherichia coli replisome is inherently DNA damage tolerant. Science *334*, 235-238.

Yekezare, M., Gómez-González, B., and Diffley, J. F. (2013). Controlling DNA replication origins in response to DNA damage - inhibit globally, activate locally. J Cell Sci *126*, 1297-1306.

Yoo, H. Y., Kumagai, A., Shevchenko, A., Shevchenko, A., and Dunphy, W. G. (2004). Adaptation of a DNA replication checkpoint response depends upon inactivation of Claspin by the Polo-like kinase. Cell *117*, 575-588.

Yoshizawa-Sugata, N., and Masai, H. (2007). Human Tim/Timeless-interacting protein, Tipin, is required for efficient progression of S phase and DNA replication checkpoint. J Biol Chem *282*, 2729-2740.

Young, B. R., and Painter, R. B. (1989). Radioresistant DNA synthesis and human genetic diseases. Hum Genet *82*, 113-117.

Yusufzai, T., and Kadonaga, J. T. (2008). HARP is an ATP-driven annealing helicase. Science *322*, 748-750.

Yusufzai, T., and Kadonaga, J. T. (2010). Annealing helicase 2 (AH2), a DNA-rewinding motor with an HNH motif. Proc Natl Acad Sci U S A *107*, 20970-20973.

Zegerman, P., and Diffley, J. F. (2010). Checkpoint-dependent inhibition of DNA replication initiation by Sld3 and Dbf4 phosphorylation. Nature *467*, 474-478.

Zellweger, R., Dalcher, D., Mutreja, K., Berti, M., Schmid, J. A., Herrador, R., Vindigni, A., and Lopes, M. (2015). Rad51-mediated replication fork reversal is a global response to genotoxic treatments in human cells. J Cell Biol *208*, 563-579.

Zeman, M. K., and Cimprich, K. A. (2014). Causes and consequences of replication stress. Nat Cell Biol *16*, 2-9.

Zerulla, K., and Soppa, J. (2014). Polyploidy in haloarchaea: advantages for growth and survival. Front Microbiol *5*, 274.
Zhang, H., and Lawrence, C. W. (2005). The error-free component of the RAD6/RAD18 DNA damage tolerance pathway of budding yeast employs sister-strand recombination. Proc Natl Acad Sci U S A *102*, 15954-15959.
Zhang, Y., and Hunter, T. (2014). Roles of Chk1 in cell biology and cancer therapy. Int J Cancer *134*, 1013-1023.
Zhao, H., and Piwnica-Worms, H. (2001). ATR-mediated checkpoint pathways regulate phosphorylation and activation of human Chk1. Mol Cell Biol *21*, 4129-4139.
Zhou, B. B., and Elledge, S. J. (2000). The DNA damage response: putting checkpoints in perspective. Nature *408*, 433-439.
Zhou, Z. X., Zhang, M. J., Peng, X., Takayama, Y., Xu, X. Y., Huang, L. Z., and Du, L. L. (2013). Mapping genomic hotspots of DNA damage by a single-strand-DNA-compatible and strand-specific ChIP-seq method. Genome Res *23*, 705-715.
Zou, L., and Elledge, S. J. (2003). Sensing DNA damage through ATRIP recognition of RPA-ssDNA complexes. Science *300*, 1542-1548.
Zou, L., Liu, D., and Elledge, S. J. (2003). Replication protein A-mediated recruitment and activation of Rad17 complexes. Proc Natl Acad Sci U S A *100*, 13827-13832.